LATERAL LOAD DISTRIBUTION FACTORS FOR MILITARY VEHICLES ON MULTI-GIRDER DECK SLAB BRIDGE SYSTEMS

JUAN C. PIÑERO

Thesis submitted to the Faculty of the
Virginia Polytechnic Institute and State University
in fulfillment of the requirements for the degree of

Master of Science
in
Engineering Mechanics

M.P. Singh, Chair
R.M. Barker
S. Thangjitham

May 2001
Blacksburg, Virginia

Keywords: Load Distribution Factors, Harmonic Decomposition Approach, Multi-Girder Bridge Systems, Military Vehicles.

LATERAL LOAD DISTRIBUTION FACTORS FOR MILITARY VEHICLES ON MULTI-GIRDER DECK SLAB BRIDGE SYSTEMS

Juan C. Piñero

Mahendra P. Singh, Chair

Engineering Mechanics

(ABSTRACT)

American Association of State Highway and Transportation Officials (ASHTO) specifications have prescribed lateral load distribution factors to calculate the bending moments and shear forces for the design of highway bridges for civilian highway traffic. The maximum bending moments and shear forces caused by a wheel line load (or the entire vehicle) placed on the girders are multiplied by the distribution factors to calculate the design forces to include the effect of the load distribution laterally to the girders by the bridge deck. However, the use of these AASHTO distribution factors may not provide accurate estimate of the maximum forces for military vehicles, which usually have significantly different loading pattern than those of the civilian vehicles. Therefore, this study was conducted to develop new formulas for the lateral load distribution factors for military vehicles.

The study considered six different types of military vehicles, three wheeled vehicles and the other three tracked vehicles. The bridge database used

for developing AASHTO distribution factors formulas was also used in this study. The focus of this study was to develop the distribution factors formulas for three different types of bridges: steel girder bridges, pre-stressed concrete bridges, and concrete T-beam bridges.

The bridges in each category were analyzed for the six types of military vehicles by the harmonic decomposition approach to calculate the distribution factor. This thesis provides a total of 52 new formulas for different types of vehicles, different types of bridges, bending moment and shear force values, interior and exterior girders, and for single and multiple lane loading cases. The distribution factors calculated with the formulas were compared with those calculated by direct analyses of the bridges to evaluate the accuracy of the proposed formulas. Comparisons were also made between the values calculated by the new formulas, post-LRFD formulas prescribed in 1996 AASHTO Standard Specification, and simple pre-LRFD formulas that were prescribed by AASHTO before 1994.

DEDICATION

To my wife, Luz, and son, Christian, whose love and support made this thesis possible.

ACKNOWLEDGEMENTS

I would like to thank Dr. M.P. Singh, the chairman of my advisory committee, for his advice, support and guidance throughout my graduate studies. I would like to express my sincere appreciation to my advisory committee members Dr. R.M. Barker and Dr. S. Thangjitham for serving in my committee and reviewing this document.

This project was sponsored by the US Army Corps of Engineers, Waterways Experiment Station, Vicksburg under contract No. DACCW39-98-K-0005. At Waterways Experiment Station, Mr. James Ray was the project monitor. His advice and direction on the project work is sincerely appreciated.

I would like to extend my gratitude to all my friends from Walton Pentecostal Holiness Church. Thank you for your prayers and support. I love you all.

I would also like to thank my parents and in-laws for their unconditional support and love for my family and me.

I want to dedicate this achievement to my wife, Luz, and my son, Christian. Luz, thank you for your love and support, "*TE AMO*".

Especially, I want to thank you God, because you gave me the strength, patient, health and wisdom to make this possible.

CONTENTS

LIST OF FIGURES

LIST OF TABLES

LIST OF APPENDICES

CHAPTER 1

INTRODUCTION

1.1 PROBLEM STATEMENT

1.1.1 Background

For an assessment of the load carrying capacity or load rating analysis of a bridge, one needs to know the maximum bending moment and shear force induced in the beams or girders of the bridge by the vehicle loads. These maximum design load effects in a bridge can be calculated by any of the rigorous analytical procedures such as grillage method, finite element method, finite strip method, or harmonic analysis approach.

These rigorous methods are accurate but cumbersome to use for a quick assessment of the capacity or rating factor. For a quick estimate of the maximum load effects that include the lateral load distribution characteristics of the deck slab and girder systems, AASHTO (1996) has prescribed simple formulas for lateral load distribution factors for civilian vehicle loads. The distribution factor is used as a multiplier to the bending moment and shear force, calculated for the entire vehicle load applied to the girder as a line load, to obtain the design values of the bending moment and shear force. The distribution factor depends upon the relative stiffness characteristics of the deck-slab and supporting girders, and of course, on the loading pattern of the vehicle on the bridge.

The load distribution factors prescribed in the AASHTO Standard Specifications (1996) and AASHTO Guide Specifications for Distribution of Loads for Highway Bridges (1994) were primarily developed for civilian highway traffic [Zokai, et al., 1992]. The vehicle considered for the development of these formulas was an HS-20 truck with only two sets of wheel line loads. However, some military vehicles have more than two sets of wheel line loads, with axle loads different from those of an HS-20 truck. In addition, the load distribution patterns of the tracked military vehicle are quite different from that of an HS-20 truck. These different loading characteristics of military vehicles are likely to cause different distributions of bending moments and shear forces in a bridge than those caused by an HS-20 vehicle.

The use of the distribution factors based on the civilian vehicles could provide an over or under estimation of the design force values (bending moment and shear forces) for military vehicles. If the forces caused by military vehicles are over estimated, it might unnecessarily restrict the usage of a quite safe bridge by the military vehicles. On the other hand, if the forces are underestimated, then it might also permit the use of a weak bridge by a heavy military vehicle. It is, therefore, desirable to obtain more realistic distribution factors to be applied to military loading to estimate their load effects on the beams and girders of multi-girder bridge systems.

1.1.2 Recent Related Studies

The topic of defining the lateral load distribution factors for highway bridges has been of continued research interest for several decades and, as such, there have been numerous studies in the past. The primary motivation behind all these studies was to define these factors in a simple form as possible to calculate the

maximum load effect in the load carrying members of a bridge structure, without carrying out complicated analysis of girder and deck slab systems.

Earlier studies in this topic, and the distribution factor formulas developed therefrom, were limited and constrained by the then available analytical and numerical capabilities. Therefore, in the late eighties, the NCHRP sponsored a comprehensive research study by Zokai, Osterkemp, and Imbsen (1991) to develop more accurate, yet simple, formulas to define distribution factors for the design of highway bridges in the United States. A large data set of 850 bridges from 18 different states in the country was considered in this study. The database included five different types of bridges. The effect of skew angle and that of the continuity of the beams over the supports were also considered. The "AASHTO HS family" of trucks as the vehicle loads in the analysis was primarily considered in the study.

In our opinion, this was the most comprehensive study conducted so far on the lateral load distribution factor analysis. The study led to new and more accurate formulas for calculating the load distribution factors. The formulas were expressed as functions of girder spacing, girder span, girder moment of inertia, slab thickness, and the number loaded lanes. The study also made recommendations about the use of some computer programs for bridge analysis, with the primary focus on the finite element and grillage methods.

Although the above study indicated that the proposed distribution factors were insensitive to different types of vehicle loading patterns, this conclusion was not based on any study with military vehicles. To address the issue of the distribution of load effects by military vehicles, the Military Traffic Management Command and the Federal Highway Administration Bridge Division sponsored an initial study. The intent was to evaluate a series of bridges in New Mexico using the

New Mexico State Highway and Transportation Department program called OVLOAD. The study examined 539 bridges from the National Bridge Inventory (NBI) for different military vehicle including the HETS (Heavy Equipment Transporter System). It was observed that several bridges in this database were not passable by some loaded military vehicles including HETS. This apparent deficiency of several bridges for military vehicles was attributed to incomplete consideration of the lateral load distribution of military vehicles by the OVLOAD program. Therefore, this initial study was followed by a more comprehensive study started in October 1998 by the New Mexico State University (NMSU).

The purpose of this follow-up study was to develop a more accurate computer program to evaluate the passability of the bridges in the NBI database, and to verify the findings with the field test on a few selected bridges. The HETS vehicle was the primary focus of this study, as this particular vehicle was observed to place the most demand on the bridge systems.

This NMSU study used a computer code SECAN to calculate the bridge response (bending moments and shear forces), including the lateral load distribution effect, for the HETS loading. This computer code is based in the method of harmonic analysis – the method also used by Singh et al (1998) in their study on the sensitivity analysis of load rating factors conducted for Waterways Experiment Station. The analytically calculated design force values with SECAN program were validated by the field tests on selected bridges in Colorado and Texas. This analytical method was then used in program BRGCK, developed to provide capacity rating factors for the bridges in the NBI database to assess their passability for HETS vehicles. The details of this NMSU study are provided in the report by Minor and Woodward (1999).

1.2 SCOPE AND OBJECTIVES

1.2.1 Scope of the Research

The scope of the present study is to developed a simple approach to calculate maximum bending moments and shear forces (load effects) caused by military vehicles in different types of simply supported multi-girder bridge systems. Computer programs that are now available for bridge system analysis can calculate these load effects. However, the intent was not to use these programs but to use the lateral load distribution factors to provide accurate values of the load effects caused by military vehicles. These easy-to-calculate lateral load distribution factors are intended to provide a quick, convenient, and accurate method for rating capacity analysis and evaluation of a bridge for military vehicle loading.

1.2.2 Specific Objectives

The specific objectives that were realized by this research are as follows:

- Earlier studies defining the lateral load distribution factors for highway bridges were comprehensively studied.
- Simple formulas similar to those prescribed in AASHTO Standard Specifications (1996) and AASHTO Guide Specifications (1994) to provide accurate values of the lateral distribution factors were developed. These lateral load distribution factors can then be used with a simple beam analysis to obtain the maximum load effect in the girders of a bridge system.
- General formulas considering all bridges as well as the three different types of bridges were defined separately. The formulas define the distribution factors as functions of girder spacing, girder span, girder moment of inertia, and slab thickness.

- Formulas both for the bending moment and shear force, in the interior and exterior girders, are provided separately.
- Specialized formulas were developed separately for the (1) HETS vehicles, (2) PLS and HEMMT vehicles, (3) ABRAMS vehicles and, (4) M113 and Bradley vehicles.
- The accuracy of the proposed formulas were evaluated by comparing the distribution factors calculated with the formulas with those calculated by direct analyses of the bridges.
- Comparisons were also made between the values calculated by the new formulas and formulas primarily developed for civilian highway traffic.

1.3 METHODOLOGY AND RESULTS OBTAINED

1.3.1 Methodology

To obtain the distribution factor formulas, first the maximum load effects (bending moments and shear forces) were calculated by a rigorous analytical approach for the six different types of military vehicles placed on three different types of multi-beam slab bridge systems.

The analytical approach appropriately considers the interaction between the beam girders and the supporting slab, and thus provides accurate values of the maximum load effects including the lateral load distribution. These calculated maximum load effect values were divided by the corresponding maximum values obtained for a simply supported beam loaded with the vehicle load applied as a line load placed directly on the beam. The calculated load distribution factor values are next processed by SAS package to obtain the exponents of the regression equations. The regression equations are expressed in terms of nondimensional bridge parameters that can also be established by similarity

analysis (Douglas, 1969). These factors are essentially the same as in the NCHRP study by Zokai et al (1991). Separate "best fit" equations were developed for the following different cases:

1. Three bridge types:
   a) Steel Beam Bridges
   b) Reinforced Concrete T-beam Bridges
   c) Pre-stressed Concrete Beam Bridges
2. Interior and Exterior Girders
3. Single Lane and Multiple Lane Loading Patterns

As mentioned earlier, equations were developed separately for four classes of military vehicle considered, as well as a single equation representing all military vehicles.

1.3.2 Research Products

The products of this research were the following:

- A development of 52 new formulas for the lateral load distribution factors for military vehicle for with different types of vehicles, different types of bridges, bending moment and shear force values, interior and exterior girders, and for single and multiple lane loading cases.
- A comprehensive comparisons between the values calculated by the new formulas, post-LRFD formulas prescribed in 1996 AASHTO Standard Specification, and simple pre-LRFD formulas that were prescribed by AASHTO before 1994.

1.4 THESIS OUTLINE

This thesis presents the development of new formulas for the lateral load distribution factors considering military vehicles loading. In Chapter 2, the harmonic decomposition approach used to calculate the live load effect in a deck and multi-girder system is discussed. This rigorous method was implemented in a computer program to calculate the maximum load effect for any arbitrary pattern of wheel loads on a simply supported multi-beam slab bridge system. The numerical accuracy of the computer program as well as the different type of bridges and vehicles considered in this study are presented in Chapter 3.

In Chapter 4, the procedure followed to determine the distribution factors formulas for the three different types of bridges considered in this study: steel girder bridges, pre-stressed concrete bridges, and concrete T-beam bridges is presented in detail. Finally, the main conclusions of this study are summarized in Chapter 5.

CHAPTER 2

HARMONIC DECOMPOSITION APPROACH

2.1 INTRODUCTION

In this chapter the basic formulation of the harmonic analysis approach is presented. This approach is described in the text by Jaeger and Bhakt (1989). Singh et al (1998) re-formulated this method in order to calculate the maximum load effect for any arbitrary pattern of wheel loads on a simply supported multi-beam slab bridge system. Since this approach was used for calculating numerical results in this report and also for the sake of completeness. Here a brief analytical description of this approach is provided.

In this method, the deck is modeled as a slab with transverse bending and torsional stiffness, supported at discrete locations by one dimensional beam elements representing the individual girders. This rigorous method will provide the most accurate load effect values in the analysis of deck and multi-girder systems.

2.2 HARMONIC REPRESENTATION OF VEHICLE LOADS

The first step in the formulation of the harmonic analysis approach is to discuss how vehicles loading are represented on the bridges. For any multi-axle vehicle placed at a particular location on the bridge, the total weight, W, can be expressed as follows:

$$W = \sum_{m=1}^{M} W_m \tag{2.1}$$

where W is the sum of the wheel loads of the vehicle, W_m is the known fraction of the vehicle weight carried by the mth wheel applied at coordinates (x_m, y_m), and M is the number of wheels in the vehicle. Figure 2.1 presents the coordinate system (x_m, y_m) considered in this formulation.

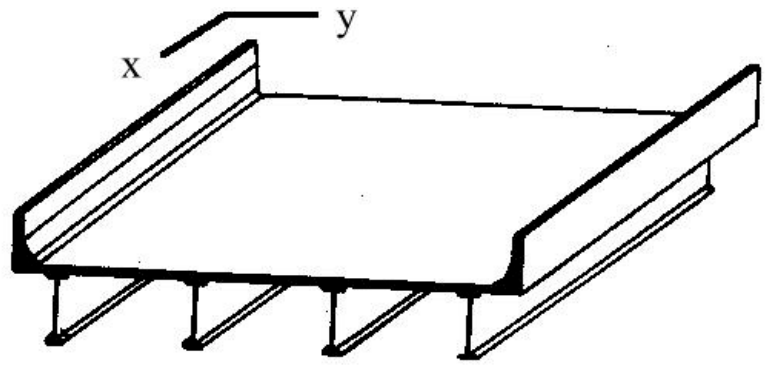

Figure 2.1: Coordinate System

In order to obtain the total response of the bridge due to the entire vehicle weight, the individual responses of a particular girder due to each wheel load W_m are obtained and then those responses are superimposed.

2.2.1 Fourier Harmonics Representation

For convenience in the analysis, the applied loads are represented by means of a harmonic series in the longitudinal direction. This procedure is performed as follows:

- **<u>Point Load Effect.</u>** Two-dimensional load distribution function is used to represent the effect of the point load W_m applied at a particular point (x_m,y_m). The function looks as follows:

$$p_m (x, y) = W_m \delta (x - x_m) \delta (y - y_m) \tag{2.2}$$

where δ (ζ - a) is the Dirac's delta function defined as

$$\delta(\zeta - a) = \begin{cases} 1 & when \quad \zeta = a \\ 0 & when \quad \zeta \neq a \end{cases} \tag{2.3}$$

- **<u>Fourier Harmonics of Applied Loads.</u>** Equation (2.3) is modeled as the sum of an infinite number of harmonic line loads, applied at a transverse distance $y = y_m$. such that

$$p_m, (x,y) = \sum_{n=1}^{\infty} p_{mn}(x)\, \delta(y - y_m) \tag{2.4}$$

In the previous equation p_{mn} (x) is the distribution of the nth harmonic line load. This distribution is defined as follows:

$$p_{mn}(x) = P_{mn} \sin \frac{n\pi x}{L_x} \tag{2.5}$$

where L_x is the bridge span, and P_{mn}, is the amplitude of the nth harmonic for the mth wheel load. The amplitude P_{mn} is defined by the following equation:

$$P_{mn} = \frac{2W_m}{L_x} \sin \frac{n\pi x_m}{L_x} \tag{2.6}$$

where x_m is the x-coordinate of the wheel fraction point of application.

- **<u>Fourier Harmonics of Force between Girder and Slab.</u>** To simplify the analysis, it has been assumed that no-torsion exist between the girders and the deck. In other words, the reactive force between a girder and the slab

simply consists of a vertical reaction along the length of the girder, at a transverse distance $y = y_j$ as shown in Figure 2.2.

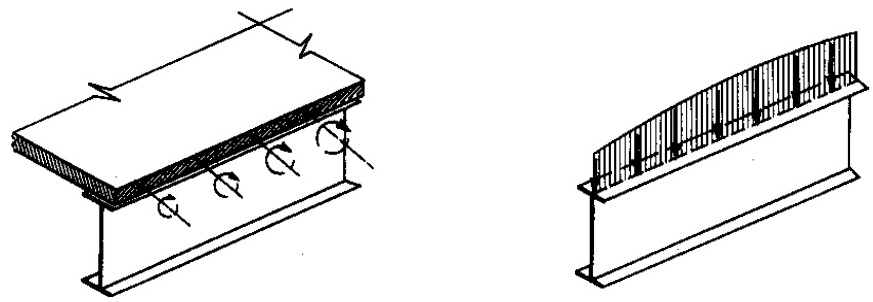

(a) Torsion Restrain (b) No-Torsion Restrain

Figure 2.2: Restrains between Girder and Deck Slab

Resolving this load into its Fourier harmonics, the following expressions is obtained:

$$p_m^j(x,y) = \sum_{n=1}^{\infty} p_{mn}^j \sin\frac{n\pi x}{L_x}\delta\left(y - y_j\right) \tag{2.7}$$

where p^j_m (x, y) is the reactive line load applied by the jth girder. Using the definition presented for the previous scenario (Eq. 2.5), p^j_{mn} (x) can be defined as:

$$p_{mn}^j(x,y) = P_{mn}^j \sin\frac{n\pi x}{L_x} \tag{2.8}$$

where P_{mn}^j is the unknown amplitude of the nth harmonic component of the load shared by the jth girder.

In order to be able to calculate the shear force and bending moment responses, the values for these unknown P_{mn}^j amplitude for each girder needs to be founded. In

the next sections, a method that considers the equilibrium and displacement compatibility conditions of the deck-girder system will be used to obtain these amplitudes and finally the design quantities.

2.3 BENDING ANALYSIS OF DECK SLAB AND GIRDERS

First, the behavior of the deck slab in the transverse direction needed to be examined under harmonic loading in order to obtain the displacement compatibility conditions of the deck-girder system. As seen on the previous section, two main loads act on the deck of the bridge: the wheel load W_m acting downwards, and the loads from the girders acting upwards. The combination of these loads can be expressed by using Eqs. (2.5) and (2.8) as follows:

$$q(x,y) = \sum_{j=1}^{N}\sum_{n=1}^{\infty} P_{mn}^{j} \sin\frac{n\pi x}{L_x}\delta(y-y_j) - \sum P_{mn} \sin\frac{n\pi x}{L_x}\delta(y-y_m) \qquad (2.9)$$

Simplifying the previous equation, we obtain the following representation,

$$q(x,y) = \sum_{n=1}^{\infty} q_{mn}(y) \sin\frac{n\pi x}{L_x} \qquad (2.10)$$

where $q_{mn}(y)$ is the amplitude of load distribution function of the nth harmonic in the transverse direction, which is given by:

$$q_{mn}(y) = \sum_{j=1}^{N} P_{mn}^{j}\delta(y-y_j) - P_{mn}\delta(y-y_m) \qquad (2.11)$$

2.3.1 Structural Responses

The next steps are needed to obtain the total structural response of the deck slab due to a series of harmonic loads.

1) **Deck Slab Strip.** Consider a strip of the deck slab in the transverse direction with the width of the strip be unity and its length be L_y. By using force and moment equilibrium conditions, the distribution of shear force $V_{mn}(y)$ and bending moment $M_{mn}(y)$ of the beam (strip) can be given by:

$$V_{mn}(y) = \sum_{j=1}^{N} P_{mn}^{j}(y - y_j)^0 - P_{mn}(y - y_m)^0 \tag{2.12}$$

$$M_{mn}(y) = \sum_{j=1}^{N} P_{mn}^{j}(y - y_j) - P_{mn}(y - y_m) \tag{2.13}$$

where $(y - a)^n$ is the nth-order singularity function defined as:

$$\langle y - a \rangle^n = \begin{cases} (x-a)^n & when \quad x \geq a \\ 0 & when \quad x < a \end{cases} \tag{2.14}$$

2) **Transverse Displacement.** In order to describe the transverse displacement function w_{mn} (y) for the strip corresponding to the loadings presented in Eq.(2.11), the following second-order differential equation can be used,

$$-D_T \frac{d^2 w_{mn}}{dy^2} = M_{mn}(y) \tag{2.15}$$

where $D_T = (EI)_T/L_x$ is the flexural stiffness of the strip, and $(EI)_T$ the total transverse flexural stiffness of the bridge deck. By substituting Eq. (2.13) into Eq. (2.15) the following expression is obtained,

$$-D_T w_{mn}(y) = \sum_{j=1}^{N} \frac{P_{mn}^{j}}{6}(y - y_j)^3 - \frac{P_{mn}}{6}(y - y_m)^3 + C_{1y} + C_2 \tag{2.16}$$

where C_1 and C_2 are unknown constants.

3) **Displacement Function.** In order to obtain the unknowns in Eq.(2.16), the displacement compatibility conditions of the deck with girders at N locations $y = y_j$, $j = 1, 2, ...N$, and static force and moment equilibrium conditions are considered below. First, lets define using simple beam analysis the fourth order displacement function for the simply-supported j^{th} girder as follows:

$$-K_j \frac{d^4 w_{mnj}}{dx^4} = P_{mn}^j \sin \frac{n\pi x}{L_x} \tag{2.17}$$

where $K_j = (EI)_j$ is the flexural rigidity of the jth girder. By integrating the previous equation four times, and applying the boundary conditions at the girder ends, the following expression is obtained,

$$w_{mnj}(x) = a_{mnj} \sin \frac{n\pi x}{L_x} \tag{2.18}$$

The a_{mnj} coefficient in Eq.(2.18) is the displacement amplitude corresponding to the nth harmonic. This amplitude is defined as:

$$a_{mnj} = \frac{1}{K_j} \left(\frac{L_x}{n\pi} \right)^4 P_{mn}^j \tag{2.19}$$

4) **Compatibility Equations.** The next step is to obtain the constants C_1 and C_2 . This can be done by considering th next two displacements

compatibility equations of the deck slab at any two girders locations r and s ,

$$w_{mn}\ (y = y_r) = a_{mnr} \tag{2.20}$$

$$w_{mn}\ (y = y_s) = a_{mns} \tag{2.21}$$

This equations are for the nth harmonic component. After some rearrangement of terms the two equations to obtain C_1 and C_2 look as follows:

$$C_1 = -\frac{1}{y_s - y_r}\left[D_T\left(\frac{L_x}{n\pi}\right)^4\left(\frac{P_{mn}^s}{K_s} - \frac{P_{mn}^r}{K_r}\right) + \sum_{j=1}^{N}\frac{P_{mn}^j}{6}\left(\langle y_s - y_j\rangle^3 - \langle y_r - y_j\rangle^3\right)\right.$$
$$\left. - \frac{P_{mn}}{6}\left(\langle y_s - y_m\rangle^3 - \langle y_r - y_m\rangle^3\right)\right] \tag{2.22}$$

$$C_2 = -\frac{1}{y_s - y_r}\left[D_T\left(\frac{L_x}{n\pi}\right)^4\left(y_s\frac{P_{mn}^s}{K_s} - y_r\frac{P_{mn}^r}{K_r}\right) + \sum_{j=1}^{N}\frac{P_{mn}^j}{6}\left(y_s\langle y_r - y_j\rangle^3 - y_r\langle y_s - y_j\rangle^3\right)\right.$$
$$\left. - \frac{P_{mn}}{6}\left(y_s\langle y_r - y_m\rangle^3 - y_r\langle y_s - y_m\rangle^3\right)\right] \tag{2.23}$$

With this equations for C_1 and C_2 , then the amplitude of the nth harmonic of the deck slab displacement can be obtained by substituting into Eq.(2.16) as follows:

$$-D_T w_{mn}(y) = \sum_{j=1}^{N}\frac{P_{mn}^j}{6}\left[\langle y - y_j\rangle^3 - \frac{1}{y_s - y_r}\left((y - y_r)\langle y_s - y_j\rangle^3 - (y - y_s)\langle y_r - y_j\rangle^3\right)\right]$$
$$-\frac{P_{mn}}{6}\left[\langle y - y_m\rangle^3 - \frac{1}{y_s - y_r}\left((y - y_r)\langle y_s - y_m\rangle^3 - (y - y_s)\langle y_r - y_m\rangle^3\right)\right]$$
$$-D_T\left(\frac{L_x}{n\pi}\right)^4\frac{1}{y_s - y_r}\left((y - y_r)\frac{P_{mn}^s}{K_s} - (y - y_s)\frac{P_{mn}^r}{K_r}\right) \tag{2.24}$$

5) **Displacement and Equilibrium Conditions.** The last step in obtaining the unknown amplitudes of the girder reactive forces, P_{mn}^{j}, is to impose N-2 displacement conditions on the remaining girders(i.e., $i \neq$ r, s) and two force and moment equilibrium conditions. The displacement conditions are given by:

$$w_{mn}\,(y = y_i) = a_{mni},\ i = 1, \ldots, N, \text{ with } i \neq r, s \tag{2.25}$$

On the other hand, the vertical force and moment equations, respectively, are given by the following equations:

$$\sum_{j=1}^{N} \frac{P_{mn}^{j}}{6} - P_{mn} = 0 \tag{2.26}$$

$$\sum_{j=1}^{N} P_{mn}^{j} y_j - P_{mn} y_m = 0 \tag{2.27}$$

Finally, substituting for $w_{mn}\,(y = y_i)$ from Eq. (2.24) into Eq. (2.25), the following expression is obtained

$$\begin{aligned}
&\sum_{j=1}^{N} \frac{P_{mn}^{j}}{6}\left[\langle y_i - y_j\rangle^3 - \frac{1}{y_s - y_r}\left((y_i - y_r)\langle y_s - y_j\rangle^3 - (y_i - y_s)\langle y_r - y_j\rangle^3\right)\right] \\
&\quad + D_T\left(\frac{L_x}{n\pi}\right)^4\left[\frac{P_{mn}^{i}}{K_i} - \frac{1}{y_s - y_r}\left((y_i - y_r)\frac{P_{mn}^{s}}{K_s} - (y_i - y_s)\frac{P_{mn}^{r}}{K_r}\right)\right] \\
&\quad = \frac{P_{mn}}{6}\left[\langle y_i - y_m\rangle^3 - \frac{1}{y_s - y_r}\left((y_i - y_r)\langle y_s - y_m\rangle^3 - (y_i - y_s)\langle y_r - y_m\rangle^3\right)\right]
\end{aligned} \tag{2.28}$$

for $i = 1, 2, \ldots, N;\ i \neq r, s$

2.3.2 Representation in Matrix Form

The previous Eqs (2.26), (2.27), and (2.28) can be expressed in the matrix form considering the following general format:

$$[A]\ \{\rho\} = \{B\} \tag{2.29}$$

where the components of matrix $[A]$, vectors $\{\rho\}$ and $\{B\}$ are given as

$$A_{ij} = \frac{1}{6}\left[\langle y_i - y_j\rangle^3 - \frac{1}{y_s - y_r}\left((y_i - y_r)\langle y_s - y_j\rangle^3 - (y_i - y_s)\langle y_r - y_j\rangle^3\right)\right]$$
$$+ D_T\left(\frac{L_x}{n\pi}\right)^4\left[\frac{\delta_{ij}}{K_i} - \frac{1}{y_s - y_r}\left((y_i - y_r)\frac{\delta_{js}}{K_s} - (y_i - y_s)\frac{\delta_{jr}}{K_r}\right)\right];\ i \neq r,\ s \tag{2.30}$$

$$B_i = \frac{1}{6}\left[\langle y_i - y_m\rangle^3 - \frac{1}{y_s - y_r}\left((y_i - y_r)\langle y_s - y_m\rangle^3 - (y_i - y_s)\langle y_r - y_m\rangle^3\right)\right] \tag{2.30}$$

$$\rho_i = \frac{P_{mn}^i}{P_{mn}} \tag{2.32}$$

where δ_{ij} is the Kronecker's delta function, $D_T = (EI)_T/L_x = K_T/L_x$ and $k_i = (EI)_i$.

2.4 BENDING MOMENT AND SHEAR FORCES IN GIRDERS

By solving Eq. (2.29) from Eq.(2.8), the following unknown harmonic function coefficients to define the distributed load on the jth girder are given

$$p_m^j(x) = \sum_{n=1}^{N} P_{mn}^j \sin\frac{n\pi x}{L_x} \tag{2.33}$$

From the previous equation, the total distributed load on j^{th} girder are obtained by considering the loading from all wheels of the vehicle as follows:

$$p^{j}(x) = \sum_{m=1}^{M}\sum_{n=1}^{\infty} P_{mn}^{j} \sin\frac{n\pi x}{L_x} \tag{2.34}$$

Similarly, the total deflection of the jth girder is obtained from Eq. (2.18) and Eq.(2.19) as

$$w_j(x) = \sum_{m=1}^{M}\sum_{n=1}^{\infty} \frac{1}{K_j}\left(\frac{L_x}{n\pi}\right)^4 P_{mn}^{j} \sin\frac{n\pi x}{L_x} \tag{2.35}$$

The corresponding slope of the displacement curve, θ_j (x), bending moment, M_j (x), shear force, and V_j (x) are obtained as

$$\theta_j(x) = \frac{dw_j}{dx} = \sum_{m=1}^{M}\sum_{n=1}^{\infty} \theta_{mnnj} \cos\frac{n\pi x}{L_x} = \sum_{m=1}^{M}\sum_{n=1}^{\infty} \frac{1}{K_j}\left(\frac{L_x}{n\pi}\right)^3 P_{mn}^{j} \sin\frac{n\pi x}{L_x} \tag{2.36}$$

$$M_j(x) = -K_j\frac{d^2w}{dx^2} = \sum_{m=1}^{M}\sum_{n=1}^{\infty} M_{mnnj} \sin\frac{n\pi x}{L_x} = K_j\sum_{m=1}^{M}\sum_{n=1}^{\infty} \frac{1}{K_j}\left(\frac{L_x}{n\pi}\right)^2 P_{mn}^{j} \sin\frac{n\pi x}{L_x} \tag{2.37}$$

$$V_j(x) = -K_j\frac{d^3w}{dx^3} = \sum_{m=1}^{M}\sum_{n=1}^{\infty} V_{mnnj} \cos\frac{n\pi x}{L_x} = K_j\sum_{m=1}^{M}\sum_{n=1}^{\infty} \frac{1}{K_j}\left(\frac{L_x}{n\pi}\right) P_{mn}^{j} \cos\frac{n\pi x}{L_x} \tag{2.38}$$

where θ_{mnj}, M_{mnj}, and V_{mnj} are, respectively, the amplitudes of slope, bending moment, and shear force corresponding to the nth harmonic line load.

2.5 SHEAR FORCE AND BENDING MOMENT IN THE DECK SLAB

Using Eq.(2.12) and Eq.(2.13), the total shear force and bending moment in the deck slab at location (*x, y*) were founded. By considering superposition of all the harmonics and wheel loads, the final expressions are given as

$$V(x,y)=\sum_{m=1}^{M}\sum_{n=1}^{\infty}V_{mn}(y)\sin\frac{n\pi x}{L_x}=\sum_{m=1}^{M}\sum_{n=1}^{\infty}\left(\sum_{j=1}^{N}P_{mn}^{j}\left\langle y-y_j\right\rangle^0-P_{mn}\left\langle y-y_m\right\rangle^0\right)\sin\frac{n\pi x}{L_x} \quad (2.39)$$

$$M(x,y)=\sum_{m=1}^{M}\sum_{n=1}^{\infty}M_{mn}(y)\sin\frac{n\pi x}{L_x}=\sum_{m=1}^{M}\sum_{n=1}^{\infty}\left(\sum_{j=1}^{N}P_{mn}^{j}\left\langle y-y_j\right\rangle-P_{mn}\left\langle y-y_m\right\rangle\right)\sin\frac{n\pi x}{L_x} \quad (2.40)$$

2.6 CONCLUSIONS

The basic formulation of the harmonic analysis approach, adjusted to calculate the maximum load effect on a simply supported multi-beam slab bridge system, has been presented. For convenience, harmonic series was introduced to represent the applied loads as well as the structural responses. Expressions for the bending moment and shear forces for both the girders and deck slab were founded.

This harmonic analysis approach was incorporated in a computer program to obtain the lateral load distribution factors for the different multi-beam slab bridge system considered in this study. Detail description of the procedure followed to obtain the new formulas for the distribution factors is presented in the next chapter.

CHAPTER 3

ANALYSIS OF BRIDGES FOR MILITARY VEHICLES

3.1 INTRODUCTION

This chapter describes the different types of bridges and military vehicles load configurations considered in this study. In addition, numerical validation and accuracy of the computer program used in this study to calculate the maximum load effect for any arbitrary pattern of wheel loads on a simply supported multi-beam slab bridge system is discussed in detail.

3.1.1 Types of Bridges

The focus of this thesis was to develop lateral distribution factor formulas for the steel beam girder bridges, T-beam reinforced concrete bridges, and pre-stressed concrete girder bridges. The study considers the same database of bridges as the one considered by Zokai et al (1991) for the development of distribution factor formulas for the NCHRP project. The same database has also been considered by the NMSU study (Minor and Woodward 1999).

The Zokai et al data was analyzed by the NMSU team to define the "typical bridges" that represents the populations of the following bridges:

(1) Steel Girder Bridges
(2) Reinforced Concrete T-beam Bridges
(3) Pre-stressed Concrete Girder Bridges
(4) Slab Bridges

These typical bridges were created to represent the existing variations in the span, beam spacing, moments of inertia of girders, and slab thickness in the four types of bridges in the database. In this thesis, only the first three beam bridges are considered. Typical cross-sections of these bridges are presented in Figure 3.1.

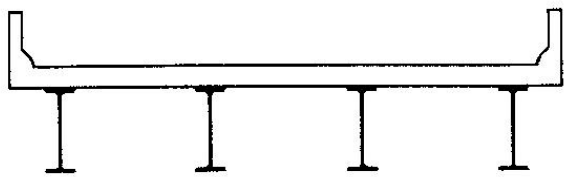

(a) Steel Girder Bridge

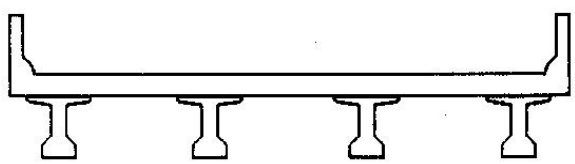

(b) Prestressed Concrete Girder Bridge

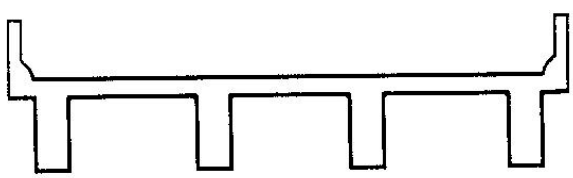

(c) Reinforced Concrete T-beam Bridge

Figure 3.1: Typical Bridges Cross-Sections

Steel Girder Bridges

A total of 90 different steel girder bridges were considered in this study. The properties of the typical steel girder bridges developed in the NMSU study are presented on Table 3.1.

Table 3.1: Properties of Typical Steel Girder Bridges in the NMSU Study

Span	Beam Spacing (fts)				
(fts)	4	5	6	7	8
50	3842	4620	5556	6682	8035
70	5864	7052	8480	10198	12264
90	8950	10763	12943	15565	18718
110	13659	16426	19754	23756	28568
130	20848	25071	30150	36258	43603
140	25756	30973	37248	44793	53868
No. of Beams	7	6	5	5	4

Note: Three slab thickness have been considered: 7, 8 and 9 in.

The NMSU team obtained the values shown in Table 1 by regression analysis of the Zokai et al (1991) database. The regression equation is given as:

$$\text{Ln}(I) = 6.4588 + 0.021141\,L + 0.184468\,S \qquad (3.1)$$

where I is the moment of inertia (in^4), L is the span length (ft), and S is the beam spacing (ft). This regression equation has been used to define the moments of inertia for the typical set of steel bridges for each set of span and beam spacing values indicated in the table.

Prestressed Girder Bridges

The different types of prestressed concrete girder bridges considered in this study are presented in Table 3.2. A total of 138 different prestressed concrete girder bridges have been considered in the analysis. These bridges were developed by the NMSU (Minor and Woodward 1999) and they represented the population of the typical prestressed concrete girder bridges from the NBI database.

Table 3.2: Properties of Typical Prestressed Girder Bridges in the NMSU Study

Span	Beam Spacing (fts)						
(fts)	4	5	6	7	8	9	10
40	II	II	II	II	II	N/A	N/A
50	III	III	III	III	III	N/A	N/A
60	II	II	II	II	II	N/A	N/A
65	III	III	III	III	III	N/A	N/A
70	IV	IV	IV	IV	IV	IV	IV
80	III	III	III	III	III	N/A	N/A
85	IV	IV	IV	IV	IV	IV	IV
100	IV	IV	IV	IV	IV	IV	IV
No. of Beams	7	6	5	5	4	4	4

Note: Three slab thickness have been considered: 7, 8 and 9 in.

As shown in Table 3.2, three common types of prestressed concrete beams were assigned to the typical bridges. According to the NMSU study, the assignment of each beam section to each one of the combinations of span and spacing was based on the typical usage observed in the real bridges database. Section properties and moment of inertia for each type of prestressed concrete beam are presented in Table 3.3 and Figure 3.2.

Table 3.3: Prestressed Concrete Section Properties and Moment of Inertia

Type of Beam	bu (in)	bb (in)	X1 (in)	X2 (in)	X3 (in)	X4 (in)	bw (in)	h (in)	I (in^4)
II	12	18	6	3	6	6	6	36	50979
III	16	22	7	4.5	7	7.5	7	45	125390
IV	20	26	8	6	8	9	8	54	260741

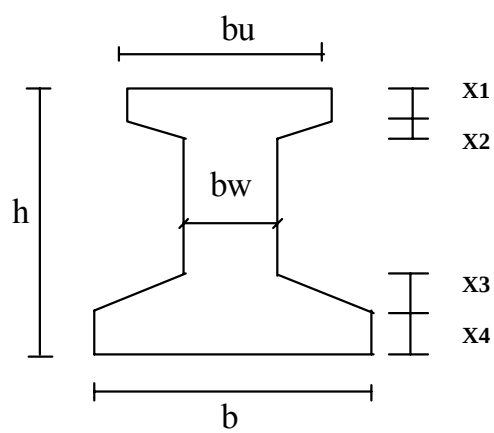

Figure 3.2: Prestressed Concrete Section Dimensions

T-beam Reinforced Concrete Bridges

According to Minor and Woodward 1999 (NMSU Study), the data contained in Zokaie et al database shows that there was no standard amounts of reinforcing steel for the concrete T-beams. For this reason, it was necessary to calculate the cracked moment of inertia assuming an amount of tension reinforcing steel in the sections. Working Stress procedures with a steel yield stress of 40 ksi was used in order to estimate the amount of steel. The 30 different types of reinforced concrete T-beam bridges considered in this study are presented in Table 3.4.

Table 3.4: Properties of Typical Reinforced Concrete T-beam Bridges in the NMSU Study

Span (fts)	Beam Spacing (fts)	No. of Beams	Width (fts)	I_{cr} (in^4)
27	9	4	27	49250
29.2	8.33	4	25	39390
35	4.75	6	23.75	25370
42	5.85	5	23.4	40580
46.8	5.61	6	28.05	40290
56	9	4	27	141500
60	4.87	6	24.35	122900
62.4	5.61	6	28.05	59590
70	9	4	27	222130
78	9	4	27	322500

Note: Three slab thickness have been considered: 7, 8 and 9 in.

At the beginning of this study, only the typical bridges previously defined were analyzed to develop the distribution factor formulas. The distribution factors calculated from these formulas showed a very good fit with those obtained by the direct analysis of these bridges. However, when such a comparison was made for the existing bridges presented in Table A.1 (Appendix A), the fit was not as good as with the typical bridges. This prompted the inclusion of the existing bridges with the typical bridges in the analysis to develop new formulas for the distribution factors for the steel and prestressed concrete girder bridges. For the T-beam concrete bridge, however, only the existing bridge data was utilized. The results from the new formulas were again compared with those obtained by direct analysis, and an improved fit was obtained for the steel and prestressed concrete

bridges. The comparison for the T-beam bridges remained the same qualitatively. This comparison of the results is discussed in Chapter 4. The new formulas are finally proposed for use with military vehicles.

3.1.2 Military Vehicles

Six different type of military vehicles provided by the U.S. Army Corps of Engineers were included in this study. The military vehicles considered are the following:

Wheeled Vehicles

- **HETS.** This is the biggest vehicle considered in this study. It has six separate wheel lines of loading and a total of nine axes.
- **PLS.** This vehicle has two separate wheel lines of loading and a total of eight axes.
- **HEMMT.** Two separate wheel lines of loading and a total of seven axes characterized this vehicle.

Tracked Vehicles

- **M113 Tank.** This vehicle has two separate wheel lines of loading and a total of five axes.
- **ABRAMS Tank.** This one is the biggest of the tracked vehicles. It has two separate wheel lines of loading and a total of seven axes.
- **BRADLEY Tank.** Two separate wheel lines of loading and a total of six axes characterized this vehicle.

The footprints and the axle load for each of these six vehicles are shown in Figures 3.3 through 3.8. It is noted that except for the HETS vehicle, all other vehicles have only two wheel lines of loading.

The computer program used in the present study considers the actual footprint of the vehicles to obtain the maximum load effect. The wheel loads are applied as concentrated loads, although in the program one could also represent them as distributed loads over each wheel footprint area; such a refinement was, however, considered unnecessary in this study.

3.1.2.1 Loading Placement for Maximum Response

The maximum load effects in a girder depend upon the location of the vehicle on the deck. The longitudinal and lateral positions of the vehicles corresponding to the maximum load effect were obtained by varying the position in small increments along and across the bridge. Figure 3.9 shows the variation of the vehicle position in the transverse direction to obtain the maximum moment and shear response on the bridge. Figure 3.10 shows the variations in the bending moments and shear forces in different girders of a typical five-girder steel bridge for different transverse positions of the vehicle on the bridge.

For the maximum bending effect in the girders, the position of the vehicle along the bridge was the essentially same as for a simply supported beam loaded with the vehicle load treated as a line load. The maximum bending moment occurred under one of the heavy axles when the axle and the vehicle centroid were equidistant from the two opposite end supports. This longitudinal position for the maximum bending effect was, thus, different for each of the considered vehicles. The maximum shear forces in the girders were usually obtained when one of the vehicle's heavy axles (usually the last axle) was on or next to the rear end support.

The exterior girders experienced the largest load effects when the centroid of the vehicle was as far as it could go towards the girder from the bridge centerline.

This position is be usually dictated by the position of the curbs with respect to the position of the exterior girders.

Both single lane and multi-lane-loading patterns were considered. In the multi-lane loading case, the outside wheel lines of the two adjacent vehicles were kept 4 ft apart.

3.2 COMPUTER PROGRAMS

3.2.1 Our New Program

All typical bridges listed in Tables 3.1, 3.2, and 3.4, along with the existing bridges listed in Table A.1 (Appendix A), were analyzed for all six military vehicles using the harmonic analysis approach described in Chapter 2. In this study, the harmonic analysis was incorporated in a new computer program to calculate the maximum load effect for any arbitrary pattern of wheel loads on a simply supported multi-beam slab bridge system.

The SECAN, program used in the NMSU study, also used the harmonic analysis approach. The accuracy of the SECAN program was verified by the field tests conducted on some selected bridges in Colorado and Texas (Minor and Woodward, 1999).

3.2.2 LDFAC Program

To verify the numerical accuracy of the program used in our study, several sets of numerical results were obtained for the distribution factors for the HS-20 vehicle, and compared with the results obtained from the equations by Zokai et al (1991) and those obtained by the computer program LDFAC (Zokai et al, 1993).

This later program was recommended by Zokai et al for level two type of analysis of highway bridge systems. This program is based on the grillage method of

analysis. It represents a multi-girder and deck system by a grillage consisting of interconnected beam elements. It is important that the equivalent bending and torsional stiffness properties of these beam elements are properly chosen to represent the girders and deck of a bridge. The wheel loads also need to be transferred properly to the nodes of the interconnecting nodes of the grillage. Zokai et al (1993) have a developed a computer code to conduct such an analysis. The numerical results calculated with this code have been compared with those obtained by our harmonic analysis program.

3.2.3 Numerical Accuracy of Our Computer Program

The comparison of the distribution factor results is made in Figures 3.11 through 3.22. The first six figures are for the bending moment distribution factors, and the next six for the shear force distribution factors. Both single lane and multi-lane-loading scenarios are included. It is noted that the bending moment distribution factors calculated by different methods are reasonably close to each other, some being closer than others. There seems to be a somewhat larger difference in the shear force results, especially for the multi-lane-loading pattern.

In general, the differences in the results obtained by the two computer programs (harmonic analysis and LDFAC) can be justified as they use quite different analytical formulations. The LDFAC results, based on the grillage approach, would be considered to produce less accurate results because of the representation of the bridge continuum by discrete interconnected beam elements. The small differences between the results obtained by the Zokai et al formulas and those obtained by harmonic analysis can also be justified as the Zokai formulas were developed to represent a wide range of bridge types and parameters.

Furthermore, the validation of the harmonic analysis results obtained by SECAN with those of the field tests conducted on five bridges in Colorado and Texas adds further credence to the harmonic analysis approach.

3.3 CONCLUSIONS

The main properties for the steel beam girder bridges, T-beam reinforced concrete bridges, and pre-stressed concrete girder bridges considered in this study described in detail. In addition, the characteristics of the wheeled military vehicles (HETS, PLS, HEMMT) and the tracked vehicles (M113, ABRAMS, BRADLEY) have been presented.

The development and validation of the computer program develop as part of this study has been presented. The numerical results of the distribution factors obtained with our computer program, in comparison with the results obtained with the LDFAC program, were considered acceptable and reasonably close to each other.

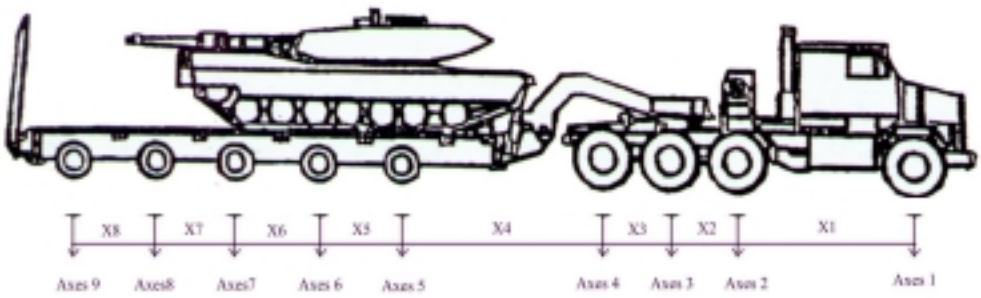

(a) Side View

Loading Data:

		Axes 1	Axes 2	Axes 3	Axes 4	Axes 5	Axes 6	Axes 7	Axes 8	Axes 9
Loads (kips)	Empty	18.4	7.6	7.6	7.4	6.0	6.0	6.0	11.6	11.6
	Laden	20.8	22.8	21.6	20.0	28.2	27.6	27.6	30.8	30.8

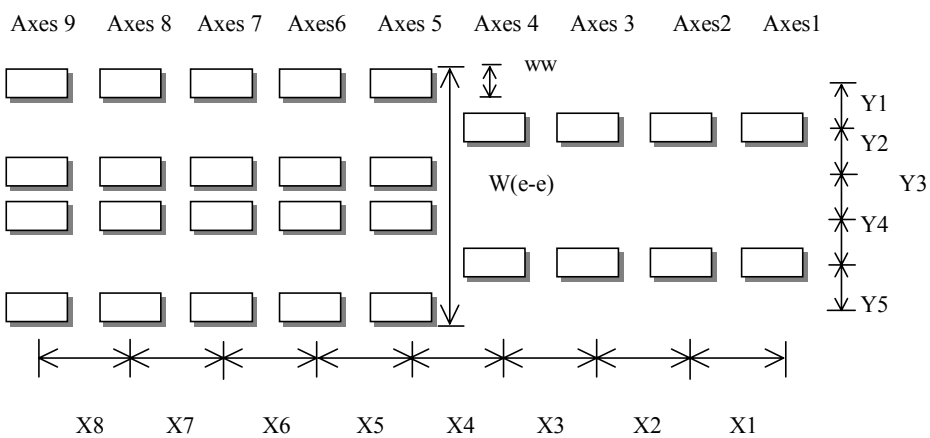

(b) Top View

Dimensions:

	ww	W(e-e)	Y1	Y2	Y3	Y4	Y5	x 1	x 2	x 3	x 4	x 5	x 6	x 7	x 8
width (fts)	1.43	12	1.58	1.11	4.85	1.11	1.58	9.2	3.8	3.8	3.7	3.0	3.0	3.0	5.8

Figure 3.3: Configuration of HETS Vehicle Load Distribution

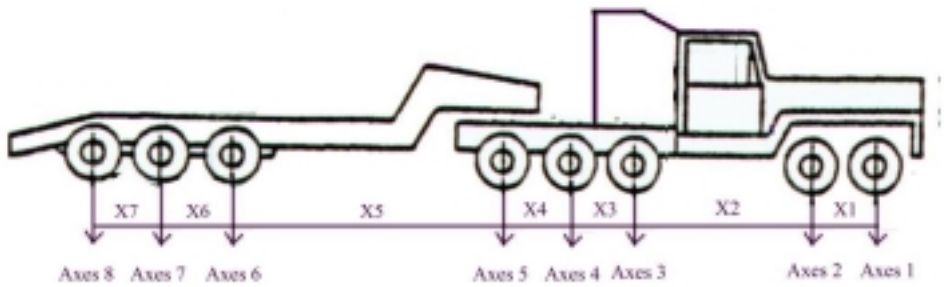

(a) Side View

Loading Data:

		Axes 1	Axes 2	Axes 3	Axes 4	Axes 5	Axes 6	Axes 7	Axes 8
Loads (kips)	Empty	10.4	10.4	11	11.2	11.2	6.6	5.6	5.6
	Laden	11.4	11.4	21.2	21.2	21.2	9.8	20.6	20.6

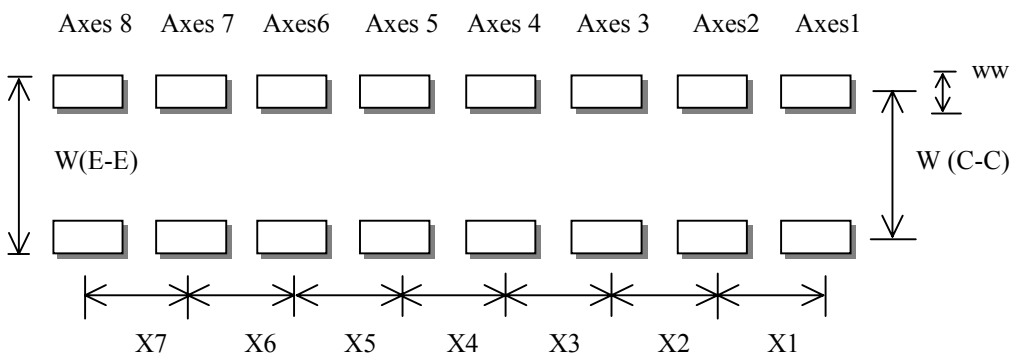

(b) Top View

Dimensions:

	ww	W(E-E)	W(c-c)	x 1	x 2	x 3	x 4	x 5	x 6	x 7
width (fts)	1.33	8	6.667	5.0	11.2	4.9	5.0	8.5	10.0	4.6

Figure 3.4: Configuration of PLS Vehicle Load Distribution

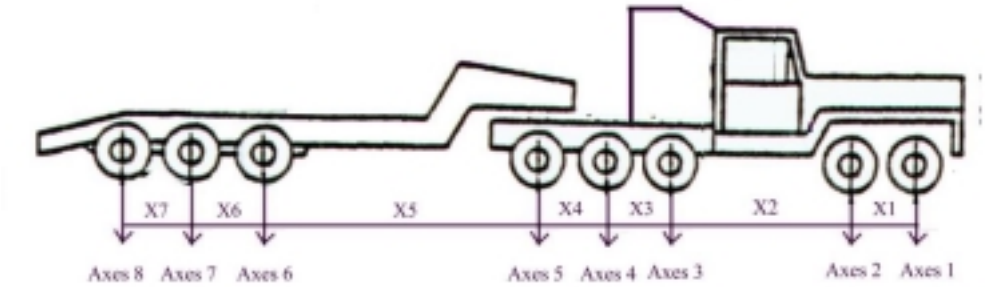

(a) Side View

Loading Data:

		Axes 1	Axes 2	Axes 3	Axes 4	Axes 5	Axes 6	Axes 7
Loads (kips)	Empty	12	12	8	8	6.6	5.6	5.6
	Laden	14	14	16.4	16.4	9.8	20.6	20.6

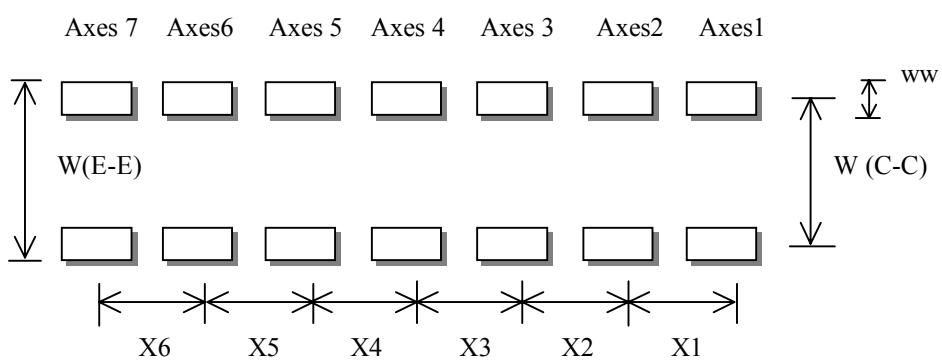

(b) Top View

Dimensions:

	ww	W(E-E)	W(c-c)	x 1	x 2	x 3	x 4	x 5	x 6
width (fts)	1.5	8	6.5	5.0	12.5	5.0	8.0	10.0	4.6

Figure 3.5: Configuration of HEMTT Vehicle Load Distribution

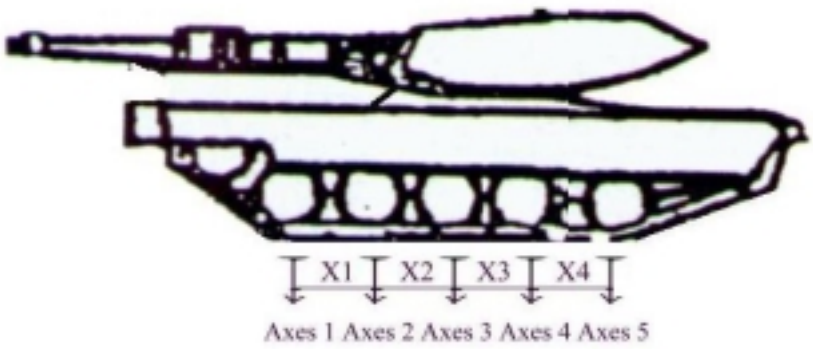

(a) Side View

Loading Data:

		Axes 1	Axes 2	Axes 3	Axes 4	Axes 5
Loads (kips)	Laden	4.6	4.6	4.6	4.6	4.6

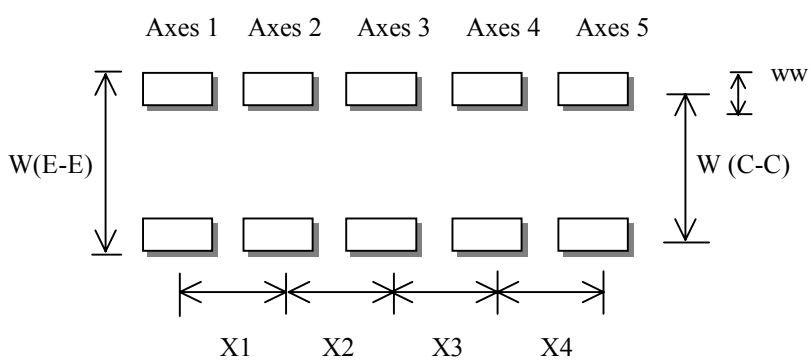

(b) Top View

Dimensions:

	ww	W(E-E)	W(c-c)	x 1	x 2	x 3	x 4
width (fts)	1.67	8.75	7.08	2.19	2.19	2.19	2.19

Figure 3.6: Configuration of M113 Tracked Vehicle Load Distribution

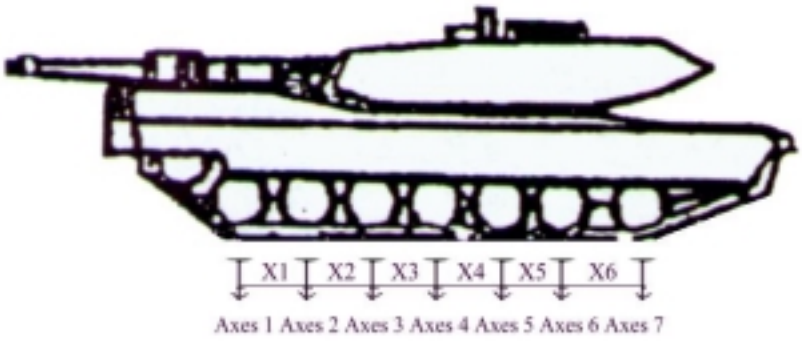

(a) Side View

Loading Data:

		Axes 1	Axes 2	Axes 3	Axes 4	Axes 5	Axes 6	Axes 7
Loads (kips)	Laden	20	20	20	20	20	20	20

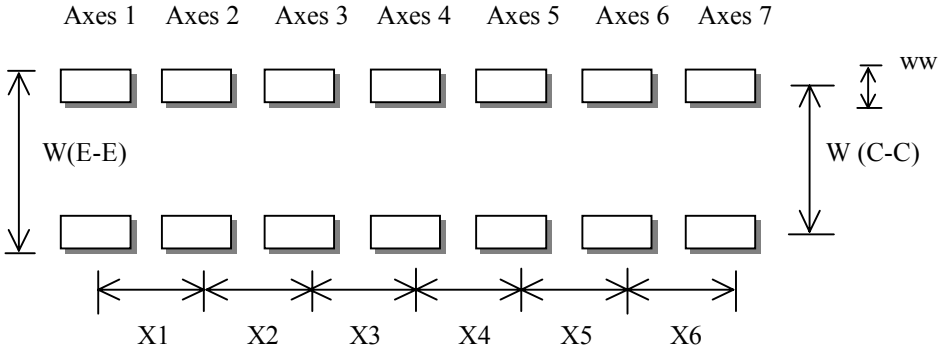

(b) Top View

Dimensions:

	ww	W(E-E)	W(c-c)	x 1	x 2	x 3	x 4	x 5	x 6
width (fts)	2.083	11.417	9.337	3	2.4	2.4	2.4	2.4	2.44

Figure 3.7: Configuration of ABRAMS Tracked Vehicle Load Distribution

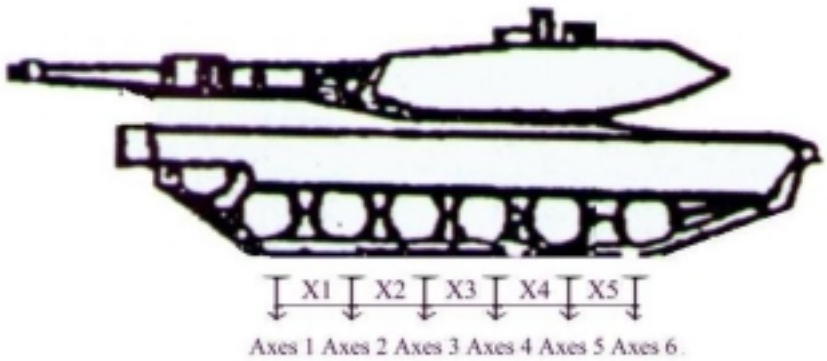

(a) Side View

Loading Data:

		Axes 1	Axes 2	Axes 3	Axes 4	Axes 5	Axes 6
Loads (kips)	Laden	8.4	8.4	8.4	8.4	8.4	8.4

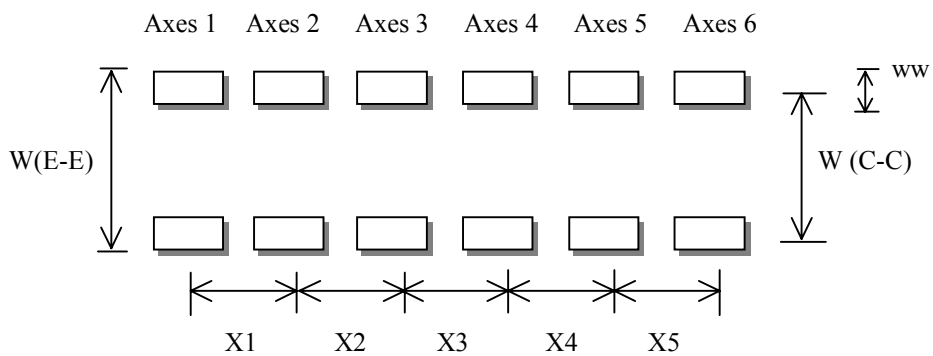

(b) Top View

Dimensions:

	ww	W(E-E)	W(c-c)	x 1	x 2	x 3	x 4	x 5
width (fts)	1.75	10.5	8.75	2.57	2.57	2.57	2.57	2.57

Figure 3.8: Configuration of BRADLEY Tracked Vehicle Load Distribution

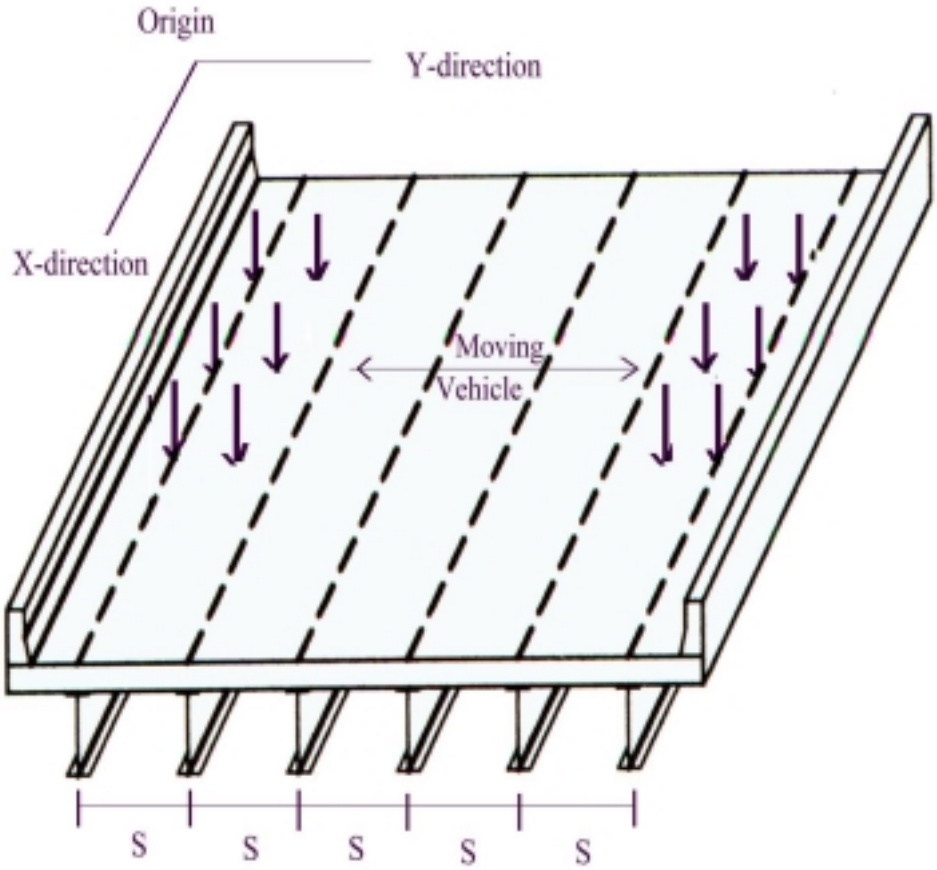

Figure 3.9: Variation of Vehicle Position in the transverse Direction to obtain Maximum Moment and Shear Response

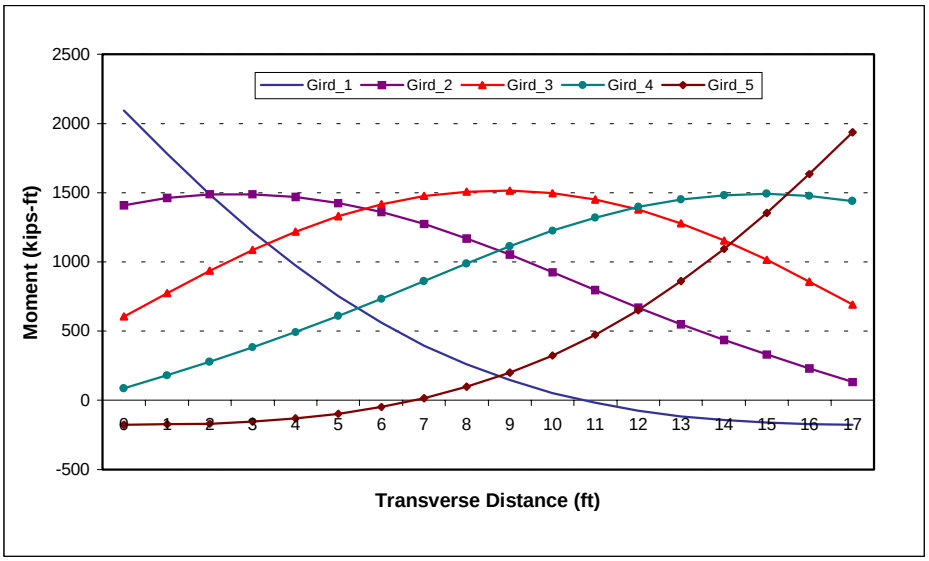

(a) Moment Response

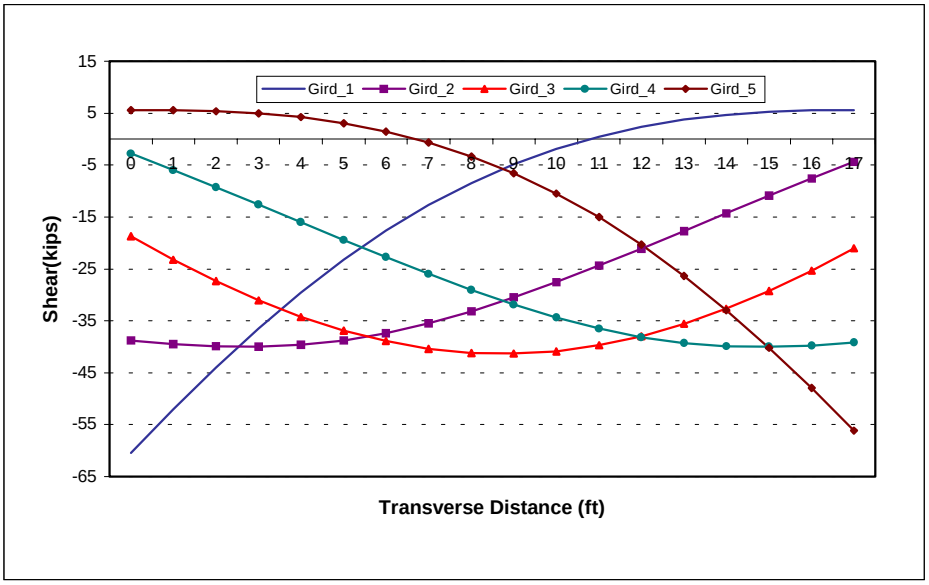

(b) Shear Response

Figure 3.10: Bending Moment and Shear Forces in different Girders calculated by Harmonic Analysis Approach for different Vehicle Locations in the Transverse Direction

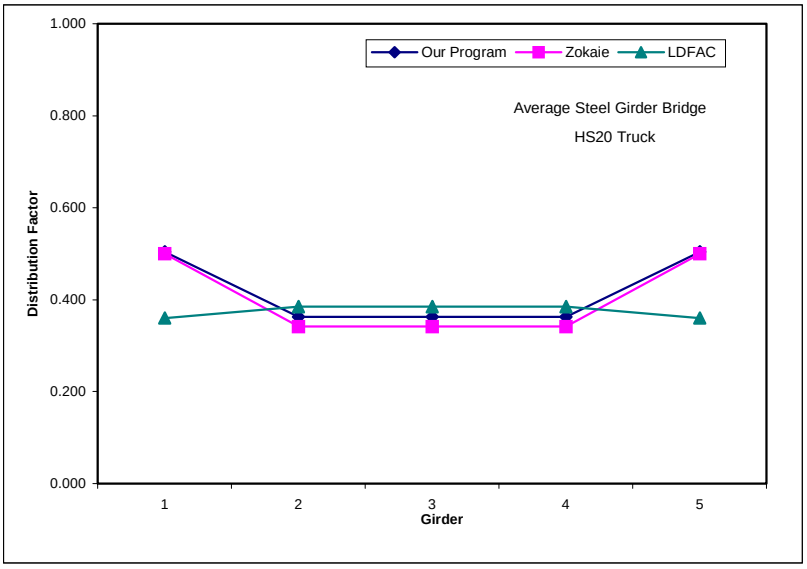

Figure 3.11: Comparison of Bending Moment Distribution Factors calculated by Harmonic Analysis approach, Zokaie et al. Formulas, and LDFAC Program, Average Steel Girder Bridge, Single Lane Loading

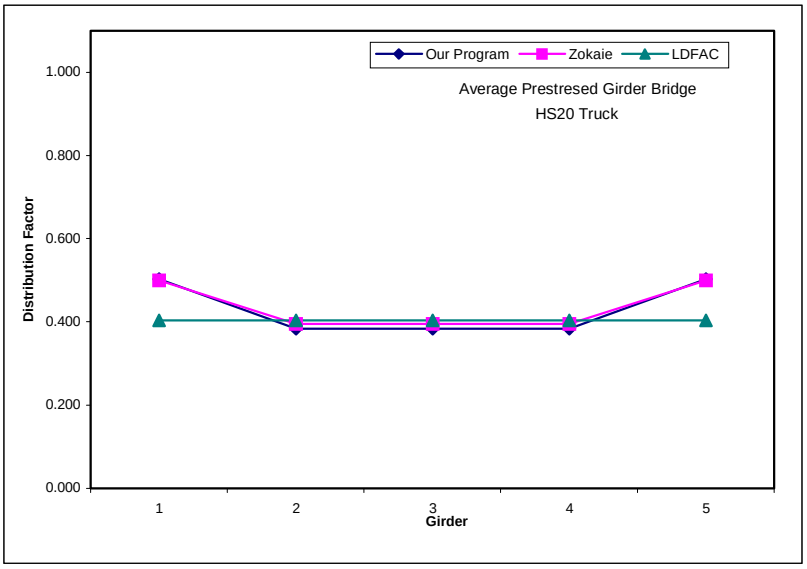

Figure 3.12: Comparison of Bending Moment Distribution Factors calculated by Harmonic Analysis approach, Zokaie et al. Formulas, and LDFAC Program, Average Prestressed Girder Bridge, Single Lane Loading

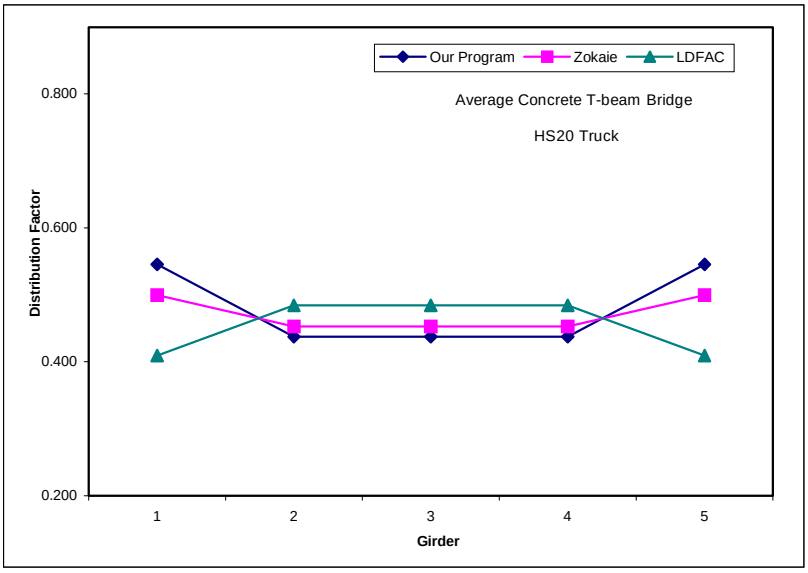

Figure 3.13: Comparison of Bending Moment Distribution Factors calculated by Harmonic Analysis approach, Zokaie et al. Formulas, and LDFAC Program, Average Concrete T-Beam Bridge, Single Lane Loading

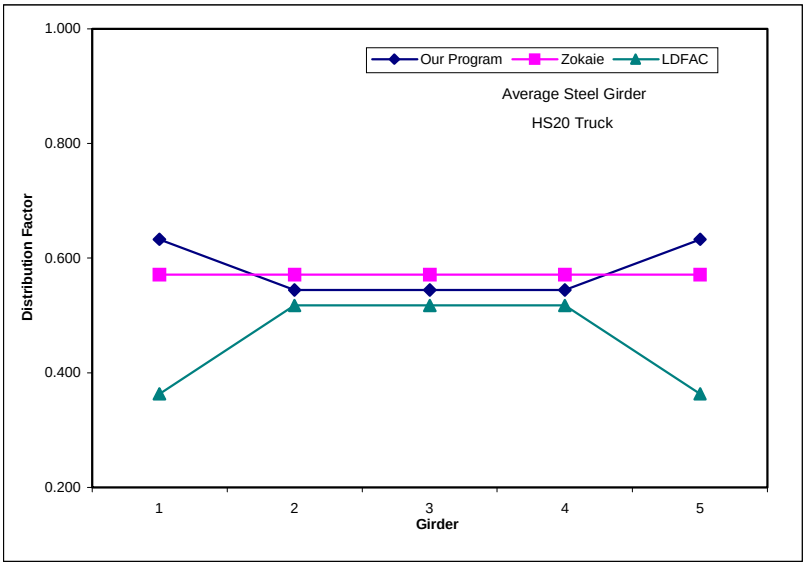

Figure 3.14: Comparison of Bending Moment Distribution Factors calculated by Harmonic Analysis approach, Zokaie et al. Formulas, and LDFAC Program, Average Steel Girder Bridge, Multi Lane Loading

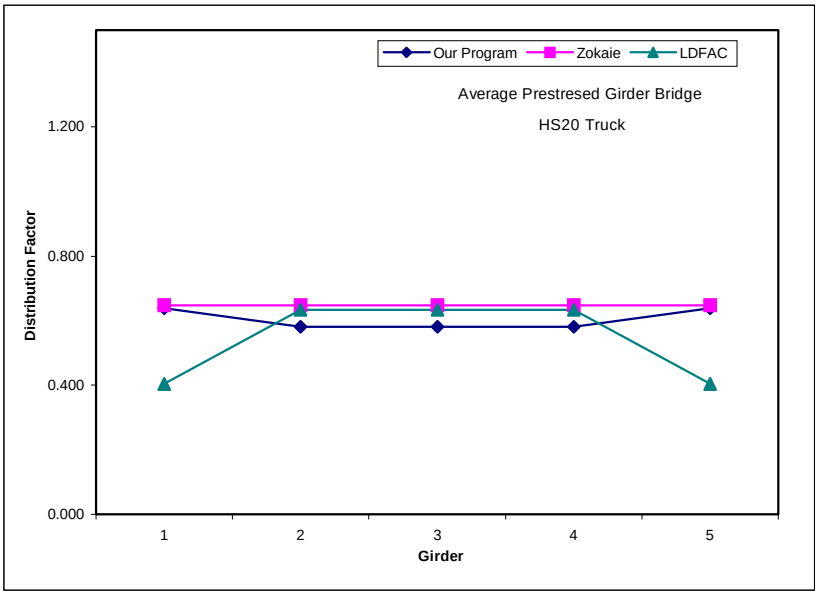

Figure 3.15: Comparison of Bending Moment Distribution Factors calculated by Harmonic Analysis approach, Zokaie et al. Formulas, and LDFAC Program, Average Prestressed Girder Bridge, Multi Lane Loading

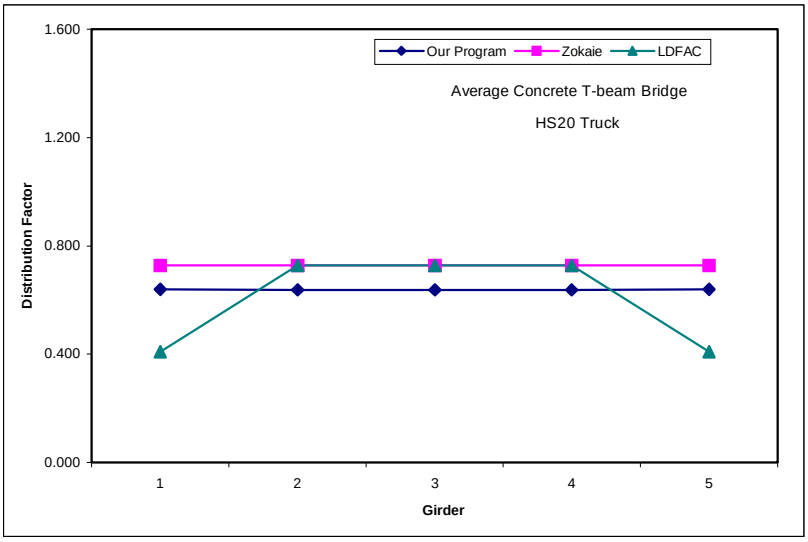

Figure 3.16: Comparison of Bending Moment Distribution Factors calculated by Harmonic Analysis approach, Zokaie et al. Formulas, and LDFAC Program, Average Concrete T-Beam Bridge, Multi Lane Loading

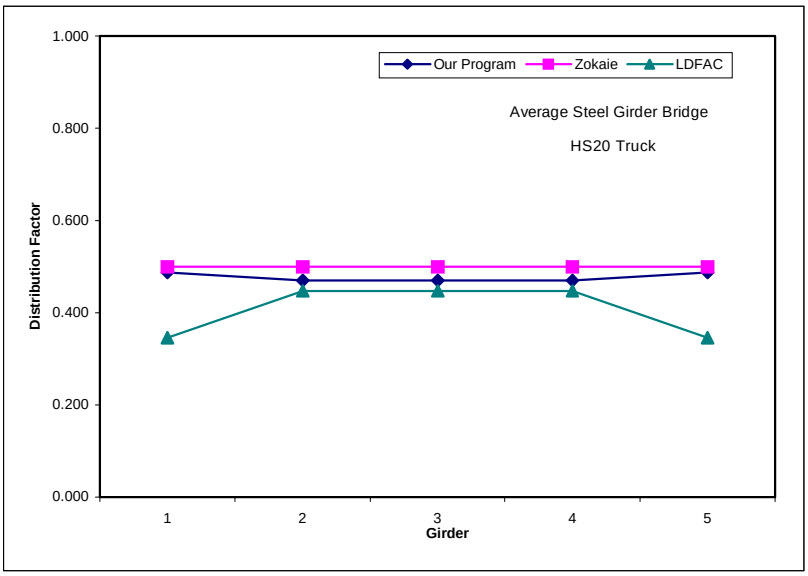

Figure 3.17: Comparison of Shear Distribution Factors calculated by Harmonic Analysis approach, Zokaie et al. Formulas, and LDFAC Program, Average Steel Girder Bridge, Single Lane Loading

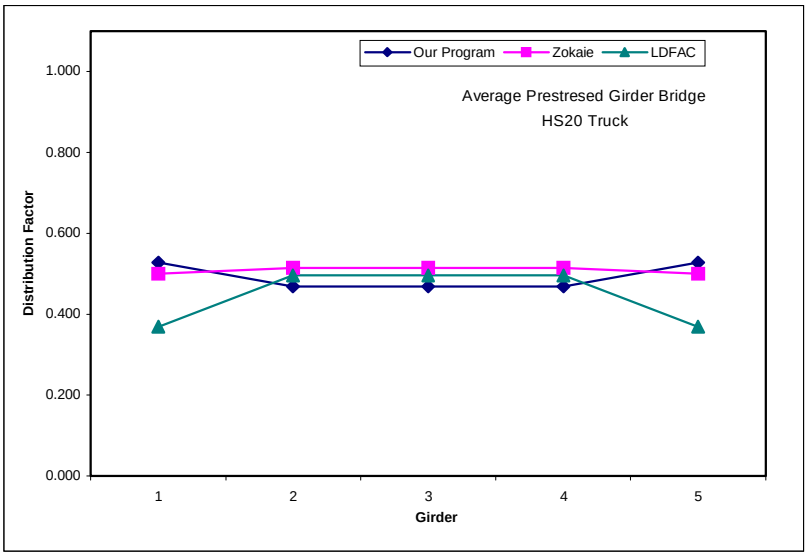

Figure 3.18: Comparison of Shear Distribution Factors calculated by Harmonic Analysis approach, Zokaie et al. Formulas, and LDFAC Program, Average Prestressed Girder Bridge, Single Lane Loading

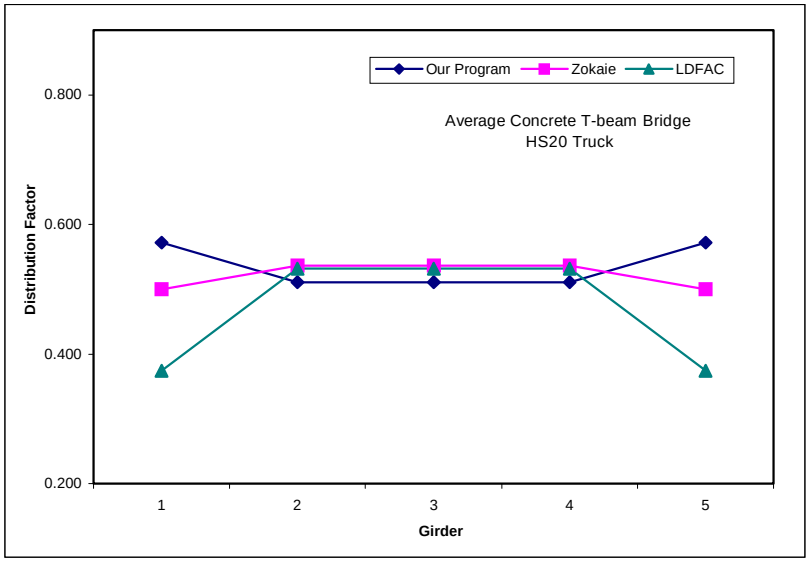

Figure 3.19: Comparison of Shear Distribution Factors calculated by Harmonic Analysis approach, Zokaie et al. Formulas, and LDFAC Program, Average Concrete T-Beam Bridge, Single Lane

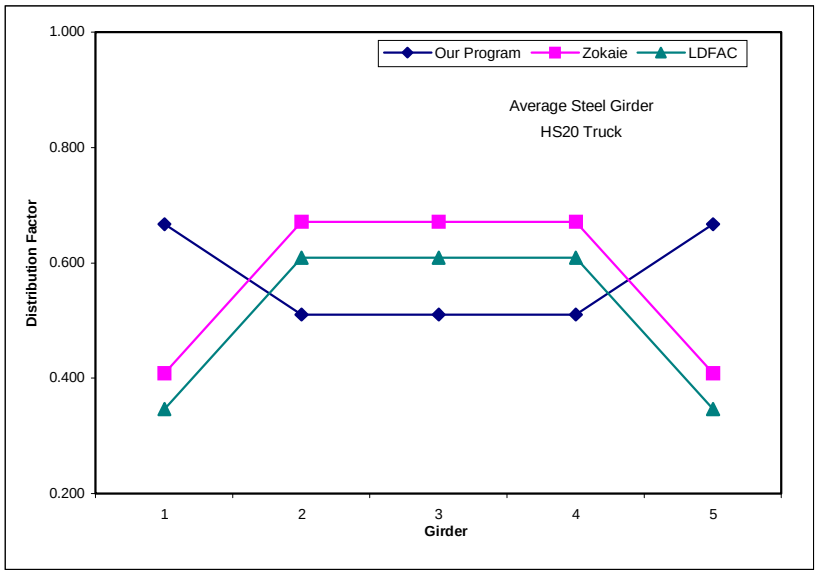

Figure 3.20: Comparison of Shear Distribution Factors calculated by Harmonic Analysis approach, Zokaie et al. Formulas, and LDFAC Program, Average Steel Girder Bridge, Multi Lane Loading

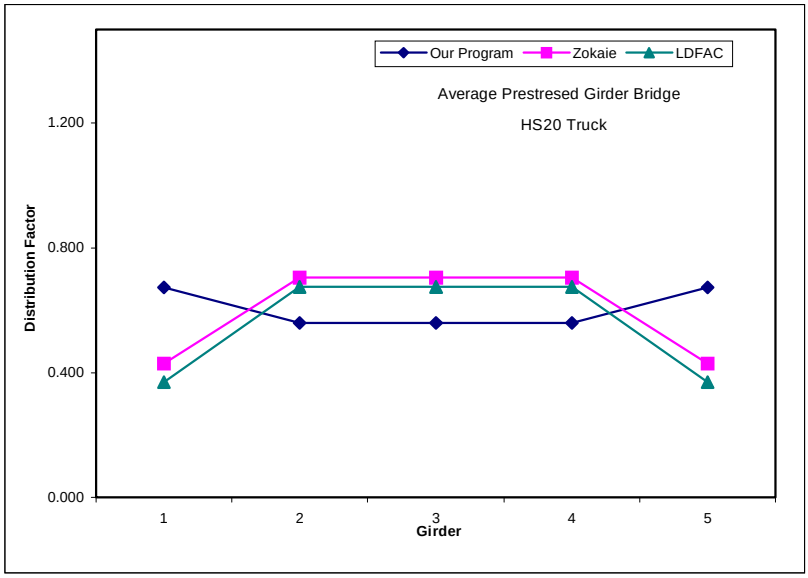

Figure 3.21: Comparison of Shear Distribution Factors calculated by Harmonic Analysis approach, Zokaie et al. Formulas, and LDFAC Program, Average Prestressed Girder Bridge, Multi Lane Loading

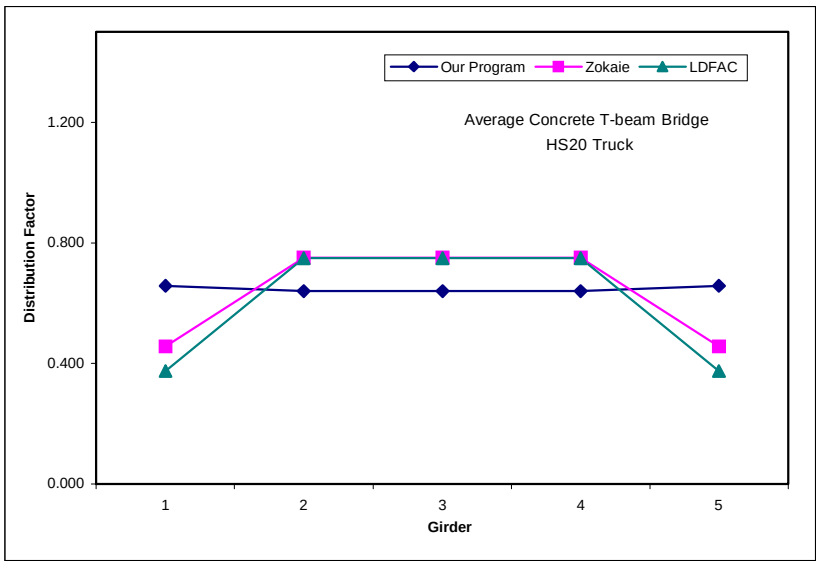

Figure 3.22: Comparison of Shear Distribution Factors calculated by Harmonic Analysis approach, Zokaie et al. Formulas, and LDFAC Program, Average Concrete T-Beam Bridge, Multi Lane Loading

CHAPTER 4

LOAD DISTRIBUTION FACTOR FORMULAS FOR MILITARY VEHICLES

4.1 INTRODUCTION

This chapter focuses in the procedure followed to determine the distribution factors formulas for three different types of bridges: steel girder bridges, pre-stressed concrete bridges, and concrete T-beam bridges. A total of 52 new formulas for different types of vehicles, different types of bridges, bending moment and shear force values, interior and exterior girders, and for single and multiple lane loading cases have been created.

In addition, a sensitivity study and comparisons between the values calculated by the new formulas, post-LRFD formulas prescribed in 1996 AASHTO Standard Specification, and simple pre-LRFD formulas that were prescribed by AASHTO before 1994 are presented.

4.2 SENSITIVITY STUDY

It is of interest to examine the sensitivity of the load distribution factors with respect to bridge parameters that affect them. This helps to identify the parameters that are most important and thus ought to be given special consideration in their numerical measurements. The three bridge types: steel

girder, prestressed concrete girders, and reinforced concrete t-beam bridges were considered in this study. The bridge parameters considered were the span, girder spacing, slab thickness, and girder moment of inertia.

4.2.1 Bridge Model and Loading

Numerical results for sensitivity analysis were obtained for the average bridges in the three bridge categories. The average bridges were obtained by calculating the average values for each of the parameter of each type of bridge. The properties of the three averages bridges are shown in Table 4.1.

Table 4.1: Parameter Values for the Average Bridges

Type of Bridge	No. of Girders	Girder Spacing (ft)	Span (ft)	Inertia (in^4)	Width (ft)	Slab Thick (in)
Steel	5	6.00	98.33	19675	25.0	8.0
Prestressed	5	6.46	70.87	171004	25.5	8.0
T-Beam	5	7.10	50.64	106350	26.1	8.0

In order to examine the sensitivity of the load distribution factors with respect to bridge parameters, each bridge parameter was varied one at a time. Therefore, while one of the parameters was varied, the others remained at the calculated average value.

All the military vehicles loading patterns were considered on each one of the different scenarios. The final values presented in the results are the average of the values obtained for each scenario with the different vehicle loadings. Details of the results obtained are presented in the next section.

4.2.2 Numerical Results

Figure 4.1 through 4.12 show the sensitivity results for these bridges. The first six figures (Figures 4.1 through 4.6) are for the bending moment distribution factors and the next six figures (Figures 4.7 through 4.12) are for the shear force distribution factors. Both, the single lane and multi-lane loading scenarios were considered. The figures show the distribution factor values plotted against the normalized parameter value. The parameter value was normalized by dividing it with the average value of the parameter.

In general, it is noted that the girder spacing is the most important parameter. The second most important parameter is the bridge span, especially for the short span bridges. The parameters of slab thickness and girder moment of inertia do not seem to be as important as the other two parameters, except for the shear force factor in the T-beam bridges (see Figures 4.9 and 4.12).

4.3 DEVELOPMENT OF NEW FORMULAS

4.3.1 Regression Analysis

The load distribution factor values calculated for the three types of bridges and for four different vehicle types were statistically processed using the nonlinear regression analysis feature of the SAS Package (SAS Institute 1989) to develop the proposed load distribution formulas. SAS is one of the most comprehensive statistical analysis program packages for data manipulation, management, analysis, and presentation developed by the SAS Institute.

4.3.2 Summary of the New Formulas

In this study, the load distribution factor formulas were developed for the following groups of the military vehicles:

(1) HETS Vehicle

(2) PLS and HEMMT Vehicles

(3) ABRAMS vehicle
(4) M113 and Bradley Vehicles
(5) All Military Vehicles

The parameters considered in the new formulas are the following:

- ***S*** : Spacing between girders (ft)
- ***L*** : Span length (ft)
- ***t*** : Slab thickness (in)
- ***I*** : Moment of inertia of the girder (in^4)
- ***n*** : Modular ratio of the girder elastic modulus to that of the slab

The formulas were developed for three types of bridges (steel girder, reinforced concrete T-beam, and pre-stressed concrete beam bridges) separately as well as for all types of bridges considered as a group. For the first four sets of vehicles, the formulas were developed only for the bending moment in the interior girders of a bridge. For this set, there are 20 different formulas. These formulas are listed in Tables 4.2 through 4.5. The last columns in these tables also provide the range of applicability of these formulas. These values represent the range of the parameter values in the population of the three different of bridge types considered in this study.

For the case of all military vehicles considered as a group, the formulas were developed separately for the following scenarios:

- Bending Moment and Shear Force Values
- Single lane and Multi-lane Loading Scenarios
- Interior and Exterior Girders

Table 4.2: Bending Moment Load Distribution Factor Formulas for Interior Girders

PLS and HEMMT Vehicles

Bridge Type	Single Lane Loading	Multi Lane Loading	Range of Applicability
All Beam Bridges	$-0.1+\left(\frac{S}{11.27}\right)^{0.25}\left(\frac{S}{L}\right)^{0.15}\left(\frac{nI}{12Lt^3}\right)^{0.06}$	$0.086+\left(\frac{S}{7.24}\right)^{0.57}\left(\frac{S}{L}\right)^{0.24}\left(\frac{nI}{12Lt^3}\right)^{0.074}$	2.17' ≤ S ≤ 12' 12' ≤ L ≤ 205' 4.42" ≤ t ≤ 12" 234 in^4 ≤ I ≤ 733,320 in^4
Steel	$0.22+\left(\frac{S}{7.96}\right)^{0.23}\left(\frac{S}{L}\right)^{0.17}\left(\frac{nI}{12Lt^3}\right)^{0.16}$	$0.16+\left(\frac{S}{13.45}\right)^{0.59}\left(\frac{S}{L}\right)^{0.17}\left(\frac{nI}{12Lt^3}\right)^{0.08}$	2.17' ≤ S ≤ 12' 20' ≤ L ≤ 205' 4.42" ≤ t ≤ 12" 234 in^4 ≤ I ≤ 287,125 in^4
Pre-stress	$-0.53+\left(\frac{S}{1.25}\right)^{0.19}\left(\frac{S}{L}\right)^{0.1}\left(\frac{nI}{12Lt^3}\right)^{0.05}$	$-0.17+\left(\frac{S}{4.4}\right)^{0.45}\left(\frac{S}{L}\right)^{0.16}\left(\frac{nI}{12Lt^3}\right)^{0.053}$	3.21'≤S≤ 10.5' 18.75' ≤ L ≤ 136' 5" ≤ t ≤ 9" 9,599 in^4 ≤ I ≤ 733,320 in^4
T-Beam	$0.11+\left(\frac{S}{9.3}\right)^{0.73}\left(\frac{S}{L}\right)^{0.3}\left(\frac{nI}{12Lt^3}\right)^{0.045}$	$0.36+\left(\frac{S}{8.37}\right)^{1.54}\left(\frac{S}{L}\right)^{0.48}\left(\frac{nI}{12Lt^3}\right)^{0.16}$	4.75' ≤ S ≤ 9.33' 12' ≤ L ≤ 78' 5" ≤ t ≤ 9" 3,267 in^4 ≤ I ≤ 567,348 in^4

Table 4.3: Bending Moment Load Distribution Factor Formulas for Interior Girders

HETS Vehicle

Bridge Type	Single Lane Loading	Range of Applicability
All Beam Bridges	$0.14+\left(\frac{S}{9.06}\right)^{0.63}\left(\frac{S}{L}\right)^{0.35}\left(\frac{nI}{12Lt^3}\right)^{0.15}$	2.17' ≤ S ≤ 12' 12' ≤ L ≤ 205' 4.42" ≤ t ≤ 12" 234 in^4 ≤ I ≤ 733,320 in^4
Steel	$0.27+\left(\frac{S}{16}\right)^{0.93}\left(\frac{S}{L}\right)^{0.44}\left(\frac{nI}{12Lt^3}\right)^{0.24}$	2.17' ≤ S ≤ 12' 20' ≤ L ≤ 205' 4.42" ≤ t ≤ 12" 234 in^4 ≤ I ≤ 287,125 in^4
Prestressed	$-1.16+1.65(S)^{0.11}\left(\frac{S}{L}\right)^{0.082}\left(\frac{nI}{12Lt^3}\right)^{0.018}$	3.21' ≤ S ≤ 10.5' 18.75' ≤ L ≤ 136' 5" ≤ t ≤ 9" 9,599 in^4 ≤ I ≤ 733,320 in^4
T-Beam	$0.36+\left(\frac{S}{3.82}\right)^{1.5}\left(\frac{S}{L}\right)^{1.6}\left(\frac{nI}{12Lt^3}\right)^{0.5}$	4.75' ≤ S ≤ 9.33' 12' ≤ L ≤ 78' 5" ≤ t ≤ 9" 3,267 in^4 ≤ I ≤ 567,348 in^4

Table 4.4: Bending Moment Load Distribution Factor Formulas for Interior Girders

ABRAMS Vehicle

Bridge Type	Single Lane Loading	Range of Applicability
All Beam Bridges	$0.24+\left(\frac{S}{12.56}\right)^{1.58}\left(\frac{S}{L}\right)^{0.28}\left(\frac{nI}{12Lt^3}\right)^{0.15}$	2.17' ≤ S ≤ 12' 12' ≤ L ≤ 205' 4.42" ≤ t ≤ 12" 234 in^4 ≤ I ≤ 733,320 in^4
Steel	$0.095+\left(\frac{S}{69.36}\right)^{0.46}\left(\frac{S}{L}\right)^{0.05}\left(\frac{nI}{12Lt^3}\right)^{0.05}$	2.17' ≤ S ≤ 12' 20' ≤ L ≤ 205' 4.42" ≤ t ≤ 12" 234 in^4 ≤ I ≤ 287,125 in^4
Prestressed	$-0.51+\left(\frac{S}{5.77}\right)^{0.3}\left(\frac{S}{L}\right)^{0.034}\left(\frac{nI}{12Lt^3}\right)^{0.02}$	3.21' ≤ S ≤ 10.5' 18.75' ≤ L ≤ 136' 5" ≤ t ≤ 9" 9,599 in^4 ≤ I ≤ 733,320 in^4
T-Beam	$0.35+\left(\frac{S}{8.81}\right)^{2.47}\left(\frac{S}{L}\right)^{1.02}\left(\frac{nI}{12Lt^3}\right)^{0.28}$	4.75' ≤ S ≤ 9.33' 12' ≤ L ≤ 78' 5" ≤ t ≤ 9" 3,267 in^4 ≤ I ≤ 567,348 in^4

Table 4.5: Bending Moment Load Distribution Factor Formulas for Interior Girders M113 and BRADLEY Vehicles

Bridge Type	Single Lane Loading	Range of Applicability
All Beam Bridges	$0.24+\left(\frac{S}{11.89}\right)^{1.35}\left(\frac{S}{L}\right)^{0.29}\left(\frac{nI}{12Lt^3}\right)^{0.14}$	2.17' ≤ S ≤ 12' 12' ≤ L ≤ 205' 4.42" ≤ t ≤ 12" 234 in^4 ≤ I ≤ 733,320 in^4
Steel	$0.27+\left(\frac{S}{22.8}\right)^{0.86}\left(\frac{S}{L}\right)^{0.3}\left(\frac{nI}{12Lt^3}\right)^{0.23}$	2.17' ≤ S ≤ 12' 20' ≤ L ≤ 205' 4.42" ≤ t ≤ 12" 234 in^4 ≤ I ≤ 287,125 in^4
Prestressed	$-1.52+1.74(S)^{0.13}\left(\frac{S}{L}\right)^{0.038}\left(\frac{nI}{12Lt^3}\right)^{0.019}$	3.21' ≤ S ≤ 10.5' 18.75' ≤ L ≤ 136' 5" ≤ t ≤ 9" 9,599 in^4 ≤ I ≤ 733,320 in^4
T-Beam	$0.34+\left(\frac{S}{8.03}\right)^{1.95}\left(\frac{S}{L}\right)^{0.8}\left(\frac{nI}{12Lt^3}\right)^{0.33}$	4.75' ≤ S ≤ 9.33' 12' ≤ L ≤ 78' 5" ≤ t ≤ 9" 3,267 in^4 ≤ I ≤ 567,348 in^4

There are 32 different formulas for the previous case (military vehicles considered as a group). These formulas are listed in Tables 4.6 through 4.9. Tables 4.8 and 4.9 provide the formulas for bending moment and shear force, respectively, in the external girders. These tables are divided in the following two parts:

- **Part (a).** The actual expressions of the formulas are presented in this part of the tables.
- **Part (b).** Gives the amplification factor that must be applied to the values calculated from the formulas on Part (a) of the tables.

The amplification factors applied depend on the size of the overhang on the outside of a girder. In this study, four different overhang values were considered. In addition, as shown in Part (b) of the tables, amplification factor values are provided for single lane loading and multi lane loading scenarios.

The following steps need to be followed in order to assure the proper estimate of the distribution factors for the exterior girders.

1) Select the amplification factor that applied to the bridge in consideration.
2) Multiply the distribution factor by the amplification factor for the exterior girders of the bridge.
3) If the amplified distribution factor for the exterior girders is less than the value for an interior girder, then the distribution factor value for the interior girders should be used to compute the design bending moment and shear force values.

It is reiterated here that these formulas should be used with the entire wheel load.

Table 4.6: Bending Moment Load Distribution Factor Formulas for Interior Girders

All Military Vehicles

Bridge Type	Single Lane Loading	Multi Lane Loading	Range of Applicability
All Beam Bridge	$0.21+\left(\frac{S}{12.24}\right)^{0.73}\left(\frac{S}{L}\right)^{0.37}\left(\frac{nI}{12Lt^3}\right)^{0.18}$	$-0.014+\left(\frac{S}{6.91}\right)^{0.54}\left(\frac{S}{L}\right)^{0.19}\left(\frac{nI}{12Lt^3}\right)^{0.066}$	2.17' ≤ S ≤ 12' 12' ≤ L ≤ 205' 4.42" ≤ t ≤ 12" 234 in^4 ≤ I ≤ 733,320 in^4
Steel	$0.3+\left(\frac{S}{18.2}\right)\left(\frac{S}{L}\right)^{0.41}\left(\frac{nI}{12Lt^3}\right)^{0.28}$	$0.05+\left(\frac{S}{11}\right)^{0.56}\left(\frac{S}{L}\right)^{0.14}\left(\frac{nI}{12Lt^3}\right)^{0.068}$	2.17' ≤ S ≤ 12' 20' ≤ L ≤ 205' 4.42" ≤ t ≤ 12" 234 in^4 ≤ I ≤ 287,125 in^4
Pre-stress	$-0.92+1.23(S)^{0.16}\left(\frac{S}{L}\right)^{0.063}\left(\frac{nI}{12Lt^3}\right)^{0.03}$	$-0.12+\left(\frac{S}{6.12}\right)^{0.53}\left(\frac{S}{L}\right)^{0.14}\left(\frac{nI}{12Lt^3}\right)^{0.053}$	3.21'≤S≤ 10.5' 18.75' ≤ L ≤ 136' 5" ≤ t ≤ 9" 9,599 in^4 ≤ I ≤ 733,320 in^4
T-Beam	$0.36+\left(\frac{S}{4.57}\right)^{1.63}\left(\frac{S}{L}\right)^{1.55}\left(\frac{nI}{12Lt^3}\right)^{0.44}$	$0.31+\left(\frac{S}{9.03}\right)^{1.33}\left(\frac{S}{L}\right)^{0.38}\left(\frac{nI}{12Lt^3}\right)^{0.12}$	4.75' ≤ S ≤ 9.33' 12' ≤ L ≤ 78' 5" ≤ t ≤ 9" 3,267 in^4 ≤ I ≤ 567,348 in^4

Table 4.7: Shear Load Distribution Factor Formulas for Interior Girders

All Military Vehicles

Bridge Type	Single Lane Loading	Multi Lane Loading	Range of Applicability
All Beam Bridge	$-0.12+\left(\frac{S}{9.94}\right)^{0.18}\left(\frac{S}{L}\right)^{0.12}\left(\frac{nI}{12Lt^3}\right)^{0.06}$	$0.16+\left(\frac{S}{10.17}\right)^{0.61}\left(\frac{S}{L}\right)^{0.24}\left(\frac{nI}{12Lt^3}\right)^{0.073}$	2.17' ≤ S ≤ 12' 12' ≤ L ≤ 205' 4.42" ≤ t ≤ 12" 234 in^4 ≤ I ≤ 733,320 in^4
Steel	$0.22+\left(\frac{S}{118.7}\right)^{0.23}\left(\frac{S}{L}\right)^{0.35}\left(\frac{nI}{12Lt^3}\right)^{0.14}$	$0.14+\left(\frac{S}{18.78}\right)^{0.5}\left(\frac{S}{L}\right)^{0.15}\left(\frac{nI}{12Lt^3}\right)^{0.057}$	2.17' ≤ S ≤ 12' 20' ≤ L ≤ 205' 4.42" ≤ t ≤ 12" 234 in^4 ≤ I ≤ 287,125 in^4
Pre-stress	$-0.8+1.2(S)^{0.16}\left(\frac{S}{L}\right)^{0.08}\left(\frac{nI}{12Lt^3}\right)^{0.034}$	$-0.75+\left(\frac{S}{1.41}\right)^{0.25}\left(\frac{S}{L}\right)^{0.034}\left(\frac{nI}{12Lt^3}\right)^{0.012}$	3.21'≤S≤ 10.5' 18.75' ≤ L ≤ 136' 5" ≤ t ≤ 9" 9,599 in^4 ≤ I ≤ 733,320 in^4
T-Beam	$0.32+\left(\frac{S}{11.79}\right)\left(\frac{S}{L}\right)^{0.95}\left(\frac{nI}{12Lt^3}\right)^{0.35}$	$0.08+\left(\frac{S}{7.56}\right)^{0.56}\left(\frac{S}{L}\right)^{0.25}\left(\frac{nI}{12Lt^3}\right)^{0.079}$	4.75' ≤ S ≤ 9.33' 12' ≤ L ≤ 78' 5" ≤ t ≤ 9" 3,267 in^4 ≤ I ≤ 567,348 in^4

Table 4.8(a): Bending Moment Load Distribution Factor Formulas for Exterior Girders

All Military Vehicles

Bridge Type	Single Lane Loading	Multi Lane Loading	Range of Applicability
All Beam Bridge	$-0.51+\left(\frac{S}{6.1}\right)^{0.22}\left(\frac{S}{L}\right)^{0.004}\left(\frac{nI}{12Lt^3}\right)^{0.005}$	$0.22+\left(\frac{S}{25.43}\right)^{1.16}\left(\frac{S}{L}\right)^{-0.14}\left(\frac{nI}{12Lt^3}\right)^{-0.07}$	2.17' ≤ S ≤ 12' 12' ≤ L ≤ 205' 4.42" ≤ t ≤ 12" 234 in^4 ≤ I ≤ 733,320 in^4
Steel	$-0.11+\left(\frac{S}{19.6}\right)^{0.43}\left(\frac{S}{L}\right)^{0.01}\left(\frac{nI}{12Lt^3}\right)^{0.005}$	$-0.03+\left(\frac{S}{16.84}\right)^{0.7}\left(\frac{S}{L}\right)^{-0.047}\left(\frac{nI}{12Lt^3}\right)^{-0.034}$	2.17' ≤ S ≤ 12' 20' ≤ L ≤ 205' 4.42" ≤ t ≤ 12" 234 in^4 ≤ I ≤ 287,125 in^4
Pre-stress	$-0.03+\left(\frac{S}{36}\right)^{0.41}\left(\frac{S}{L}\right)^{-0.02}\left(\frac{nI}{12Lt^3}\right)^{-0.002}$	$0.25+\left(\frac{S}{27.53}\right)^{1.15}\left(\frac{S}{L}\right)^{-0.097}\left(\frac{nI}{12Lt^3}\right)^{-0.031}$	3.21'≤S≤ 10.5' 18.75' ≤ L ≤ 136' 5" ≤ t ≤ 9" 9,599 in^4 ≤ I ≤ 733,320 in^4
T-Beam	$0.23+\left(\frac{S}{42.83}\right)^{0.64}\left(\frac{S}{L}\right)^{0.06}\left(\frac{nI}{12Lt^3}\right)^{-0.005}$	$0.3+\left(\frac{S}{25.41}\right)^{1.24}\left(\frac{S}{L}\right)^{-0.16}\left(\frac{nI}{12Lt^3}\right)^{-0.07}$	4.75' ≤ S ≤ 9.33' 12' ≤ L ≤ 78' 5" ≤ t ≤ 9" 3,267 in^4 ≤ I ≤ 567,348 in^4

Table 4.8(b): Exterior Girders Amplification Factors to be applied to the formulas in Table 4.8(a) for different overhang values

Loading Scenario	Overhang (ft)			
	1'	2'	3'	4'
Single Lane	1	1.12	1.24	1.36
Multi Lane	1	1	1.1	1.2

Table 4.9(a): Shear Distribution Factor Formulas for Exterior Girders

All Military Vehicles

Bridge Type	Single Lane Loading	Multi Lane Loading	Range of Applicability
All Beam Bridge	$-0.74+1.065(S)^{0.12}\left(\frac{S}{L}\right)^{0.03}\left(\frac{nI}{12Lt^3}\right)^{0.01}$	$0.1+\left(\frac{S}{33.08}\right)^{0.89}\left(\frac{S}{L}\right)^{-0.23}\left(\frac{nI}{12Lt^3}\right)^{-0.056}$	2.17' ≤ S ≤ 12' 12' ≤ L ≤ 205' 4.42" ≤ t ≤ 12" 234 in^4 ≤ I ≤ 733,320 in^4
Steel	$-1.18+1.7(S)^{0.07}\left(\frac{S}{L}\right)^{0.048}\left(\frac{nI}{12Lt^3}\right)^{0.017}$	$-0.5+\left(\frac{S}{9.06}\right)^{0.39}\left(\frac{S}{L}\right)^{-0.079}\left(\frac{nI}{12Lt^3}\right)^{-0.01}$	2.17' ≤ S ≤ 12' 20' ≤ L ≤ 205' 4.42" ≤ t ≤ 12" 234 in^4 ≤ I ≤ 287,125 in^4
Pre-stress	$-0.22+\left(\frac{S}{25.17}\right)^{0.28}\left(\frac{S}{L}\right)^{-0.01}\left(\frac{nI}{12Lt^3}\right)^{-0.01}$	$0.26+\left(\frac{S}{40}\right)^{1.33}\left(\frac{S}{L}\right)^{-0.42}\left(\frac{nI}{12Lt^3}\right)^{-0.06}$	3.21'≤S≤ 10.5' 18.75' ≤ L ≤ 136' 5" ≤ t ≤ 9" 9,599 in^4 ≤ I ≤ 733,320 in^4
T-Beam	$-0.71+\left(\frac{S}{1.81}\right)^{0.15}\left(\frac{S}{L}\right)^{0.01}\left(\frac{nI}{12Lt^3}\right)^{0.006}$	$0.16+\left(\frac{S}{25.74}\right)^{0.85}\left(\frac{S}{L}\right)^{-0.12}\left(\frac{nI}{12Lt^3}\right)^{-0.05}$	4.75' ≤ S ≤ 9.33' 12' ≤ L ≤ 78' 5" ≤ t ≤ 9" 3,267 in^4 ≤ I ≤ 567,348 in^4

Table 4.9(b): Exterior Girders Amplification Factors to be applied to the formulas in Table 4.9(a) for different overhang values

Loading Scenario	Overhang (ft)			
	1'	2'	3'	4'
Single Lane	1	1.12	1.24	1.36
Multi Lane	1.1	1.2	1.3	1.4

4.4 COMPARISON OF LOAD DISTRIBUTION FACTORS FORMULAS

4.4.1 New Formulas versus Direct Bridge Analysis

To test the accuracy of the goodness-of-fit of these formulas with respect to the calculated distribution factor values, Figures B.1 through B.52 (Appendix B) were created. Here each figure pertains to a formula in Table 4.2 through 4.9. The following table lists the figures numbers that are associated with different tables numbers. For each set of figures, the table also identifies the type of vehicle (e.g., PLS and HEMMT, HETS, ABRAMS, M113 and Bradley, and All vehicles), load effect (e.g., bending moment or shear force), and beam location (i.e., interior or exterior) the figure set pertains to.

Table 4.10: Relationship between Figures B.1 through B.52 and Tables 4.2 through 4.9

Table No.	Figure No.	Vehicle Type	Load Effect	Beam Location
4.2	B.1 through B.8	PLS & HEMMT	Moment	Interior
4.3	B.9 through B.12	HETS	Moment	Interior
4.4	B.13 through B.16	ABRAMS	Moment	Interior
4.5	B.17 through B.20	M113 & Bradley	Moment	Interior
4.6	B.21 through B.28	All Vehicles	Moment	Interior
4.7	B.29 through B.36	All Vehicles	Shear	Interior
4.8	B.37 through B.44	All Vehicles	Moment	Exterior
4.9	B.45 through B.52	All Vehicles	Shear	Exterior

On each figure presented in Appendix B, two plots (Part a and b) have been included for comparison purpose. Each part is discussed below.

Part (a). Plots the value of distribution factor calculated by the formula against the value obtained by an actual bridge analysis. Each point in the plot represents a bridge in the data set. A perfect straight line with a slope of one will imply a perfect fit. It is seen that some formulas predict a better fit with a smaller scatter

from the 45-degrees straight line than other. The formulas representing a diverse group of vehicles and/or several types of bridges collectively usually have a larger scatter.

Part (b). Plots the histograms for the variable of the ratio of the distribution factor calculated by the formula to the one calculated by actual analysis of the bridge. Also, the mean and coefficient of variation values of this ratio have been included in the plots.

A narrow histogram with the mean value close to 1.0 and a low coefficient of variation value indicates a good fit between the analysis and the proposed formula. Such a good fit is usually seen for the cases of a type of vehicle on a particular type of bridge. For example for the HETS vehicle, the mean and coefficient of variation values, respectively, are 1.002 and 4.7% for steel bridges (Figure B.10), 1.023 and 10.5% for pre-stressed concrete bridges (Figure B.11), and 1.008 and 6.3% for the concrete T-beam bridges (Figure B.12). If the results of all bridge types are lumped together, then for HETS vehicle the mean and coefficient of variation values are 1.018 and 12% (Figure B.9). Concrete T-beam bridges usually have higher variations as indicated by the coefficient of variation values. The coefficient of variation of the bending moment distribution factor ratio for the T-beam concrete bridge is usually higher than for the other types of bridges. Including more types of bridges with different types of vehicles would likely increase the coefficient of variation.

In general, the coefficients of variation of the shear force distribution factors tend to be higher than that of the bending moment. A relatively large coefficient of variation value implies that the use of the proposed distribution formula might provides values that could be different from the one calculated by a detailed bridge analysis.

4.4.2 New Formulas versus Pre-LRFD and Post-LRFD Formulas

It is of interest to compare the values of the distribution factors calculated by the new proposed formulas developed for the military vehicles with the values calculated according to the pre-and post-LRFD AASHTO specifications for the civilian vehicles. The distribution factor formulas given in the 1994 and earlier versions of the AASHTO Standard specifications are considered as the pre-LRFD distribution factors. The factors defined in the 1996 AASHTO Standard Specification are considered as the post-LRFD distribution factors. For the bending moment in an interior girder for the single loading case, these formulas are given in Table 4.11. No comparison is made for the exterior girders, or multi-lane loading case or the shear force distribution factors

Table 4.11: Bending Moment Load Distribution Factor Formulas for Interior Girders Single Lane Loading Scenario

Bridge Type	Non-LRFD Formulas	LRFD Formulas
Steel	$\frac{S}{7}$	$0.06+\left(\frac{S}{14}\right)^{0.4}\left(\frac{S}{L}\right)^{0.3}\left(\frac{Kg}{12.0Lt^3}\right)^{0.1}$
Prestressed	$\frac{S}{7}$	$0.06+\left(\frac{S}{14}\right)^{0.4}\left(\frac{S}{L}\right)^{0.3}\left(\frac{Kg}{12.0Lt^3}\right)^{0.1}$
T-Beam	$\frac{S}{6.5}$	$0.06+\left(\frac{S}{14}\right)^{0.4}\left(\frac{S}{L}\right)^{0.3}\left(\frac{Kg}{12.0Lt^3}\right)^{0.1}$

The comparison of the load factors is made both quantitatively in the tabular form and qualitatively in the graphical form. Tables 4.12 through 4.16 show the mean and coefficient of variation values of the distribution factor calculated by harmonic analysis (most exact), the proposed new formulas for military vehicles, LRFD formulas in AASHTO 1996, and the pre-LRFD formulas in 1994 and earlier versions of AASHTO specifications.

Each table is for a particular type of vehicle and presents values for each of the types of bridges considered as well as the general case which includes all the beam and slab bridges together. Only the single lane loading case was considered.

Table 4.12: Mean and Coefficient of Variation Values for Bending Moment Load Distribution Factor obtained with Harmonic Analysis, LRFD, Non-LRFD, and New Formulas for Interior Girders for PLS and HEMMT Vehicles

Bridge Type	Coefficient	Single Lane Loading			
		Harmonic Analysis	New Formulas	LRFD Formulas	Non-LRFD Formulas
All Beam	Mean	0.465	0.477	0.393	0.498
	C.O.V.	0.243	0.160	0.201	0.277
Steel Girder	Mean	0.400	0.396	0.364	0.464
	C.O.V.	0.135	0.077	0.186	0.265
Pre-stressed	Mean	0.495	0.500	0.393	0.478
	C.O.V.	0.220	0.182	0.178	0.274
T-Beam	Mean	0.557	0.555	0.442	0.548
	C.O.V.	0.259	0.199	0.172	0.221

Table 4.13: Mean and Coefficient of Variation Values for Bending Moment Load Distribution Factor obtained with Harmonic Analysis, LRFD, Non-LRFD, and New Formulas for Interior Girders for HETS Vehicle

Bridge Type	Coefficient	Single Lane Loading			
		Harmonic Analysis	New Formulas	LRFD Formulas	Non-LRFD Formulas
All Beam	Mean	0.439	0.436	0.377	0.463
	C.O.V.	0.245	0.217	0.199	0.266
Steel Girder	Mean	0.382	0.382	0.366	0.467
	C.O.V.	0.154	0.144	0.190	0.270
Pre-stressed	Mean	0.474	0.480	0.393	0.474
	C.O.V.	0.229	0.194	0.177	0.270
T-Beam	Mean	0.472	0.475	0.467	0.571
	C.O.V.	0.194	0.103	0.147	0.179

Table 4.14: Mean and Coefficient of Variation Values for Bending Moment Load Distribution Factor obtained with Harmonic Analysis, LRFD, Non-LRFD, and New Formulas for Interior Girders for ABRAMS Vehicle

Bridge Type	Coefficient	Single Lane Loading			
		Harmonic Analysis	New Formulas	LRFD Formulas	Non-LRFD Formulas
All Beam	Mean	0.398	0.399	0.377	0.463
	C.O.V.	0.221	0.204	0.199	0.266
Steel Girder	Mean	0.369	0.370	0.361	0.459
	C.O.V.	0.120	0.109	0.174	0.263
Pre-stressed	Mean	0.425	0.429	0.397	0.477
	C.O.V.	0.233	0.210	0.196	0.276
T-Beam	Mean	0.440	0.444	0.467	0.571
	C.O.V.	0.161	0.142	0.147	0.179

Table 4.15: Mean and Coefficient of Variation Values for Bending Moment Load Distribution Factor obtained with Harmonic Analysis, LRFD, Non-LRFD, and New Formulas for Interior Girders for M113 & Bradley Vehicles

Bridge Type	Coefficient	Single Lane Loading			
		Harmonic Analysis	New Formulas	LRFD Formulas	Non-LRFD Formulas
All Beam	Mean	0.434	0.434	0.378	0.462
	C.O.V.	0.236	0.207	0.205	0.266
Steel Girder	Mean	0.394	0.393	0.364	0.463
	C.O.V.	0.143	0.143	0.185	0.272
Pre-stressed	Mean	0.467	0.466	0.396	0.476
	C.O.V.	0.238	0.213	0.183	0.277
T-Beam	Mean	0.476	0.509	0.474	0.566
	C.O.V.	0.180	0.151	0.165	0.178

Table 4.16: Mean and Coefficient of Variation Values for Bending Moment Load Distribution Factor obtained with Harmonic Analysis, LRFD, Non-LRFD, and New Formulas for Interior Girders for All Vehicles

Bridge Type	Coefficient	Single Lane Loading			
		Harmonic Analysis	New Formulas	LRFD Formulas	Non-LRFD Formulas
All Beam	Mean	0.437	0.436	0.383	0.476
	C.O.V.	0.226	0.184	0.182	0.256
Steel Girder	Mean	0.390	0.395	0.364	0.463
	C.O.V.	0.142	0.120	0.184	0.267
Pre-stressed	Mean	0.470	0.466	0.483	0.478
	C.O.V.	0.235	0.200	0.188	0.276
T-Beam	Mean	0.483	0.482	0.576	0.569
	C.O.V.	0.314	0.230	0.400	0.365

Graphically the mean values for the bending moment in these tables are compared in Figures 4.13 through 4.17. Each figure corresponds to a table. That is, Figure 4.13 depicts the mean values in Table 4.12, Figure 4.14 depicts the values in Table 4.13, and so on. These figures indicate that mean values calculated by the harmonic analysis and the proposed formulas are quite close to each other.

When compared with the more accurate harmonic analysis, usually the pre-LRFD formulas tend to over estimate and the post-LRFD formulas usually tend to underestimate the values of the distribution factors.

Comparison with Ratio of the Distribution Factors

Another approach to compare various distribution factor formulas is to obtain the ratio of the distribution factors calculated by the formulas to factor calculated by the direct analysis. This was done earlier in the previous section when the distribution factors calculated by the proposed formulas were evaluated vis-à-vis the values calculated by direct analysis. Tables 4.17 through 4.21 show the mean and coefficient of variation values of the distribution factor ratio calculated by the proposed, post LRFD, and pre-LRFD formulas. The denominator of these ratios is the distribution factor calculated by the harmonic analysis.

A mean value close to 1.0 with a small coefficient of variation implies that the values calculated by the formula are close to the values calculated by the analysis. The frequency distribution of these ratios is shown by the histograms shown in Figures C.1 through C.20 (Appendix C). The figure numbers associated with each table are presented in Table 4.22.

Table 4.17: Mean and Coefficient of Variation Values for Bending Moment Load Distribution Factor Ratios obtained with LRFD, Non-LRFD, and New Formulas for Interior Girders for PLS and HEMMT Vehicles

Bridge Type	Coefficient	Single Lane Loading		
		New/Harmonic	LRFD/Harmonic	Non-LRFD/Harmonic
All Beam	Mean	1.05	0.861	1.083
	C.O.V.	0.159	0.175	0.249
Steel Girder	Mean	0.999	0.911	1.157
	C.O.V.	0.078	0.147	0.226
Pre-stressed	Mean	1.023	0.806	0.964
	C.O.V.	0.115	0.118	0.184
T-Beam	Mean	1.021	0.817	1.006
	C.O.V.	0.170	0.170	0.186

Table 4.18: Mean and Coefficient of Variation Values for Bending Moment Load Distribution Factor Ratios obtained with LRFD, Non-LRFD, and New Formulas for Interior Girders for HETS Vehicle

Bridge Type	Coefficient	Single Lane Loading		
		New/Harmonic	LRFD/Harmonic	Non-LRFD/Harmonic
All Beam	Mean	1.004	0.872	1.062
	C.O.V.	0.107	0.107	0.172
Steel Girder	Mean	1.002	0.954	1.207
	C.O.V.	0.047	0.088	0.174
Pre-stressed	Mean	1.023	0.843	1.001
	C.O.V.	0.105	0.110	0.167
T-Beam	Mean	1.008	0.998	1.225
	C.O.V.	0.063	0.068	0.159

Table 4.19: Mean and Coefficient of Variation Values for Bending Moment Load Distribution Factor Ratios obtained with LRFD, Non-LRFD, and New Formulas for Interior Girders for ABRAMS Vehicle

Bridge Type	Coefficient	Single Lane Loading		
		New/Harmonic	LRFD/Harmonic	Non-LRFD/Harmonic
All Beam	Mean	1.007	0.954	1.155
	C.O.V.	0.069	0.094	0.124
Steel Girder	Mean	1.003	0.975	1.226
	C.O.V.	0.042	0.105	0.172
Pre-stressed	Mean	1.019	0.951	1.117
	C.O.V.	0.091	0.134	0.123
T-Beam	Mean	1.015	1.066	1.304
	C.O.V.	0.074	0.073	0.131

Table 4.20: Mean and Coefficient of Variation Values for Bending Moment Load Distribution Factor Ratios obtained with LRFD, Non-LRFD, and New Formulas for Interior Girders for M113 and Bradley Vehicles

Bridge Type	Coefficient	Single Lane Loading		
		New/Harmonic	LRFD/Harmonic	Non-LRFD/Harmonic
All Beam	Mean	1.010	0.881	1.064
	C.O.V.	0.098	0.114	0.148
Steel Girder	Mean	1.001	0.921	1.162
	C.O.V.	0.059	0.106	0.185
Pre-stressed	Mean	1.008	0.864	1.018
	C.O.V.	0.102	0.115	0.143
T-Beam	Mean	1.073	1.004	1.201
	C.O.V.	0.119	0.112	0.148

Table 4.21: Mean and Coefficient of Variation Values for Bending Moment Load Distribution Factor Ratios obtained with LRFD, Non-LRFD, and New Formulas for Interior Girders for All Vehicles

Bridge Type	Coefficient	Single Lane Loading		
		New/Harmonic	LRFD/Harmonic	Non-LRFD/Harmonic
All Beam	Mean	1.015	0.889	1.105
	C.O.V.	0.119	0.132	0.193
Steel Girder	Mean	1.018	0.931	1.177
	C.O.V.	0.066	0.112	0.192
Pre-stressed	Mean	1.006	1.047	1.018
	C.O.V.	0.120	0.126	0.166
T-Beam	Mean	0.997	1.206	1.199
	C.O.V.	0.111	0.094	0.170

Table 4.22: Relationship between Figures C.1 through C.20 and Tables 4.17 through 4.21

Table No.	Figure No.	Vehicle Type
4.17	C.1 through C.4	PLS & HEMMT
4.18	C.5 through C.8	HETS
4.19	C.9 through C.12	ABRAMS
4.20	C.13 through C.16	M113 & Bradley
4.21	C.17 through C.20	All Vehicles

Each figure presents three histograms. The top histograms in these figures are the same as those discussed in the previous section. They show the comparison of the distribution factor values calculated by the proposed formulas with those calculated by the analysis. The middle histograms shows the comparison of the post-LRFD values with the analytical values, and the bottom histograms shows this comparison of pre-LRFD values with the analytical values. The mean and coefficient values given in the tables are also shown on each figure. Also shown

on each histogram is a coefficient, which is similar to the skewness coefficient but here it is defined with respect to the ratio of 1.0 (and not the mean value) as follows:

$$k = \frac{\sum_{i=1}^{n} (x_i - 1)^3}{n\sigma^3} \tag{4.1}$$

where k is the skewness coefficient, x_i is the ith distribution factor ratio value, n is the number of bridges analyzed, and σ is the standard deviation of the distribution factor ratio. A positive value of this coefficient means that the frequency distribution of the ratio is skewed to the right, with more values being higher than 1.0. Similarly, a negative value means that the frequency distribution is skewed to the left, with more values being less than 1.0.

As indicated before, on an average the post LRFD formulas tend to underestimate and the pre-LRFD formulas tend to overestimate the distribution factor values for the military vehicles. Also, the simple pre- LRFD formulas show a larger dispersion in the ratio; it implies that there is a larger uncertainty associated with the values calculated by these formulas. Compared to the pre- and post LRFD formulas, the proposed formulas provide the distribution factor values closest to the analytically calculated values with least dispersion and relatively smaller underestimation of the factor values.

4.5 CONCLUSIONS

A total of 52 new formulas for the load distribution factors for different types of vehicles, different types of bridges, bending moment and shear force values, interior and exterior girders, and for single and multiple lane loading cases have been created.

In the sensitivity study performed to the distribution factors with respect to the bridge parameters that affect them, it was observed that the girder spacing was the most important parameter and the bridge span the second most important parameter. On the other hand, in the comparisons made between the values calculated by the new formulas, post-LRFD formulas prescribed in 1996 AASHTO Standard Specification, and simple pre-LRFD formulas that were prescribed by AASHTO before 1994, it was noted that the post-LRFD formulas usually tend to underestimate the values of the distribution factors under the military vehicles loading and the pre-LRFD formulas usually tend to overestimate them. In general, the proposed formulas provided values for the distribution factors closest to the analytical calculated values with relatively less dispersion in comparison with the results obtained with the pre-LRFD and post-LRFD formulas.

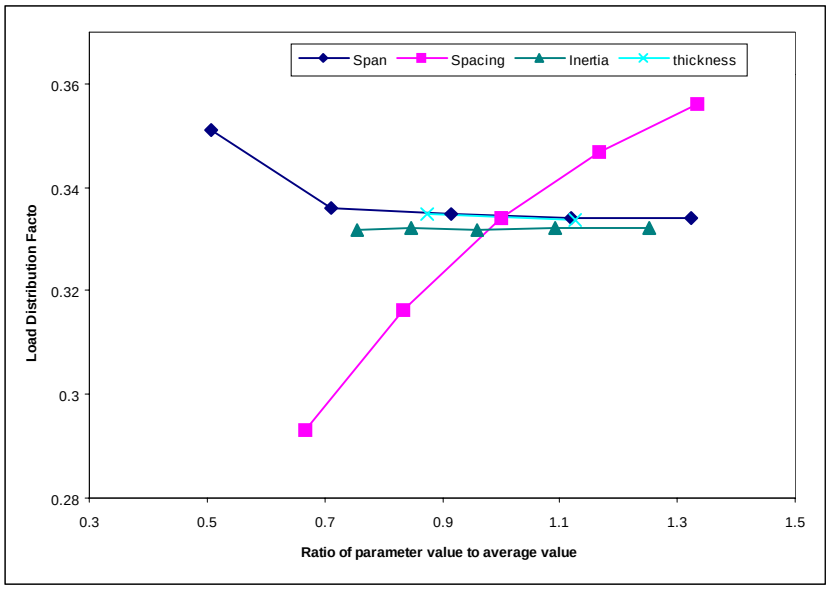

Figure 4.1: Sensitivity of Bending Moment Distribution Factors

Steel Girder Bridges

Single Lane Loading Scenario

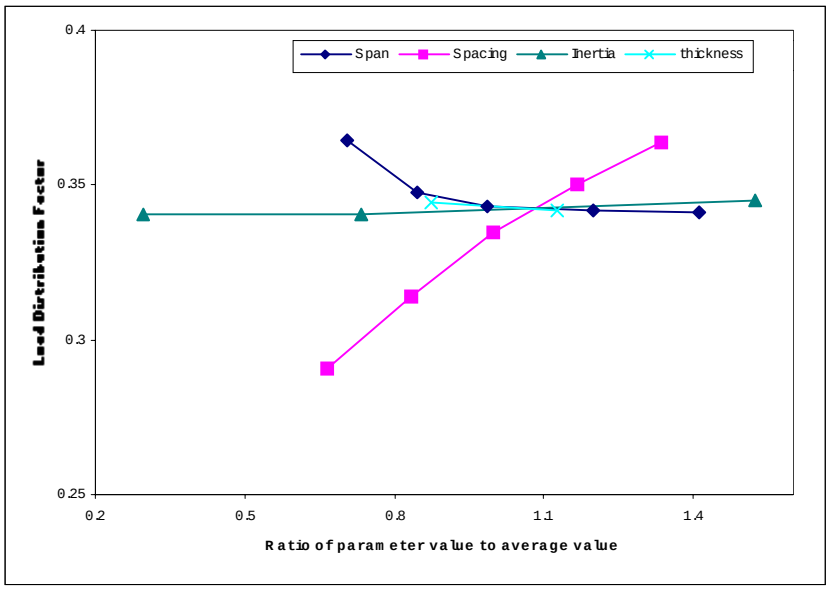

Figure 4.2: Sensitivity of Bending Moment Distribution Factors

Prestressed Girder Bridges

Single Lane Loading Scenario

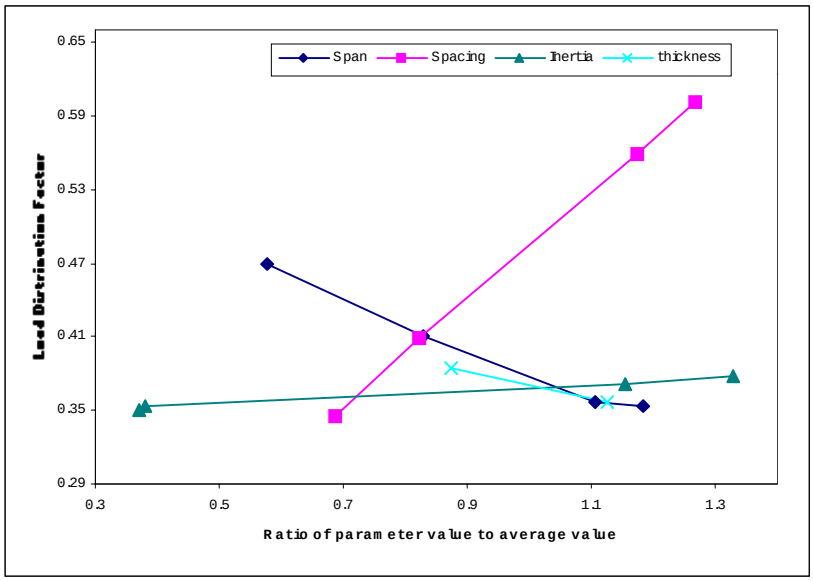

Figure 4.3: Sensitivity of Bending Moment Distribution Factors

Concrete T-beam Bridges

Single Lane Loading Scenario

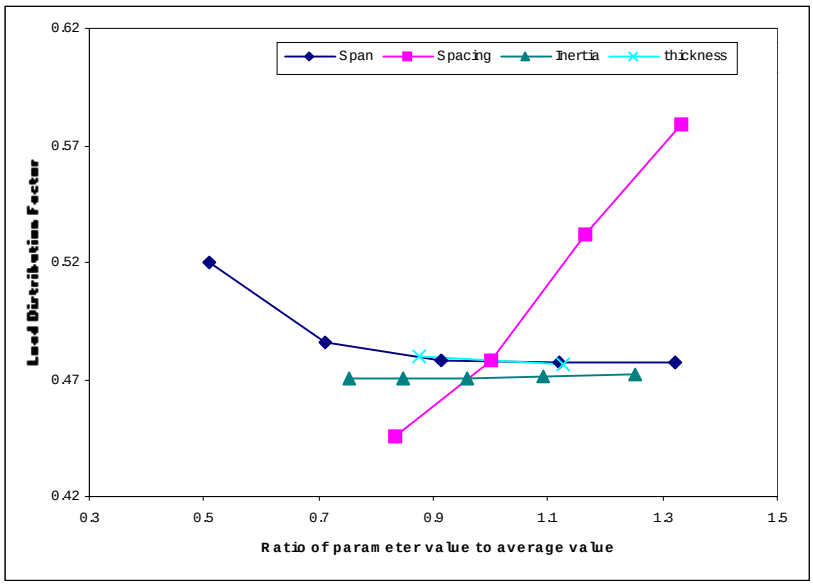

Figure 4.4: Sensitivity of Bending Moment Distribution Factors

Steel Girder Bridges

Multi Lane Loading Scenario

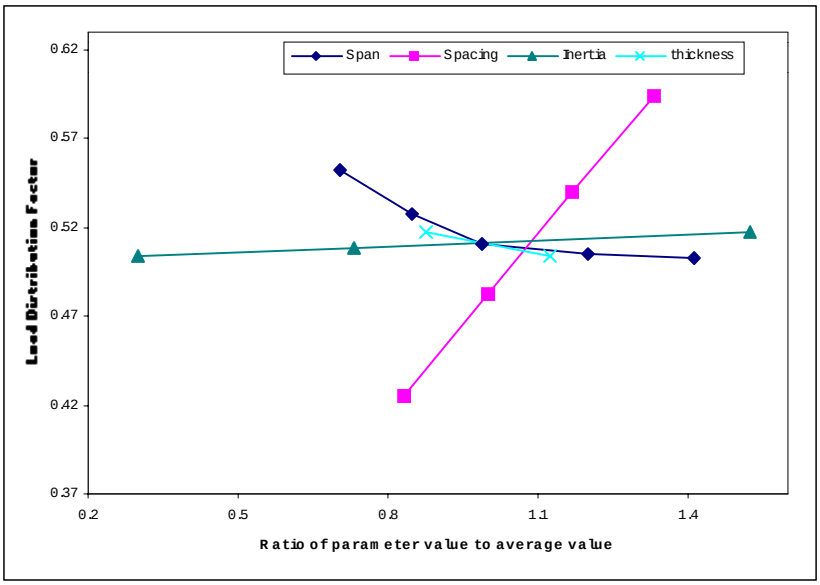

Figure 4.5: Sensitivity of Bending Moment Distribution Factors

Prestressed Girder Bridges

Multi Lane Loading Scenario

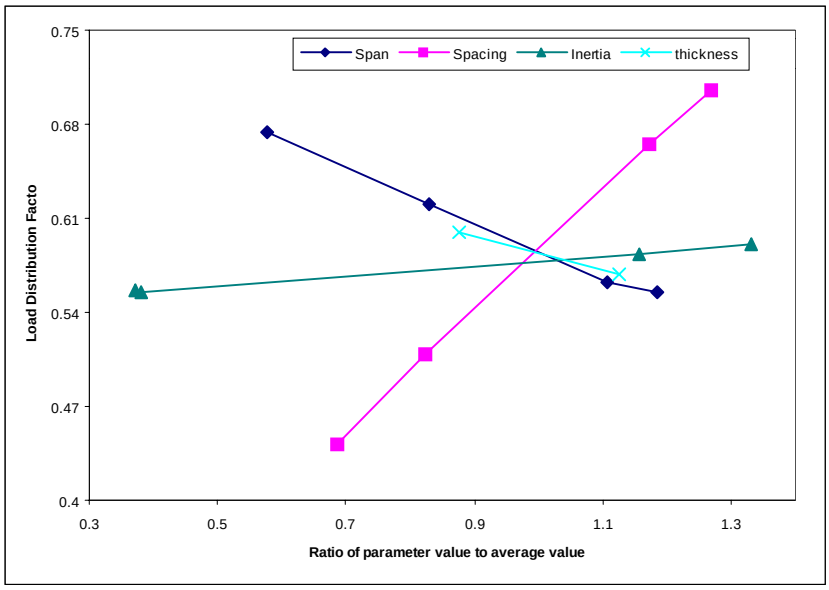

Figure 4.6: Sensitivity of Bending Moment Distribution Factors

Concrete T-beam Bridges

Multi Lane Loading Scenario

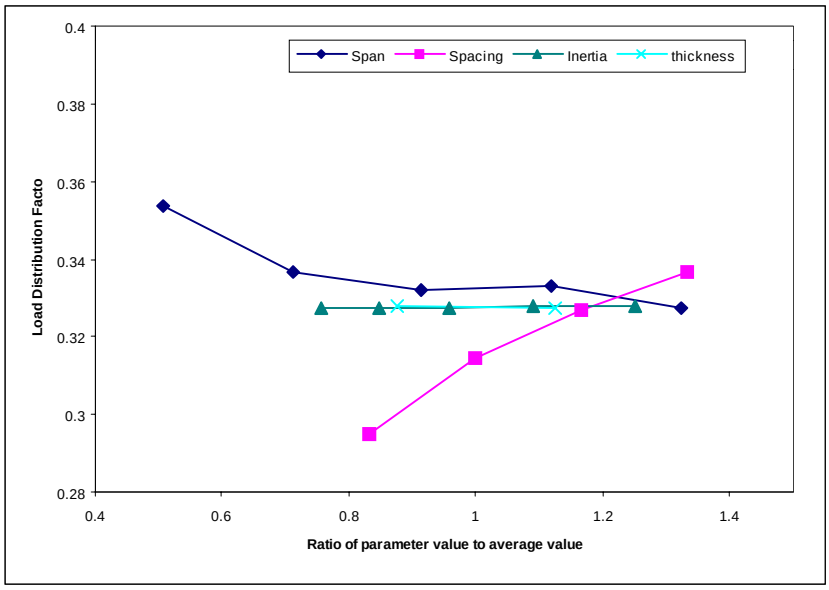

Figure 4.7: Sensitivity of Shear Distribution Factors

Steel Girder Bridges

Single Lane Loading Scenario

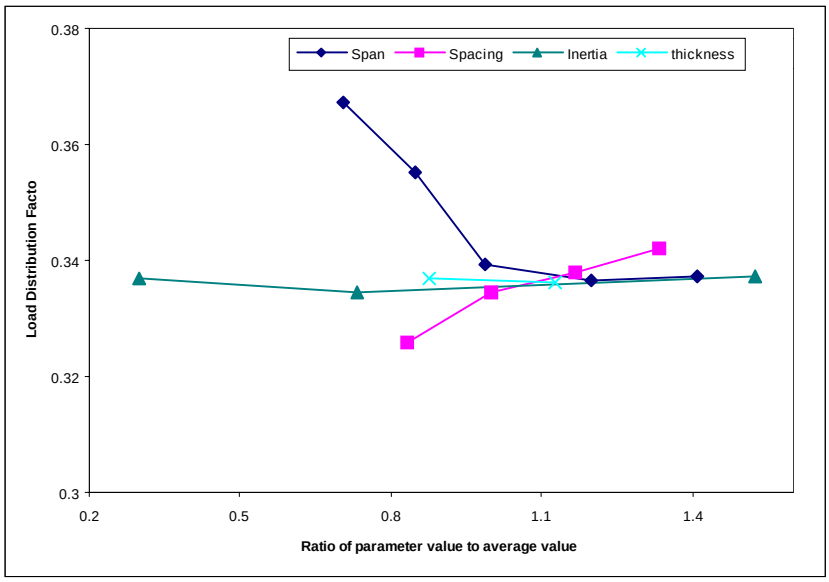

Figure 4.8: Sensitivity of Shear Distribution Factors

Prestressed Girder Bridges

Single Lane Loading Scenario

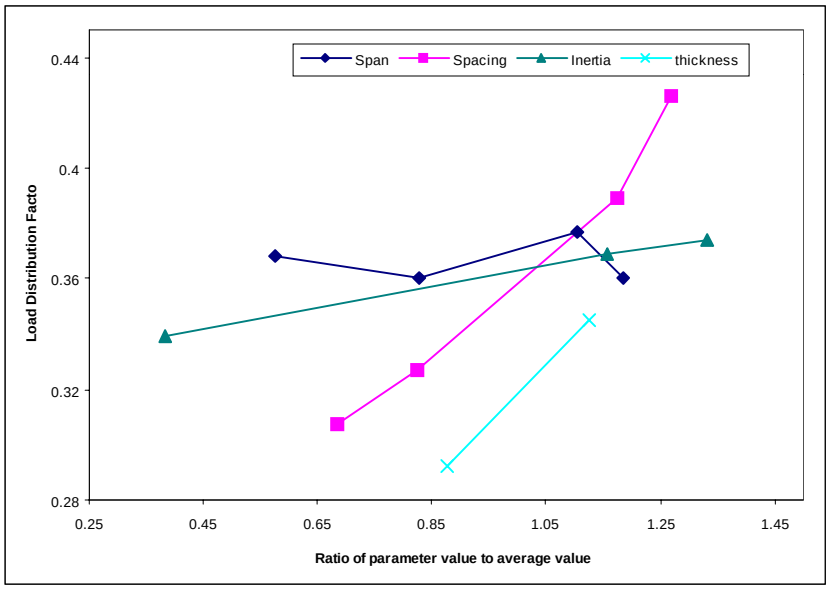

Figure 4.9: Sensitivity of Shear Distribution Factors

Concrete T-beam Bridges

Single Lane Loading Scenario

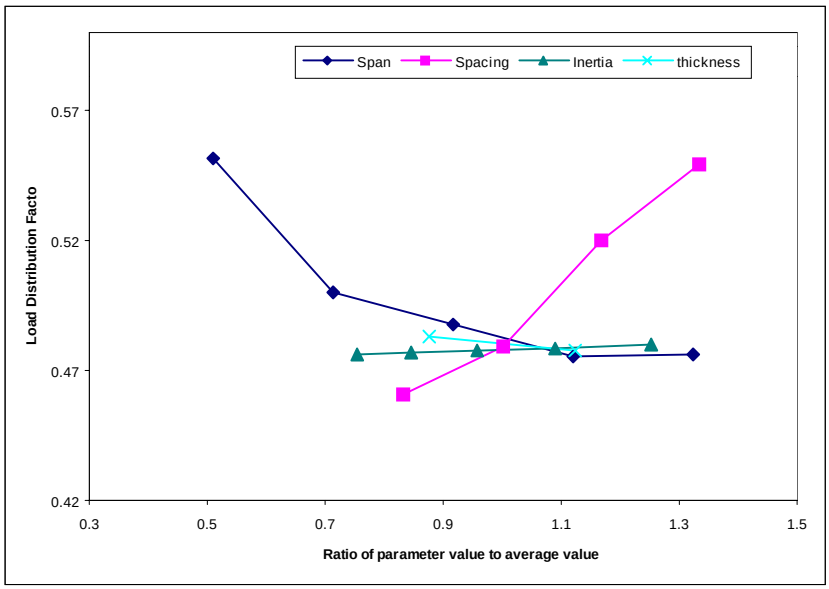

Figure 4.10: Sensitivity of Shear Distribution Factors

Steel Girder Bridges

Multi Lane Loading Scenario

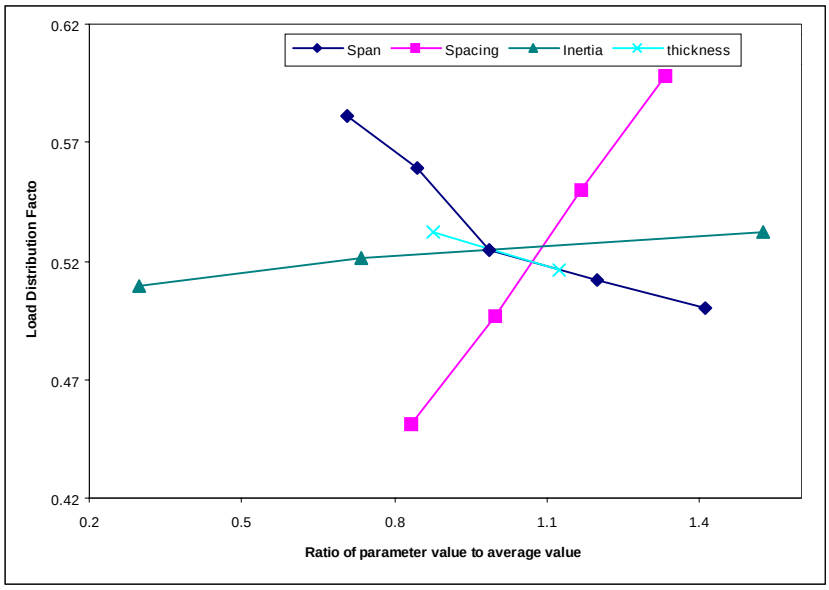

Figure 4.11: Sensitivity of Shear Distribution Factors

Prestressed Girder Bridges

Multi Lane Loading Scenario

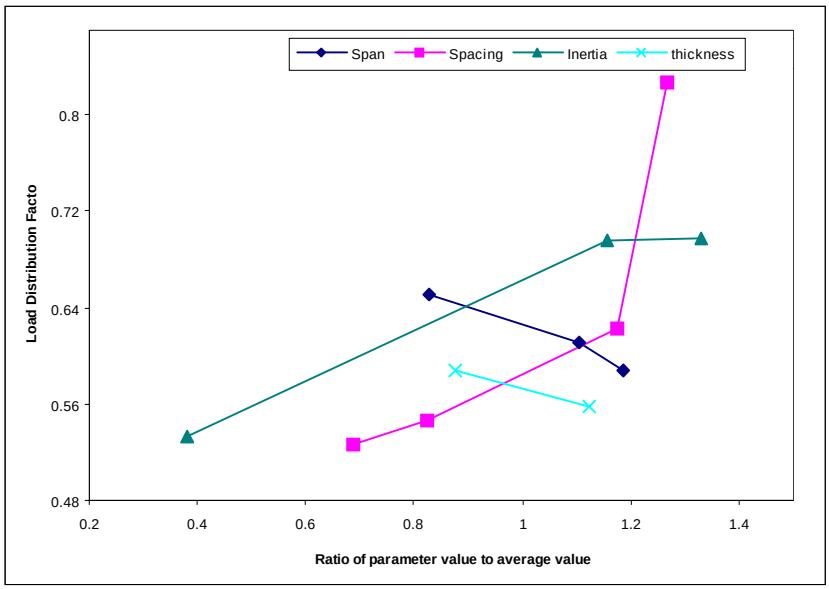

Figure 4.12: Sensitivity of Shear Distribution Factors

Concrete T-beam Bridges

Multi Lane Loading Scenario

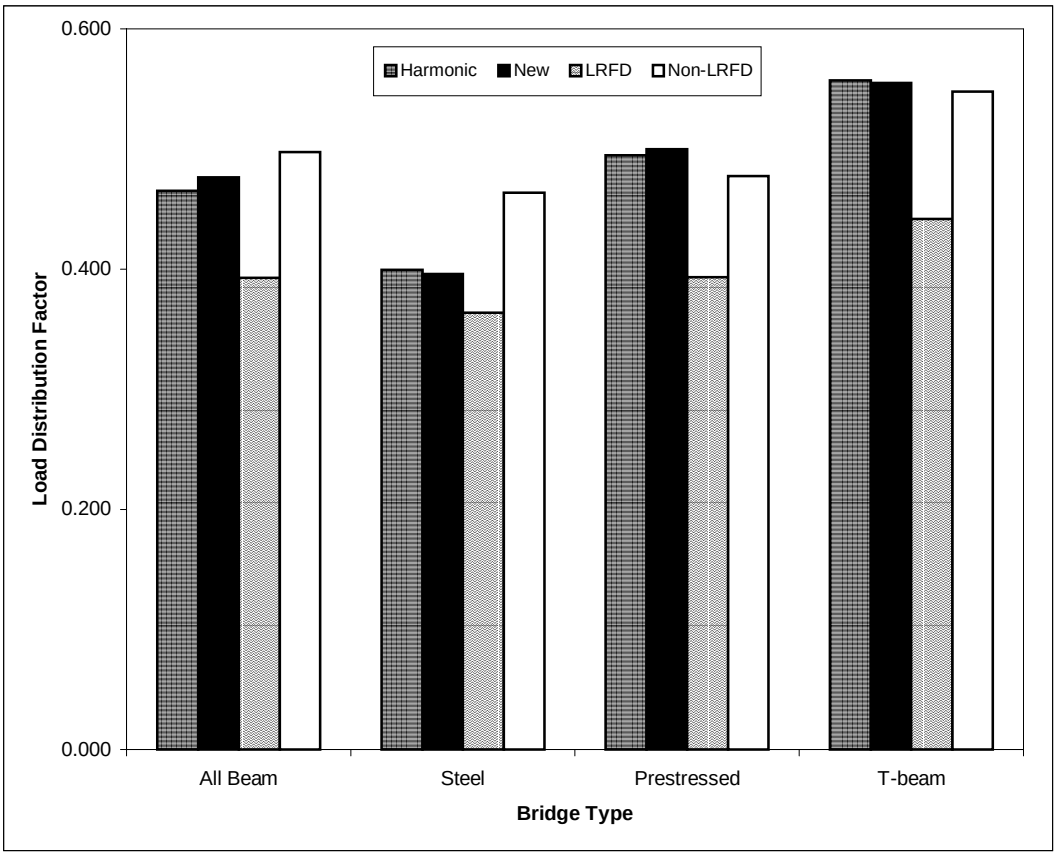

Figure 4.13. Comparison of Mean Values of the Distribution Factors calculated by Bridge Analysis, Proposed Formulas, LRFD and Non-LRFD Formulas for PLS and HEMTT Vehicles, All Bridges, Bending Moment in Interior Girders for Single Lane

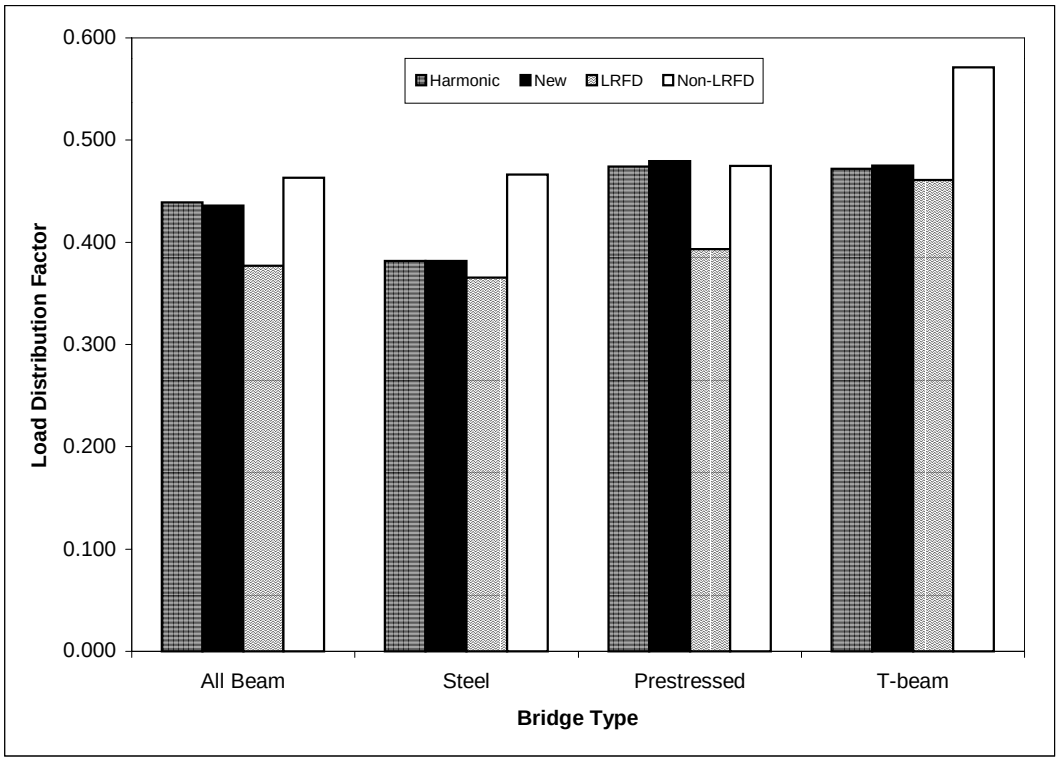

Figure 4.14. Comparison of Mean Values of the Distribution Factors calculated by Bridge Analysis, Proposed Formulas, LRFD and Non-LRFD Formulas for HETS Vehicle, All Bridges, Bending Moment in Interior Girders for Single Lane

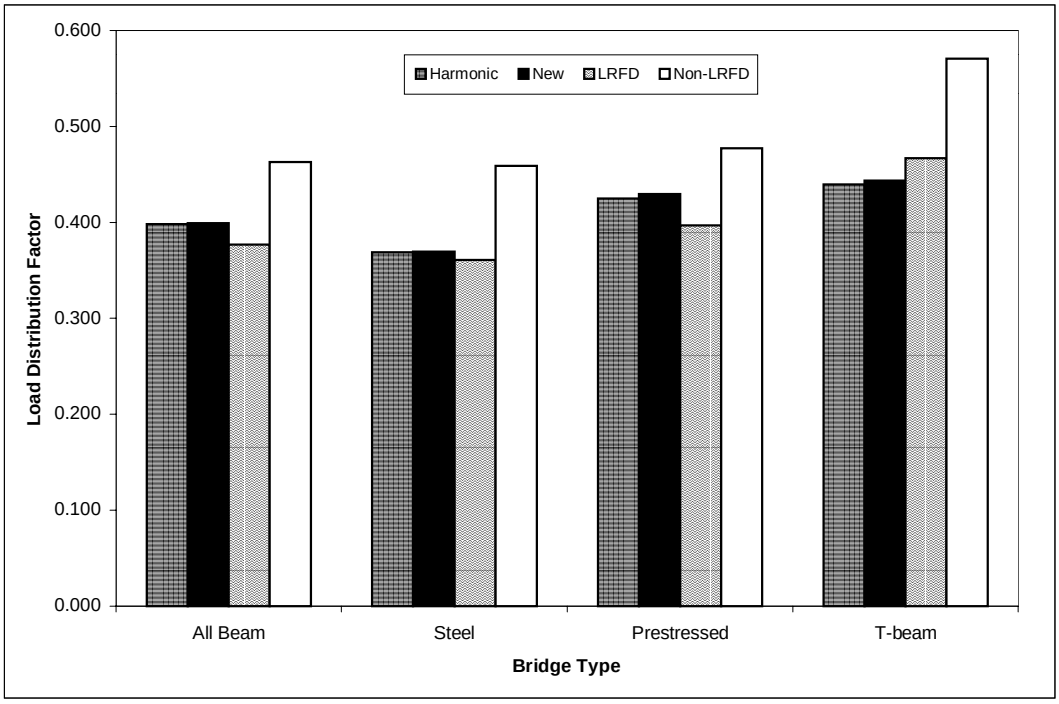

Figure 4.15. Comparison of Mean Values of the Distribution Factors calculated by Bridge Analysis, Proposed Formulas, LRFD and Non-LRFD Formulas for ABRAMS Vehicle, All Bridges, Bending Moment in Interior Girders for Single Lane

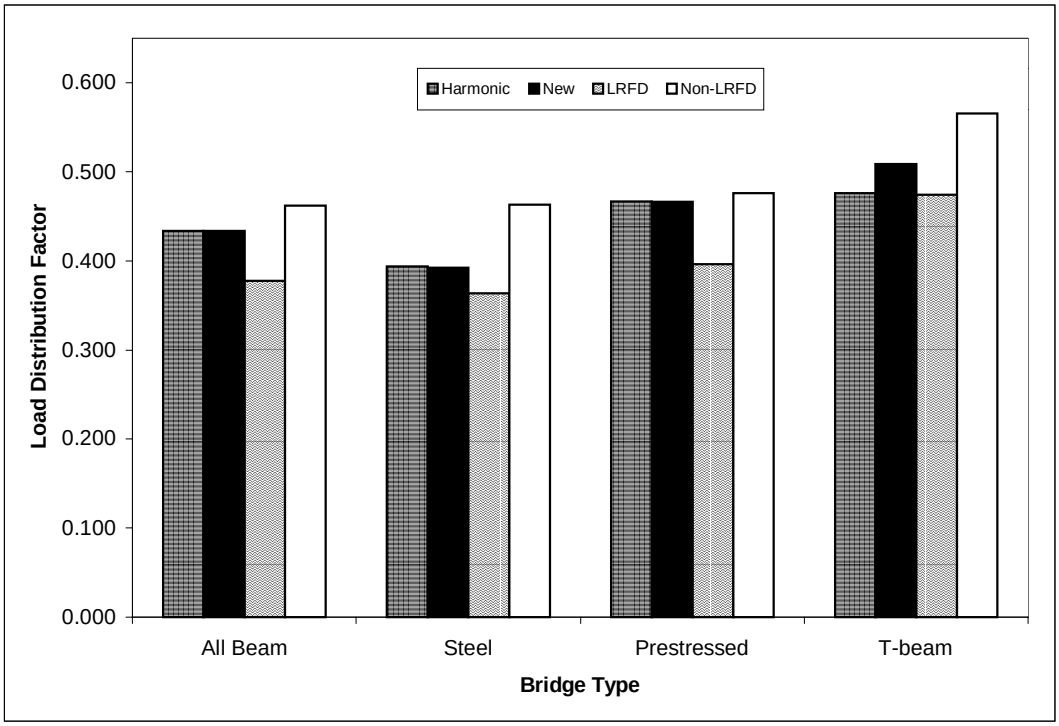

Figure 4.16. Comparison of Mean Values of the Distribution Factors calculated by Bridge Analysis, Proposed Formulas, LRFD and Non-LRFD Formulas for M113 and Bradley Vehicles, All Bridges, Bending Moment in Interior Girders for Single Lane

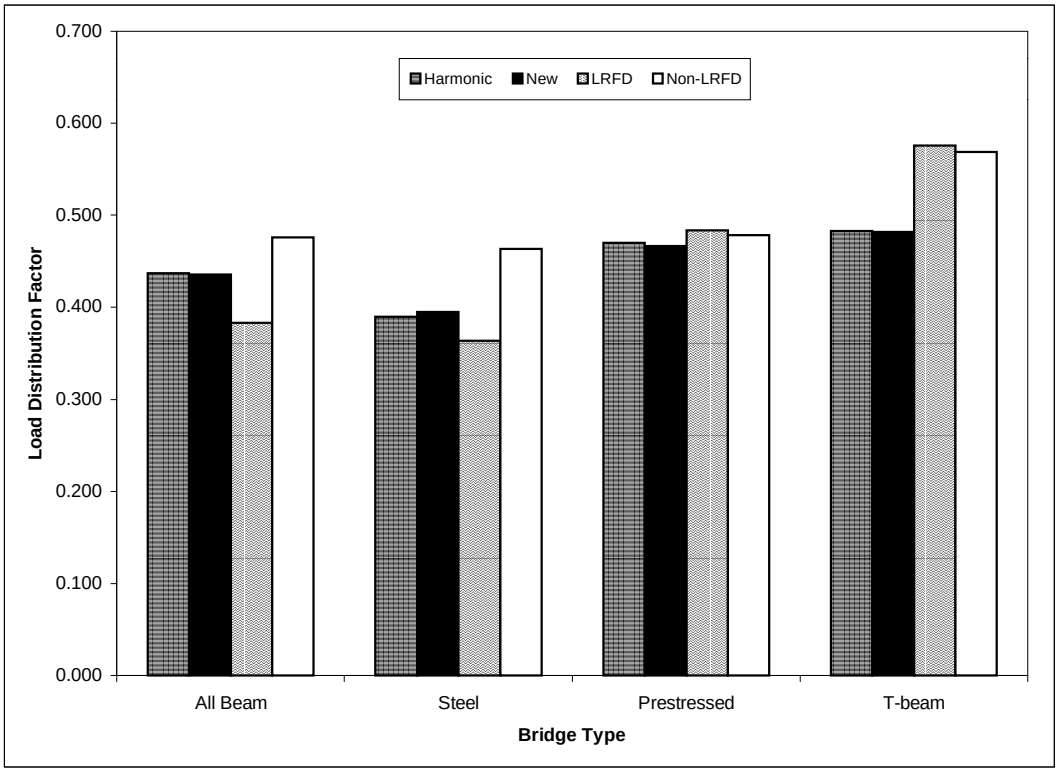

Figure 4.17. Comparison of Mean Values of the Distribution Factors calculated by Bridge Analysis, Proposed Formulas, LRFD and Non-LRFD Formulas for All Vehicles, All Bridges, Bending Moment in Interior Girders for Single Lane

CHAPTER 5

CONCLUDING REMARKS

This thesis describes a methodology to define the lateral load distribution factors for military vehicles on simply supported multi-beam and deck slab highway bridge systems. The study considers six different types of military vehicles on three different types of multi-beam slab bridge systems. Load distribution factor formulas, expressed in terms of beam and deck slab parameters, were developed for the three bridge systems considered separately as well as collectively. Twenty different formulas for bending moment distribution factors were developed separately for (1) HETS vehicle system, (2) PSL and HEMTT vehicle systems, (3) ABRAMS tracked vehicle, and (4) M111 and Bradley tracked vehicles.

In addition, a set of 32 different formulas that are intended to represent all military vehicles collectively were also developed. These formulas cover the cases of (1) single and multiple lane loading, (2) interior and exterior girders, (3) three bridge types considered separately and collectively, and (4) bending moment and shear force values. The accuracy of each of these proposed formulas with respect to harmonic analysis was also evaluated. In general, the accuracy of the distribution factors for the bending moment tends to be higher than the accuracy of the distribution factors for the shear forces. In addition, a comparison of accuracy of these proposed formulas was also made with that of the pre-LRFD and post-LRFD distribution factor formulas. On average the post LRFD formulas

tend to underestimate and the pre-LRFD formulas tend to overestimate the distribution factor values for the military vehicles.

In conclusion, the proposed formulas developed in this study provide the distribution factor values closest to the analytically calculated values with least dispersion and relatively smaller underestimation of the factor values in comparison to the pre- and post LRFD formulas.

REFERENCES

AASHTO, (1996), "Standard Specifications for Highway Bridges", 16th Edition.

AASHTO, (1994), "Guide Specification for Distribution of Loads for Highway Bridge"

Bakht, B., and Jaeger, L. G., (1989), "Bridge Analysis by Microcomputer", McGraw Hill Inc.

Bakht, B., and Jaeger, L. G., (1985), "Bridge Analysis Simplified", McGraw Hill Inc.

Barker, R.M., and Puckett, J. A., (1997), "Design of Highway Bridges, based on AASHTO LRFD Bridge Design Specifications", John Wiley & Sons, Inc., New York, USA.

Cheung, M. S., Li, W., and Chidiac, S.E., (1996), "Finite Strip Analysis of Bridges", E & FN Spon.

Cusens, A.R., and Pama, R. P., (1975), "Bridge Deck Analysis", John Wiley & Sons, Inc.

Douglas, J., (1969), "An Introduction to Dimensional Analysis for Engineers", Pitman Publishing Corp.

Hambly, E.C., (1991), "Bridge Deck Behavior", 2nd Edition, E & FN Spon.

Kuzmanovic, B. O., and Sanchez, M. R., (1986), "Lateral Distribution of Live Loads on Highway Bridges", *Journal of Structural Engineering-ASCE.,* V 112(8) , 1847-1862.

Minor, J., and Woodward, C., (1999), "Bridge Analysis Study, Phase II & Phase III", Draft Report prepared for the U.S. Army Waterways Experiment Station, New Mexico State University.

PCI, (1999), “PCI Design Handbook-Precast/Prestressed Concrete”, Fifth Edition, Prestressed Concrete Institute, Inc., USA.

SAS Institute Inc. (1989), SAS/STAT User’s Guide, Version 6, Fourth Edition, Vol 3. , Cary, NC: SAS Institute Inc.

Singh, M. P., Thangjithan, S., and Singh, S., (1998), “Parametric Sensitivity Analysis of Multi-Girder Bridge Systems”, Report Prepared for U.S. Army Waterways Experiment Station, Vicksburg, MS, December

Timoshenko, S., and Woinowsky-Krieger, S., (1959), “Theory of Plates and Shells”, McGraw Hill Inc.

Zokai, T., Osterkemp, T.A., and Imbsen, R.A., (1991), “Distribution of Wheel Loads on Highway Bridges”, NCHRP Final Reports, Vol. 1 and 2 12-26/1, March

Zokai, T., Mish, K. D., and Imbsen, R.A., (1993), “Distribution of Wheel Loads on Highway Bridges, Phase III”, NCHRP Final Report, 12-26(2), December

APPENDIX A

EXISTING BEAM AND SLAB BRIDGES

This appendix presents a list of the properties of the existing beam and slab bridges taken from the Zokaie et al database. The bridges have been classified in Table A.1 in the tree types of bridges considered in this study: steel girder, prestressed concrete, and concrete T-beam bridges.

Table A.1: Properties of Existing Bridges considered in this study (Zokaie et at Data)

Seq. No.	Description	Span (ft)	No. of Girders	Girder Spacing (ft)	Slab thick.(in)	Width (C-C) (ft)	Inertia (in^4)
1	Arizona-Steel	30	5	7.5	7.75	32	2364
2	Arizona-Steel	40	5	7.5	7.75	32	2364
3	California-Steel	113.17	4	8.5	7.13	28	27833
4	California-Steel	80.66	5	6.25	6	24	9739
5	California-Steel	130	3	15.5	9.63	39	188585
6	California-Steel	155	3	15.5	9.63	39	188585
7	California-Steel	68	4	6.66	6.75	21	14988
8	California-Steel	116	4	9	7	28	68862
9	California-Steel	51.25	9	6.5	7	52	5367
10	California-Steel	51.25	5	6.5	6.5	28	5367
11	California-Steel	75.25	6	7.75	6.63	37	17101
12	California-Steel	91.25	6	7.75	6.63	37	24195
13	California-Steel	151.13	3	12	7.75	28	287125
14	California-Steel	75	3	12	7.75	28	215965
15	Florida-Steel	142	10	9.25	7.5	79.25	59869
16	Florida-Steel	205	10	9.25	7.5	79.25	75951
17	Maine-Steel	20	5	5	6.5	22	801
18	Maine-Steel	50	5	7.92	7.5	30	8641
19	Maine-Steel	60	5	5	7	22	9012
20	Maine-Steel	75	5	8.25	6	28	16856
21	Maine-Steel	90	5	8	9	32	18554
22	Maine-Steel	110	4	8.5	8.5	28	29835
23	Maine-Steel	75	5	6	5.75	24	11048
24	Maine-Steel	20.5	12	2.17	7.5	22	234
25	Maine-Steel	70	6	7.5	8.5	39	7796
26	Maine-Steel	100	5	7	8	29.83	10460
27	Minesota-Steel	56.25	7	5.33	7.25	30	5753
28	Minesota-Steel	28	9	2.58	6.5	19	516
29	Minesota-Steel	43	7	4.83	7	27	3267
30	Minesota-Steel	51	7	6.25	6.5	30	4461
31	Minesota-Steel	50	5	7	6	30	6699
32	Minesota-Steel	68	5	7	6	30	9012
33	Minesota-Steel	65	5	7	6	30	9012
34	Minesota-Steel	121.5	8	8.08	9	46.83	41824
35	Minesota-Steel	98	5	9.83	8.25	36	29122
36	Minesota-Steel	125	5	9.83	8.25	36	27508
37	Minesota-Steel	89	4	9.33	6.75	30	10629
38	New York-Steel	105	6	8.67	12.01	36	15587
39	New York-Steel	130	6	8.67	12.01	36	19181
40	New York-Steel	100.73	8	6.6	7	33	43005

Table A.1 (cont.): Properties of Existing Bridges considered in this study (Zokaie et at Data)

Seq. No.	Description	Span (ft)	No. of Girders	Girder Spacing (ft)	Slab thick.(in)	Width (C-C) (ft)	Inertia (in^4)
41	New York-Steel	87.3	5	7	8.5	28	17871
42	Ohio-Steel	39	5	5.75	6.75	24	3267
43	Ohio-Steel	43	4	7.5	8	28	3989
44	Ohio-Steel	42.5	12	3.21	4.42	36	2096
45	Ohio-Steel	27	5	5.75	7.25	24	1327
46	Ohio-Steel	65.54	5	5.75	7.25	24	6699
47	Ohio-Steel	74.5	7	8.33	8.5	50	14988
48	Ohio-Steel	66.25	7	8.33	8.5	50	9739
49	Ohio-Steel	80	7	8.33	8.5	50	12103
50	Ohio-Steel	93.12	7	8.33	8.5	50	16092
51	Ohio-Steel	56	7	8.33	8.5	50	9739
52	Oklahoma-Steel	36	5	5.25	8.75	20	3000
53	Oklahoma-Steel	34.75	5	5.25	8.75	20	3000
54	Oklahoma-Steel	50	5	5.17	6.5	22	6699
55	Oklahoma-Steel	30	6	4.5	6	24	1327
56	Oklahoma-Steel	61	6	4.92	7.5	24	7442
57	Oklahoma-Steel	41.25	5	6.58	7.5	28	6699
58	Oklahoma-Steel	59.83	5	6.58	7.5	28	10470
59	Oklahoma-Steel	37.17	5	5.25	8.75	20	2364
60	Oklahoma-Steel	38.75	5	6.58	7.5	28	4461
61	Oklahoma-Steel	31.25	5	5.67	8	24	2096
62	Oklahoma-Steel	125	4	11	10	38	51463
63	Oklahoma-Steel	160	4	11	10	38	51463
64	Oregon-Steel	140	6	13.5	6.5	58	203546
65	Oregon-Steel	113	6	9	7	70	27429
66	Oregon-Steel	142	6	9	7	70	27429
67	California-Prestressed	113	7	6.42	6.87	40	318000
68	California-Prestressed	96	8	7.5	6.25	52	248000
69	California-Prestressed	70.5	8	7.5	6.25	52	248000
70	California-Prestressed	84	10	7	6.25	66	187800
71	California-Prestressed	61.63	10	7.66	6.25	73	63300
72	California-Prestressed	27	10	7.66	6.25	73	63300
73	California-Prestressed	84	19	9.1	7.13	188	187800
74	California-Prestressed	67.5	7	6.83	6	32	137300
75	Florida-Prestressed	40	4	9.7	7	28	50980
76	Florida-Prestressed	60	6	5.83	7	28	50980
77	Florida-Prestressed	82	5	9.69	7.5	44	260730
78	Florida-Prestressed	32.5	4	6.75	7	26	125390
79	Florida-Prestressed	72	4	6.75	7	26	125390

Table A.1 (cont.): Properties of Existing Bridges considered in this study (Zokaie et at Data)

Seq. No.	Description	Span (ft)	No. of Girders	Girder Spacing (ft)	Slab thick.(in)	Width (C-C) (ft)	Inertia (in^4)
80	Florida-Prestressed	79	9	4.75	7	38	125390
81	Florida-Prestressed	79	6	5.42	7	26	125390
82	Florida-Prestressed	47.5	4	9.03	7	26	125390
83	Florida-Prestressed	65.25	10	8.77	7.5	79.25	260730
84	Florida-Prestressed	87	10	8.77	7.5	79.25	260730
85	Florida-Prestressed	41.75	6	9.8	7	52	50980
86	Florida-Prestressed	61.5	10	5.44	7	52	125390
87	Florida-Prestressed	45.5	7	8.17	7	46	50980
88	Florida-Prestressed	91.5	7	8.17	7	46	260730
89	Florida-Prestressed	40	6	9.8	7	46	50980
90	Florida-Prestressed	95.07	14	6.51	7.5	81.5	260730
91	Florida-Prestressed	101.68	14	6.51	7.5	81.5	260730
92	Florida-Prestressed	129	12	7.77	7.5	81.5	733320
93	Florida-Prestressed	47	6	8.2	7	44	50980
94	Florida-Prestressed	82	5	9.69	7.5	44	260730
95	Florida-Prestressed	64	6	9.25	7.5	40	125390
96	Minesota-Prestressed	81	8	6.5	9	47	125390
97	Minesota-Prestressed	74.5	5	10.25	8	44	125390
98	Ohio-Prestressed	47	9	7.5	7.5	52	59077
99	Oklahoma-Prestressed	50	5	10.5	8.5	46.75	125390
100	Oregon-Prestressed	22.81	18	3.21	5	55.83	40134
101	Oregon-Prestressed	30.75	18	3.21	5	55.83	40134
102	Oregon-Prestressed	18.75	7	4.21	5.25	26	9599
103	Oregon-Prestressed	92	4	8	7.5	26	260730
104	Washington-Prestressed	136.2	8	6.75	7	52	455967
105	Arizona-Tbeam	68	4	8	6.75	29.75	417074
106	Arizona-Tbeam	71	4	8	6.75	29.75	417074
107	California-Tbeam	31	4	7.6	9	24	24600
108	California-Tbeam	29.17	5	8.33	6.5	37	53300
109	California-Tbeam	30	5	8.33	6.5	37	53300
110	California-Tbeam	71	4	8.5	6.62	28	205300
111	California-Tbeam	38	5	9	7	39	46450
112	California-Tbeam	46	4	8	8	26	10000
113	California-Tbeam	34	4	8	8	26	10000
114	California-Tbeam	34	8	7.5	6.25	52	15629
115	California-Tbeam	37	10	7	6.25	64	99550
116	Maine-Tbeam	22	4	7.5	7.5	22	15972
117	Maine-Tbeam	30	5	5.33	8	20	18250
118	Maine-Tbeam	42	5	5.85	8.25	22	31165
119	Minesota-Tbeam	58	6	6.56	5.75	30	100600

Table A.1 (cont.): Properties of Existing Bridges considered in this study (Zokaie, et at Data)

Seq. No.	Description	Span (ft)	No. of Girders	Girder Spacing (ft)	Slab thick.(in)	Width (C-C) (ft)	Inertia (in^4)
120	Minesota-Tbeam	65	8	6.27	6	46.83	74443
121	Minesota-Tbeam	68.25	7	6	6.75	38.83	567348
122	New York-Tbeam	39	4	8.33	9	22	82021
123	Ohio-Tbeam	60	6	4.87	6.5	24	177364
124	Ohio-Tbeam	40	7	4.96	6.5	29	25588
125	Oklahoma-Tbeam	50	6	7	5	40	62160
126	Oregon-Tbeam	56	4	9.33	7	30	97600
127	Oregon-Tbeam	70	4	9.33	7	30	97600
128	Oregon-Tbeam	50	4	9.33	7	30	53600
129	Oregon-Tbeam	37	4	9.33	7	30	53600
130	Oregon-Tbeam	35	4	7.33	7	26	14190
131	Oregon-Tbeam	50	4	7.33	7	26	14190
132	Oregon-Tbeam	35	9	4.75	6	30	29250
133	Washington-Tbeam	45	4	7.17	6.5	24	30200
134	Washington-Tbeam	22.5	5	8.54	6.5	36	27000
135	Washington-Tbeam	25	3	6.75	8	16	13824
136	Washington-Tbeam	12	5	7.5	6.5	34	19000
137	Washington-Tbeam	45	5	7.5	6.5	34	19000

APPENDIX B

COMPARISON OF PROPOSED FORMULAS VERSUS DIRECT BRIDGE ANALYSIS

This appendix presents the comparison of the distribution factors calculated by the Proposed Formulas and Bridge Analysis. Part (a) of the figures plots the value of the distribution factor calculated by the formula against the value obtained by an equal bridge analysis. Each point in the plot represents a bridge in the database. On the other hand, part (b) of the figures plots the histograms for the variable of the ratio of the distribution factor calculated by the formula to the one calculated by actual analysis of the bridge. The mean and coefficient of variation values of this ratio were included in the plots.

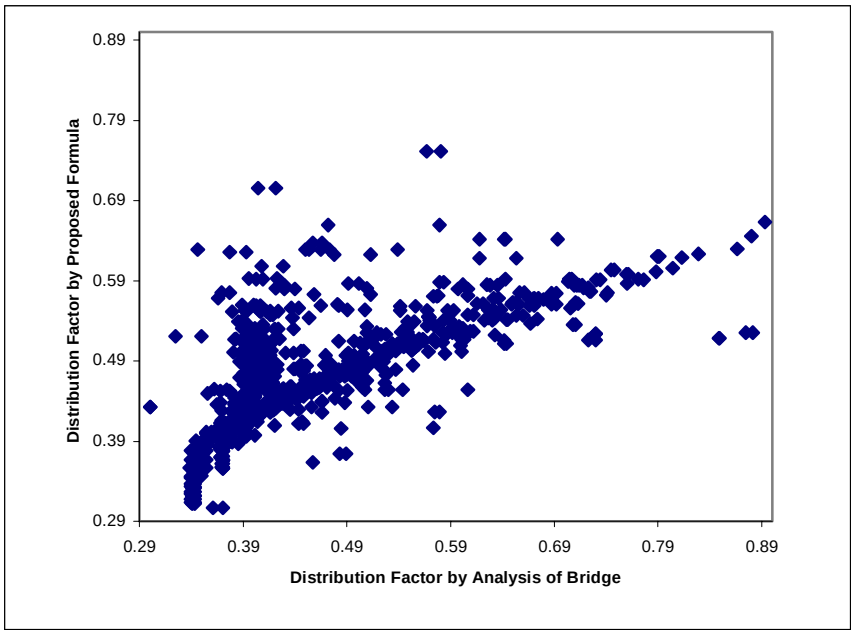

(a)

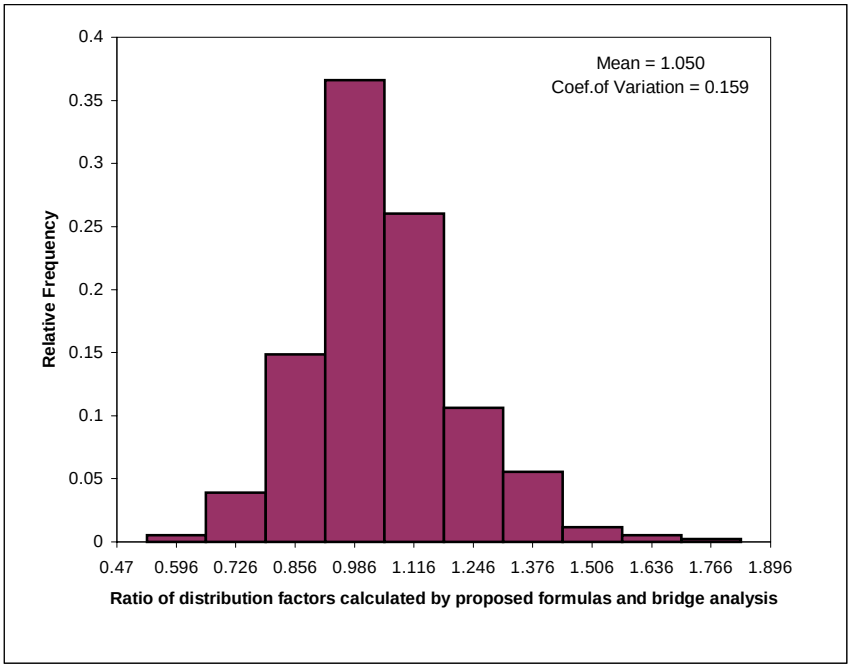

(b)

Figure B.1. Comparison of Distribution Factors calculated by Proposed Formulas and Bridge Analysis for PLS and HEMMT Vehicles, All Beam Bridges, Bending Moment in Interior Girders for Single Lane

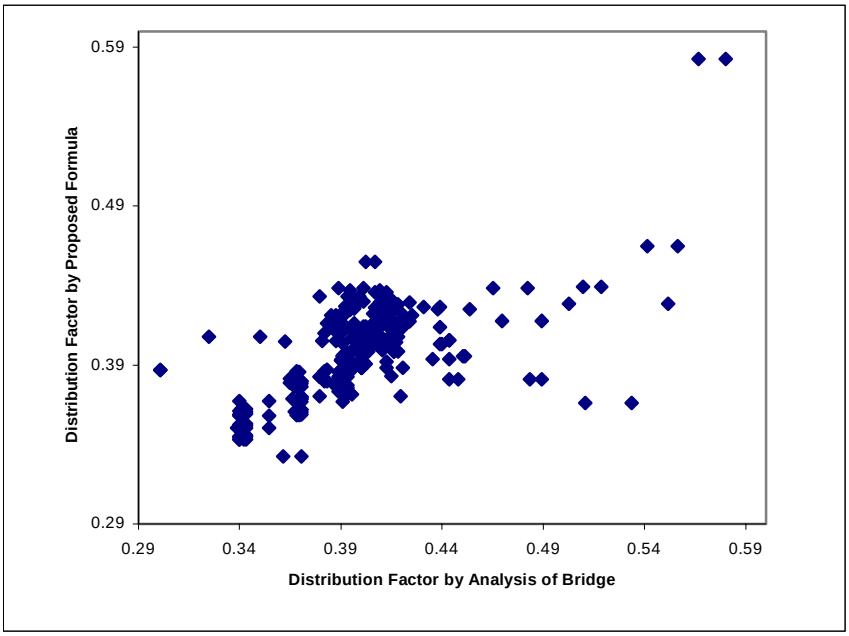

(a)

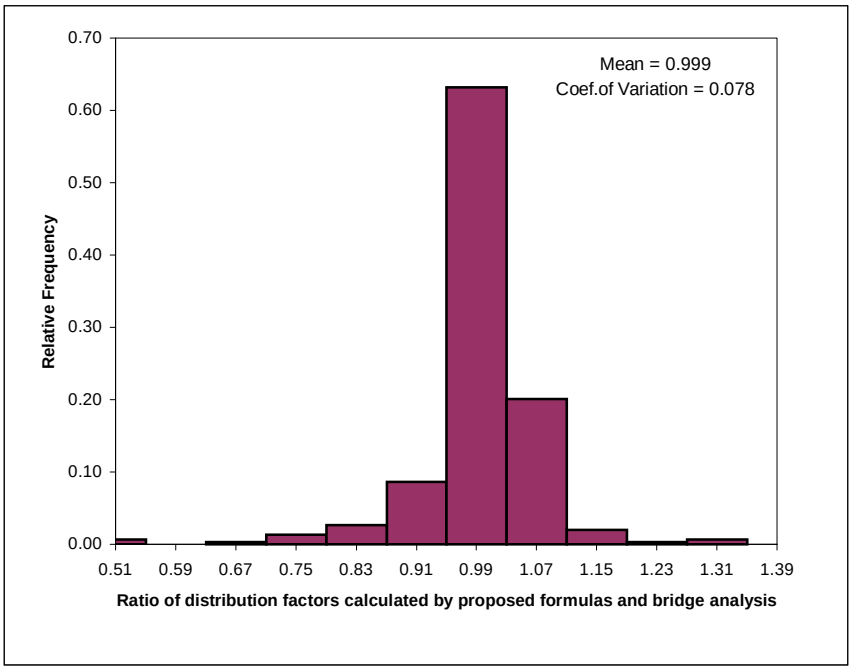

(b)

Figure B.2. Comparison of Distribution Factors calculated by Proposed Formulas and Bridge Analysis for PLS and HEMMT Vehicles, Steel Girders, Bending Moment in Interior Girders for Single Lane

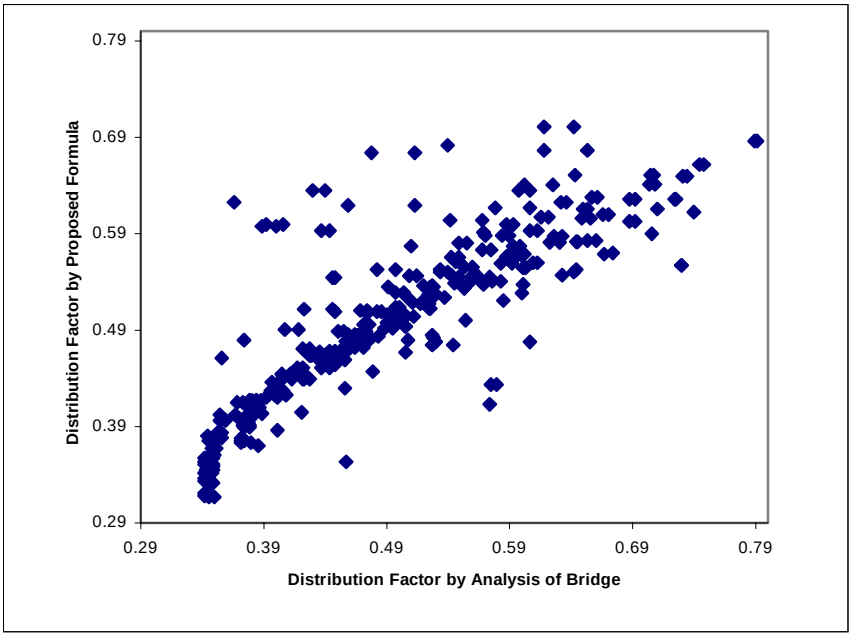

(a)

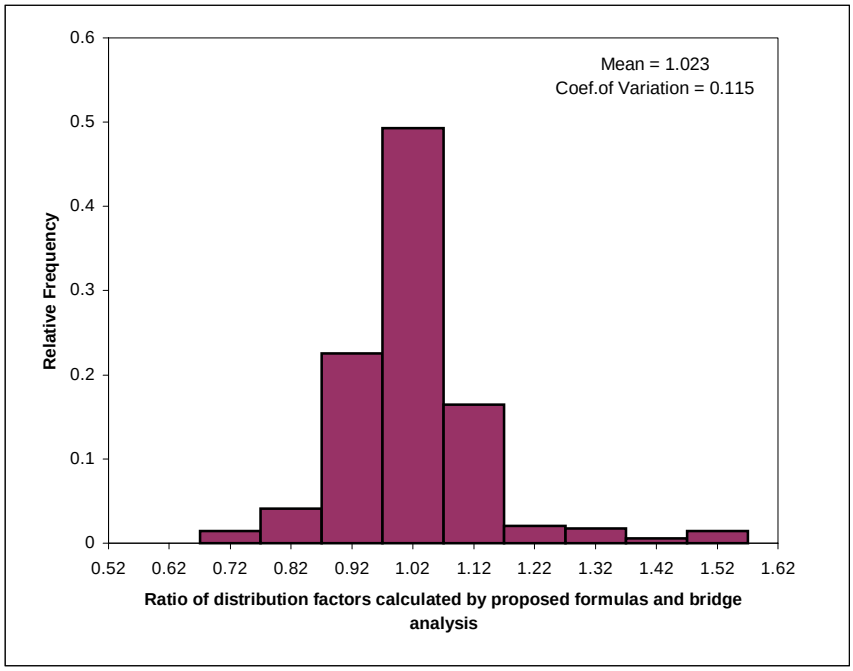

(b)

Figure B.3. Comparison of Distribution Factors calculated by Proposed Formulas and Bridge Analysis for PLS and HEMMT Vehicles, Prestressed Girders, Bending Moment in Interior Girders for Single Lane

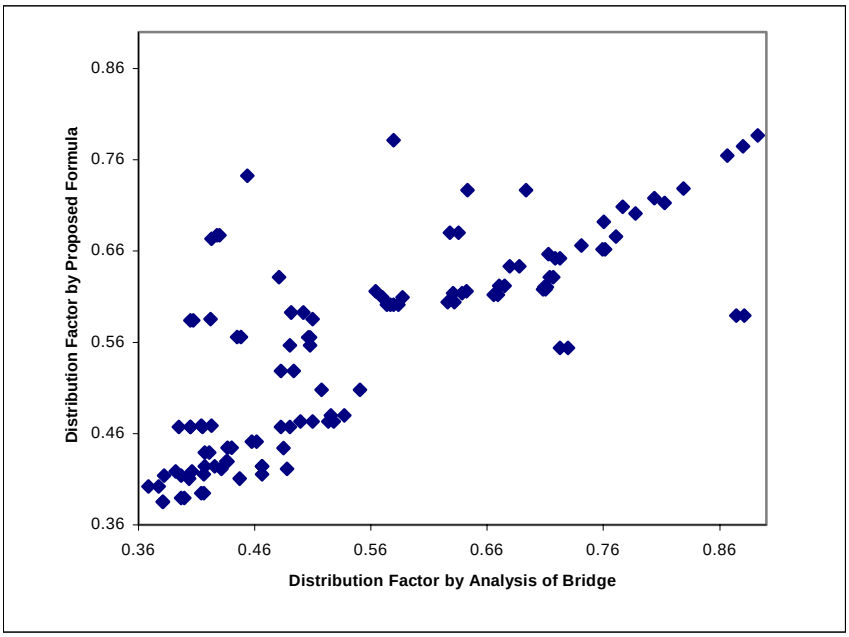

(a)

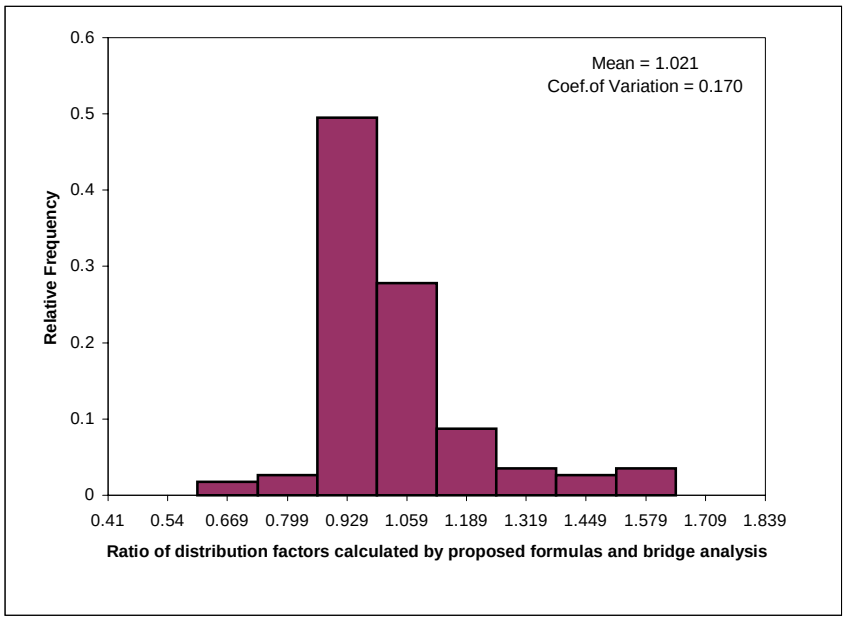

(b)

Figure B.4. Comparison of Distribution Factors calculated by Proposed Formulas and Bridge Analysis for PLS and HEMMT Vehicles, Concrete T-Beam, Bending Moment in Interior Girders for Single Lane

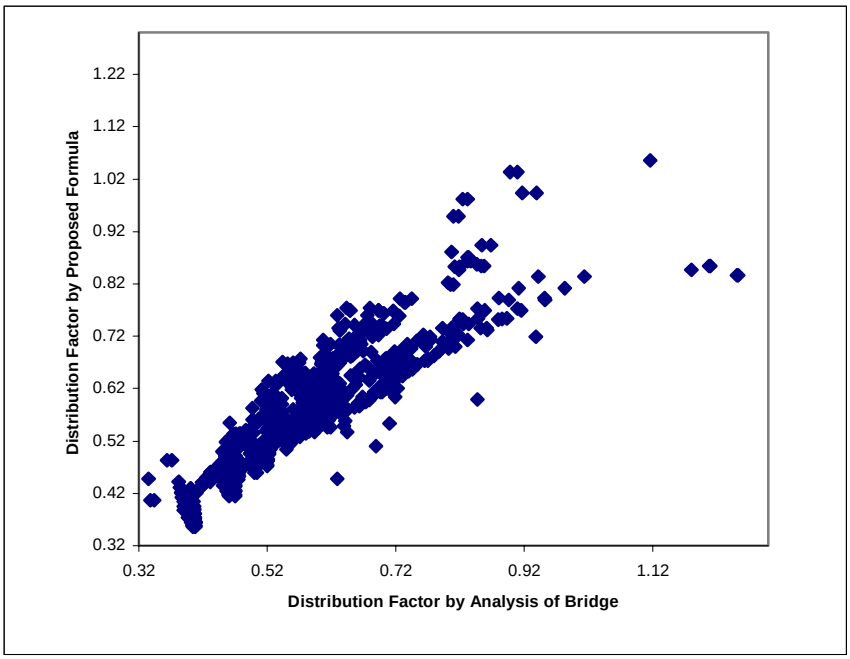

(a)

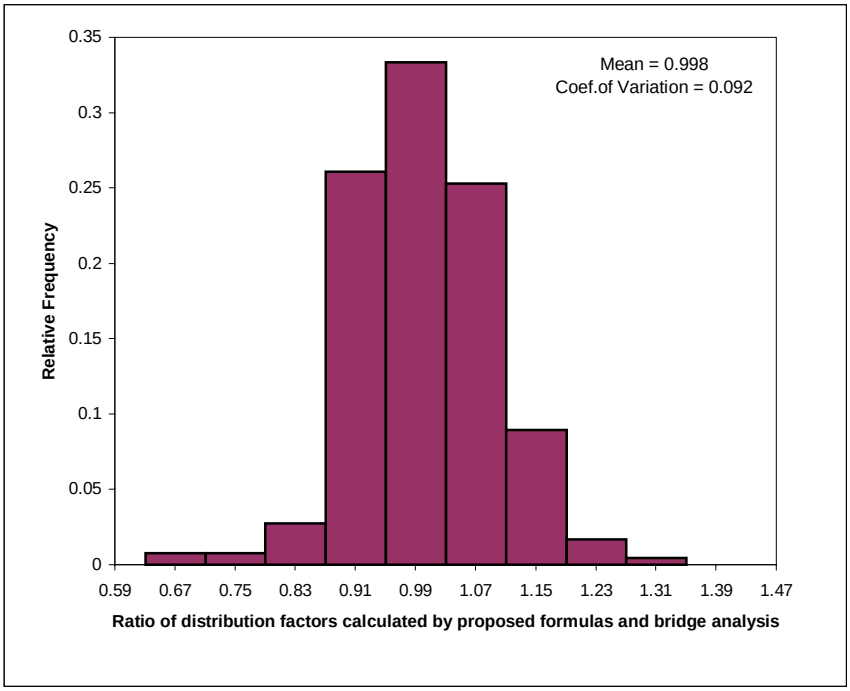

(b)

Figure B.5. Comparison of Distribution Factors calculated by Proposed Formulas and Bridge Analysis for PLS and HEMMT Vehicles, All Beam Bridges, Bending Moment in Interior Girders for Multi Lane

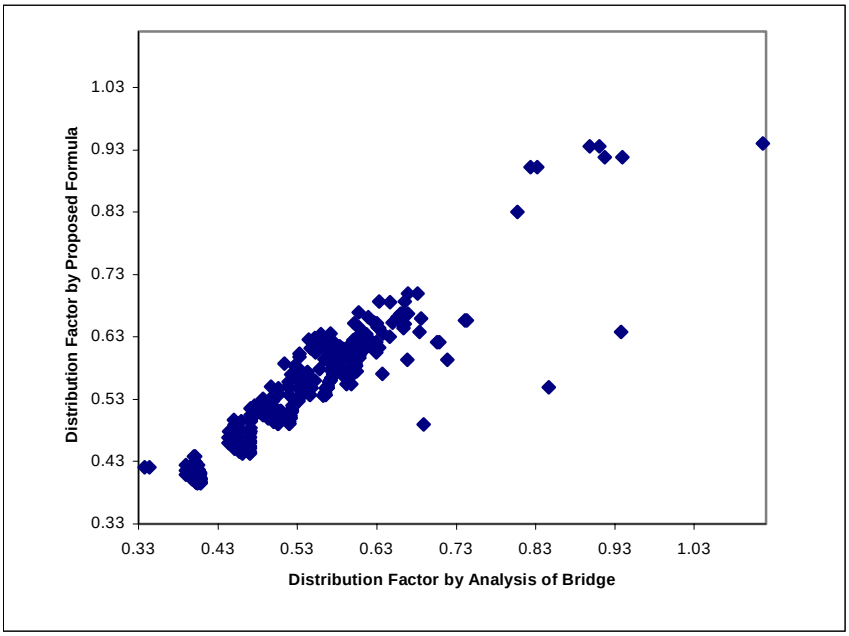

(a)

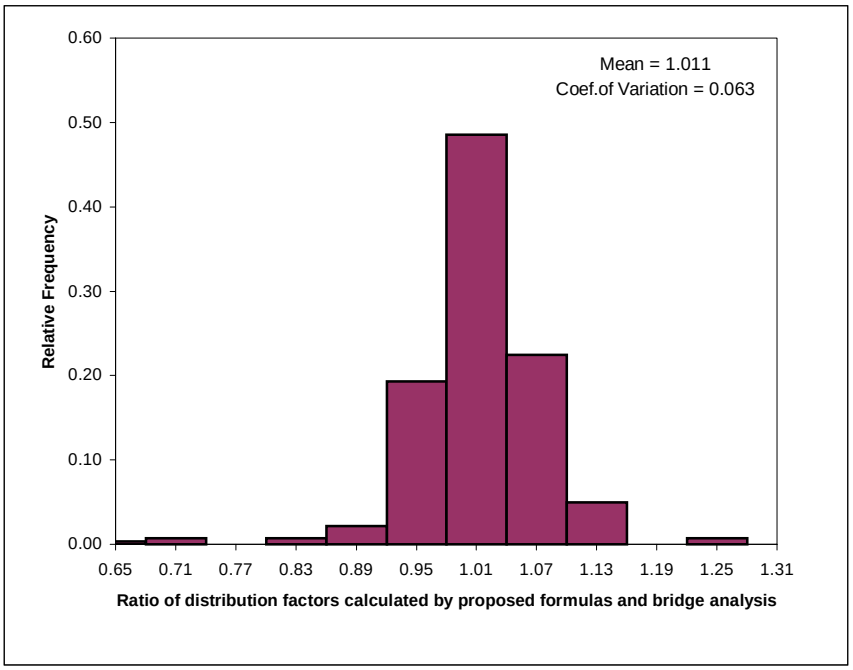

(b)

Figure B.6. Comparison of Distribution Factors calculated by Proposed Formulas and Bridge Analysis for PLS and HEMMT Vehicles, Steel Girder, Bending Moment in Interior Girders for Multi Lane

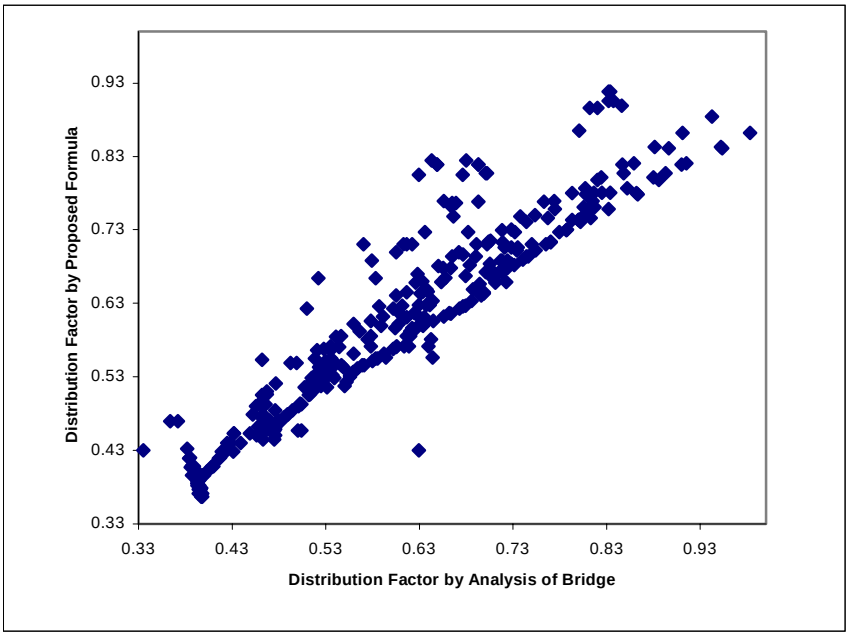

(a)

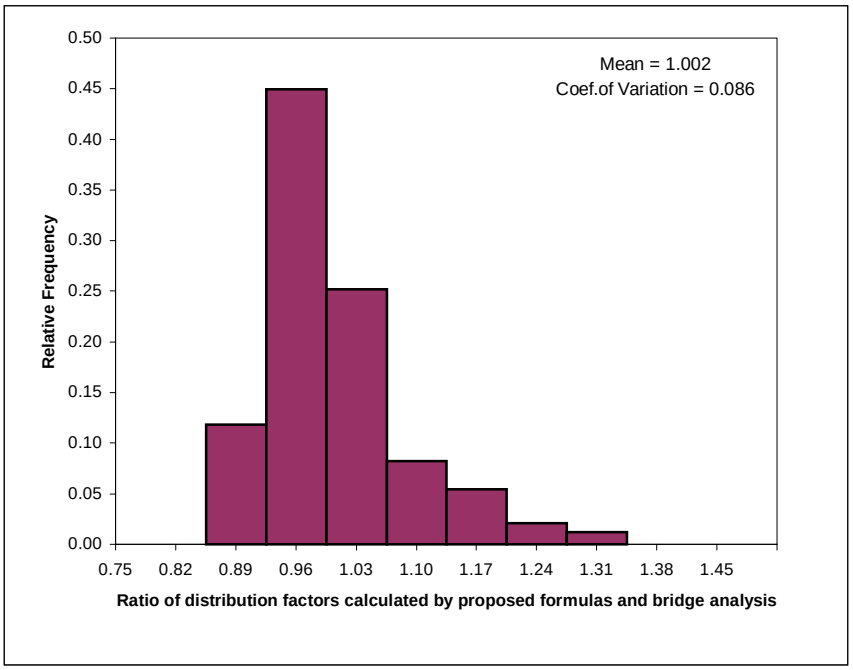

(b)

Figure B.7. Comparison of Distribution Factors calculated by Proposed Formulas and Bridge Analysis for PLS and HEMMT Vehicles, Prestressed Girder, Bending Moment in Interior Girders for Multi Lane

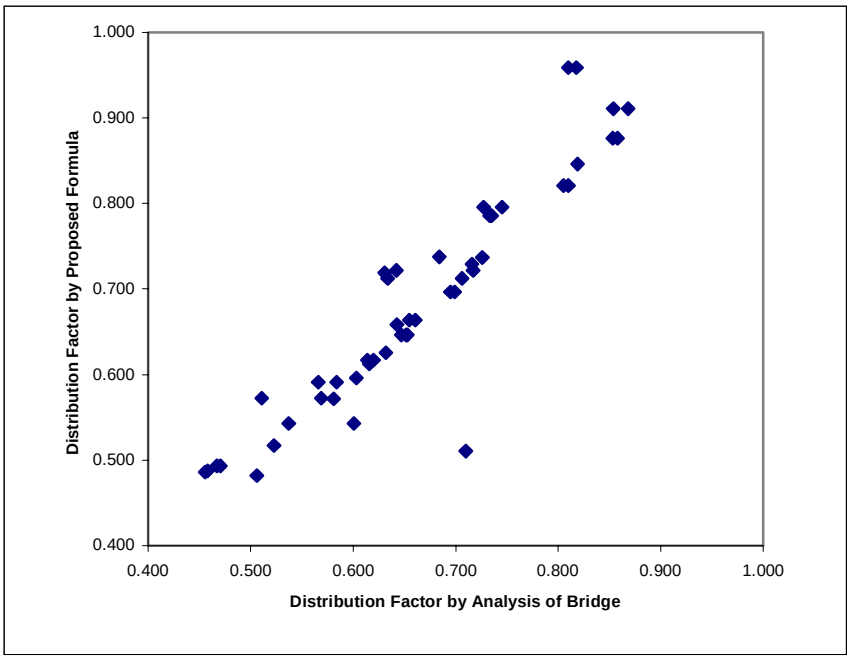

(a)

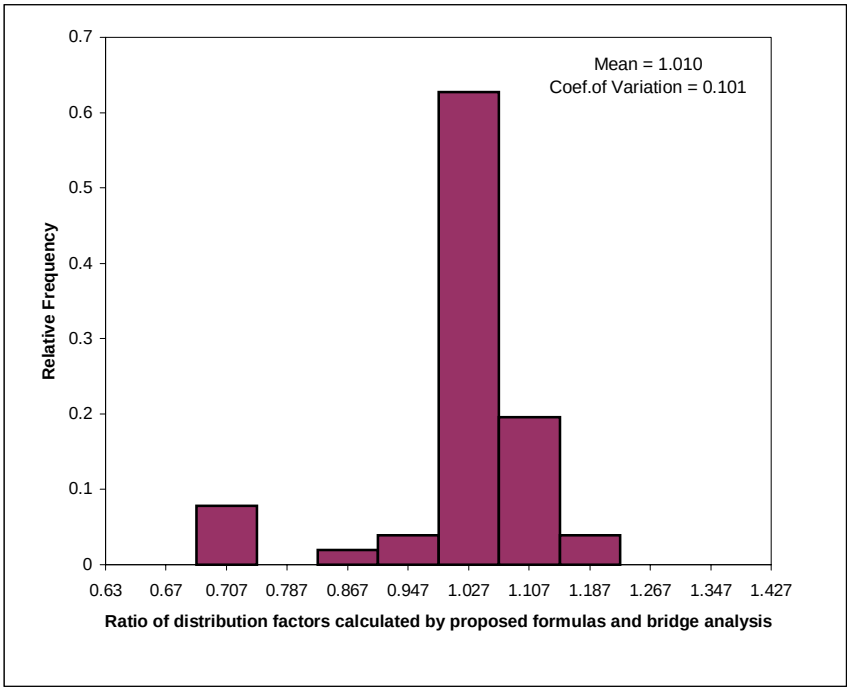

(b)

Figure B.8. Comparison of Distribution Factors calculated by Proposed Formulas and Bridge Analysis for PLS and HEMMT Vehicles, Concrete T-Beam, Bending Moment in Interior Girders for Multi Lane

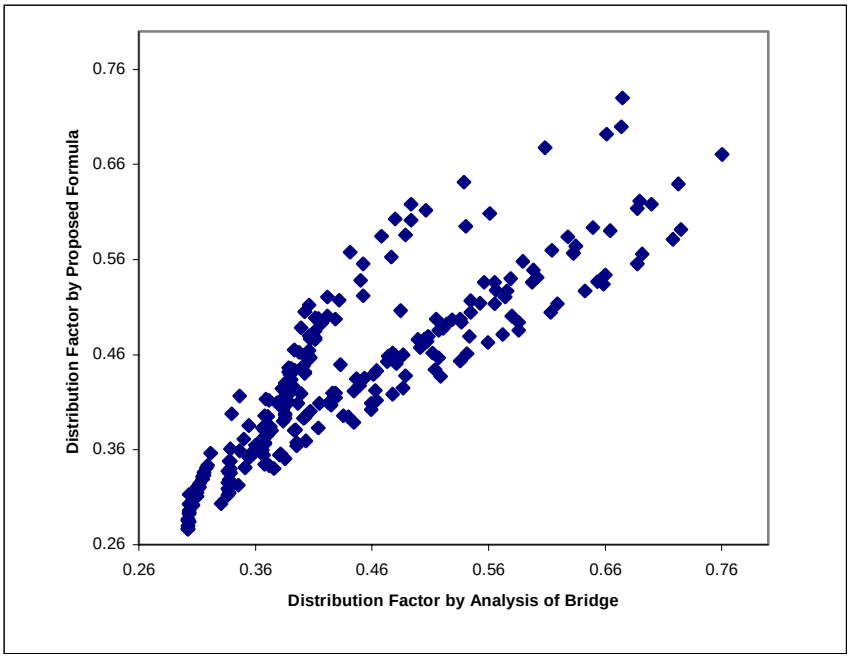

(a)

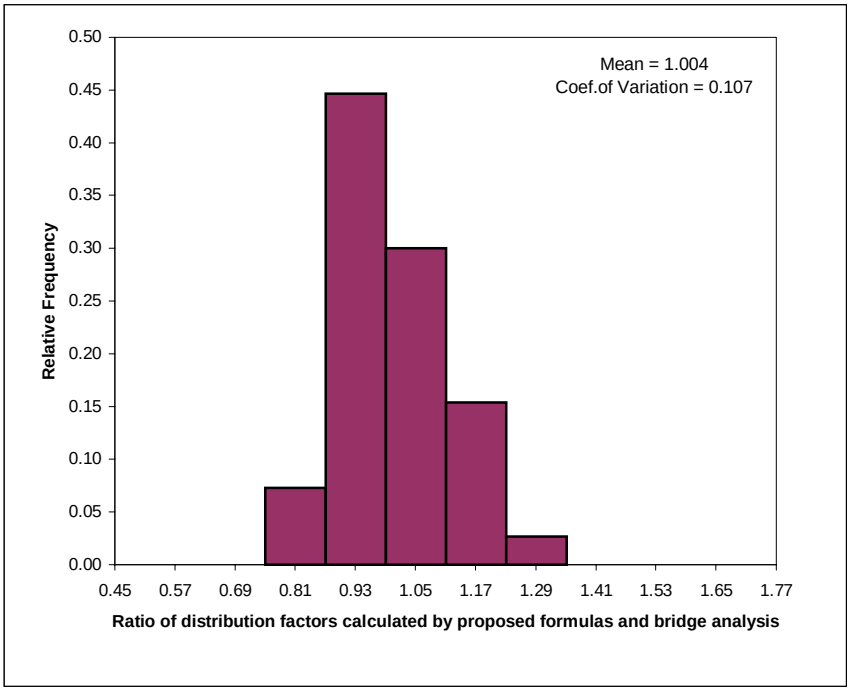

(b)

Figure B.9. Comparison of Distribution Factors calculated by Proposed Formulas and Bridge Analysis for HETS Vehicle, All Beam Bridges, Bending Moment in Interior Girders for Single Lane

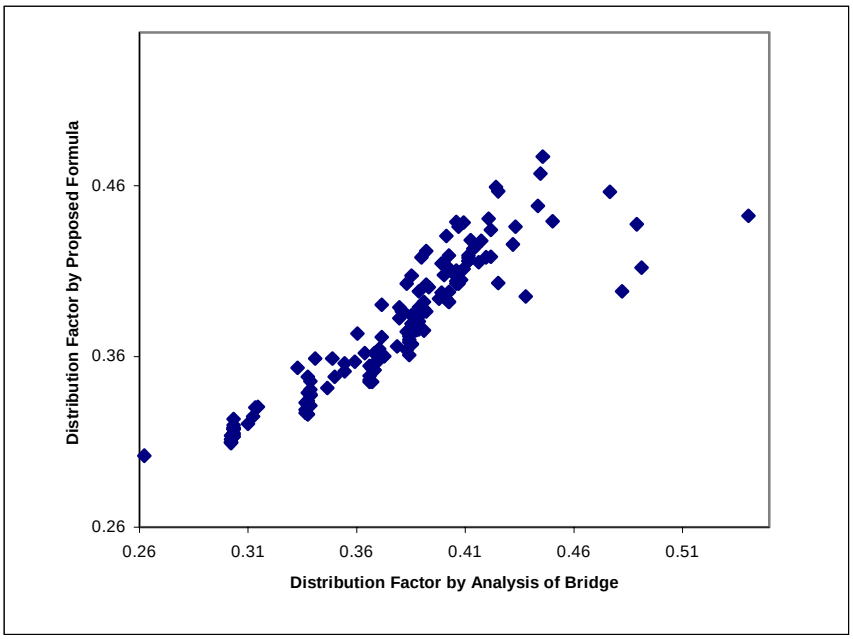

(a)

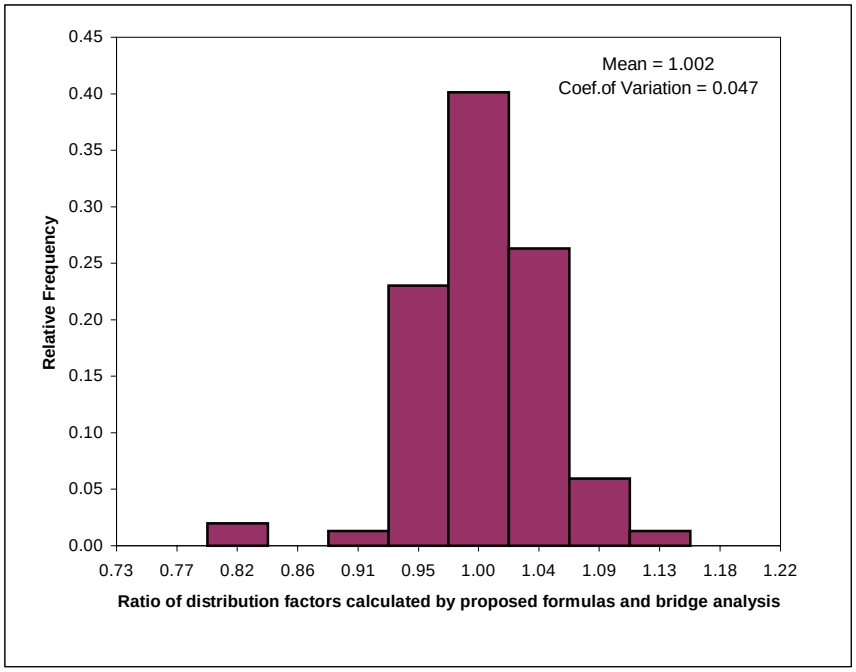

(b)

Figure B.10. Comparison of Distribution Factors calculated by Proposed Formulas and Bridge Analysis for HETS Vehicle, Steel Girders, Bending Moment in Interior Girders for Single Lane

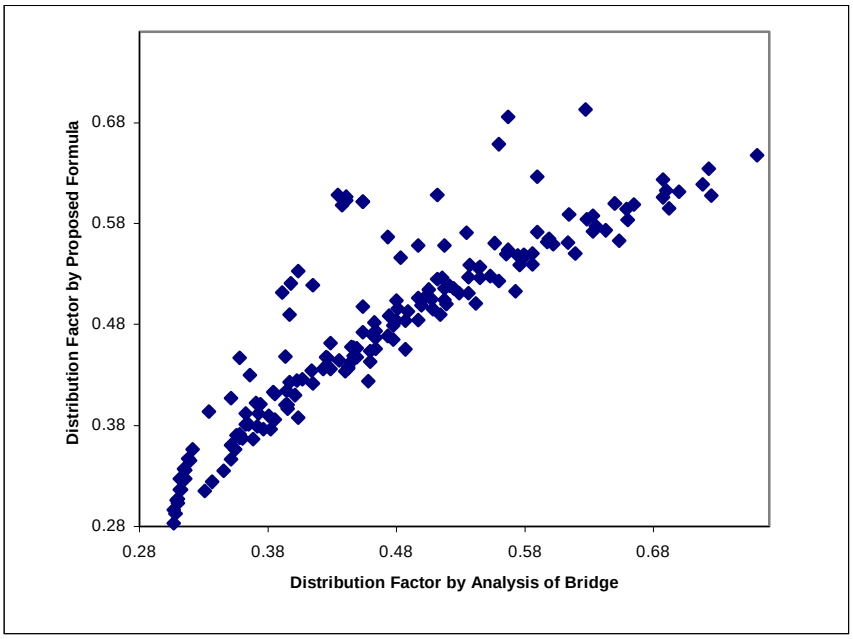

(a)

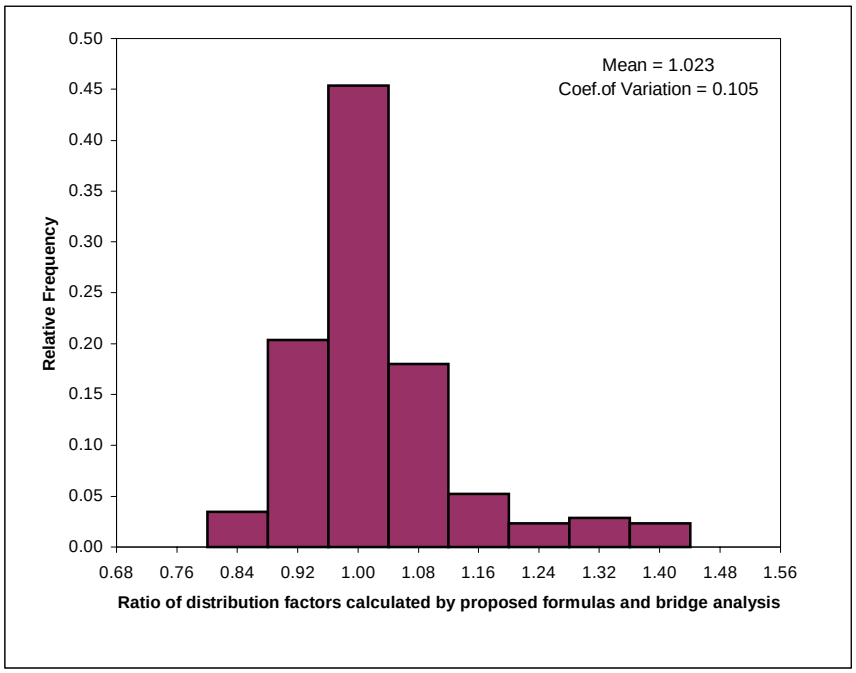

(b)

Figure B.11. Comparison of Distribution Factors calculated by Proposed Formulas and Bridge Analysis for HETS Vehicle, Prestressed Girder, Bending Moment in Interior Girders for Single Lane

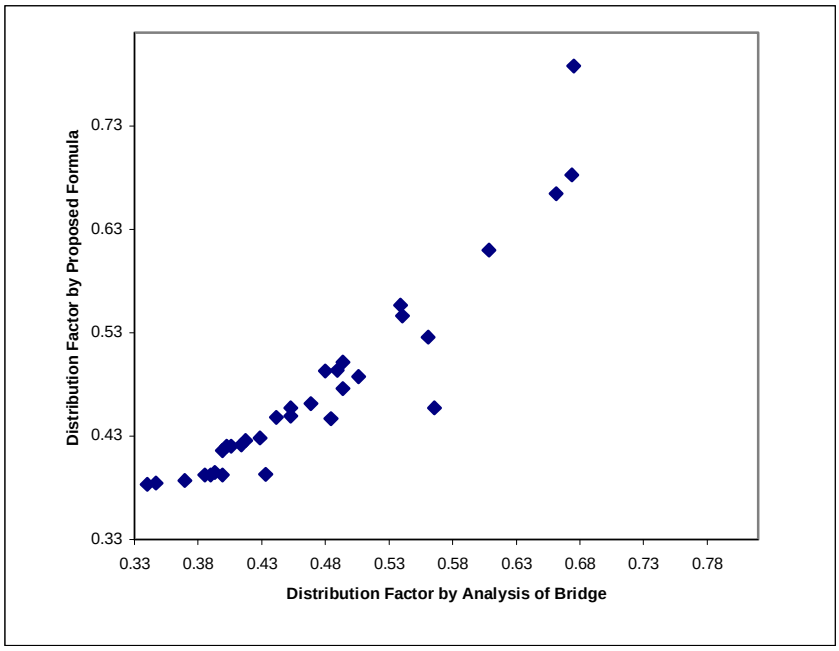

(a)

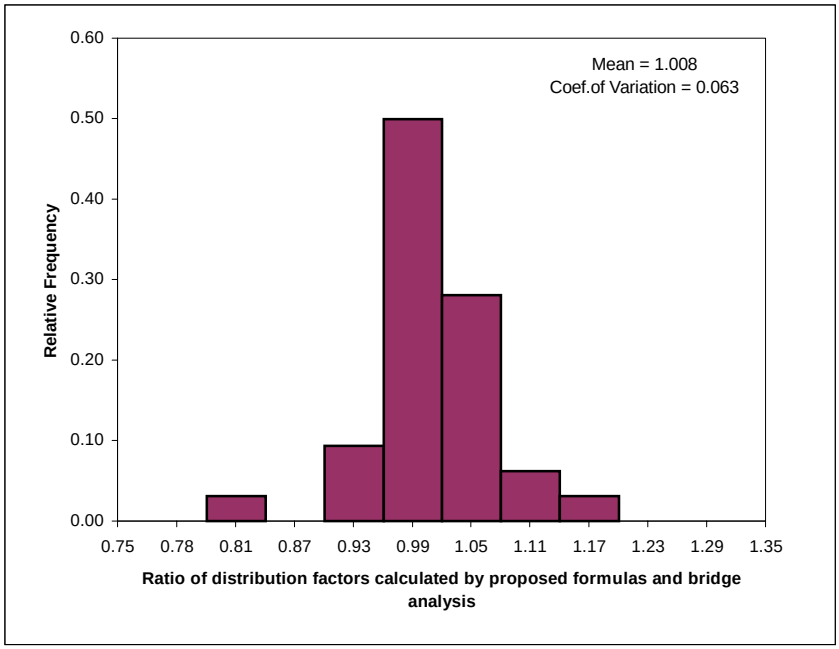

(b)

Figure B.12. Comparison of Distribution Factors calculated by Proposed Formulas and Bridge Analysis for HETS Vehicle, Concrete T-Beam, Bending Moment in Interior Girders for Single Lane

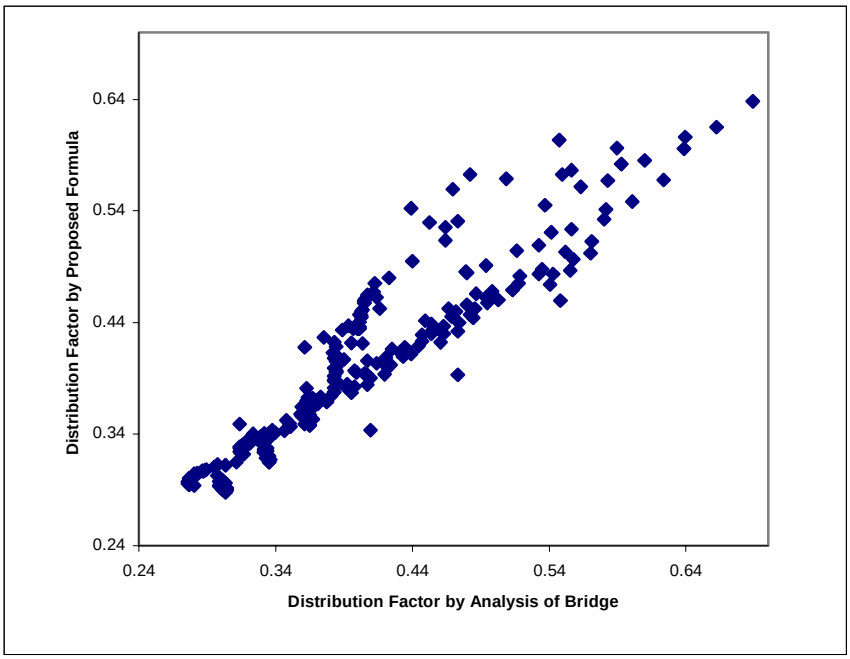

(a)

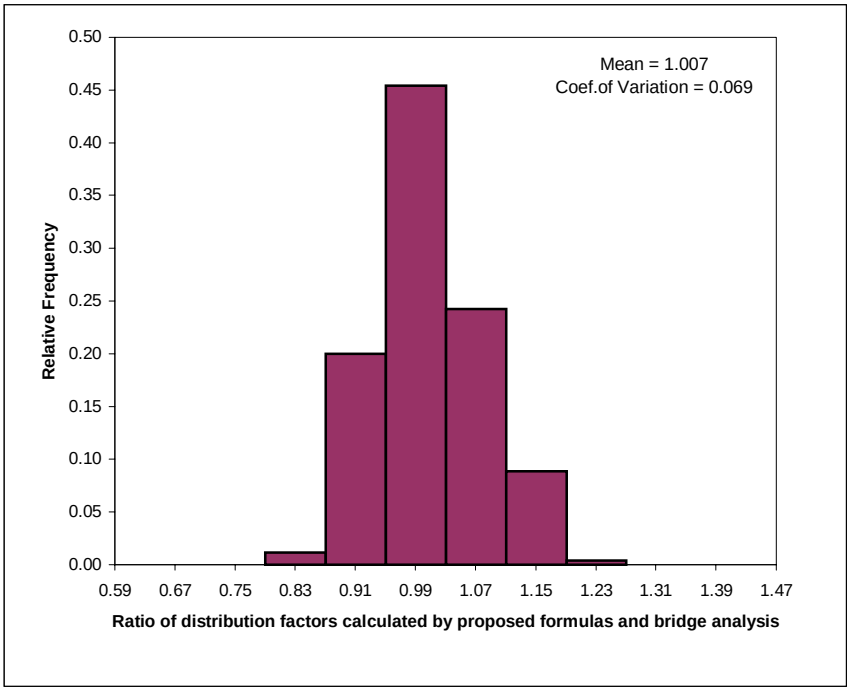

(b)

Figure B.13. Comparison of Distribution Factors calculated by Proposed Formulas and Bridge Analysis for ABRAMS Vehicle, All Beam Bridges, Bending Moment in Interior Girders for Single Lane

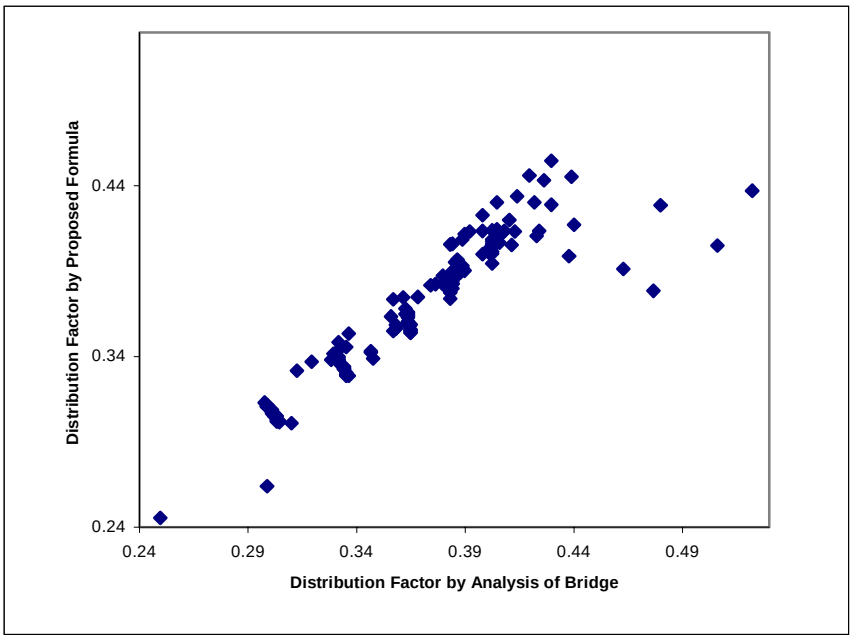

(a)

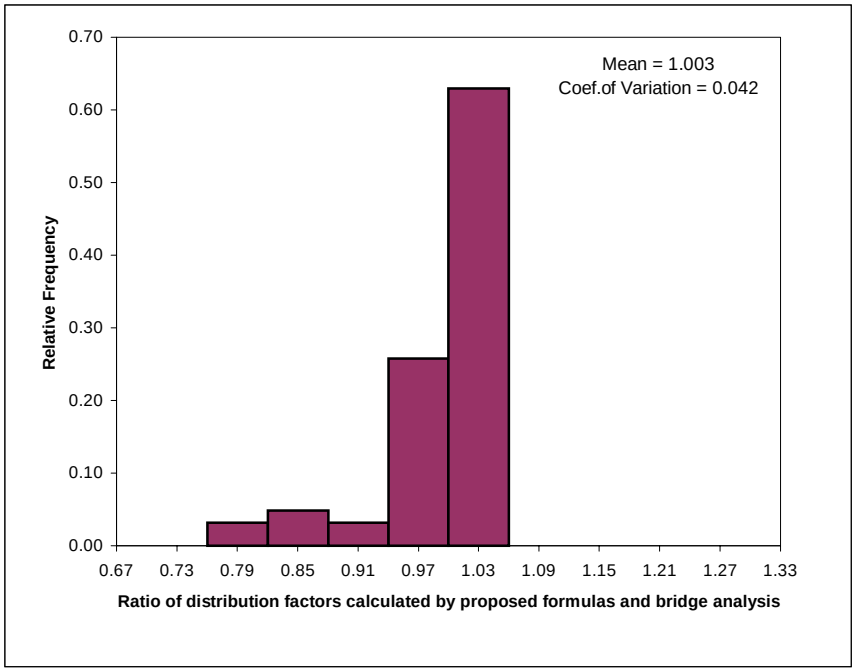

(b)

Figure B.14. Comparison of Distribution Factors calculated by Proposed Formulas and Bridge Analysis for ABRAMS Vehicle, Steel Girders, Bending Moment in Interior Girders for Single Lane

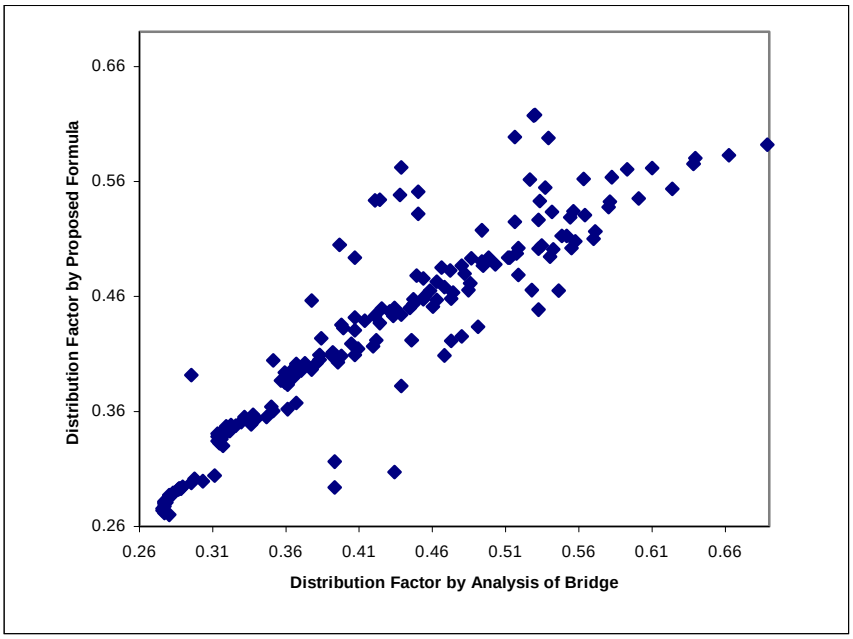

(a)

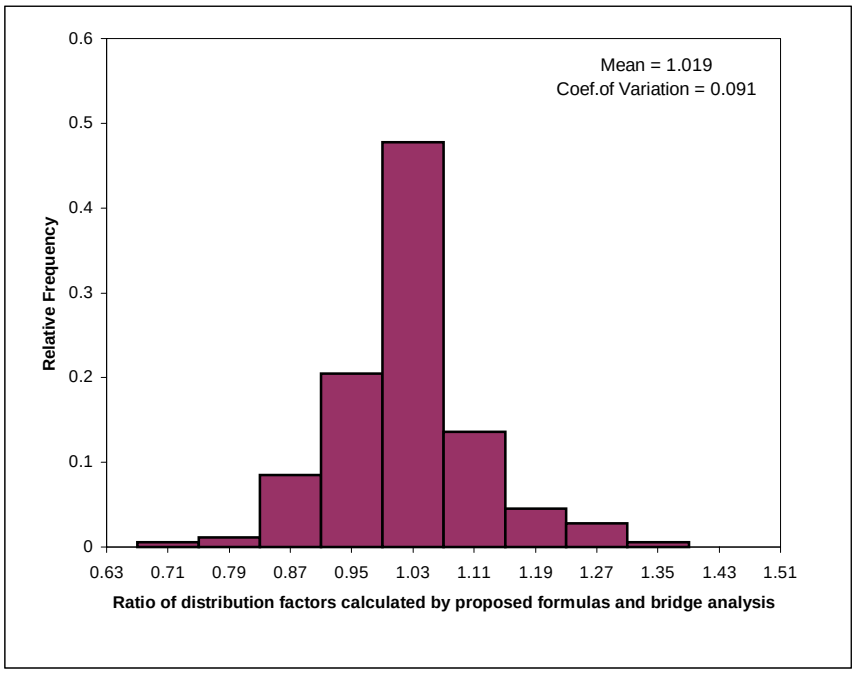

(b)

Figure B.15. Comparison of Distribution Factors calculated by Proposed Formulas and Bridge Analysis for ABRAMS Vehicle, Prestressed Girders, Bending Moment in Interior Girders for Single Lane

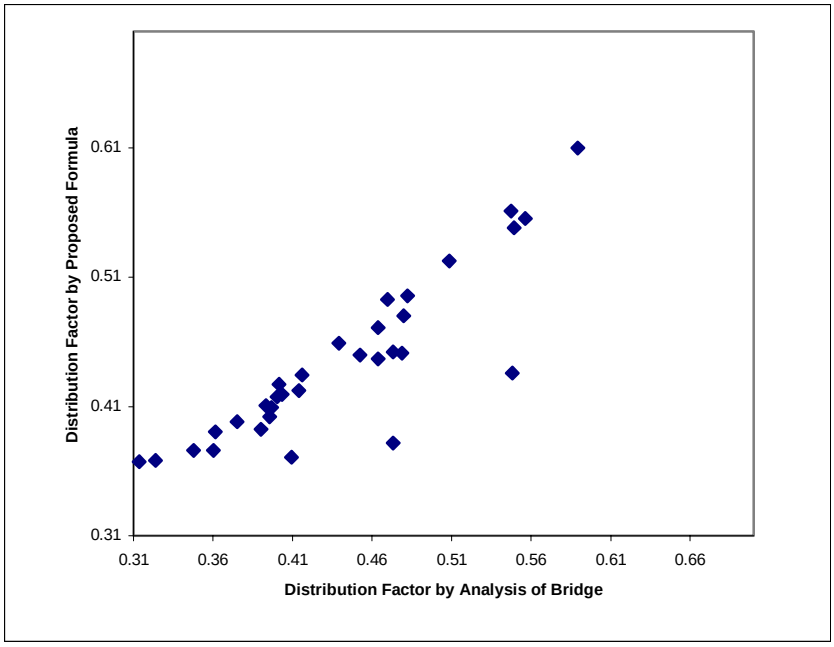

(a)

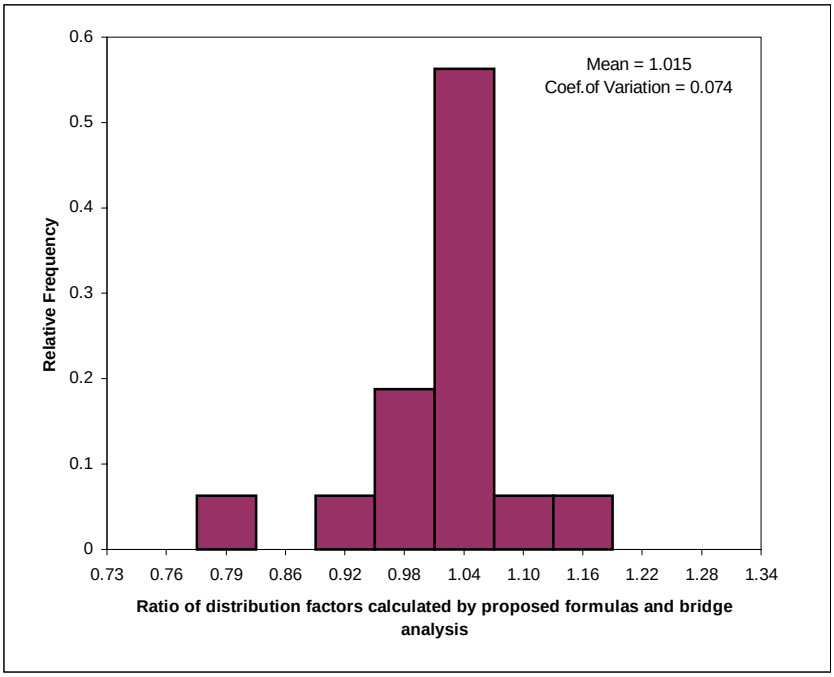

(b)

Figure B.16. Comparison of Distribution Factors calculated by Proposed Formulas and Bridge Analysis for ABRAMS Vehicle, Concrete T-Beam, Bending Moment in Interior Girders for Single Lane

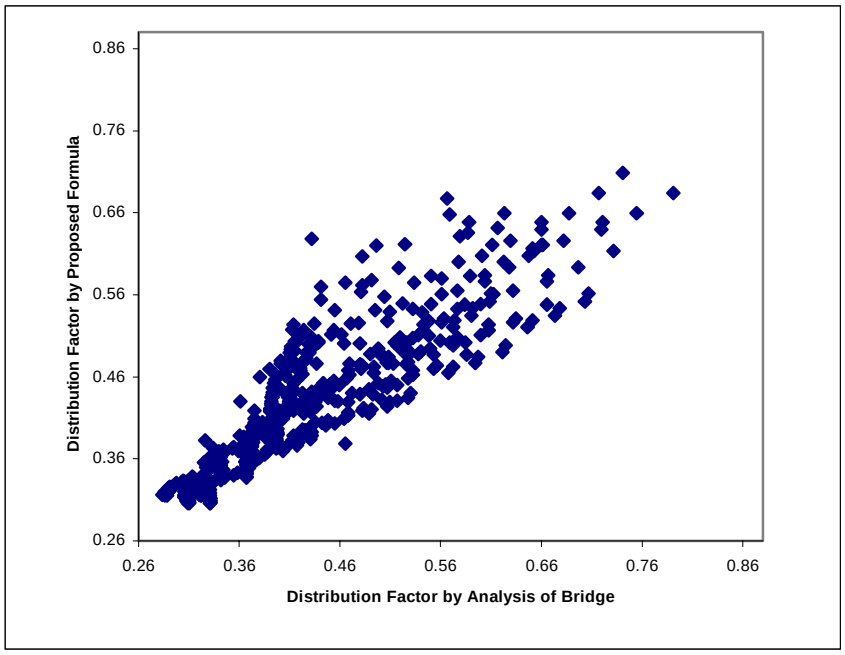

(a)

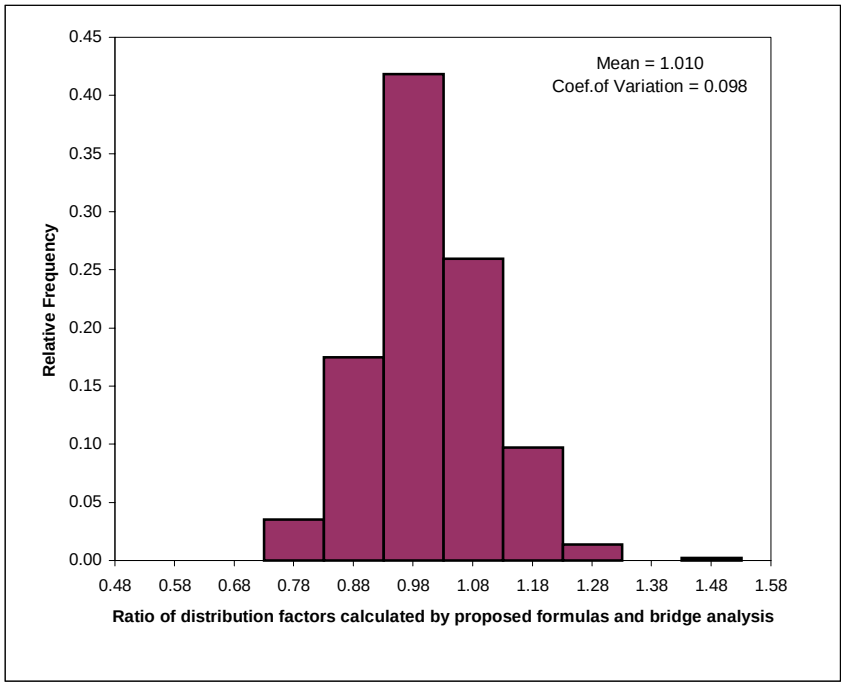

(b)

Figure B.17. Comparison of Distribution Factors calculated by Proposed Formulas and Bridge Analysis for M113 and Bradley Vehicles, All Beam Bridges, Bending Moment in Interior Girders for Single Lane

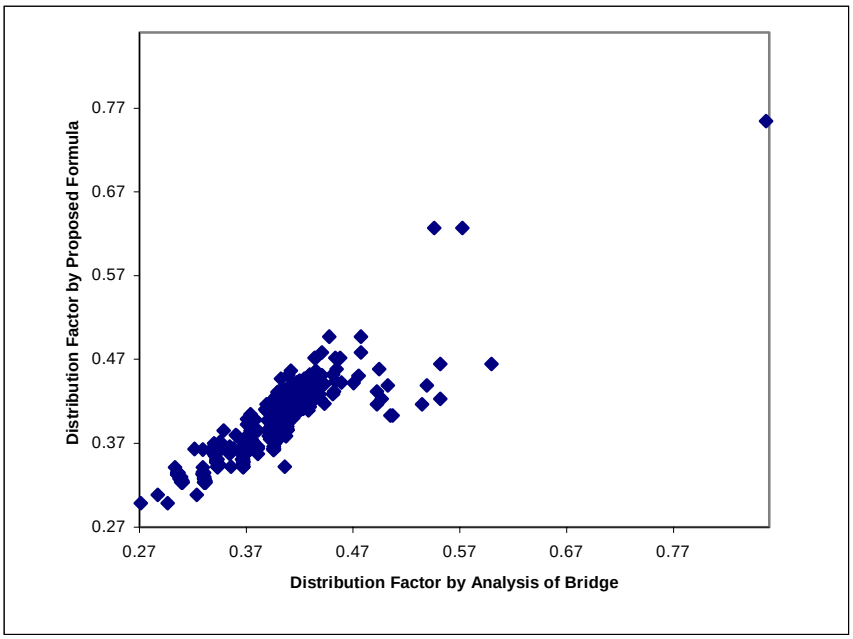

(a)

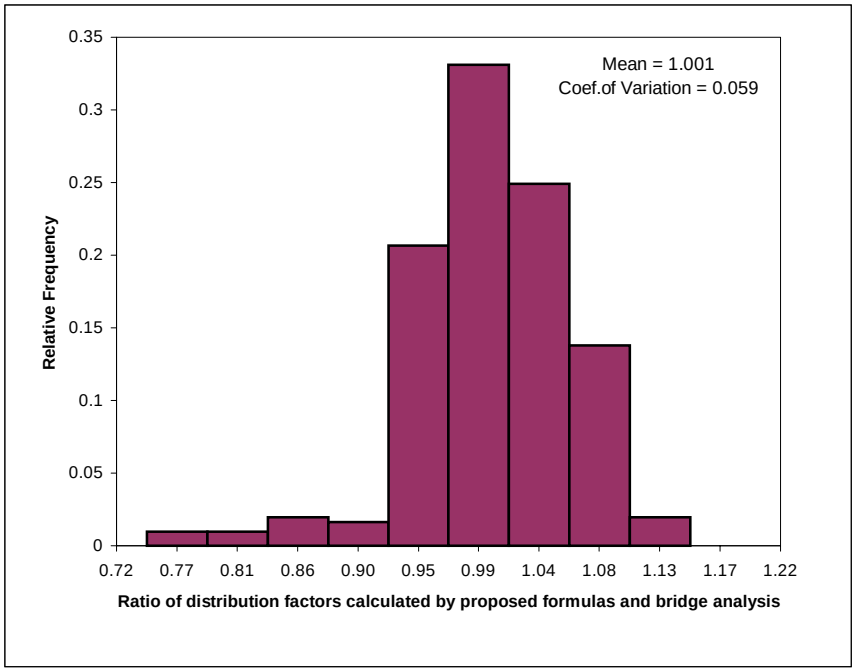

(b)

Figure B.18. Comparison of Distribution Factors calculated by Proposed Formulas and Bridge Analysis for M113 and Bradley Vehicles, Steel Girders, Bending Moment in Interior Girders for Single Lane

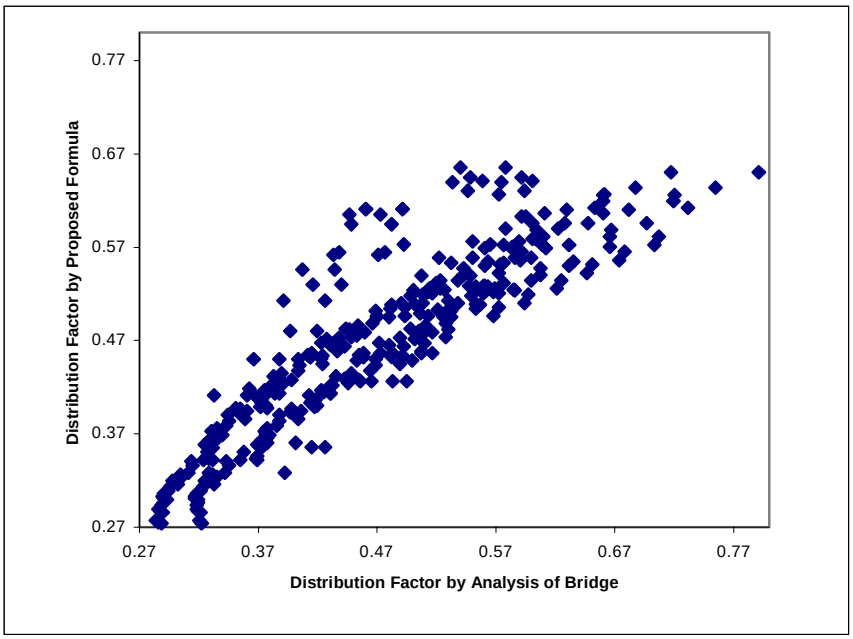

(a)

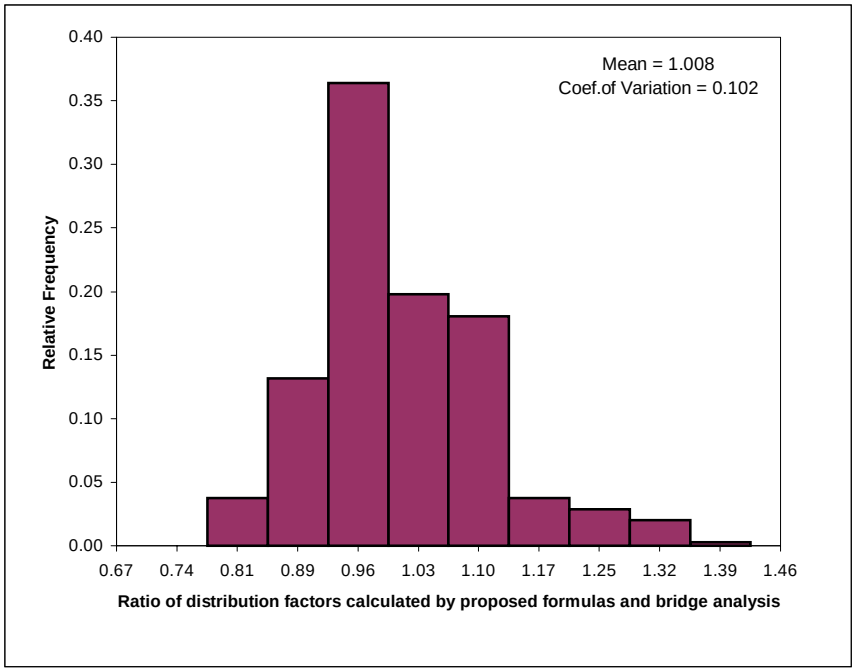

(b)

Figure B.19. Comparison of Distribution Factors calculated by Proposed Formulas and Bridge Analysis for M113 and Bradley Vehicles, Prestressed Girders, Bending Moment in Interior Girders for Single Lane

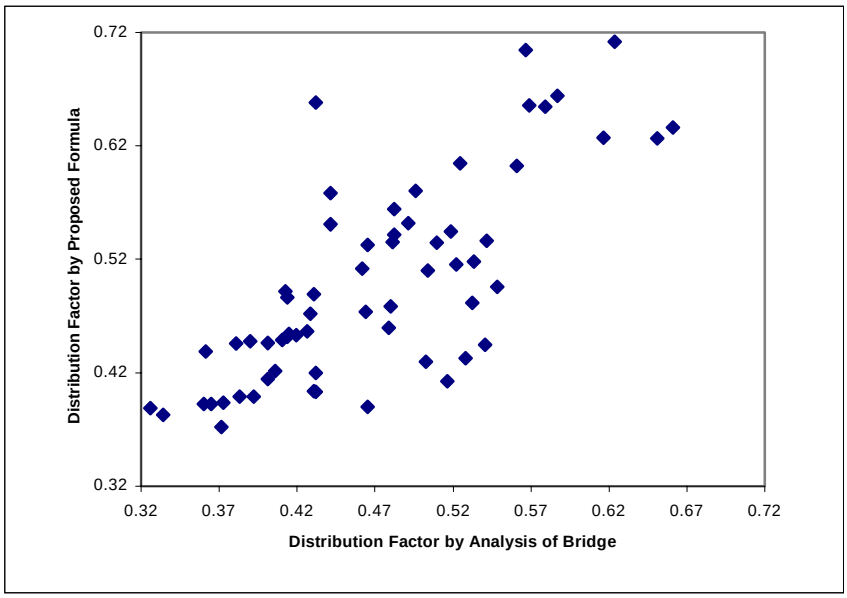

(a)

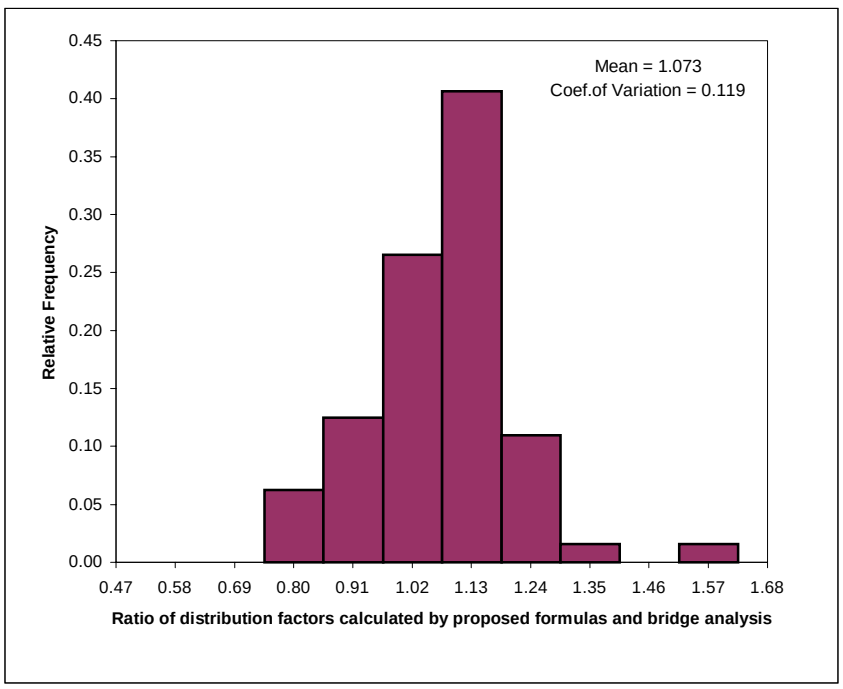

(b)

Figure B.20. Comparison of Distribution Factors calculated by Proposed Formulas and Bridge Analysis for M113 and Bradley Vehicles, Concrete T-Beam, Bending Moment in Interior Girders for Single Lane

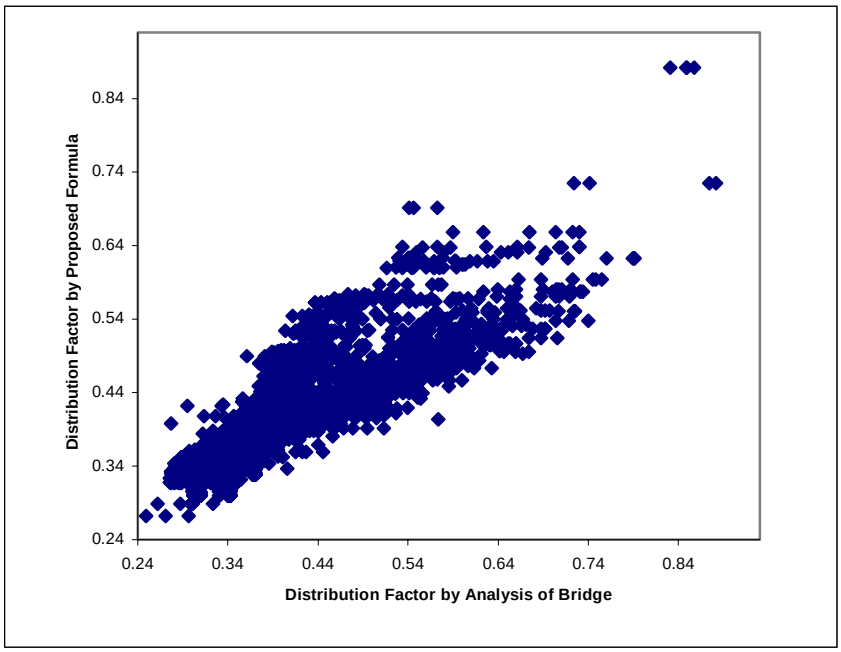

(a)

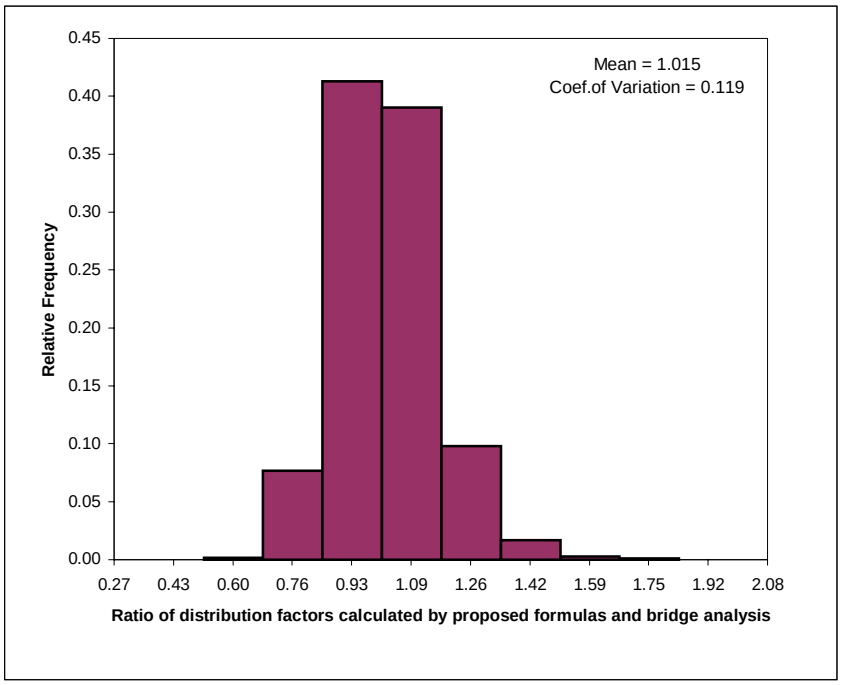

(b)

Figure B.21. Comparison of Distribution Factors calculated by Proposed Formulas and Bridge Analysis for All Vehicles, All Beam Bridges, Bending Moment in Interior Girders for Single Lane

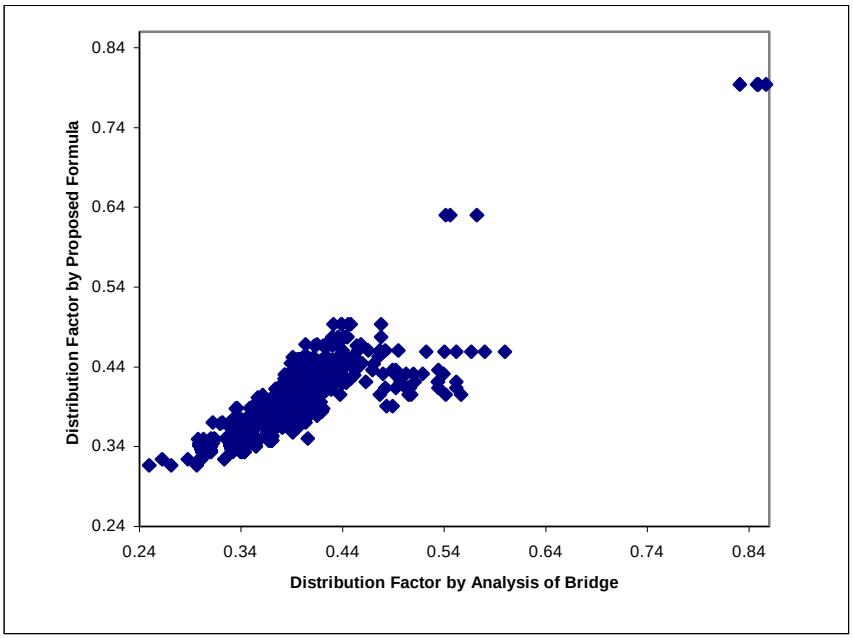

(a)

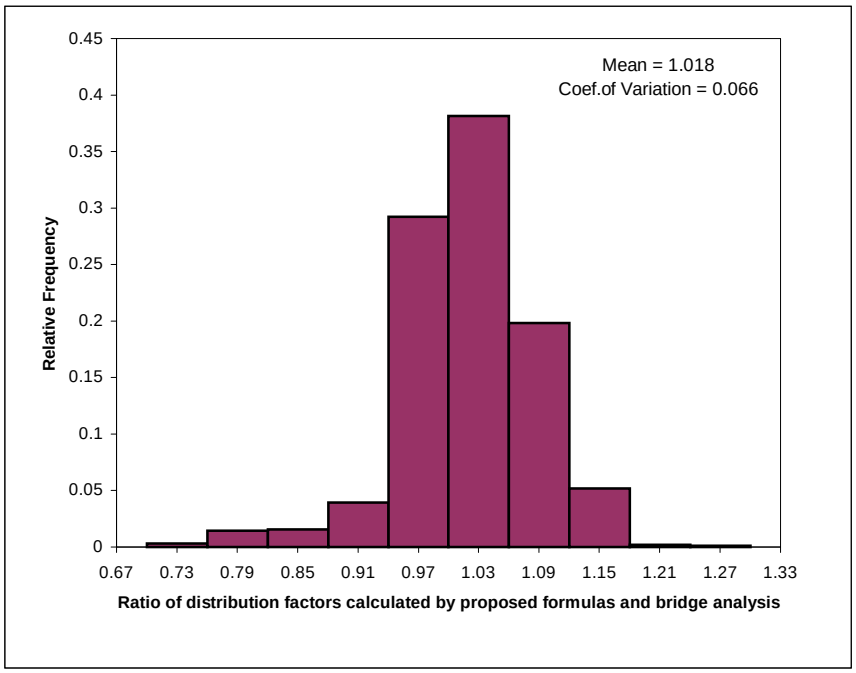

(b)

Figure B.22. Comparison of Distribution Factors calculated by Proposed Formulas and Bridge Analysis for All Vehicles, Steel Girders, Bending Moment in Interior Girders for Single Lane

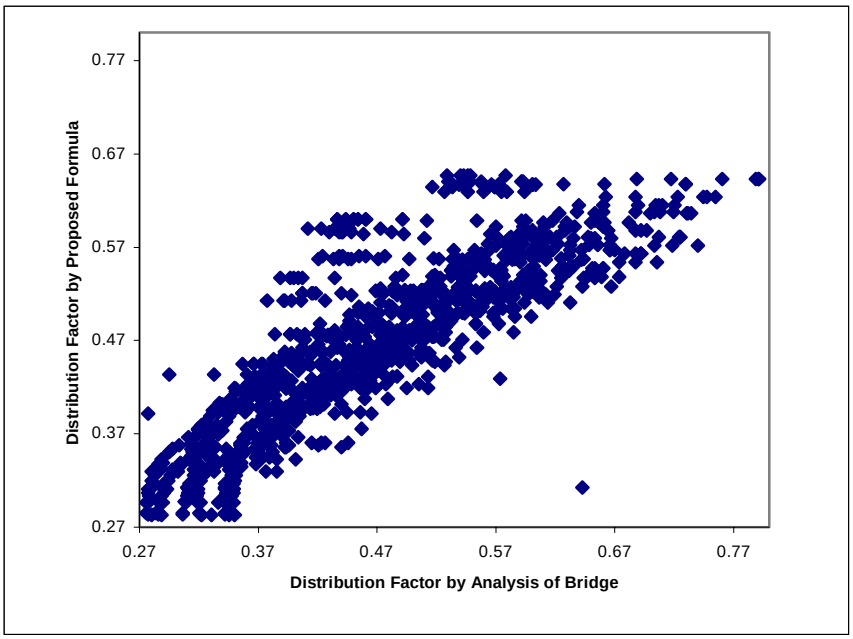

(a)

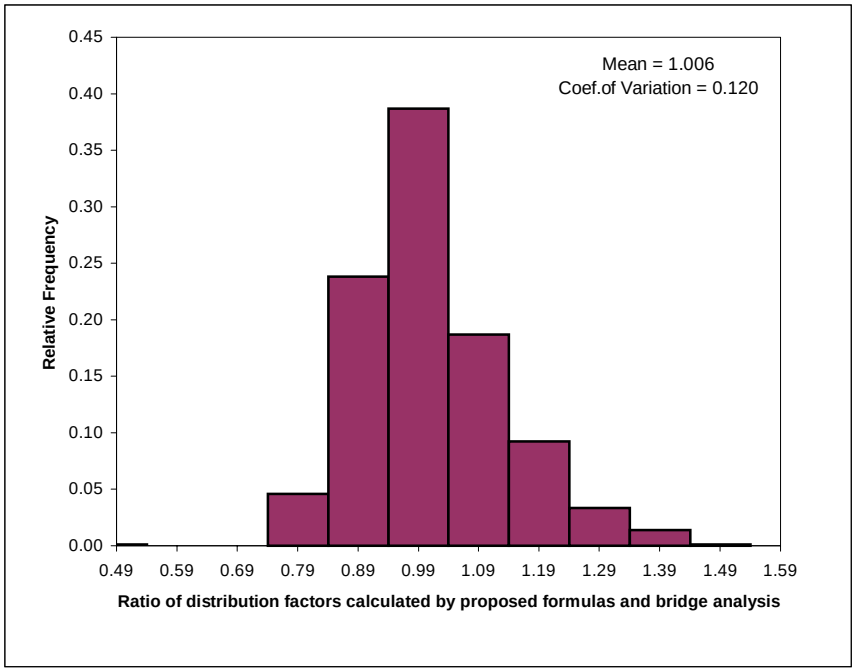

(b)

Figure B.23. Comparison of Distribution Factors calculated by Proposed Formulas and Bridge Analysis for All Vehicles, Prestressed Girders, Bending Moment in Interior Girders for Single Lane

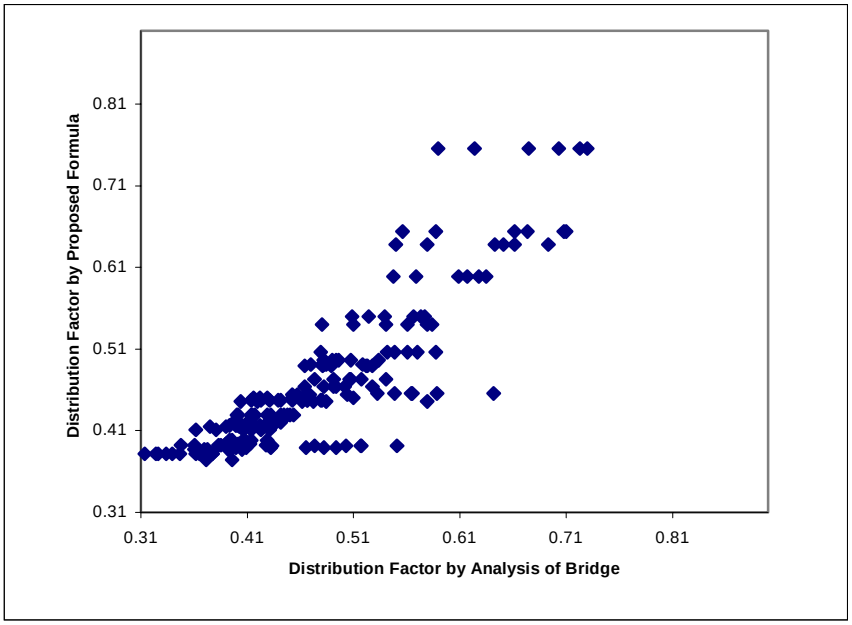

(a)

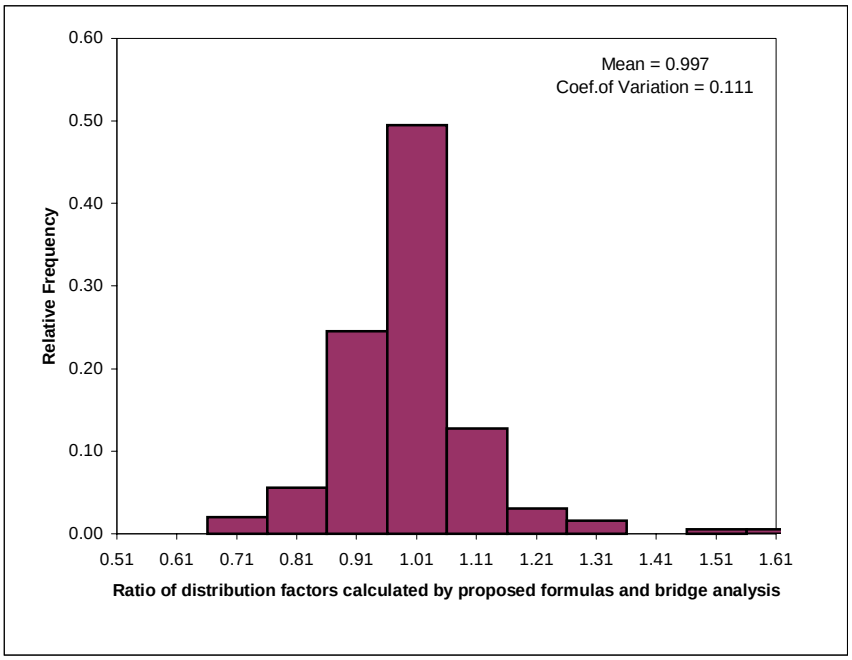

(b)

Figure B.24. Comparison of Distribution Factors calculated by Proposed Formulas and Bridge Analysis for All Vehicles, Concrete T-Beam, Bending Moment in Interior Girders for Single Lane

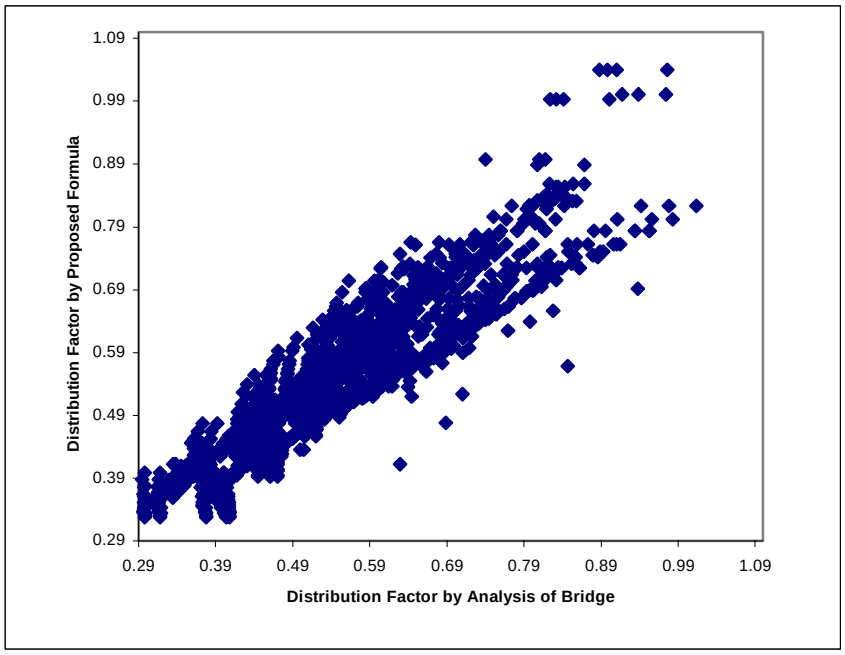

(a)

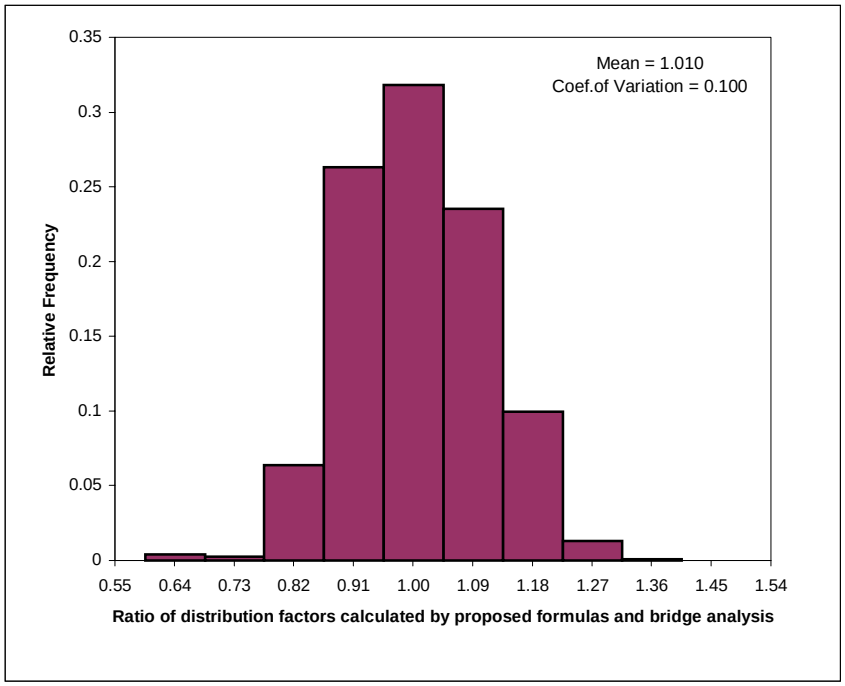

(b)

Figure B.25. Comparison of Distribution Factors calculated by Proposed Formulas and Bridge Analysis for All Vehicles, All Beam Bridges, Bending Moment in Interior Girders for Multi Lane

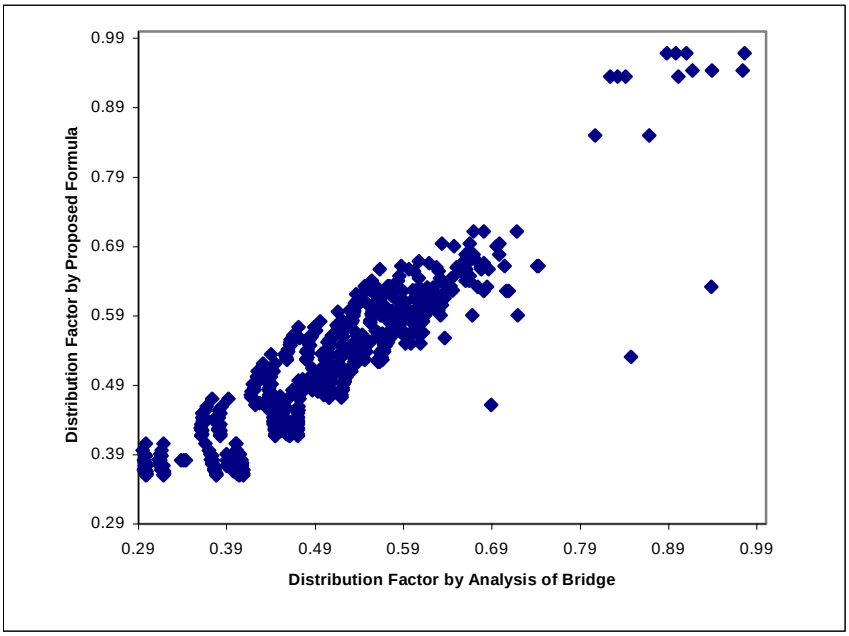

(a)

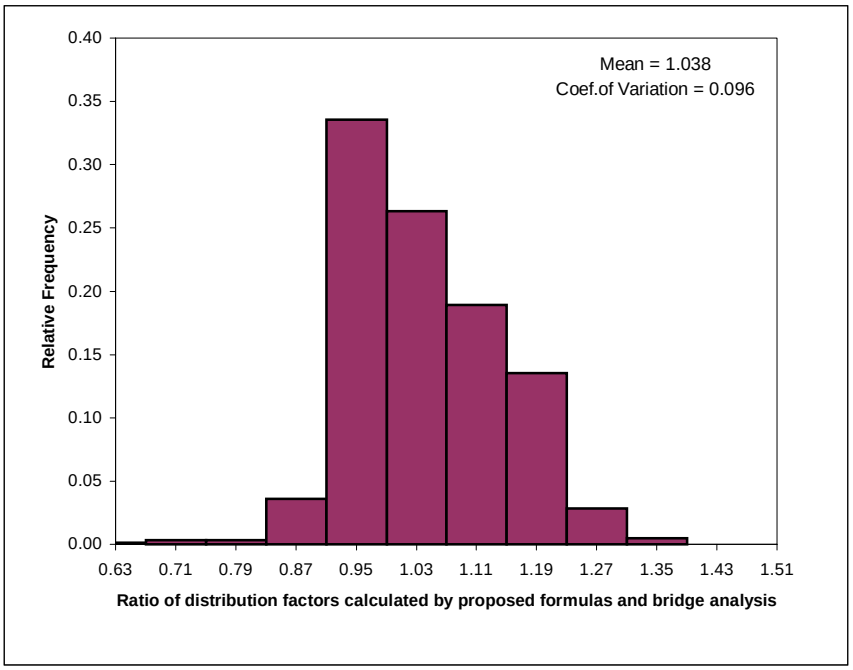

(b)

Figure B.26. Comparison of Distribution Factors calculated by Proposed Formulas and Bridge Analysis for All Vehicles, Steel Girders, Bending Moment in Interior Girders for Multi Lane

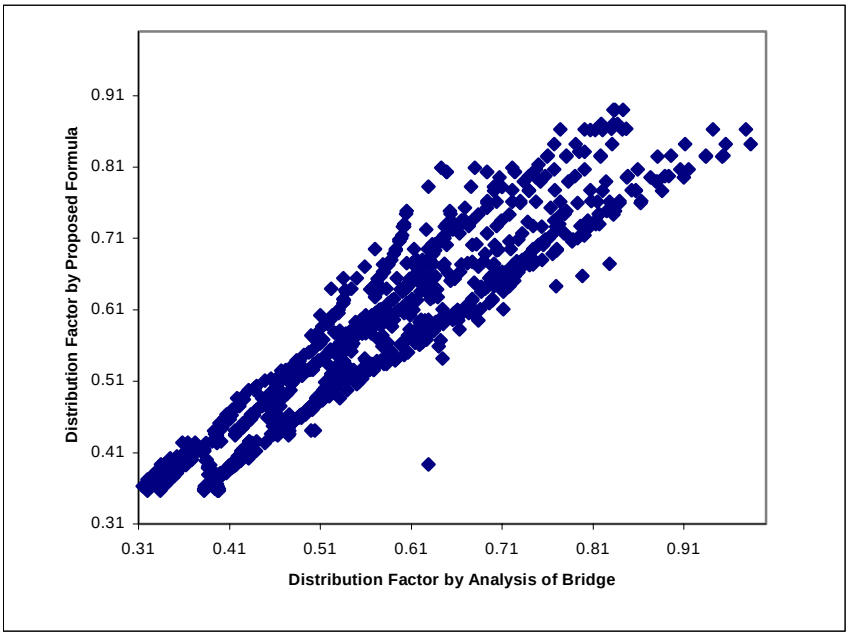

(a)

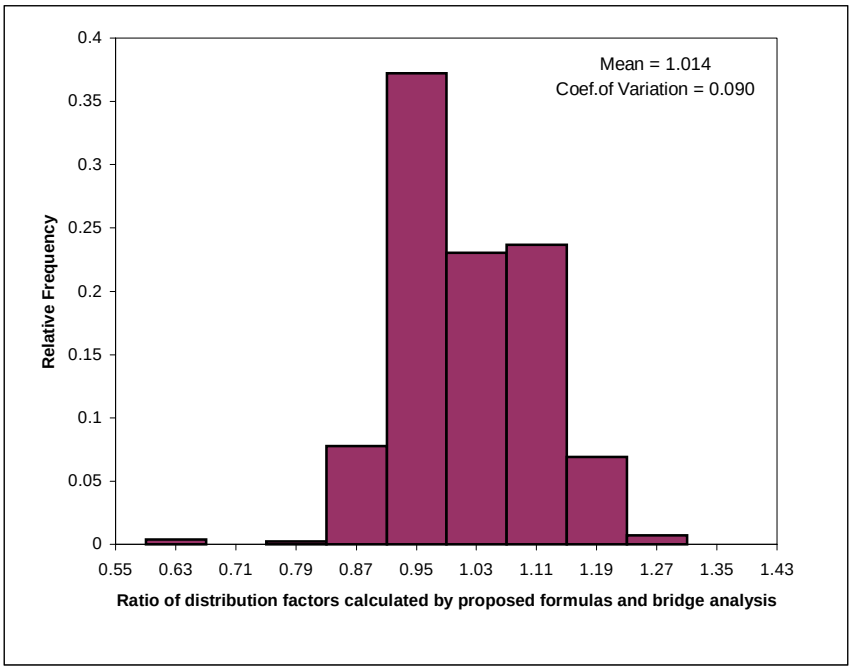

(b)

Figure B.27. Comparison of Distribution Factors calculated by Proposed Formulas and Bridge Analysis for All Vehicles, Prestressed Girders, Bending Moment in Interior Girders for Multi Lane

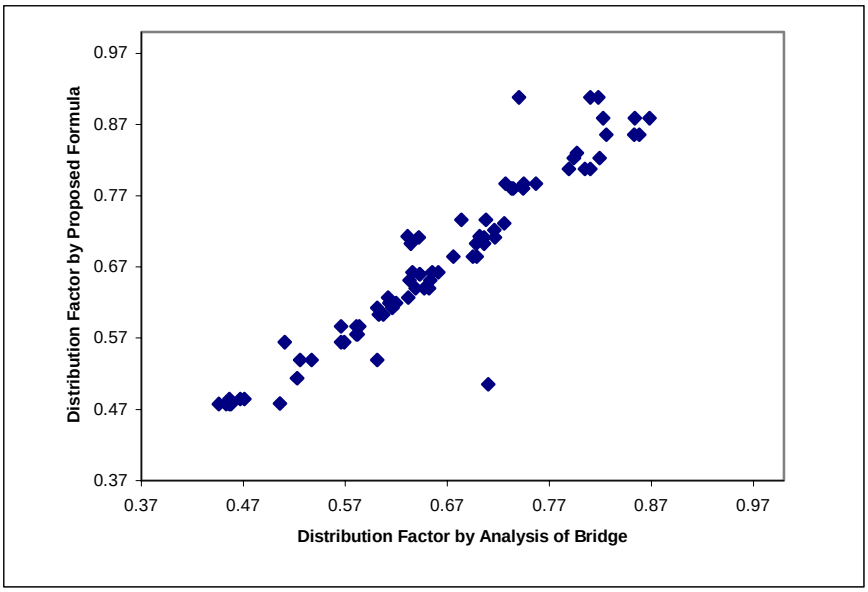

(a)

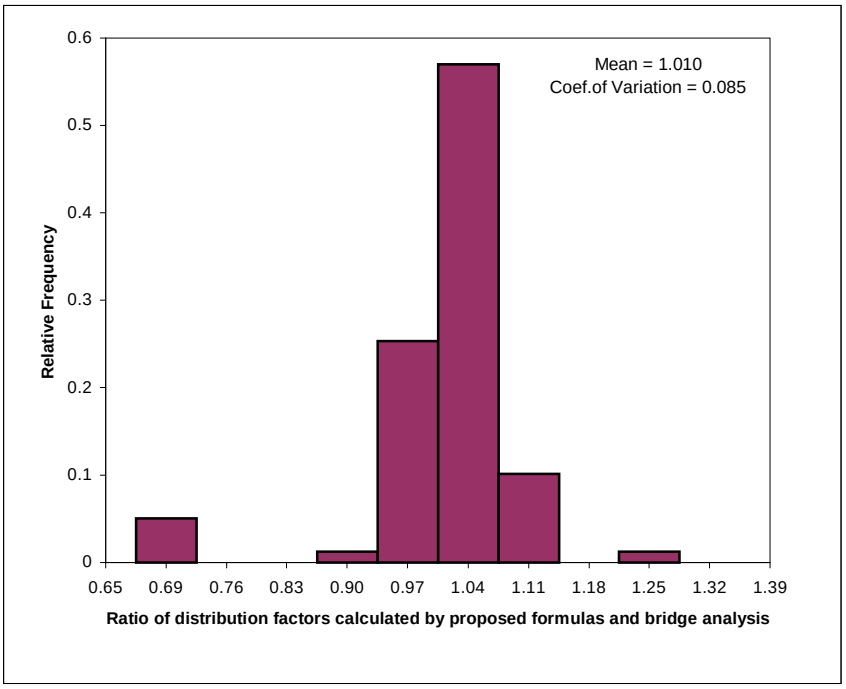

(b)

Figure B.28. Comparison of Distribution Factors calculated by Proposed Formulas and Bridge Analysis for All Vehicles, Concrete T-Beam, Bending Moment in Interior Girders for Multi Lane

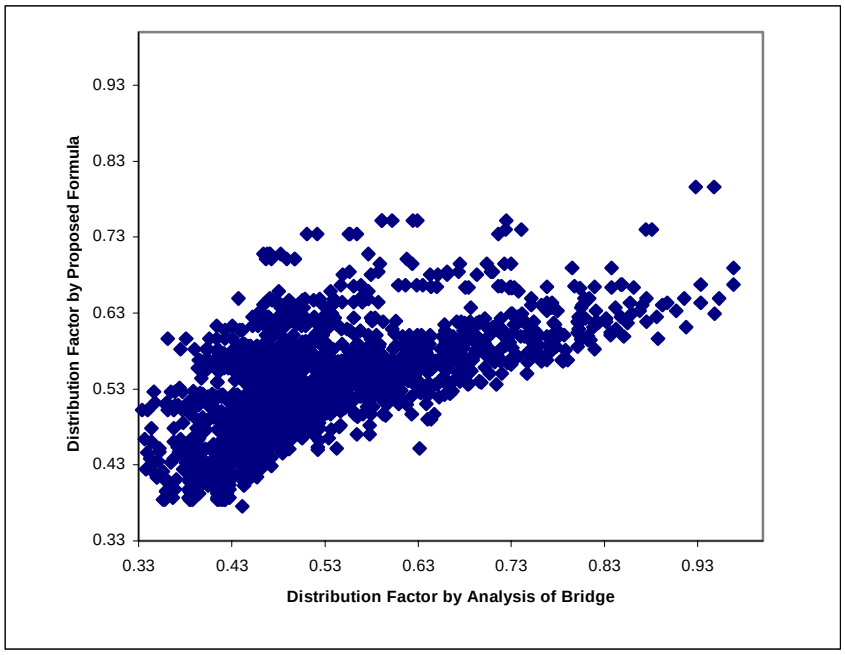

(a)

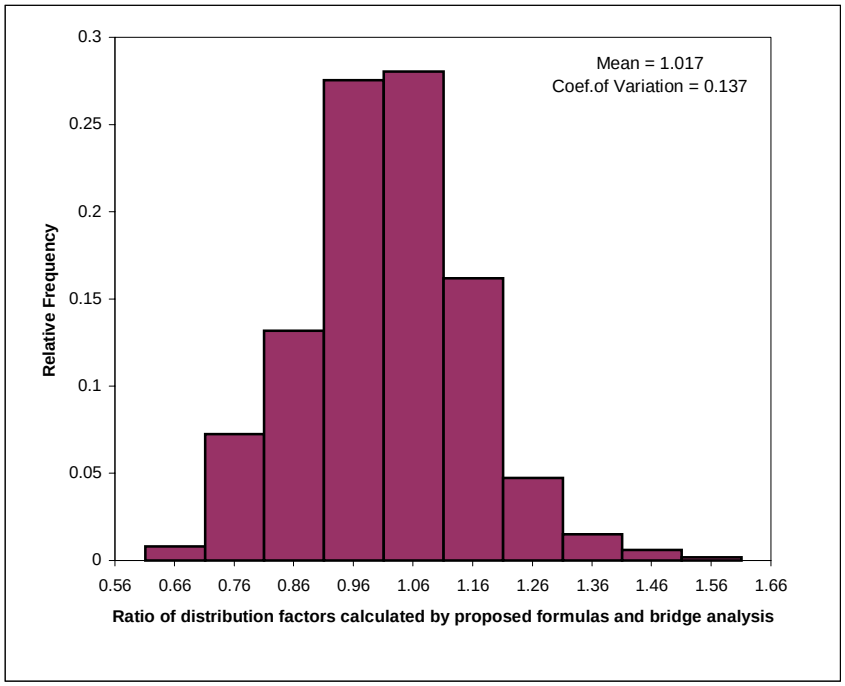

(b)

Figure B.29. Comparison of Distribution Factors calculated by Proposed Formulas and Bridge Analysis for All Vehicles, All Beam Bridges, Shear in Interior Girders for Single Lane

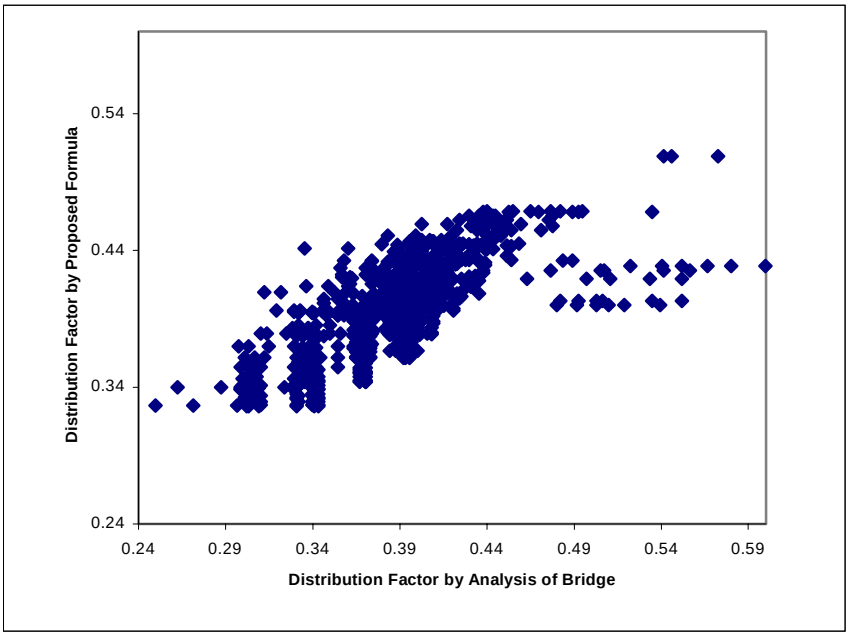

(a)

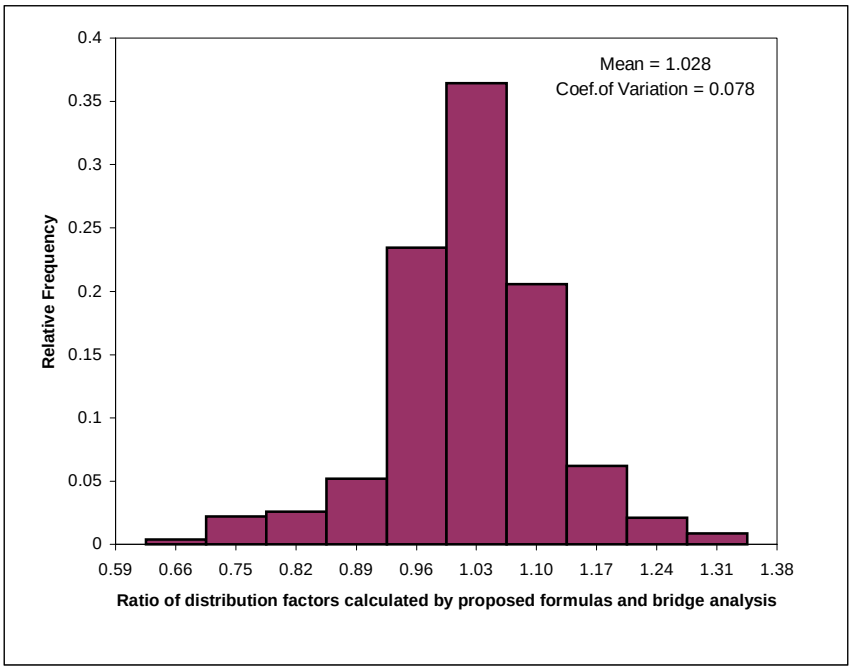

(b)

Figure B.30. Comparison of Distribution Factors calculated by Proposed Formulas and Bridge Analysis for All Vehicles, Steel Girders, Shear in Interior Girders for Single Lane

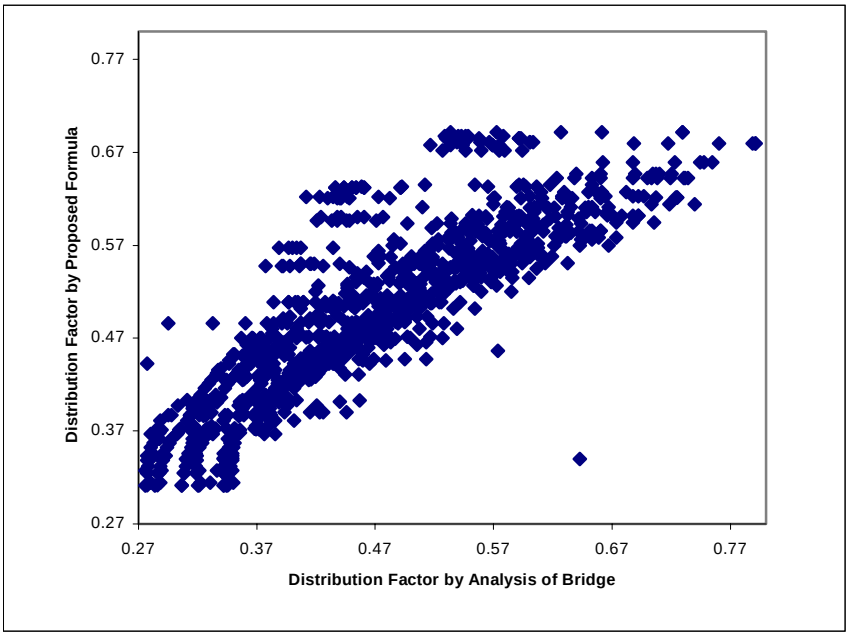

(a)

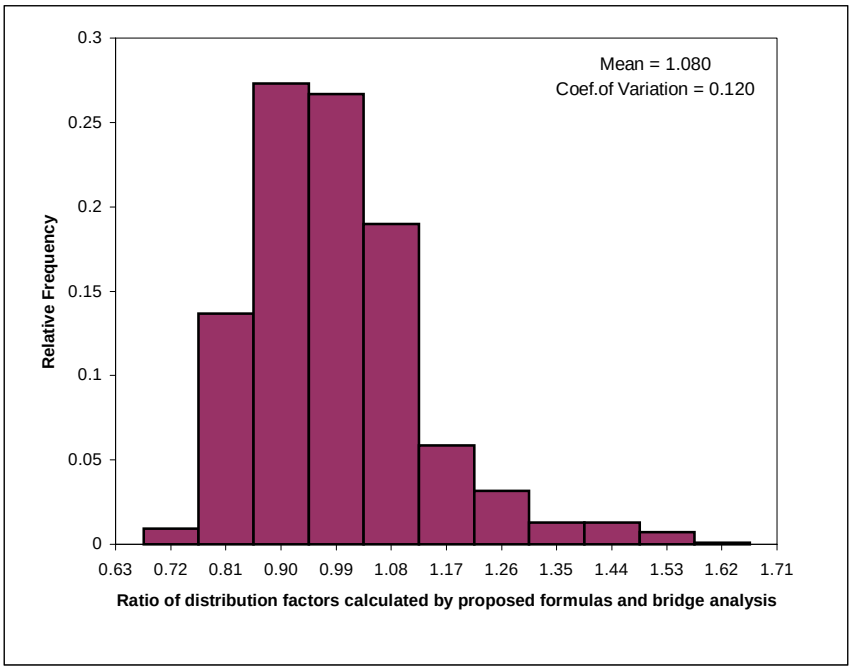

(b)

Figure B.31. Comparison of Distribution Factors calculated by Proposed Formulas and Bridge Analysis for All Vehicles, Prestressed Girders, Shear in Interior Girders for Single Lane

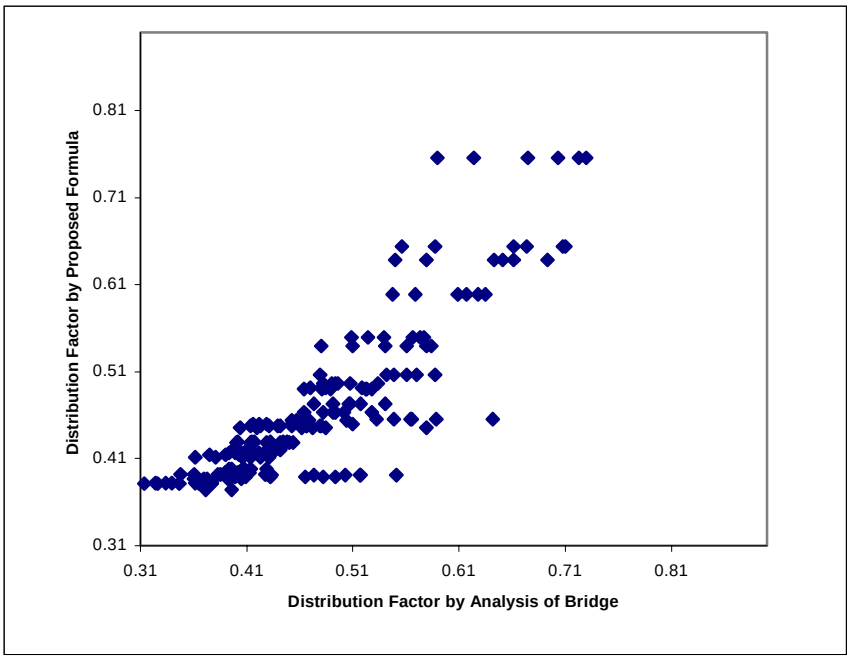

(a)

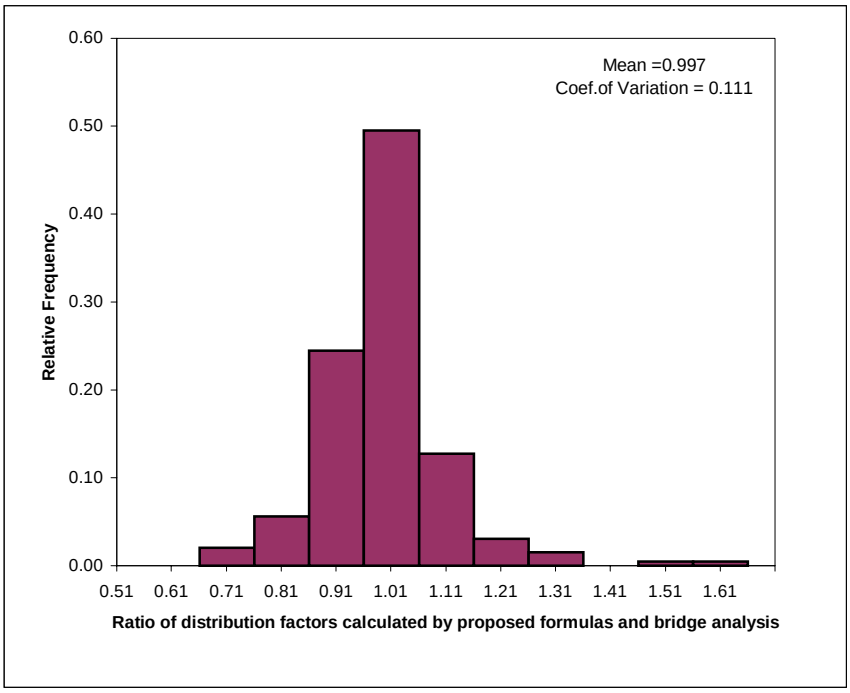

(b)

Figure B.32. Comparison of Distribution Factors calculated by Proposed Formulas and Bridge Analysis for All Vehicles, Concrete T-Beam, Shear in Interior Girders for Single Lane

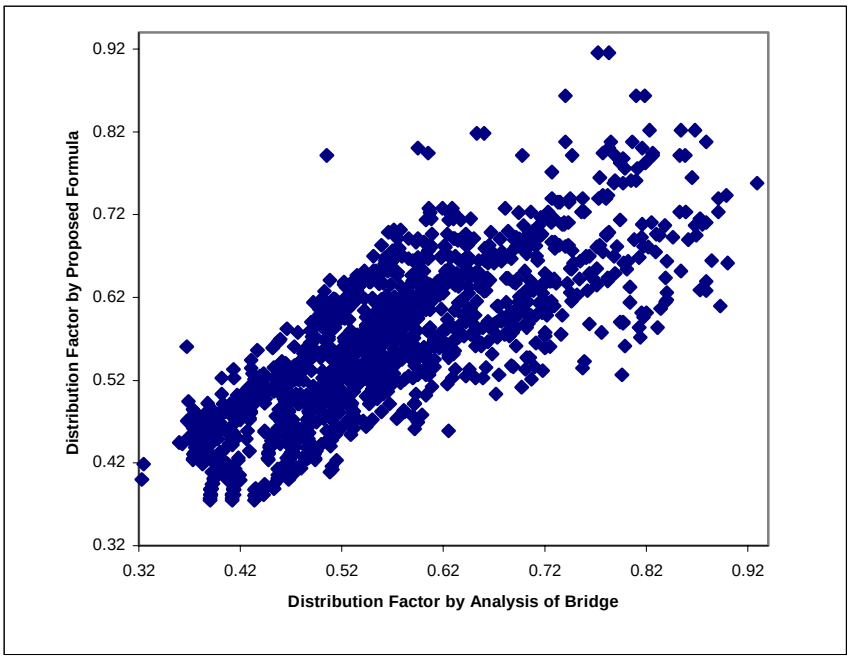

(a)

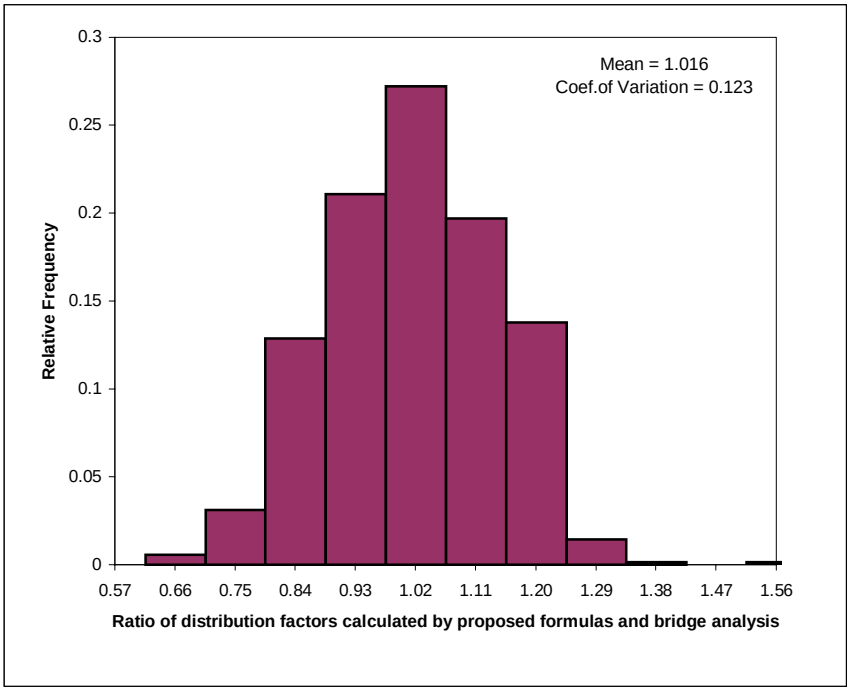

(b)

Figure B.33. Comparison of Distribution Factors calculated by Proposed Formulas and Bridge Analysis for All Vehicles, All Beam Bridges, Shear in Interior Girders for Multi Lane

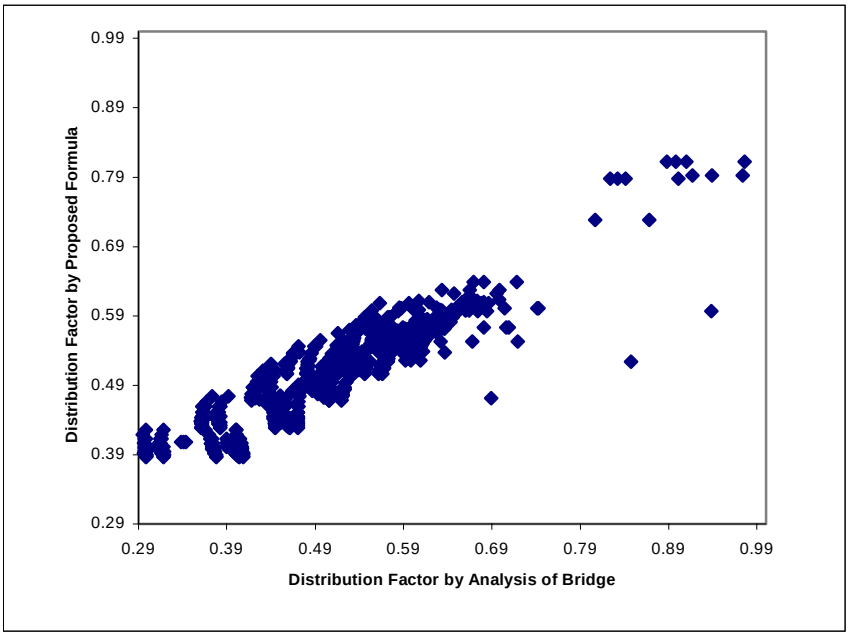

(a)

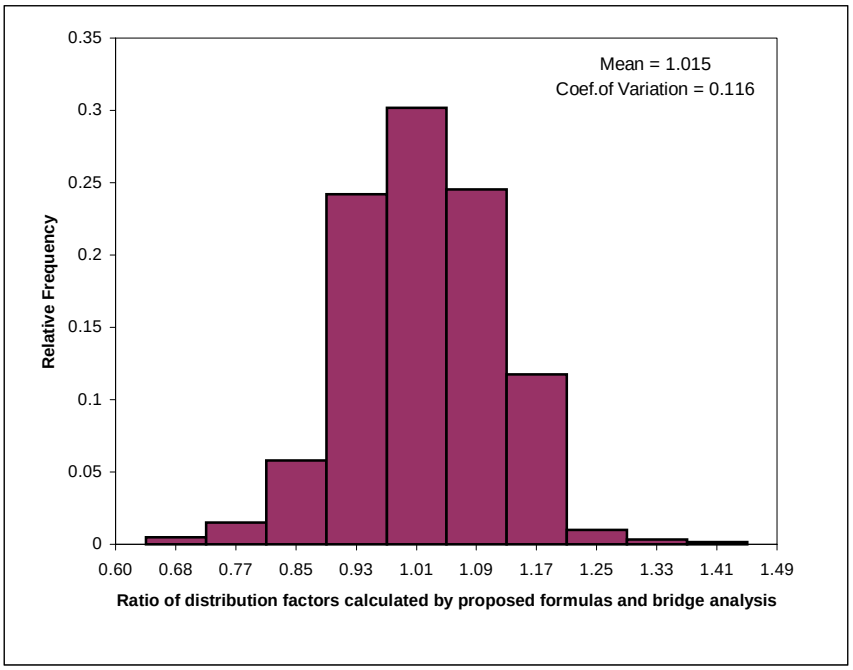

(b)

Figure B.34. Comparison of Distribution Factors calculated by Proposed Formulas and Bridge Analysis for All Vehicles, Steel Girders, Shear in Interior Girders for Multi Lane

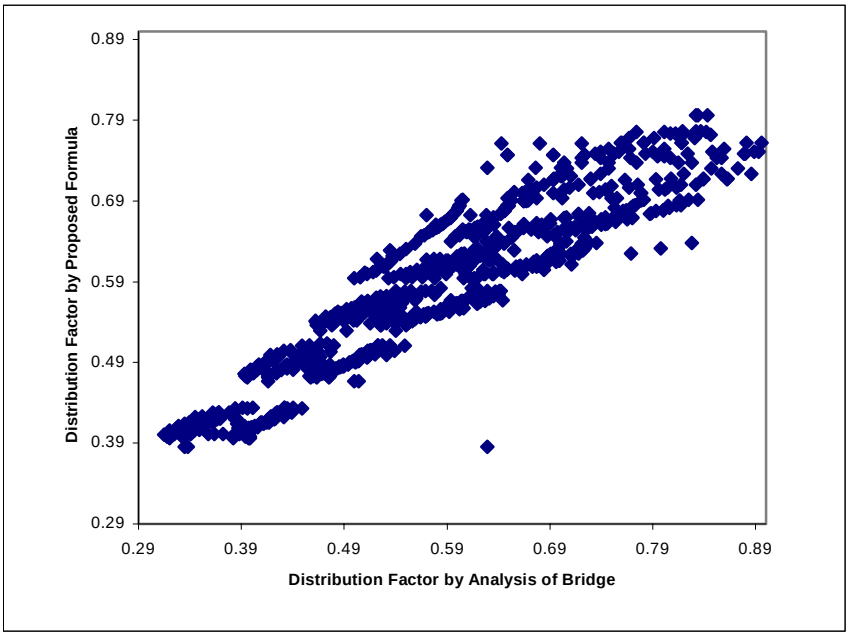

(a)

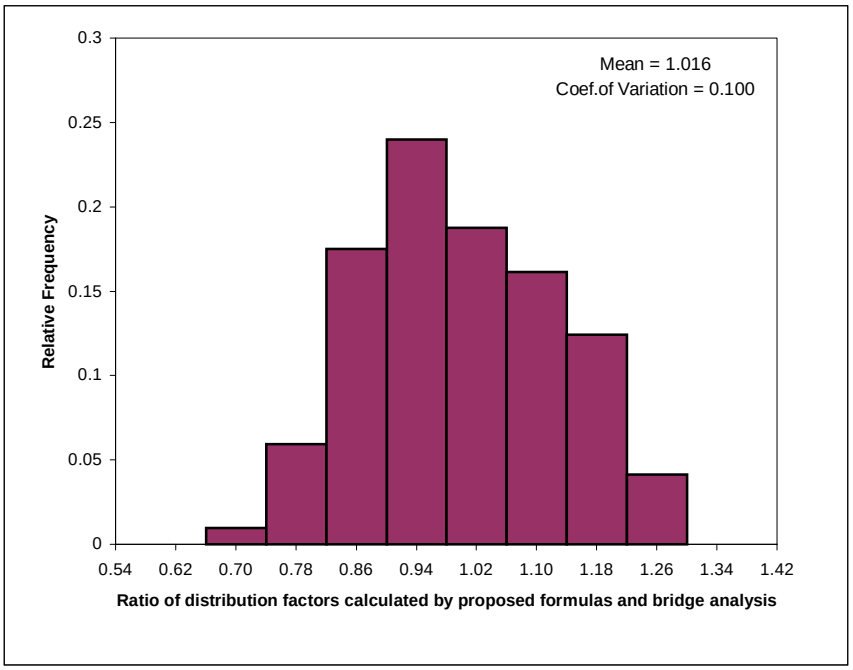

(b)

Figure B.35. Comparison of Distribution Factors calculated by Proposed Formulas and Bridge Analysis for All Vehicles, Prestressed Girders, Shear in Interior Girders for Multi Lane

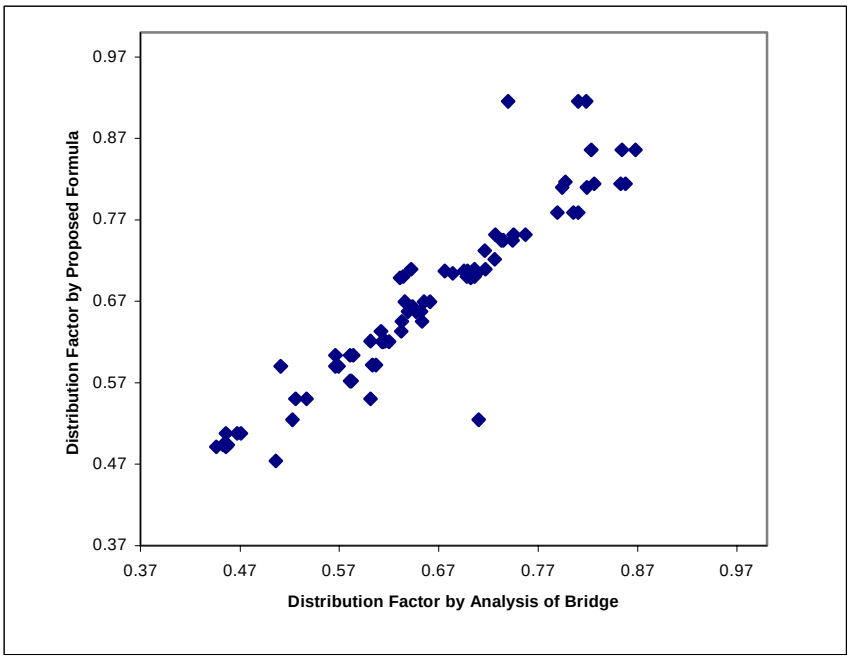

(a)

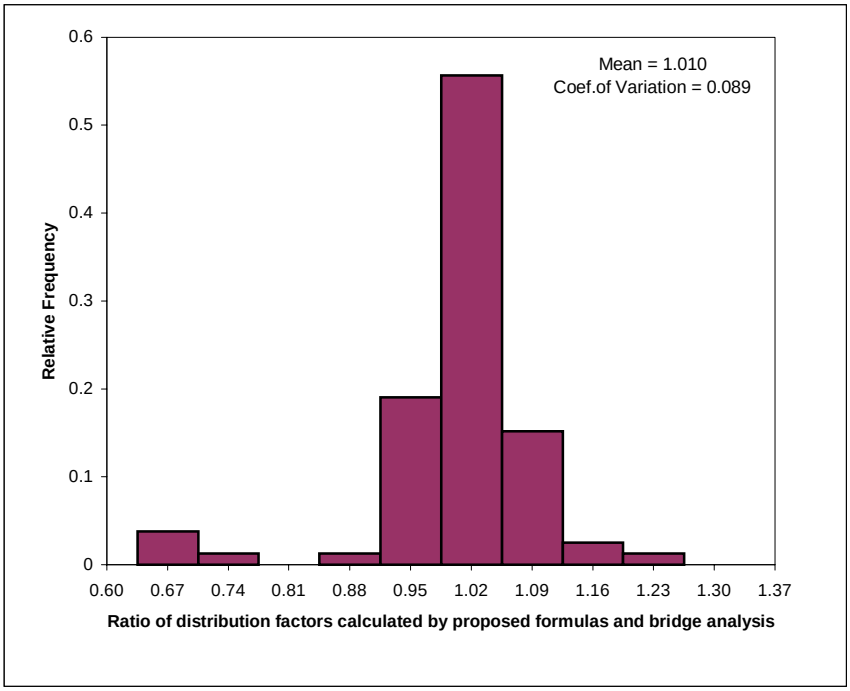

(b)

Figure B.36. Comparison of Distribution Factors calculated by Proposed Formulas and Bridge Analysis for All Vehicles, Concrete T-Beam, Shear in Interior Girders for Multi Lane

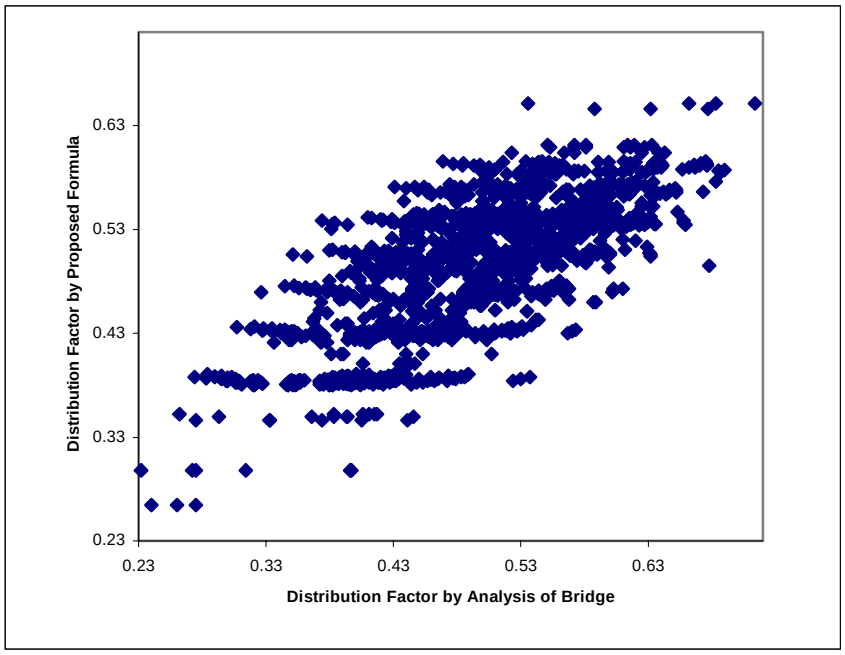

(a)

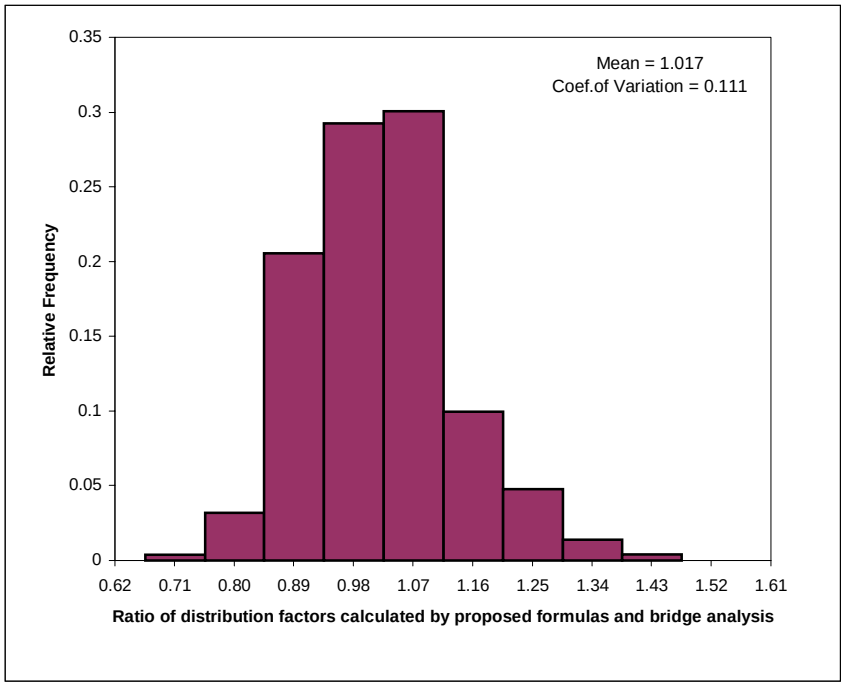

(b)

Figure B.37. Comparison of Distribution Factors calculated by Proposed Formulas and Bridge Analysis for All Vehicles, All Beam Bridges, Bending Moment in Exterior Girders for Single Lane

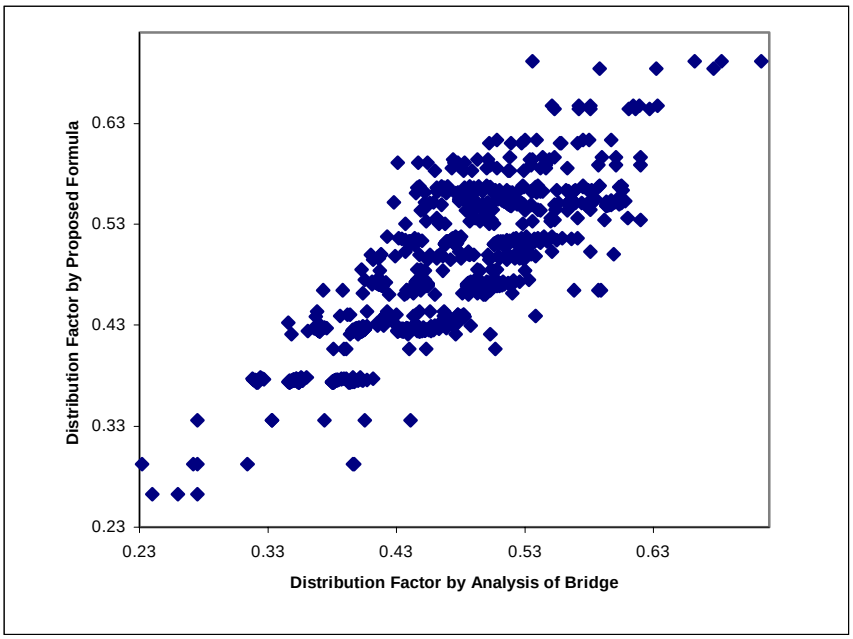

(a)

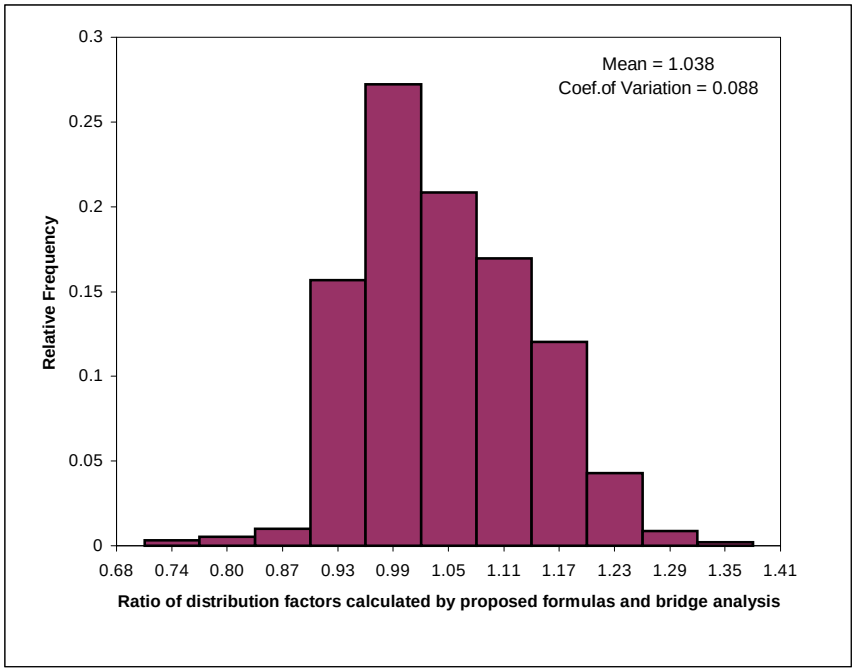

(b)

Figure B.38. Comparison of Distribution Factors calculated by Proposed Formulas and Bridge Analysis for All Vehicles, Steel Girders, Bending Moment in Exterior Girders for Single Lane

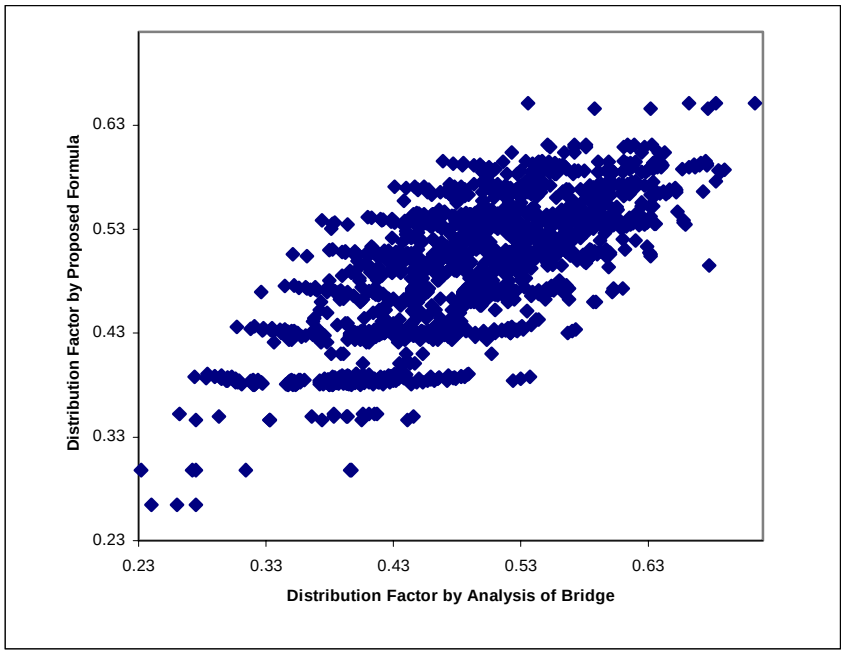

(a)

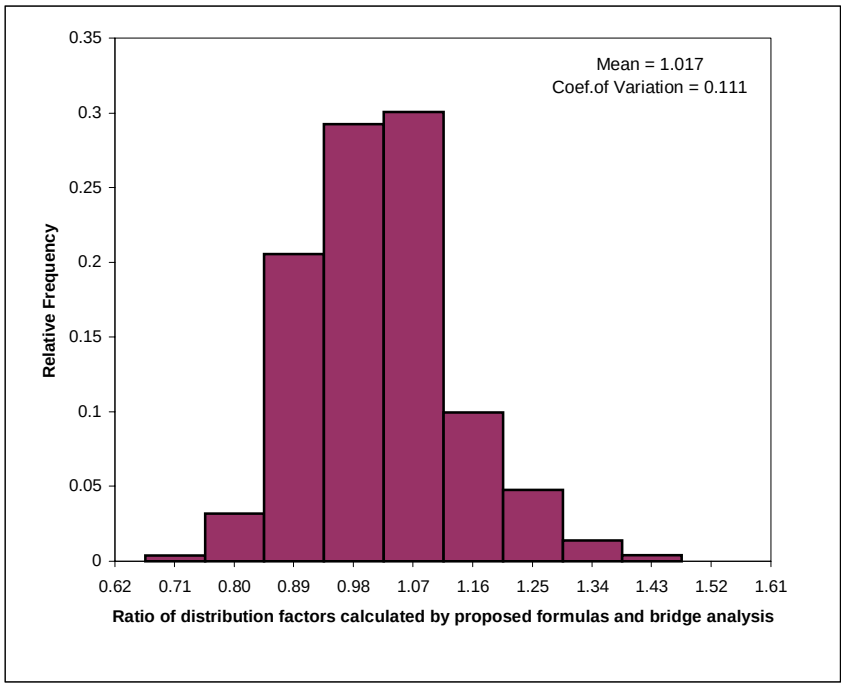

(b)

Figure B.39. Comparison of Distribution Factors calculated by Proposed Formulas and Bridge Analysis for All Vehicles, Prestressed Girders, Bending Moment in Exterior Girders for Single Lane

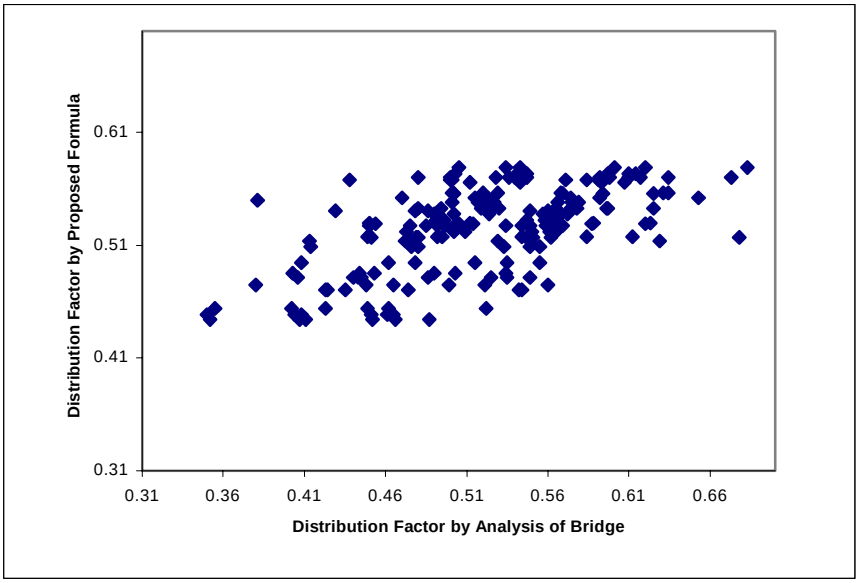

(a)

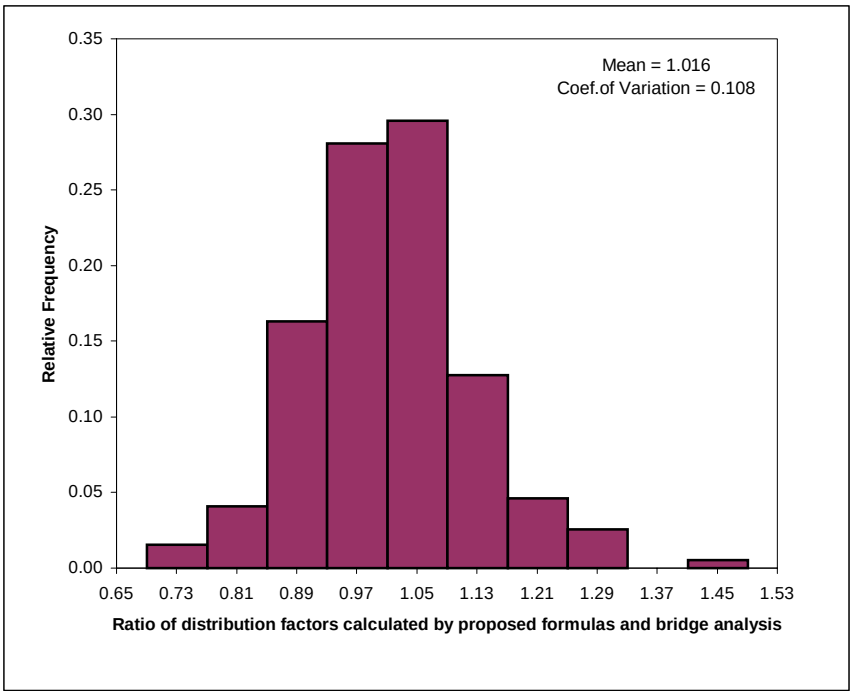

(b)

Figure B.40. Comparison of Distribution Factors calculated by Proposed Formulas and Bridge Analysis for All Vehicles, Concrete T-Beam, Bending Moment in Exterior Girders for Single Lane

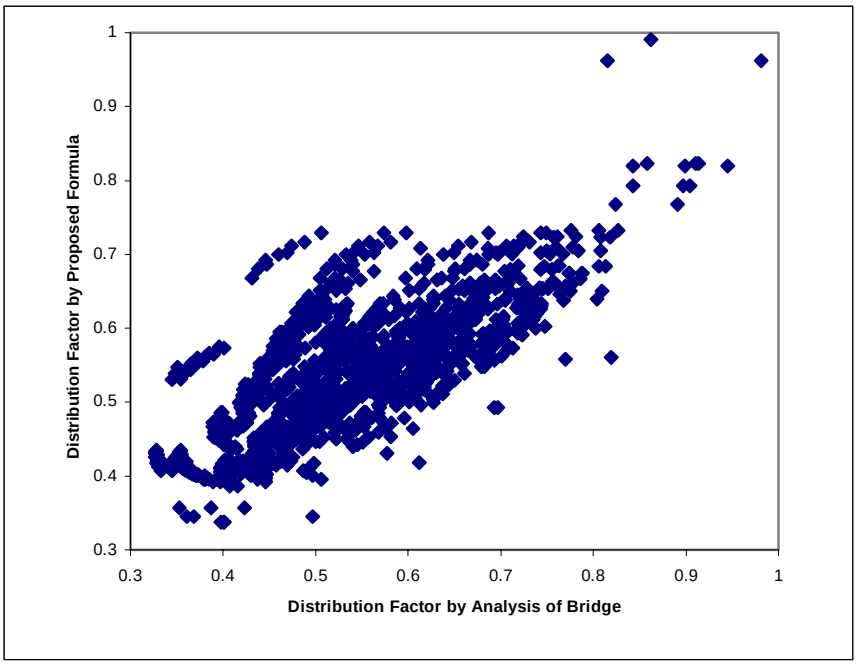

(a)

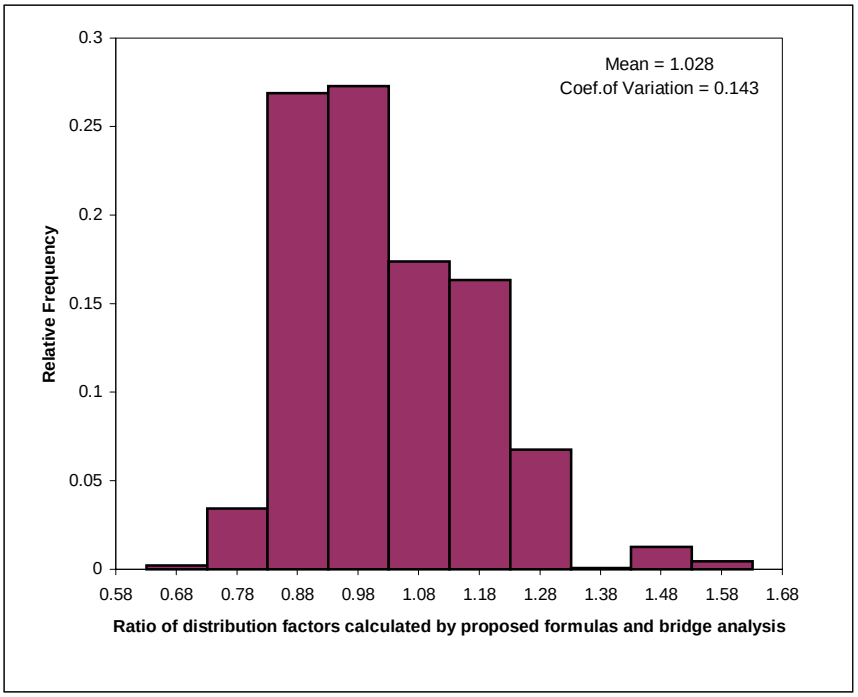

(b)

Figure B.41. Comparison of Distribution Factors calculated by Proposed Formulas and Bridge Analysis for All Vehicles, All Beam Bridges, Bending Moment in Exterior Girders for Multi Lane

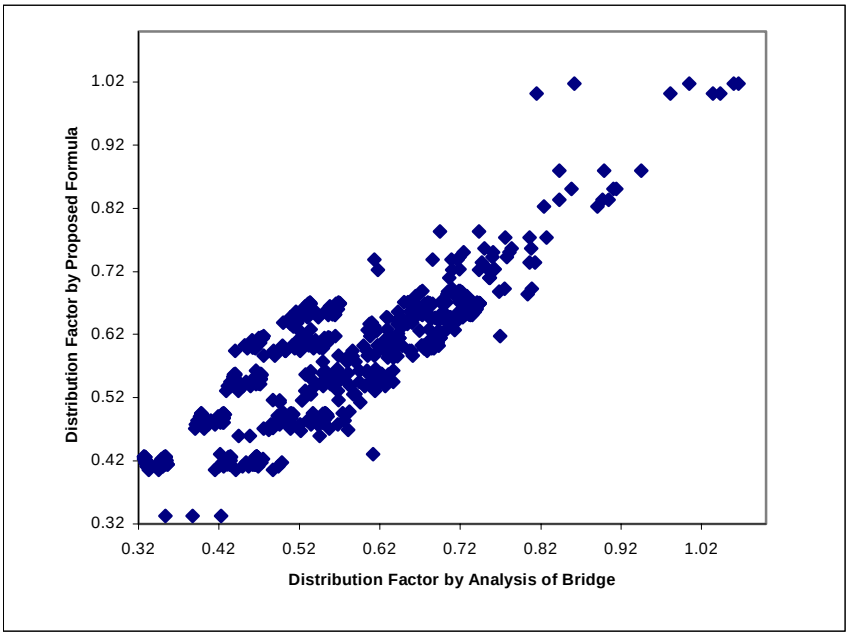

(a)

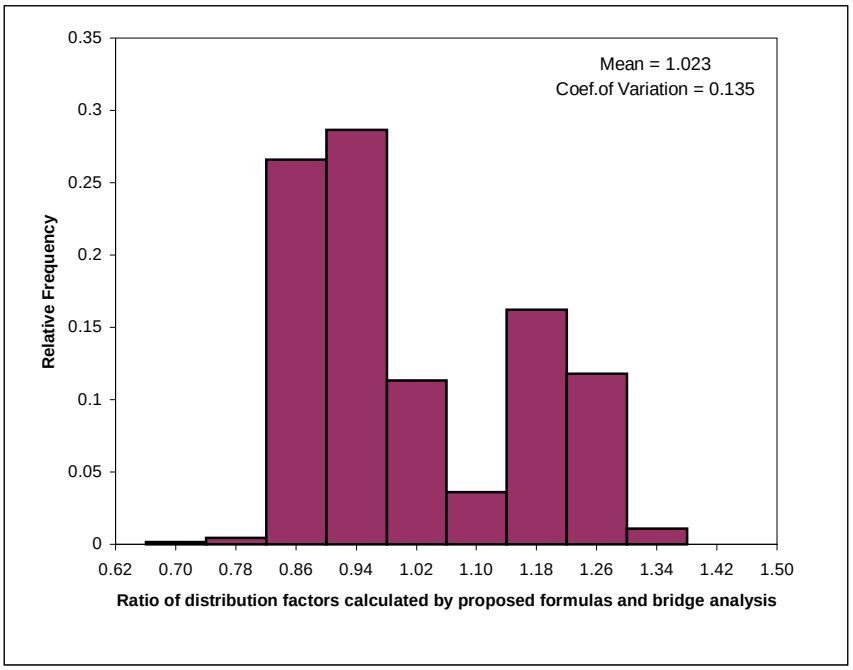

(b)

Figure B.42. Comparison of Distribution Factors calculated by Proposed Formulas and Bridge Analysis for All Vehicles, Steel Girders, Bending Moment in Exterior Girders for Multi Lane

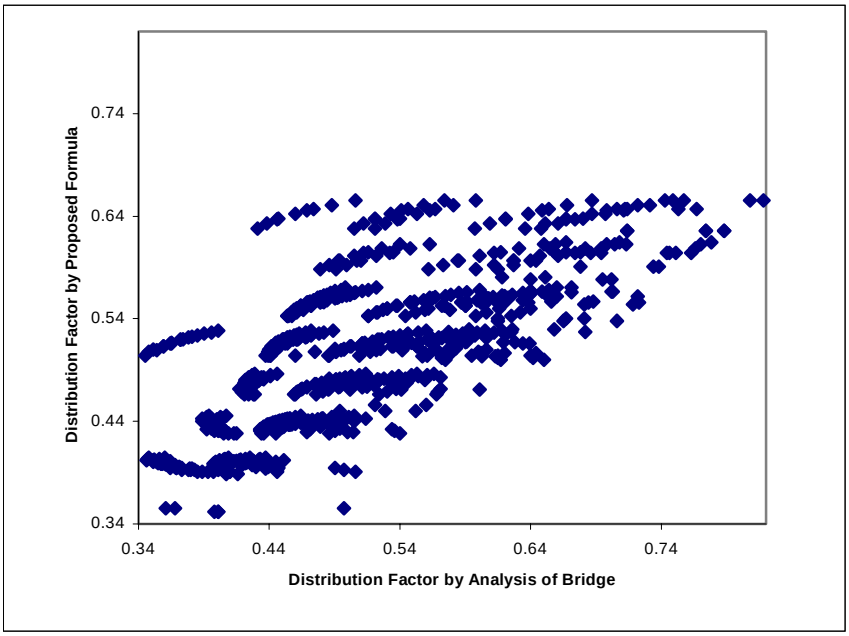

(a)

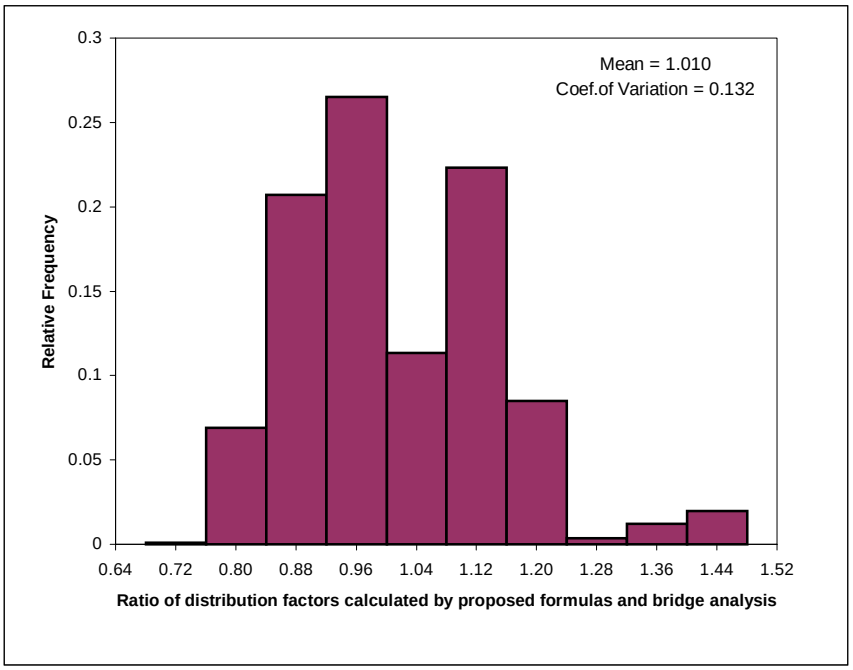

(b)

Figure B.43. Comparison of Distribution Factors calculated by Proposed Formulas and Bridge Analysis for All Vehicles, Prestressed Girders, Bending Moment in Exterior Girders for Multi Lane

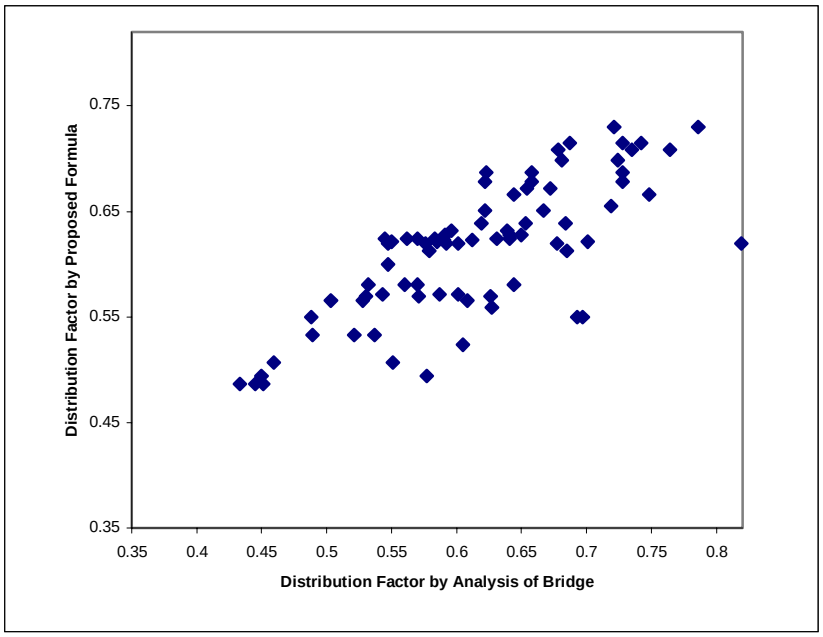

(a)

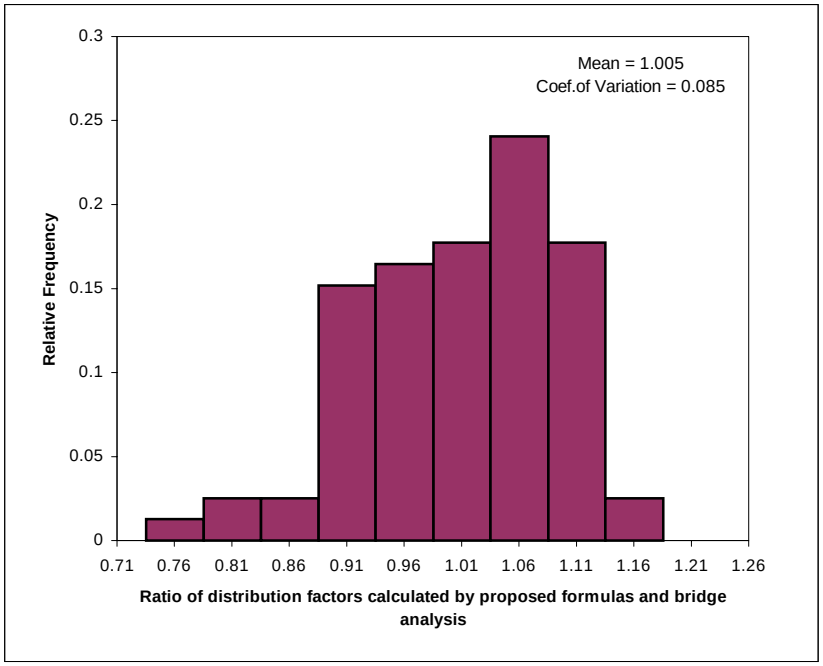

(b)

Figure B.44. Comparison of Distribution Factors calculated by Proposed Formulas and Bridge Analysis for All Vehicles, Concrete T-Beam, Bending Moment in Exterior Girders for Multi Lane

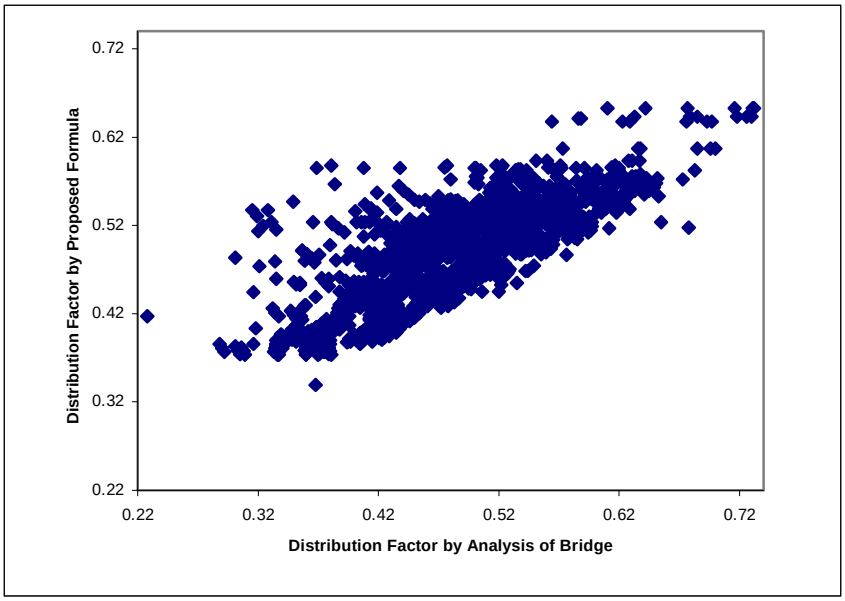

(a)

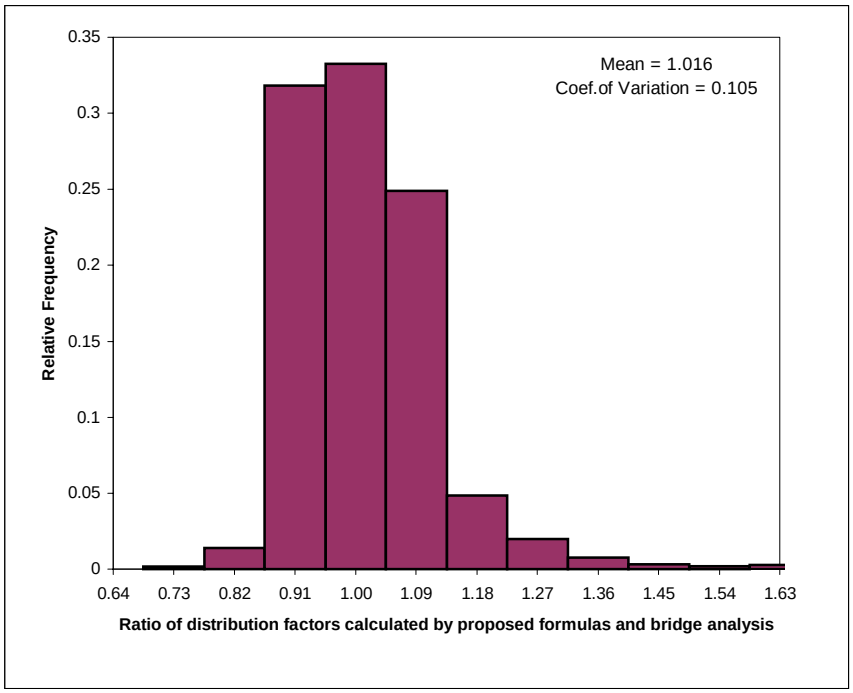

(b)

Figure B.45. Comparison of Distribution Factors calculated by Proposed Formulas and Bridge Analysis for All Vehicles, All Beam Bridges, Shear in Exterior Girders for Single Lane

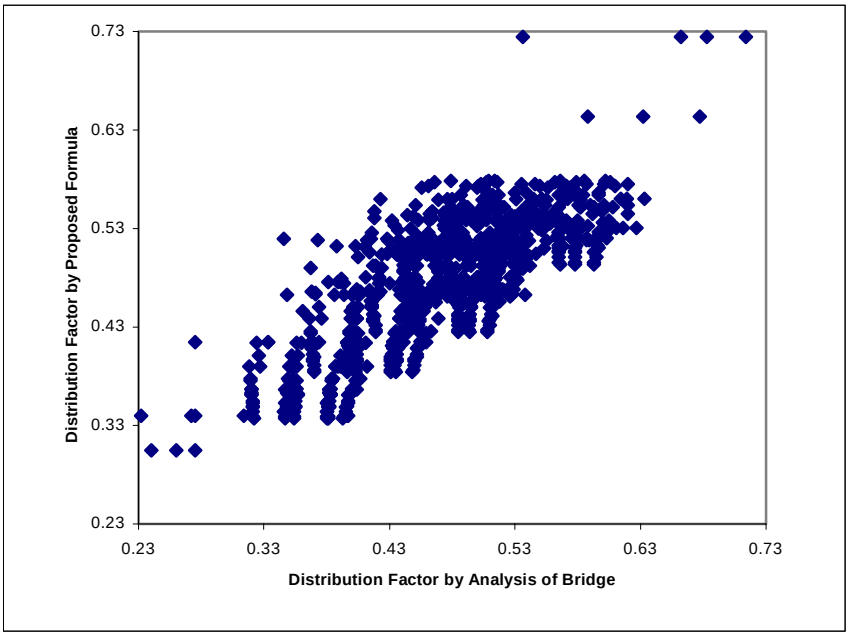

(a)

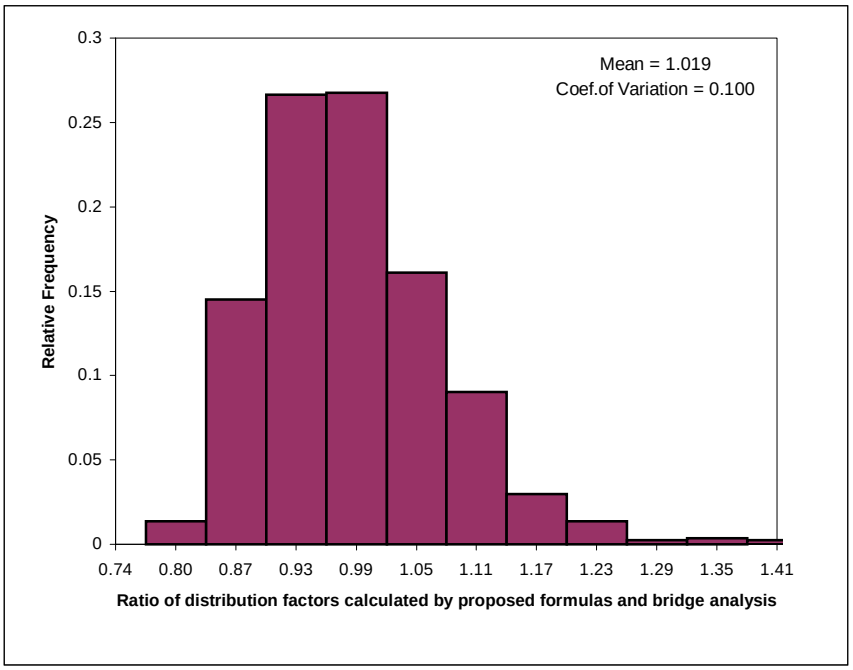

(b)

Figure B.46. Comparison of Distribution Factors calculated by Proposed Formulas and Bridge Analysis for All Vehicles, Steel Girders, Shear in Exterior Girders for Single Lane

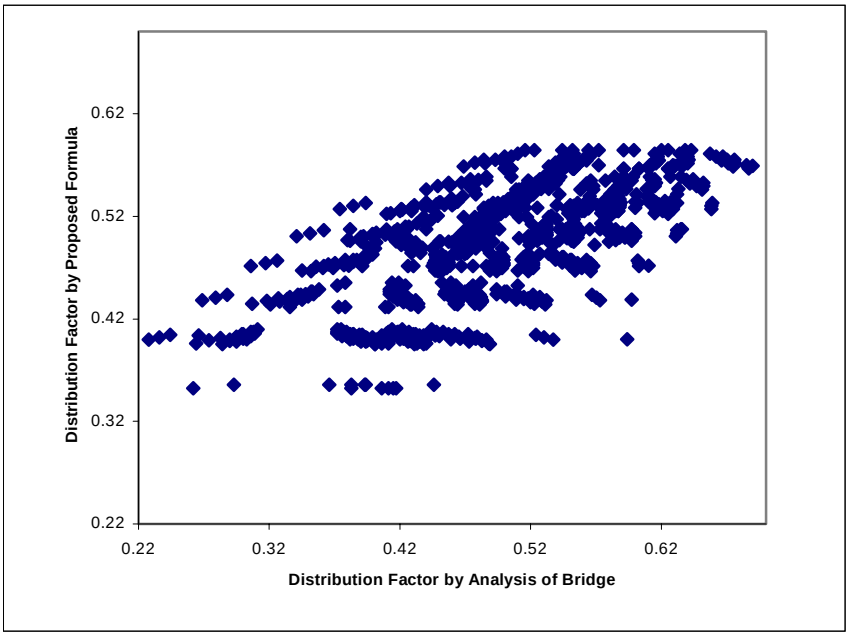

(a)

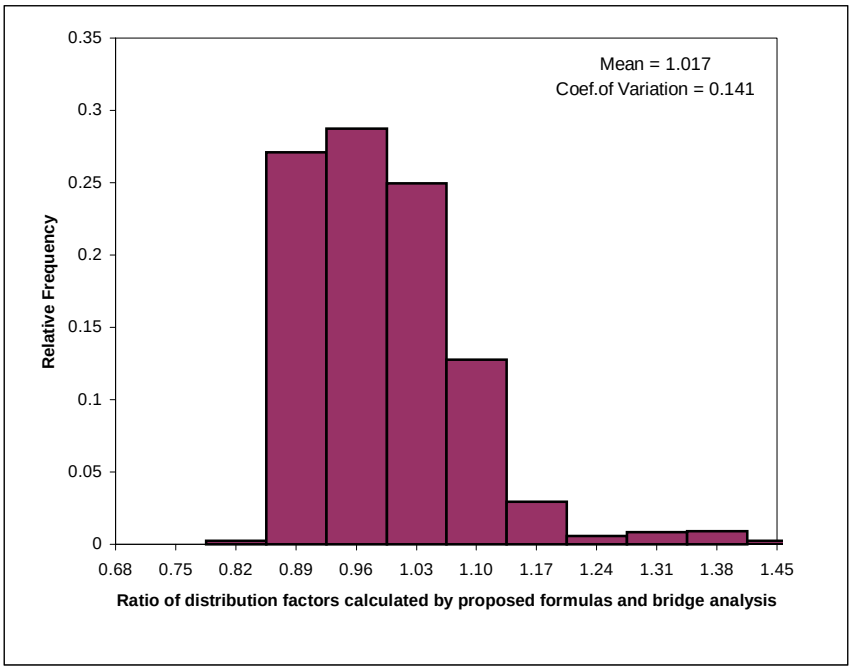

(b)

Figure B.47. Comparison of Distribution Factors calculated by Proposed Formulas and Bridge Analysis for All Vehicles, Prestressed Girders, Shear in Exterior Girders for Single Lane

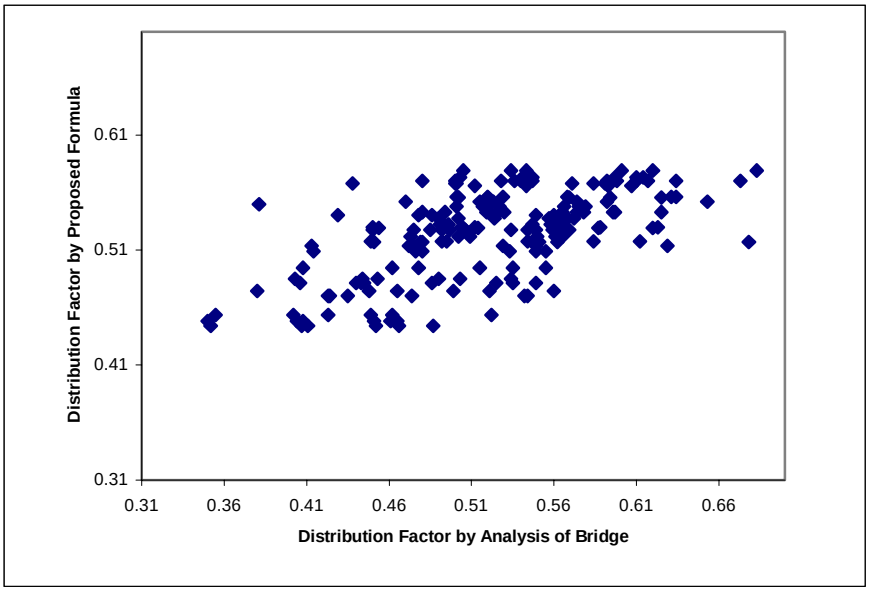

(a)

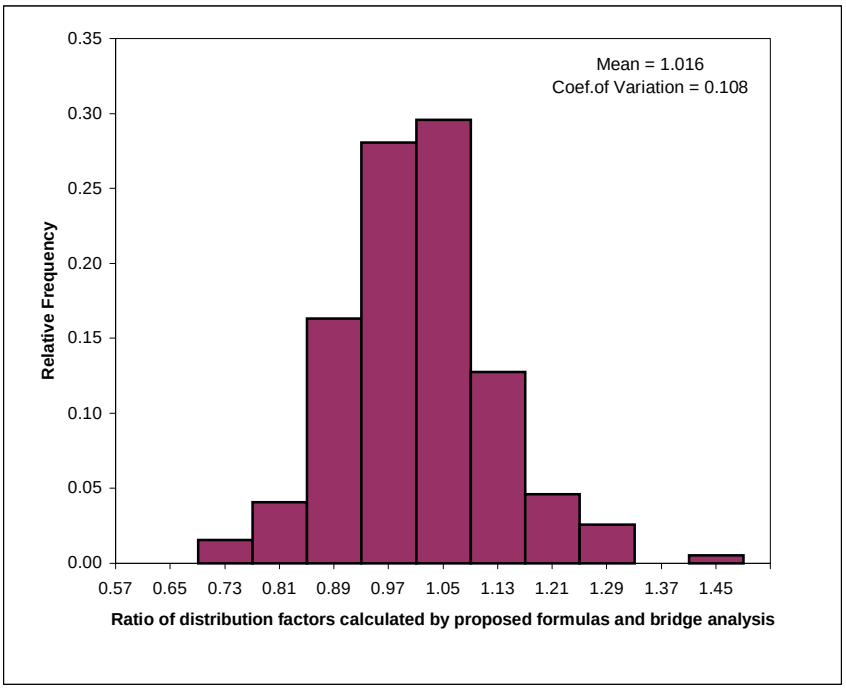

(b)

Figure B.48. Comparison of Distribution Factors calculated by Proposed Formulas and Bridge Analysis for All Vehicles, Concrete T-Beam, Shear in Exterior Girders for Single Lane

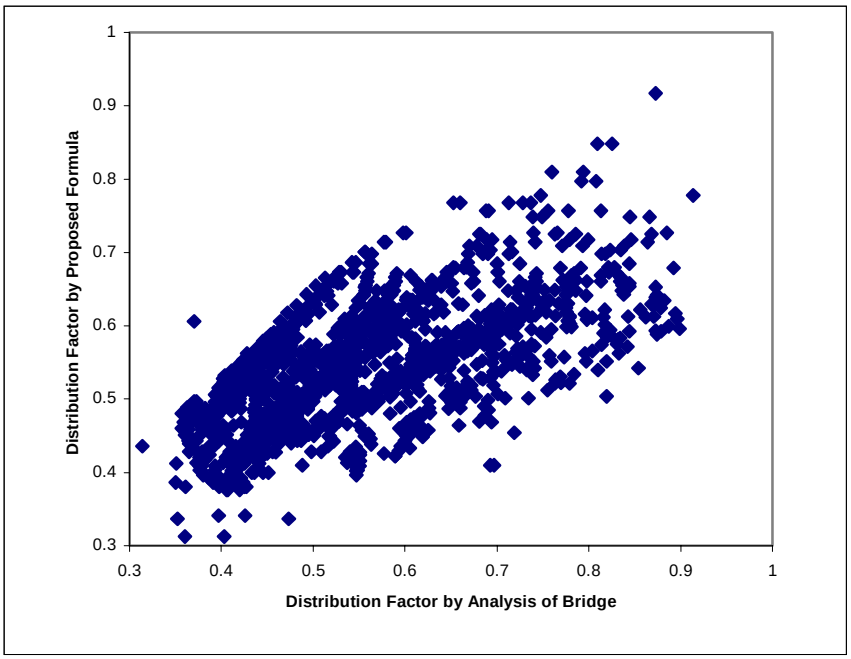

(a)

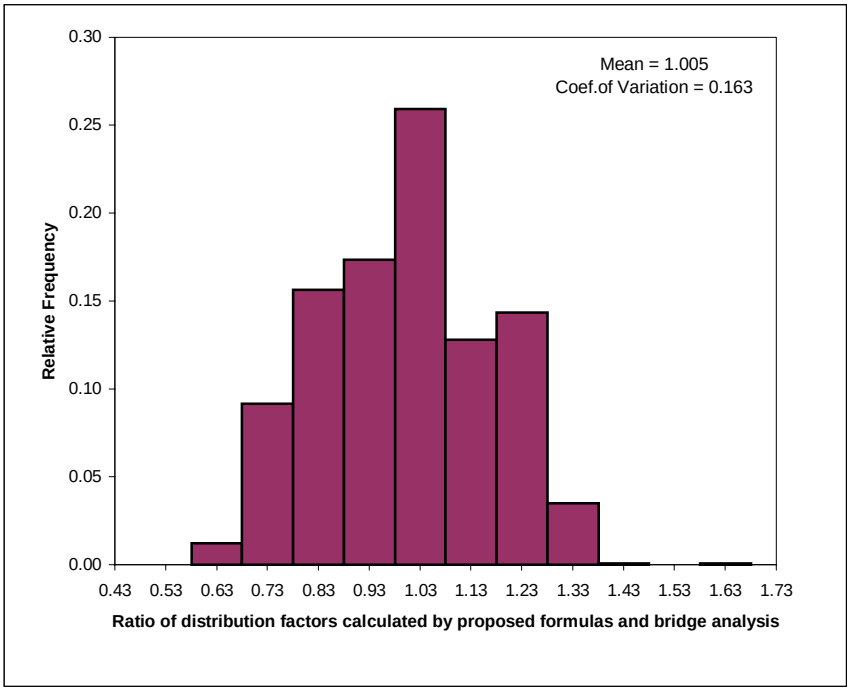

(b)

Figure B.49. Comparison of Distribution Factors calculated by Proposed Formulas and Bridge Analysis for All Vehicles, All Beam Bridges, Shear in Exterior Girders for Multi Lane

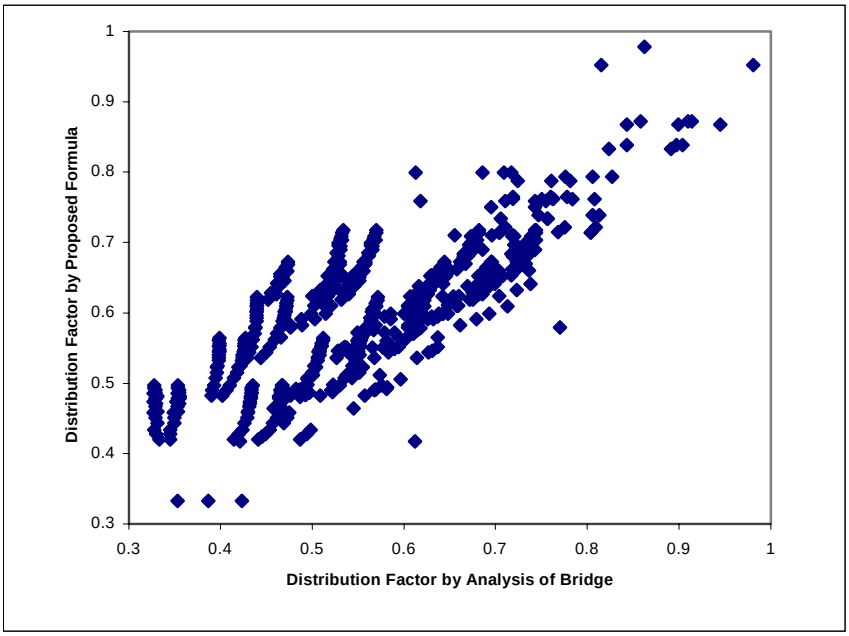

(a)

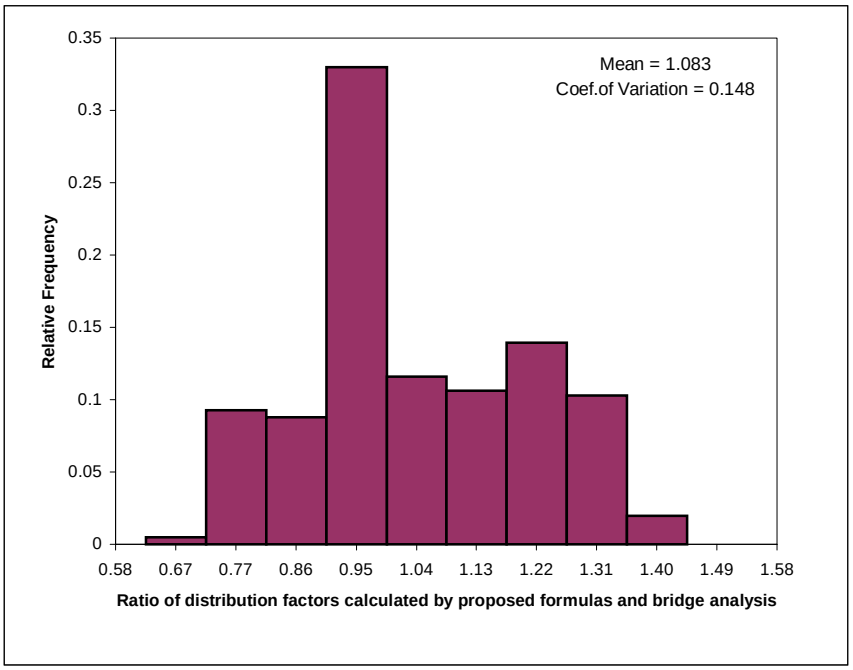

(b)

Figure B.50. Comparison of Distribution Factors calculated by Proposed Formulas and Bridge Analysis for All Vehicles, Steel Girders, Shear in Exterior Girders for Multi Lane

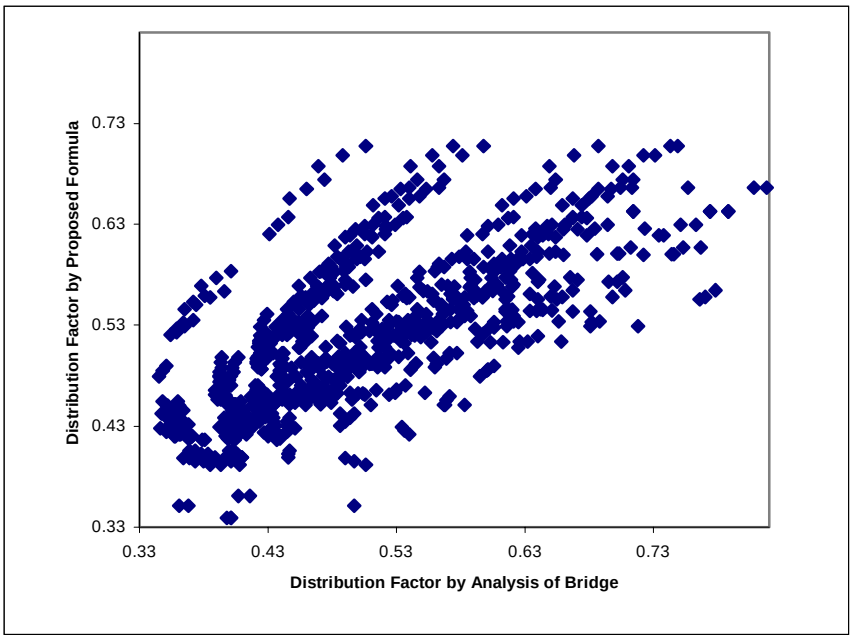

(a)

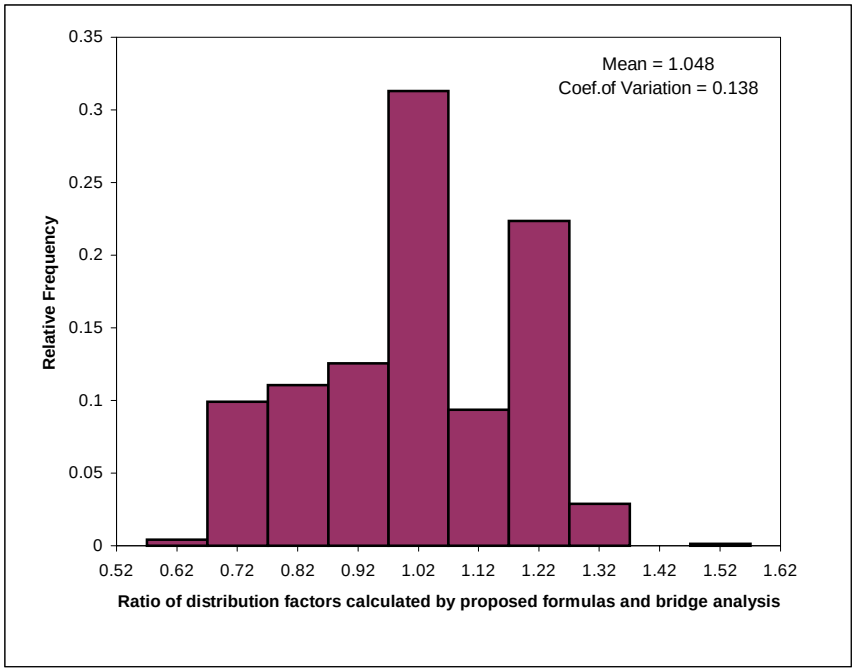

(b)

Figure B.51. Comparison of Distribution Factors calculated by Proposed Formulas and Bridge Analysis for All Vehicles, Prestressed Girders, Shear in Exterior Girders for Multi Lane

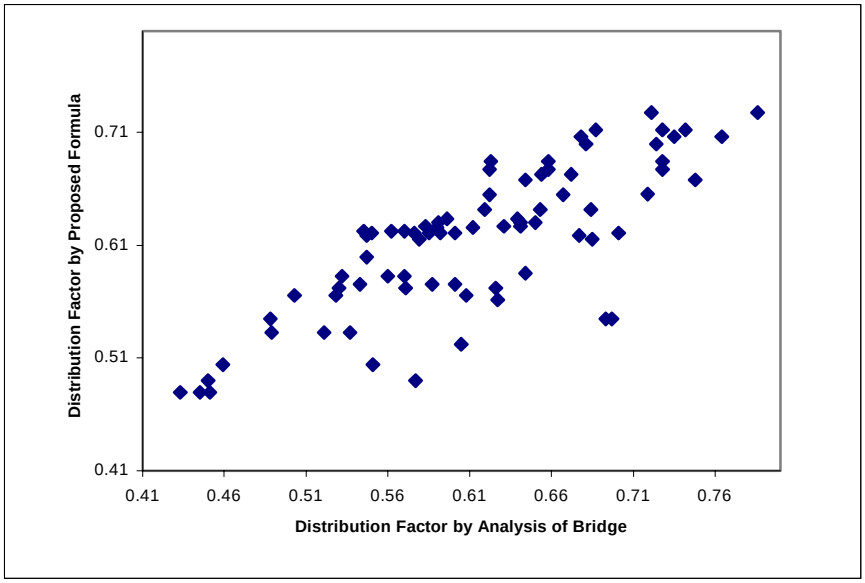

(a)

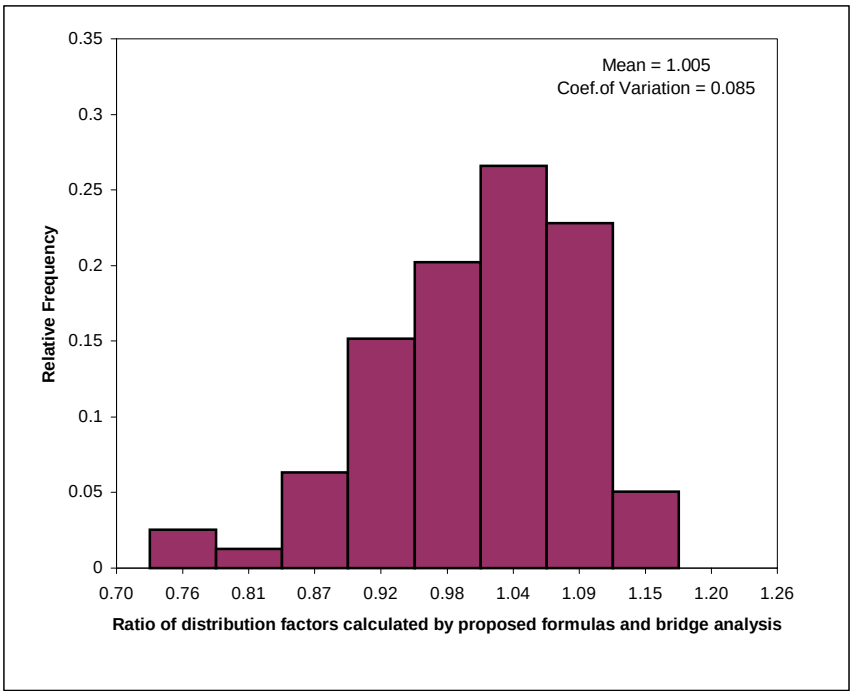

(b)

Figure B.52. Comparison of Distribution Factors calculated by Proposed Formulas and Bridge Analysis for All Vehicles, Concrete T-Beam, Shear in Exterior Girders for Multi Lane

APPENDIX C

COMPARISON OF PROPOSED FORMULAS VERSUS LRFD AND NON-LRFD FORMULAS

This appendix presents the comparisons made between the values calculated by the new formulas, post-LRFD formulas prescribed in 1996 AASHTO Standard Specification, and simple pre-LRFD formulas that were prescribed by AASHTO before 1994. The figures present the frequency distribution of the ratio of the distribution factors calculated by the new formulas to the factors calculated by direct analysis. The mean and coefficient of variation values of this ratio were included for each ratio distribution. Only single lane loading scenario was considered.

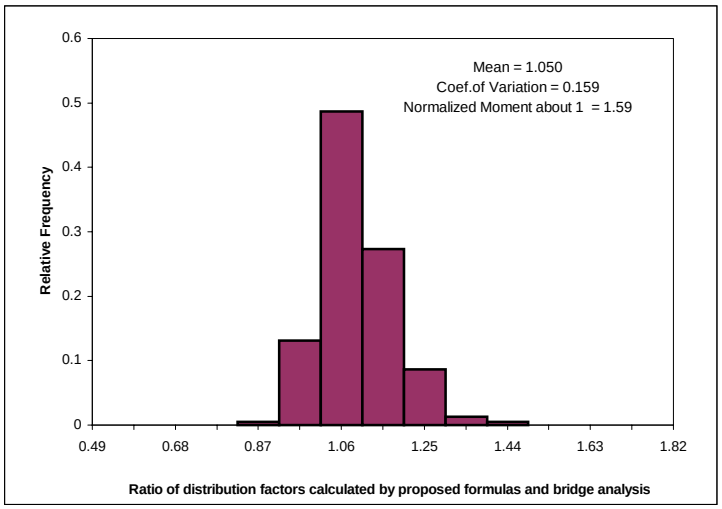

(a) New Formula

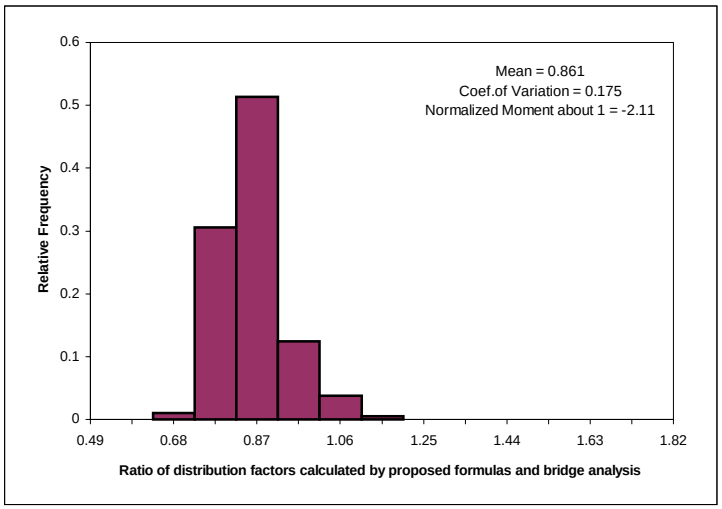

(b)LRFD Formula

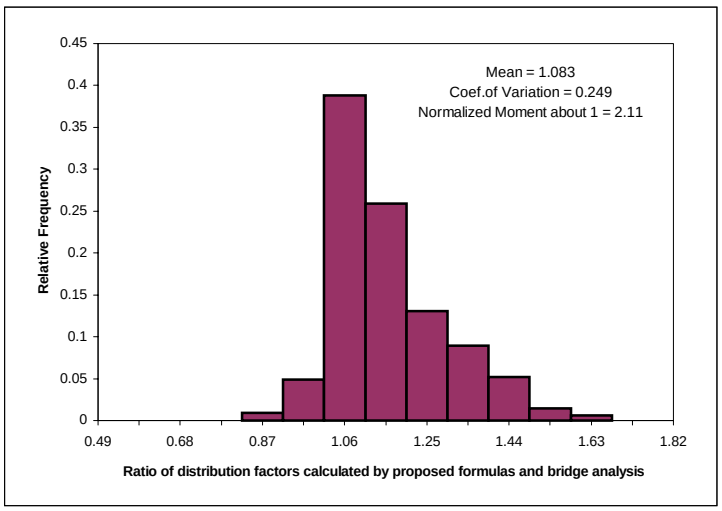

(c) Non-LRFD Formula

Figure C.1. Comparison of Distribution Factor Ratios calculated by the Proposed Formulas, LRFD Formulas, and Non-LRFD Formulas for PLS & HEMMT Vehicles, All Beam Bridges, Bending Moment in Interior Girders for Single Lane

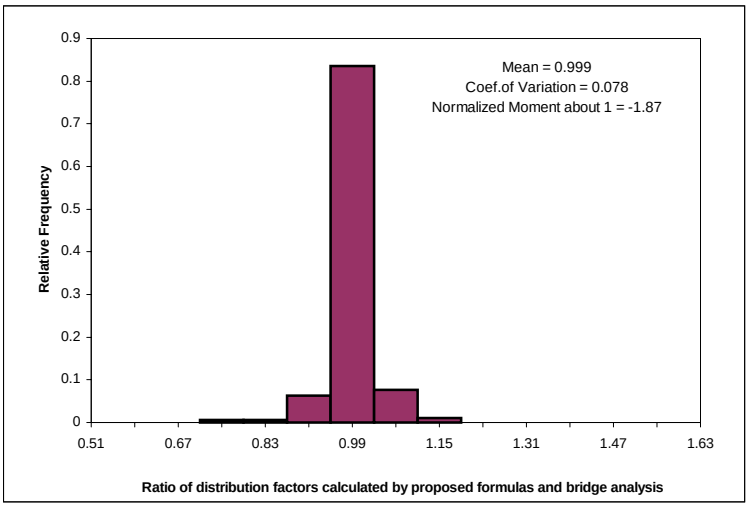

(a) New Formula

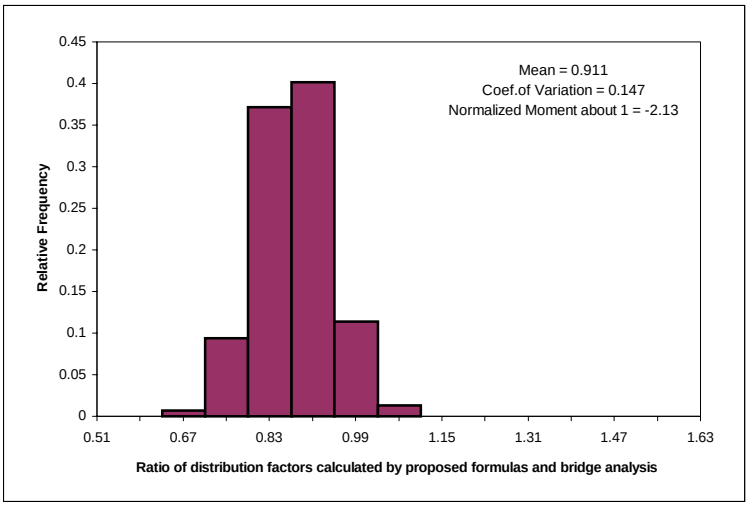

(b)LRFD Formula

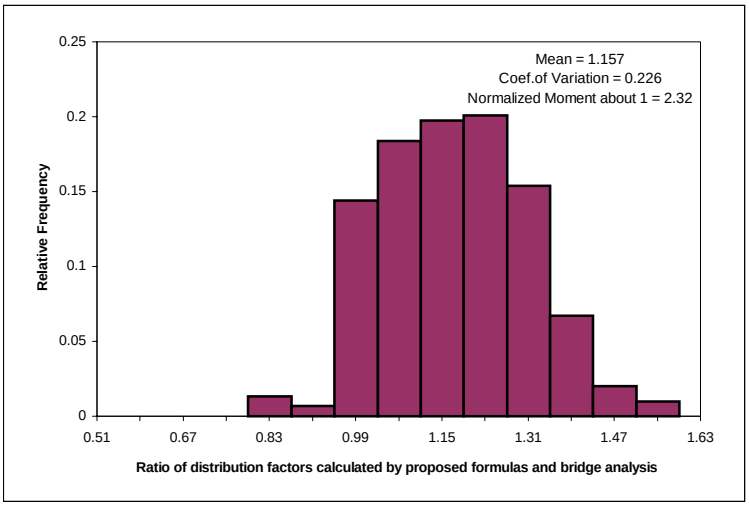

(c) Non-LRFD Formula

Figure C.2. Comparison of Distribution Factor Ratios calculated by the Proposed Formulas, LRFD Formulas, and Non-LRFD Formulas for PLS & HEMMT Vehicles, Steel Girders, Bending Moment in Interior Girders for Single Lane

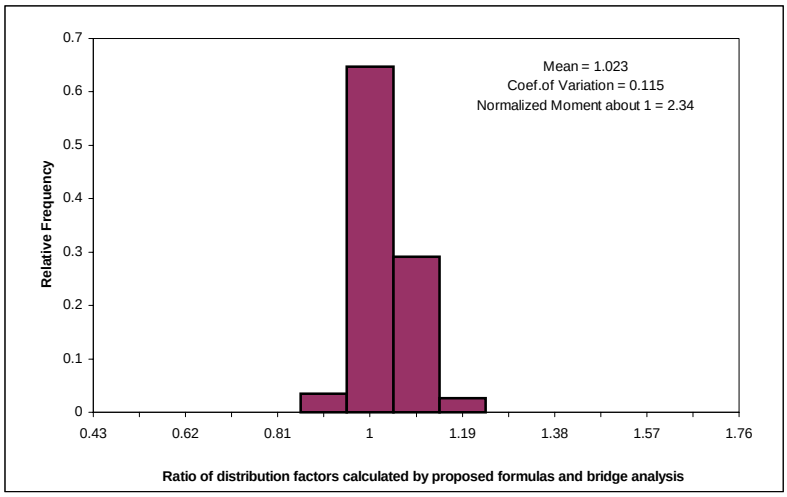

(a) New Formula

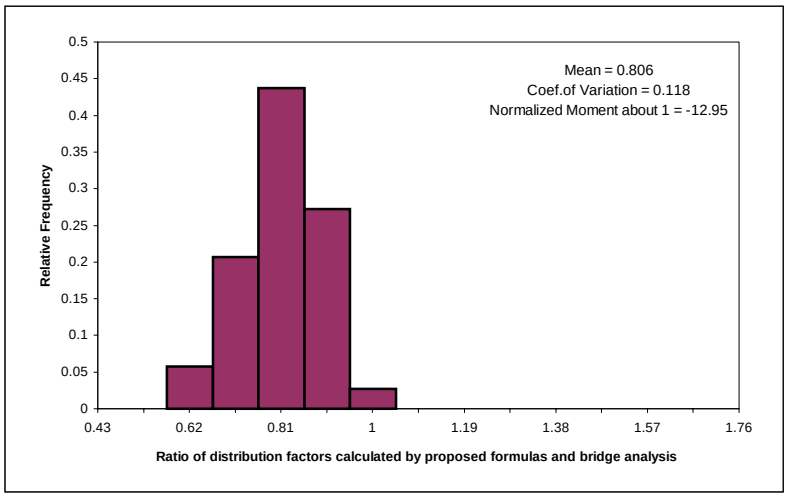

(b)LRFD Formula

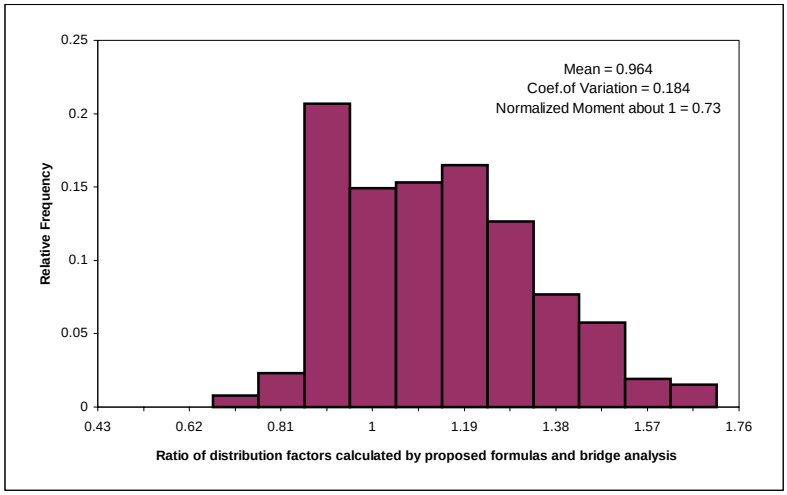

(c) Non-LRFD Formula

Figure C.3. Comparison of Distribution Factor Ratios calculated by the Proposed Formulas, LRFD Formulas, and Non-LRFD Formulas for PLS & HEMMT Vehicles, Prestressed Concrete, Bending Moment in Interior Girders for Single Lane

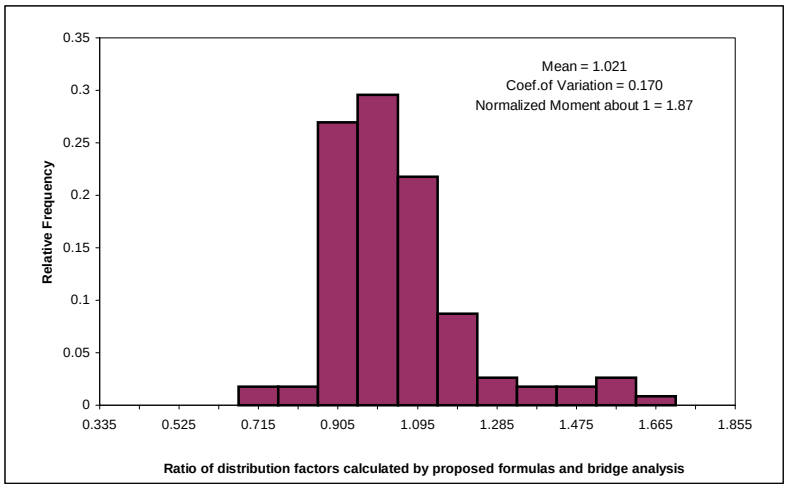

(a) New Formula

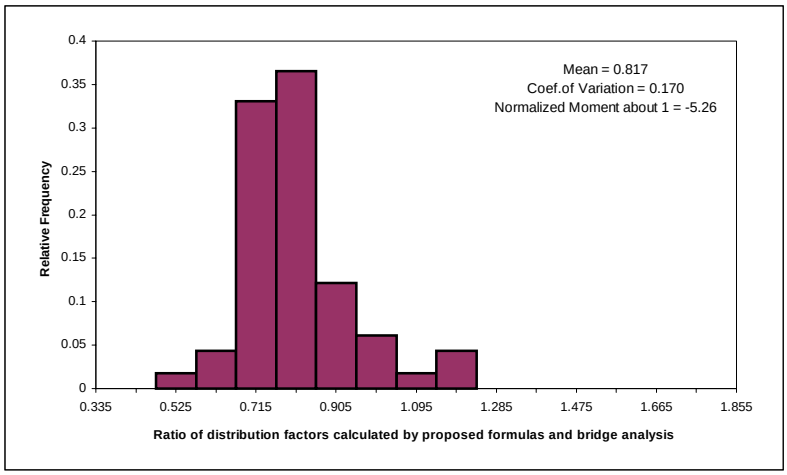

(b)LRFD Formula

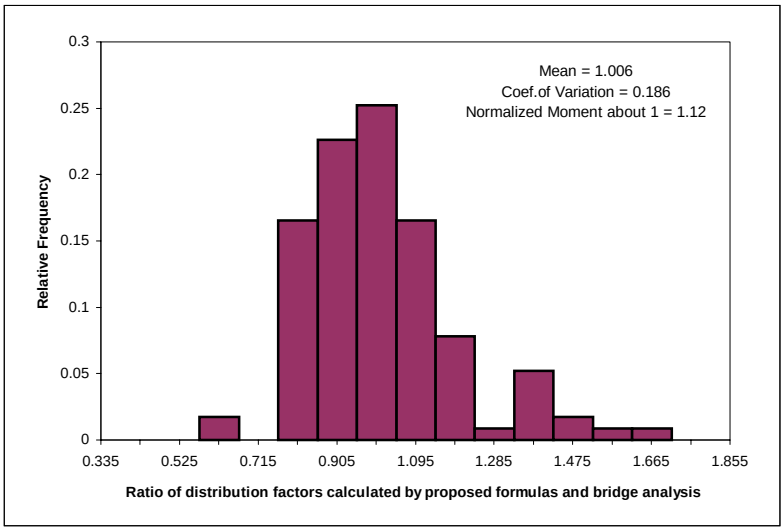

(c) Non-LRFD Formula

Figure C.4. Comparison of Distribution Factor Ratios calculated by the Proposed Formulas, LRFD Formulas, and Non-LRFD Formulas for PLS & HEMMT Vehicles, Concrete T-Beam, Bending Moment in Interior Girders for Single Lane

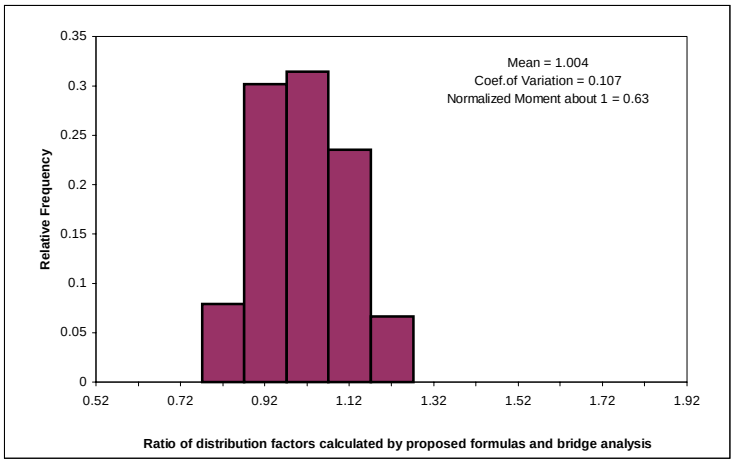

(a) New Formula

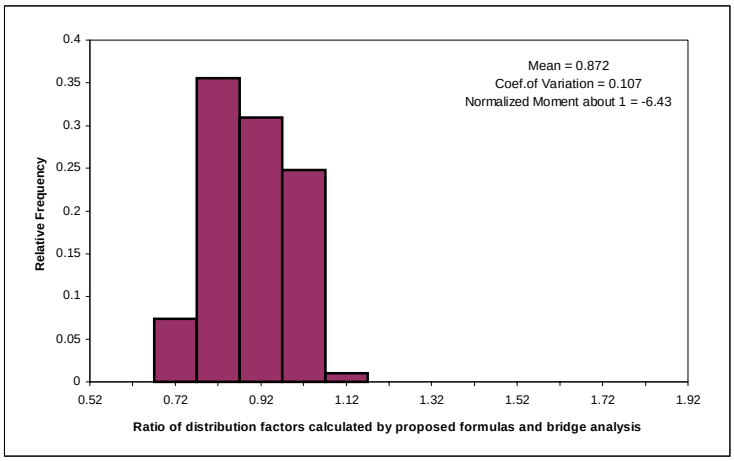

(b)LRFD Formula

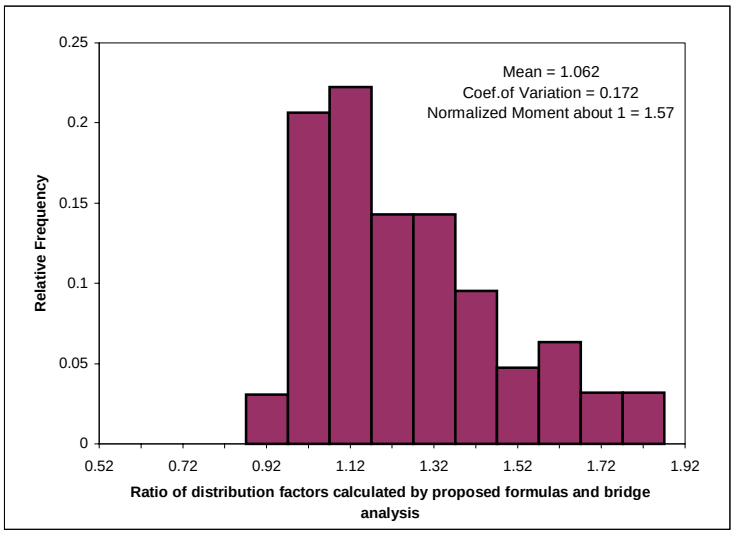

(c) Non-LRFD Formula

Figure C.5. Comparison of Distribution Factor Ratios calculated by the Proposed Formulas, LRFD Formulas, and Non-LRFD Formulas for HETS Vehicle, All Beam Bridges, Bending Moment in Interior Girders for Single Lane

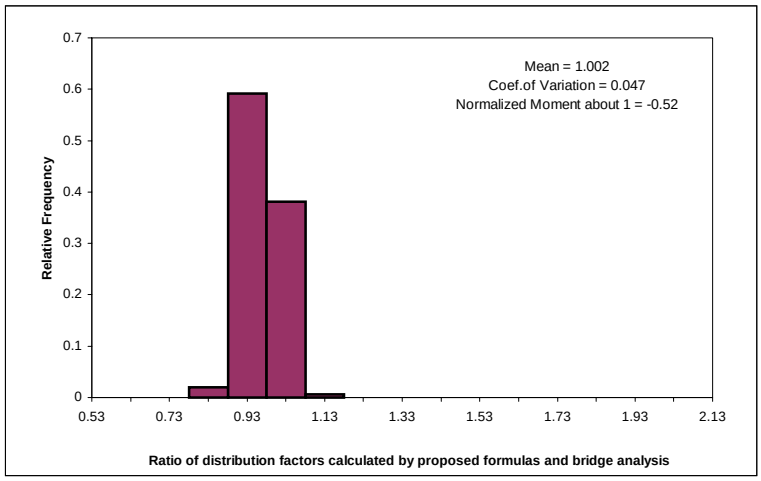

(a) New Formula

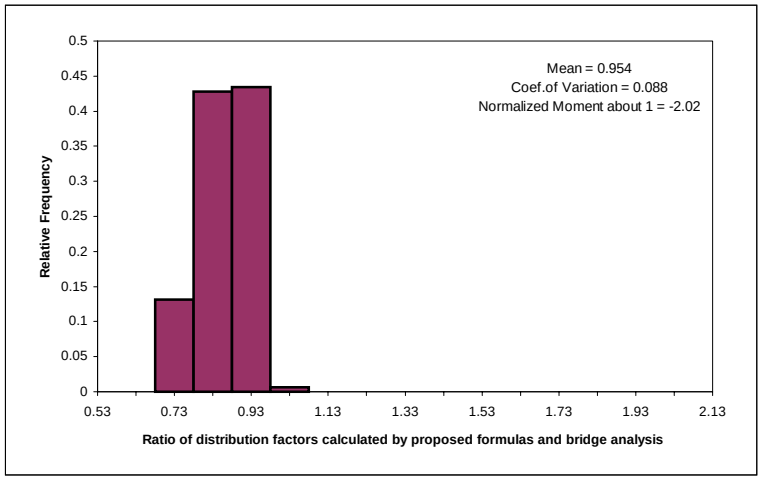

(b)LRFD Formula

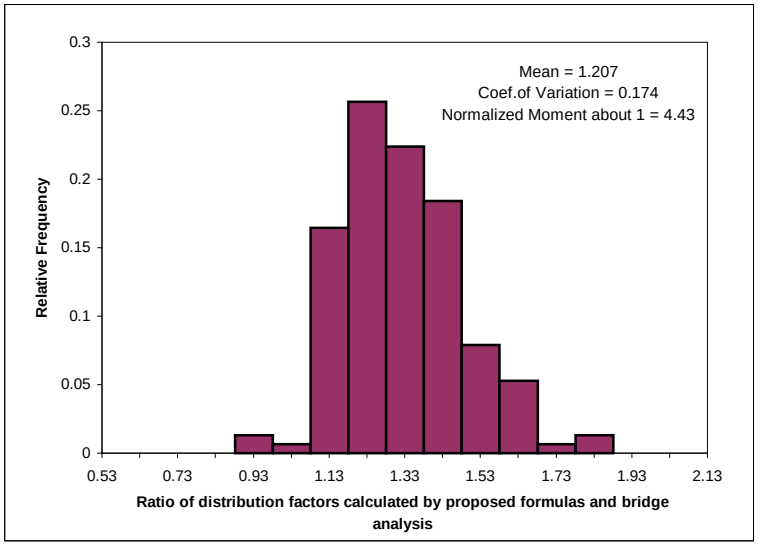

(c) Non-LRFD Formula

Figure C.6. Comparison of Distribution Factor Ratios calculated by the Proposed Formulas, LRFD Formulas, and Non-LRFD Formulas for HETS Vehicle, Steel Girders, Bending Moment in Interior Girders for Single Lane

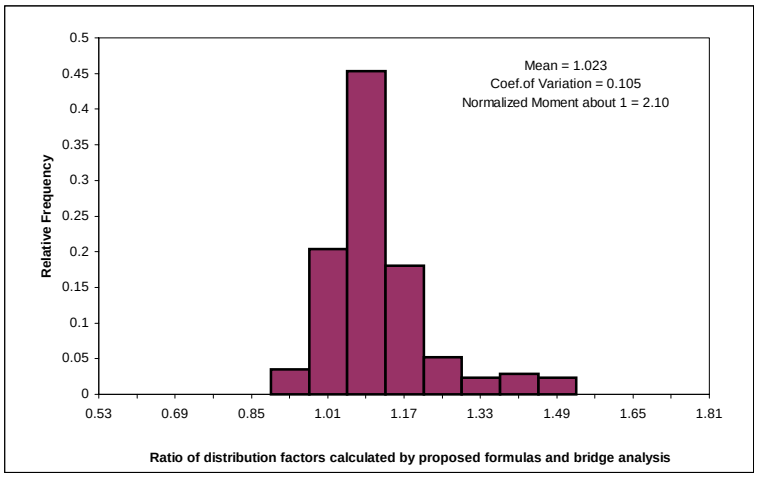

(a) New Formula

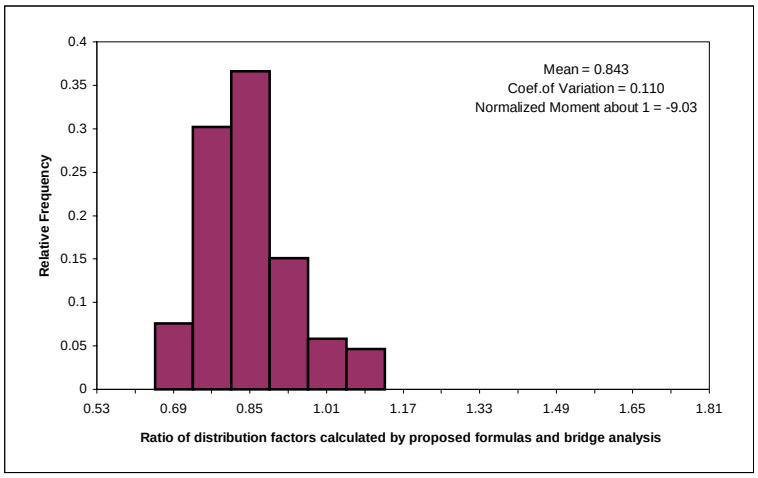

(b)LRFD Formula

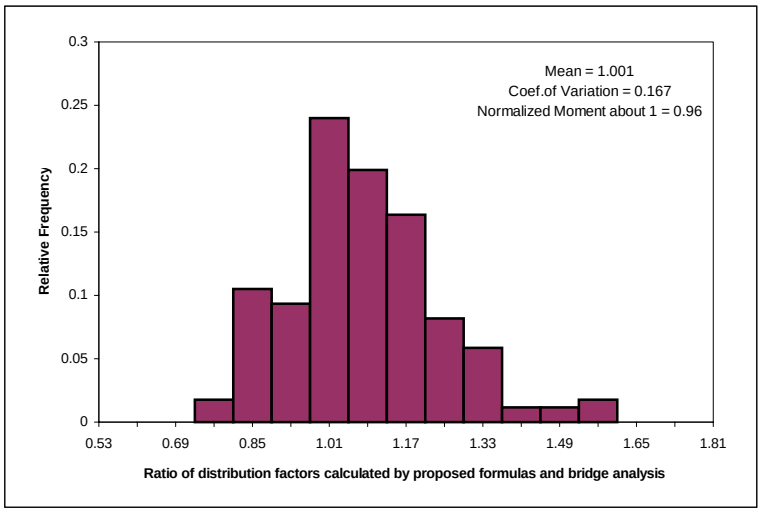

(c) Non-LRFD Formula

Figure C.7. Comparison of Distribution Factor Ratios calculated by the Proposed Formulas, LRFD Formulas, and Non-LRFD Formulas for HETS Vehicle, Prestressed Concrete, Bending Moment in Interior Girders for Single Lane

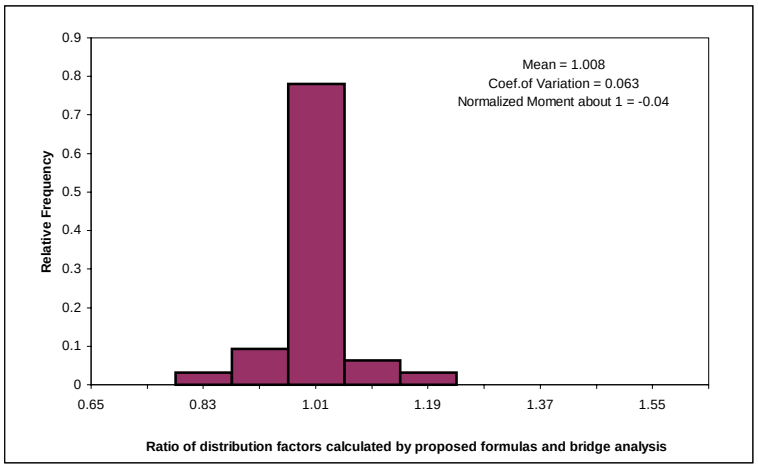

(a) New Formula

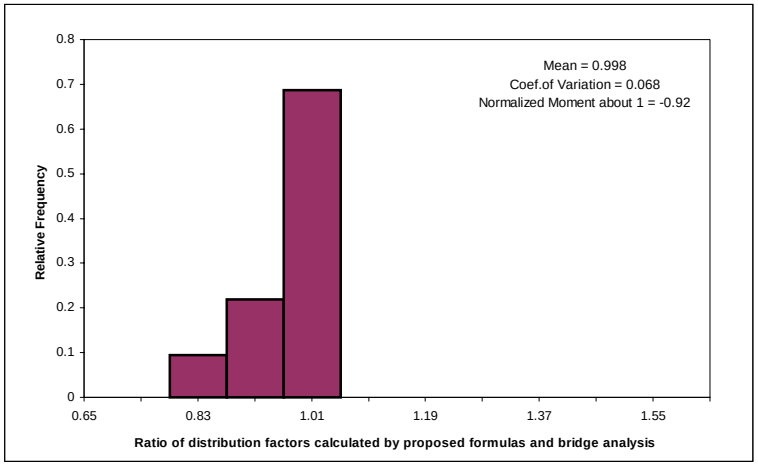

(b) LRFD Formula

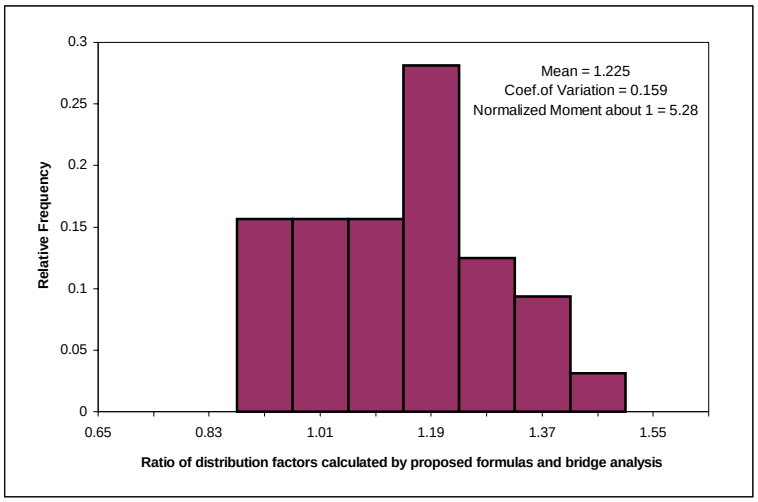

(c) Non-LRFD Formula

Figure C.8. Comparison of Distribution Factor Ratios calculated by the Proposed Formulas, LRFD Formulas, and Non-LRFD Formulas for HETS Vehicle, Concrete T-Beam, Bending Moment in Interior Girders for Single Lane

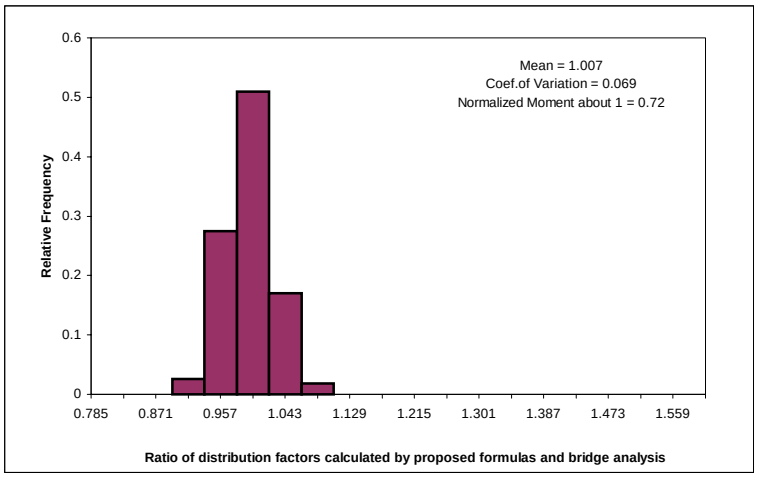

(a) New Formula

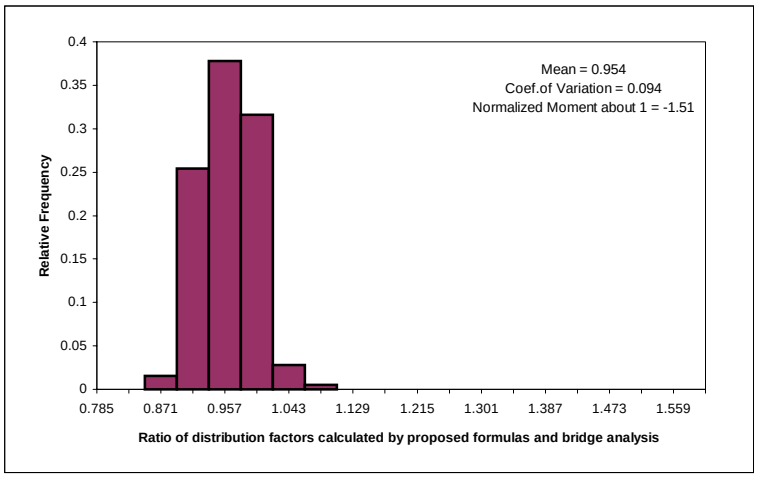

(b) LRFD Formula

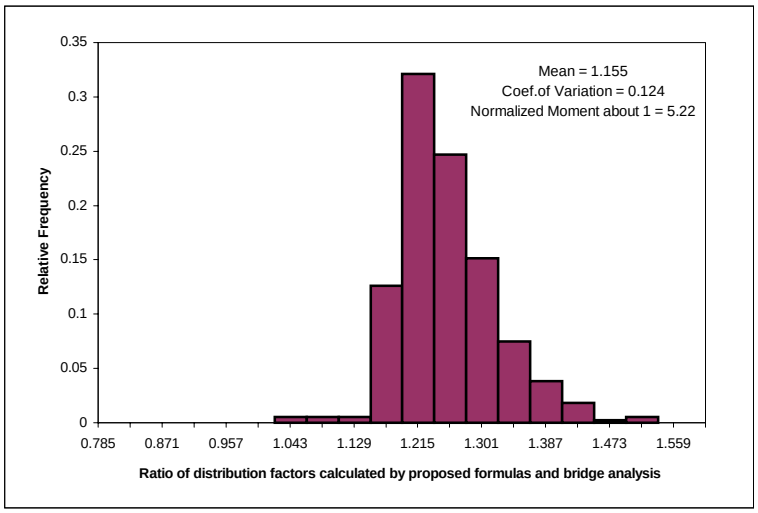

(c) Non-LRFD Formula

Figure C.9. Comparison of Distribution Factor Ratios calculated by the Proposed Formulas, LRFD Formulas, and Non-LRFD Formulas for ABRAMS Vehicle, All Beam Bridges, Bending Moment in Interior Girders for Single Lane

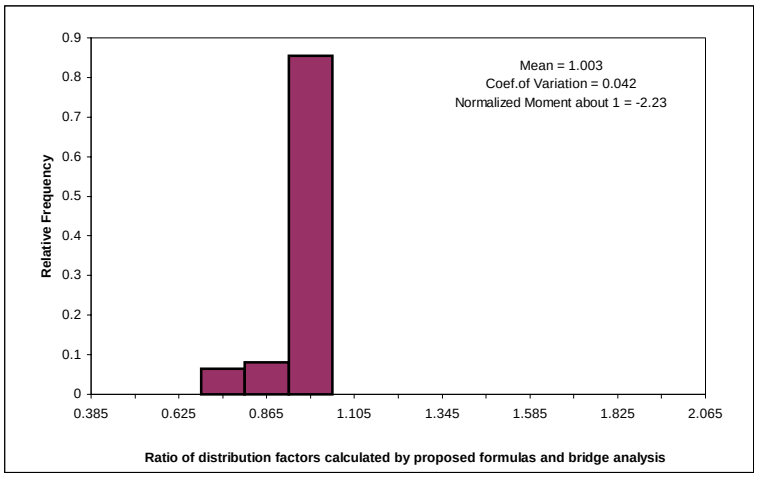

(a) New Formula

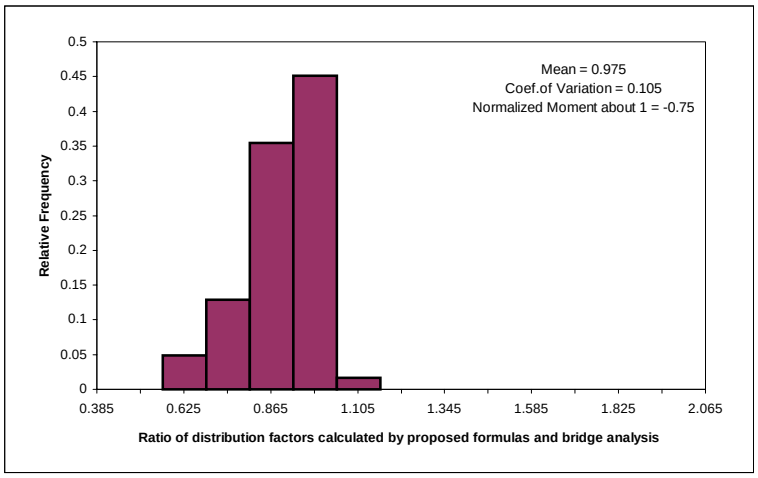

(b) LRFD Formula

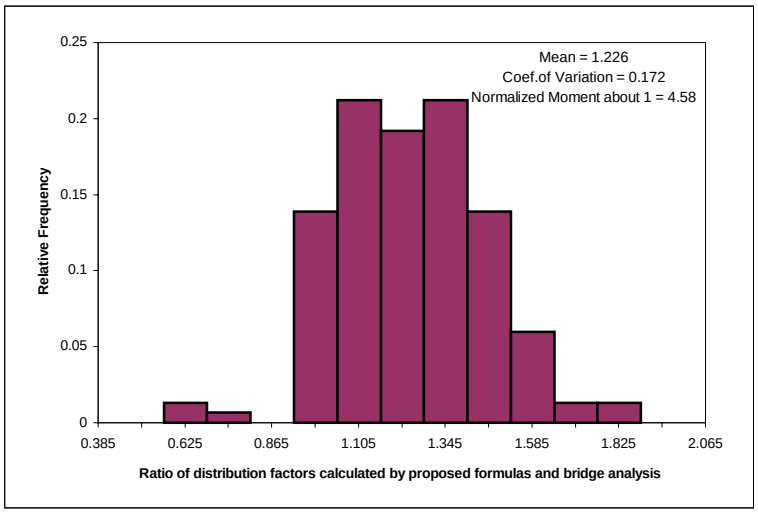

(c) Non-LRFD Formula

Figure C.10. Comparison of Distribution Factor Ratios calculated by the Proposed Formulas, LRFD Formulas, and Non-LRFD Formulas for ABRAMS Vehicle, Steel Girders, Bending Moment in Interior Girders for Single Lane

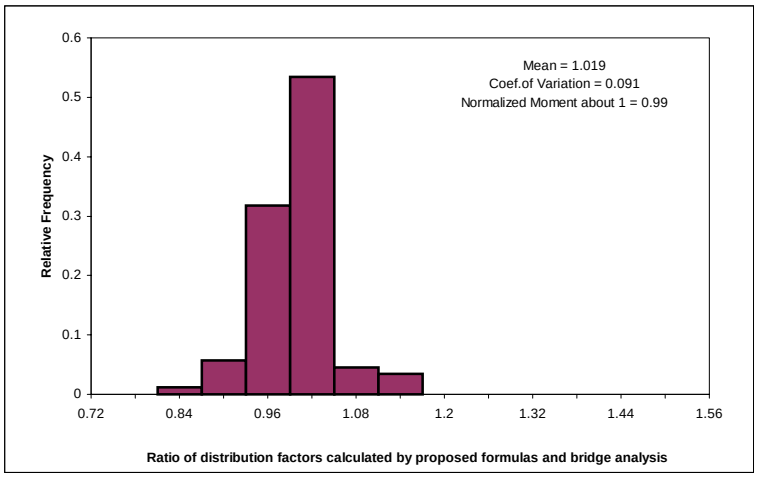

(a) New Formula

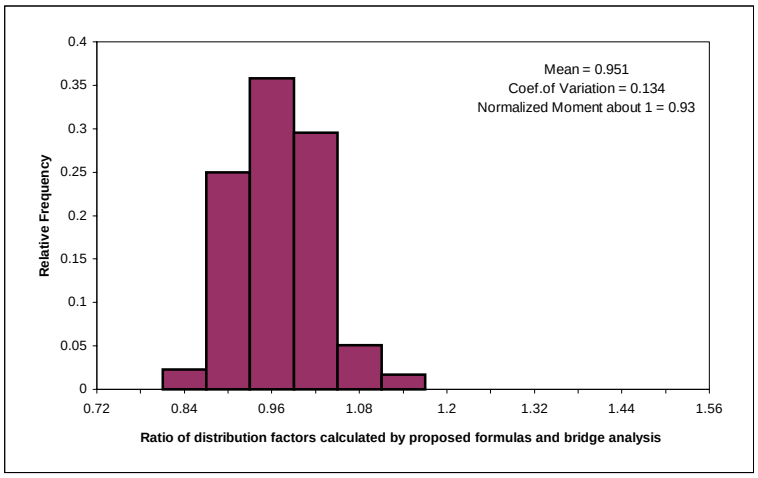

(b) LRFD Formula

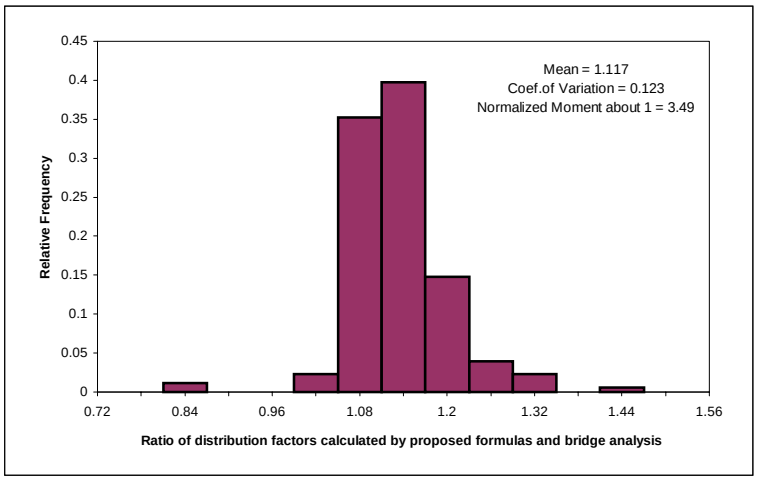

(c) Non-LRFD Formula

Figure C.11. Comparison of Distribution Factor Ratios calculated by the Proposed Formulas, LRFD Formulas, and Non-LRFD Formulas for ABRAMS Vehicle, Prestressed Concrete, Bending Moment in Interior Girders for Single Lane

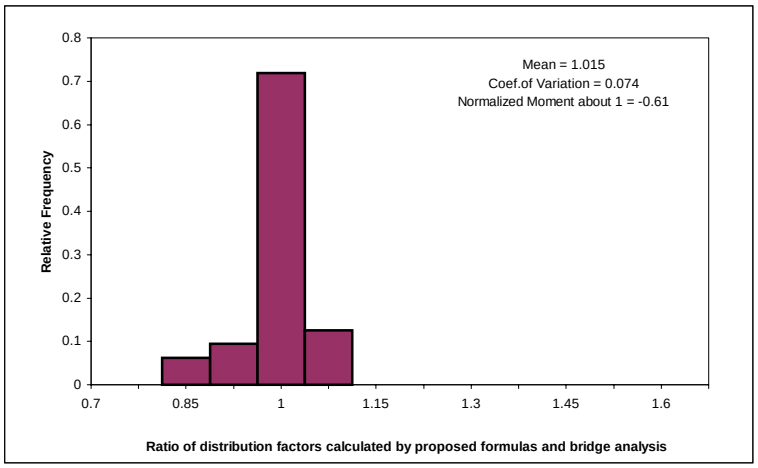

(a) New Formula

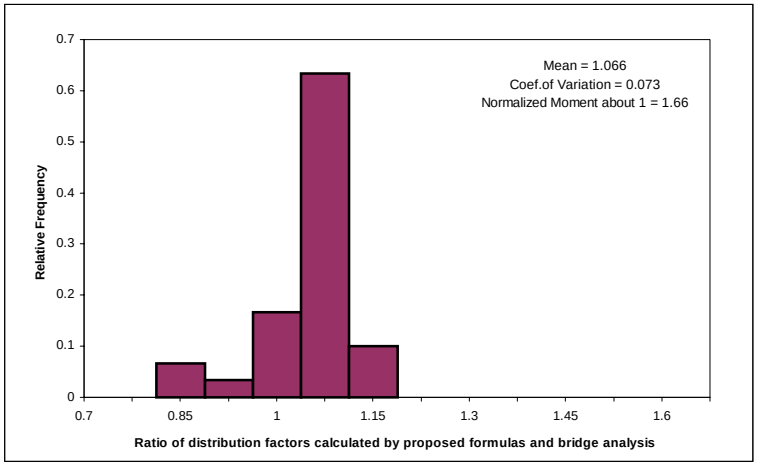

(b) LRFD Formula

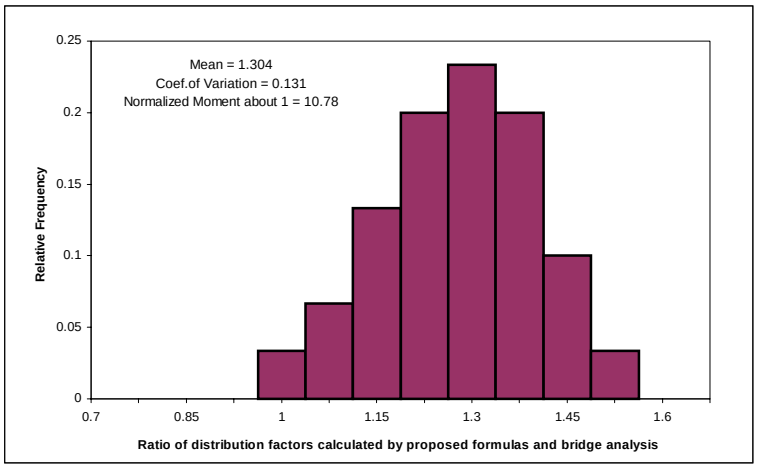

(c) Non-LRFD Formula

Figure C.12. Comparison of Distribution Factor Ratios calculated by the Proposed Formulas, LRFD Formulas, and Non-LRFD Formulas for ABRAMS Vehicle, Concrete T-Beam, Bending Moment in Interior Girders for Single Lane

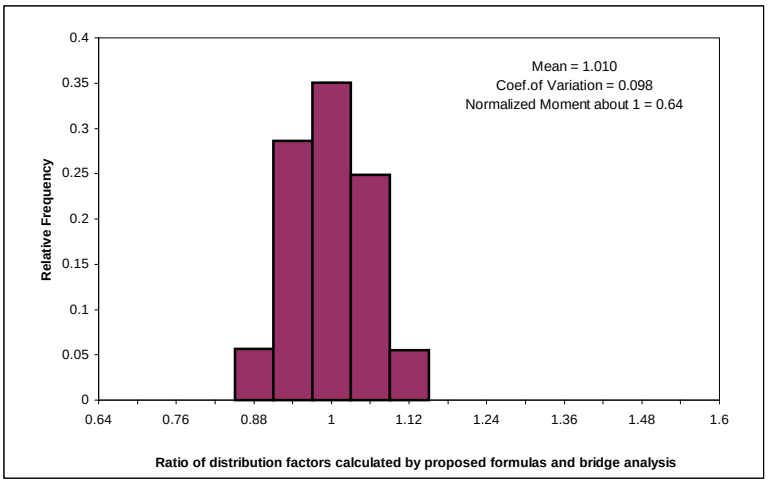

(a) New Formula

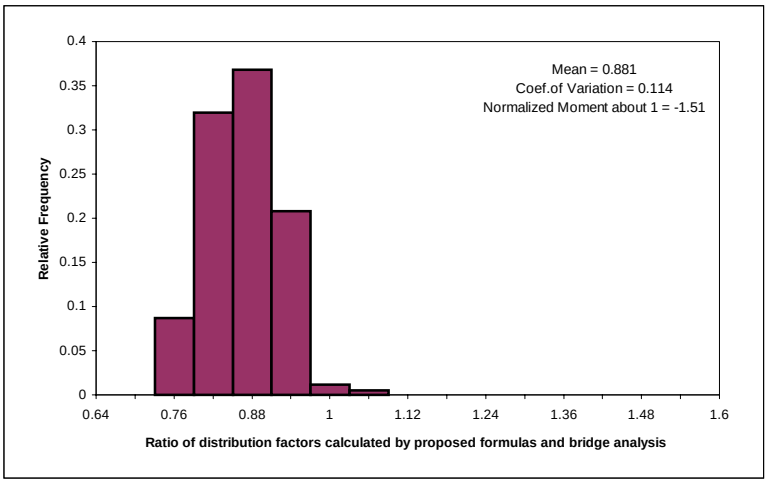

(b) LRFD Formula

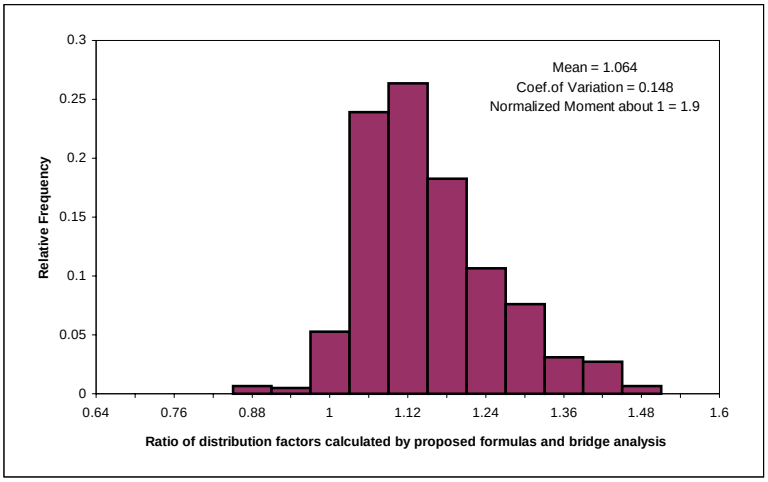

(c) Non-LRFD Formula

Figure C.13. Comparison of Distribution Factor Ratios calculated by the Proposed Formulas, LRFD Formulas, and Non-LRFD Formulas for M113 and Bradley Vehicles, All Beam Bridges, Bending Moment in Interior Girders for Single Lane

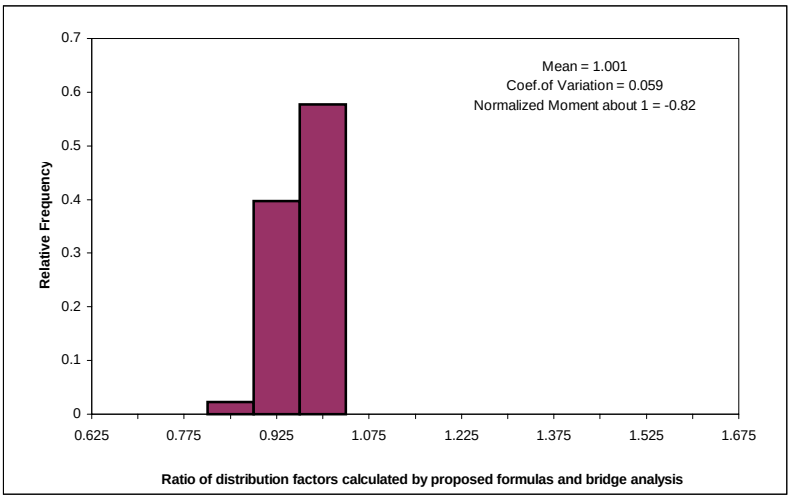

(a) New Formula

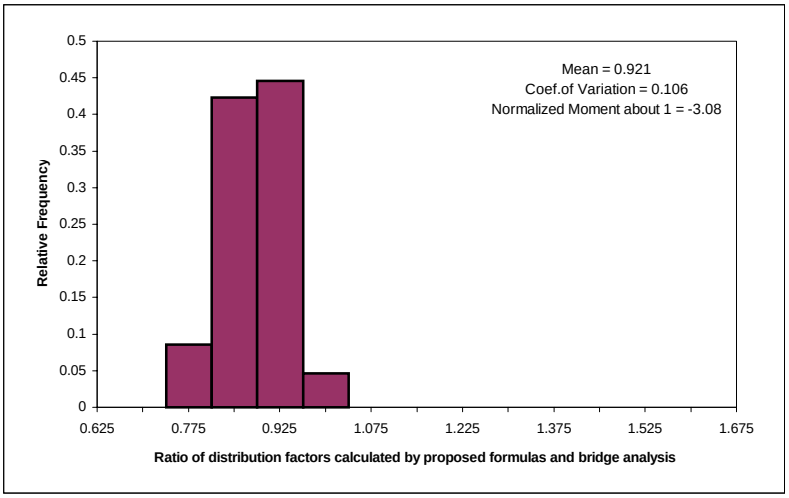

(b) LRFD Formula

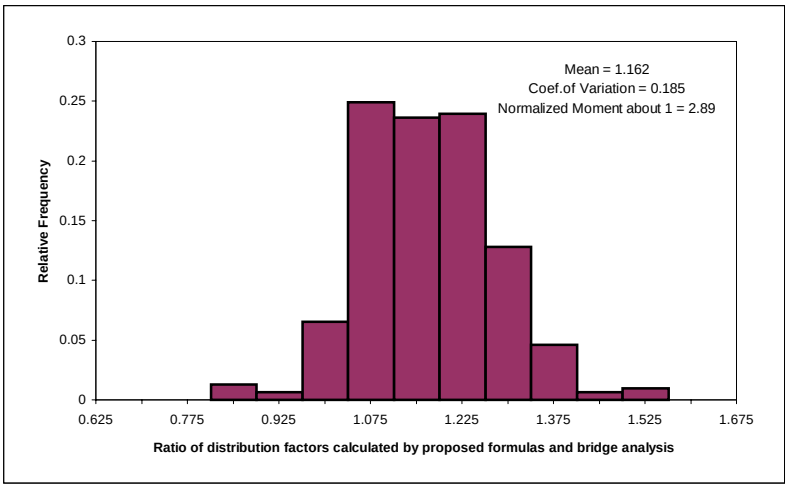

(c) Non-LRFD Formula

Figure C.14. Comparison of Distribution Factor Ratios calculated by the Proposed Formulas, LRFD Formulas, and Non-LRFD Formulas for M113 and Bradley Vehicles, Steel Girders, Bending Moment in Interior Girders for Single Lane

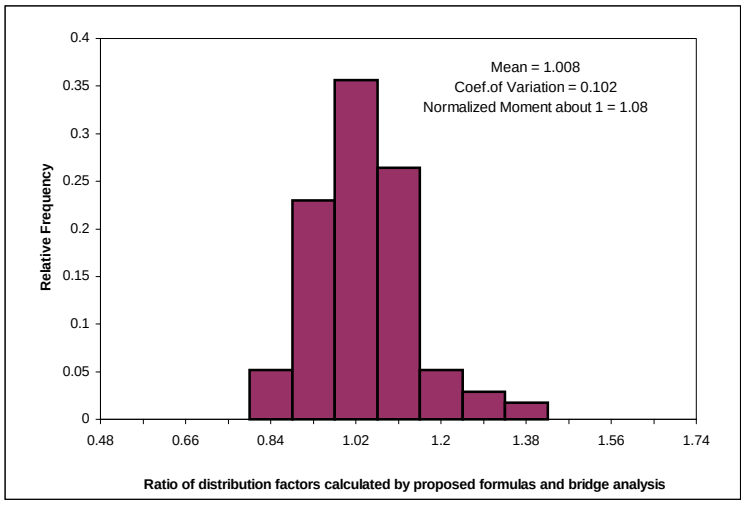

(a) New Formula

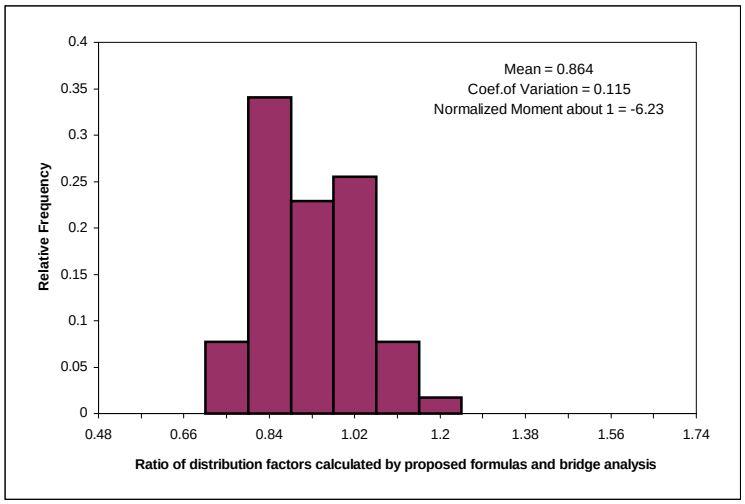

(b)LRFD Formula

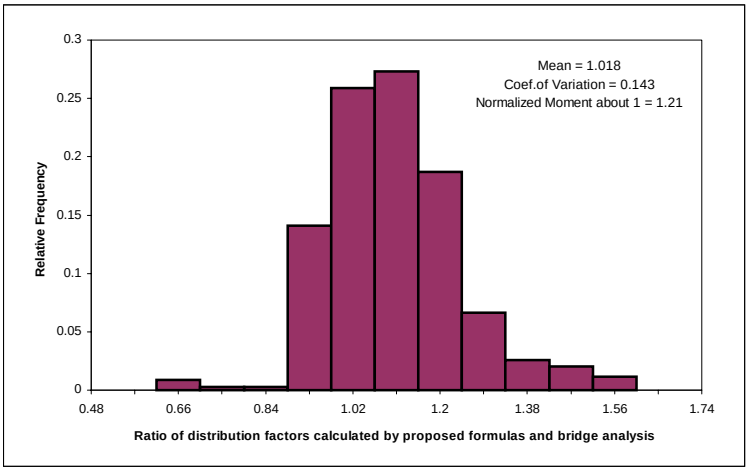

(c) Non-LRFD Formula

Figure C.15. Comparison of Distribution Factor Ratios calculated by the Proposed Formulas, LRFD Formulas, and Non-LRFD Formulas for M113 and Bradley Vehicles, Prestressed Concrete, Bending Moment in Interior Girders for Single Lane

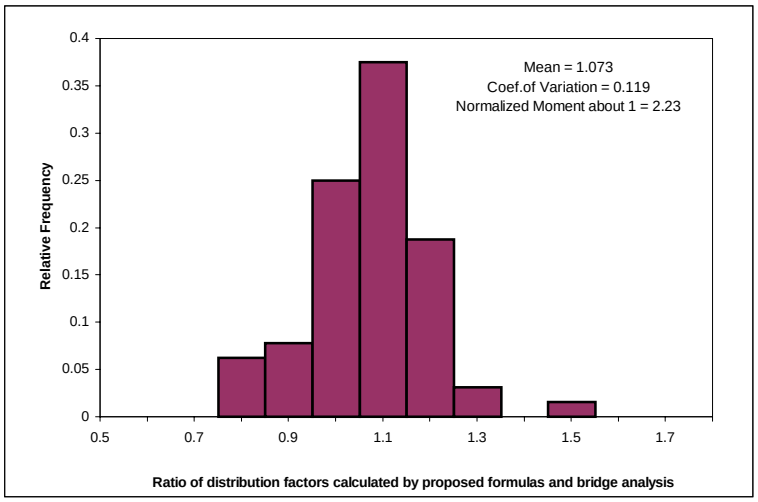

(a) New Formula

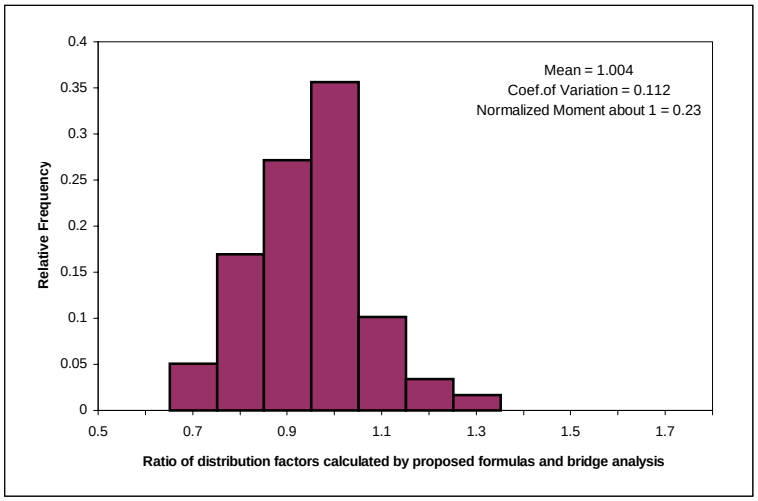

(b)LRFD Formula

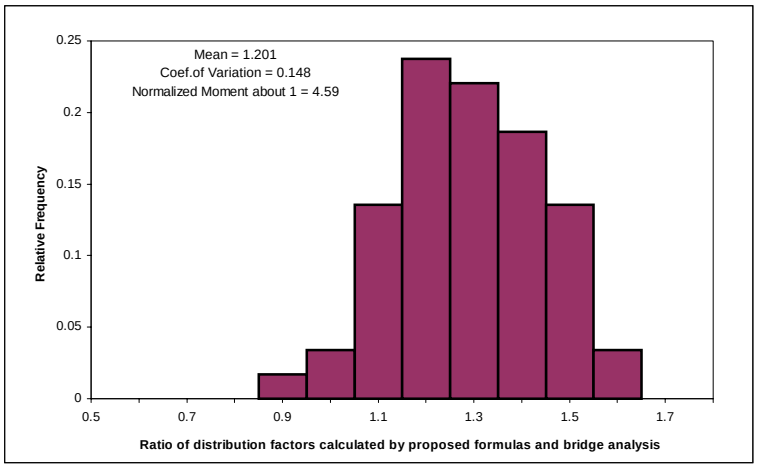

(c) Non-LRFD Formula

Figure C.16. Comparison of Distribution Factor Ratios calculated by the Proposed Formulas, LRFD Formulas, and Non-LRFD Formulas for M113 and Bradley Vehicles, Concrete T-Beam, Bending Moment in Interior Girders for Single Lane

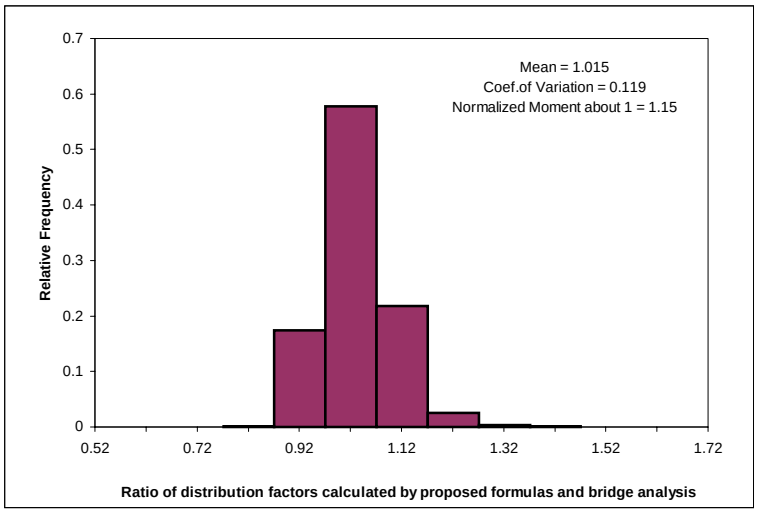

(a) New Formula

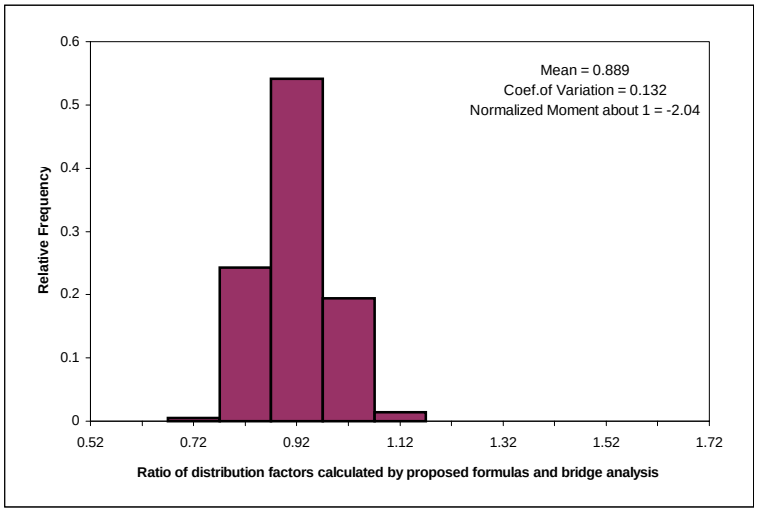

(b) LRFD Formula

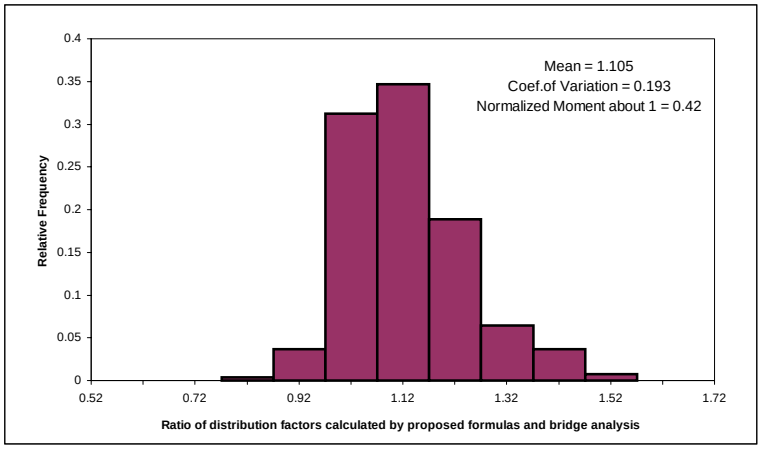

(c) Non-LRFD Formula

Figure C.17. Comparison of Distribution Factor Ratios calculated by the Proposed Formulas, LRFD Formulas, and Non-LRFD Formulas for All Vehicles, All Beam Bridges, Bending Moment in Interior Girders for Single Lane

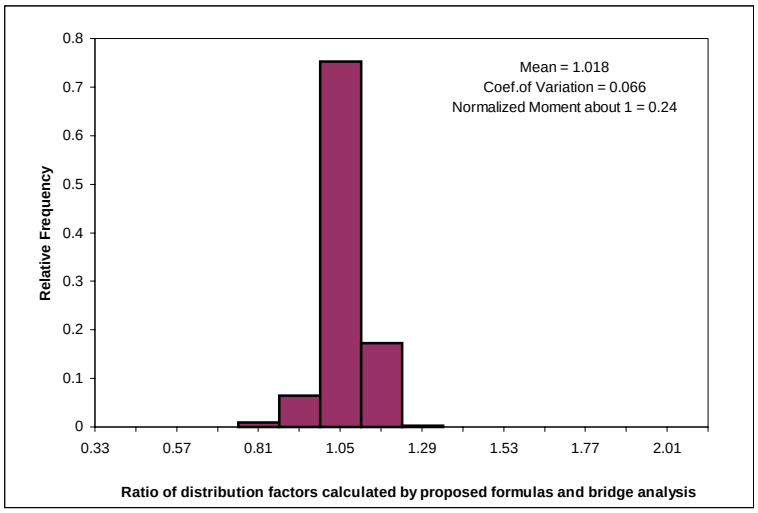

(a) New Formula

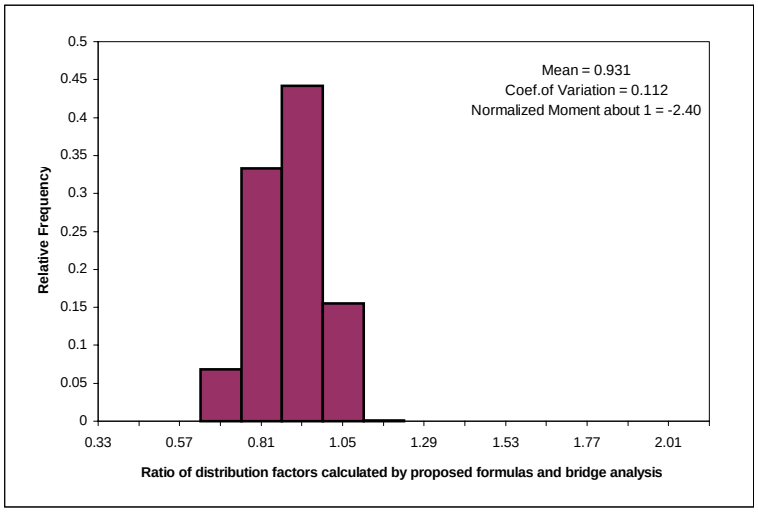

(b)LRFD Formula

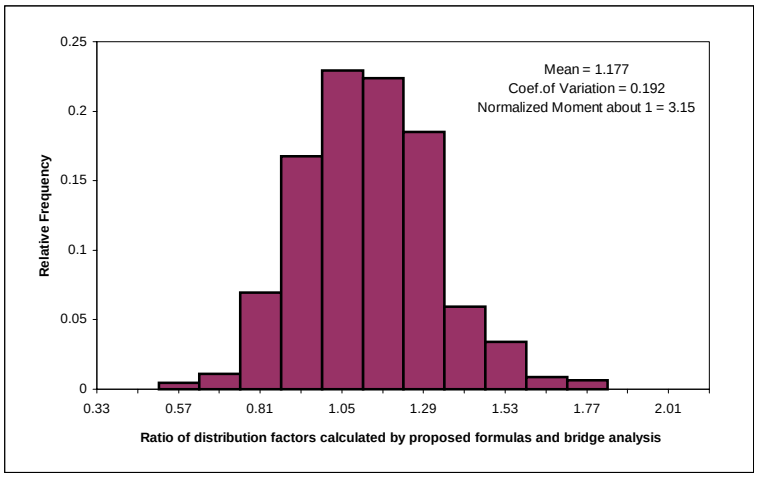

(c) Non-LRFD Formula

Figure C.18. Comparison of Distribution Factor Ratios calculated by the Proposed Formulas, LRFD Formulas, and Non-LRFD Formulas for All Vehicles, Steel Girders, Bending Moment in Interior Girders for Single Lane

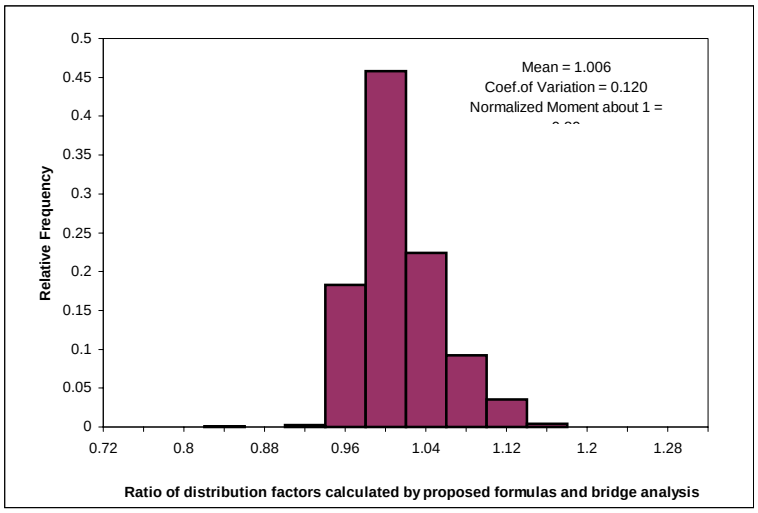

(a) New Formula

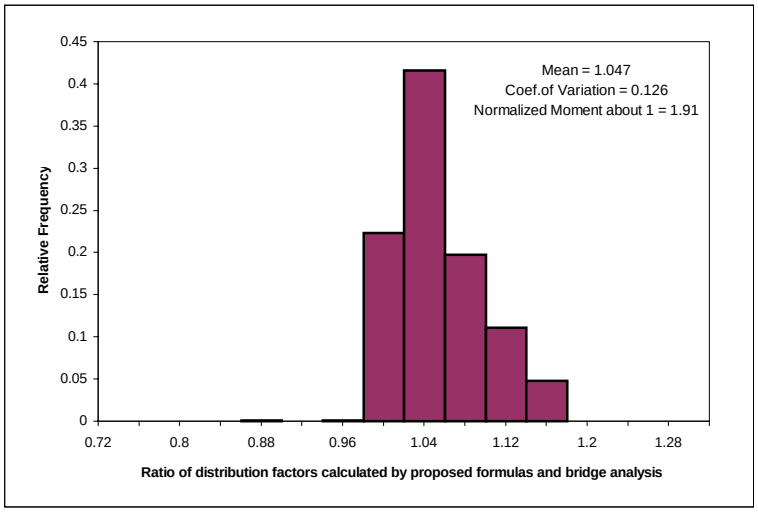

(b)LRFD Formula

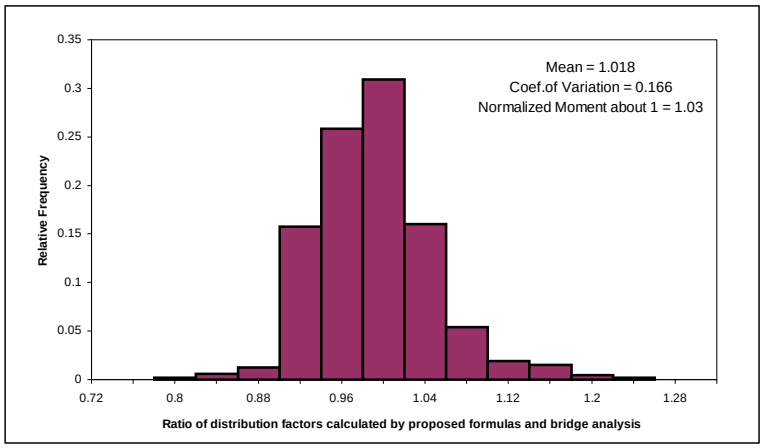

(c) Non-LRFD Formula

Figure C.19. Comparison of Distribution Factor Ratios calculated by the Proposed Formulas, LRFD Formulas, and Non-LRFD Formulas for All Vehicles, Prestressed Concrete, Bending Moment in Interior Girders for Single Lane

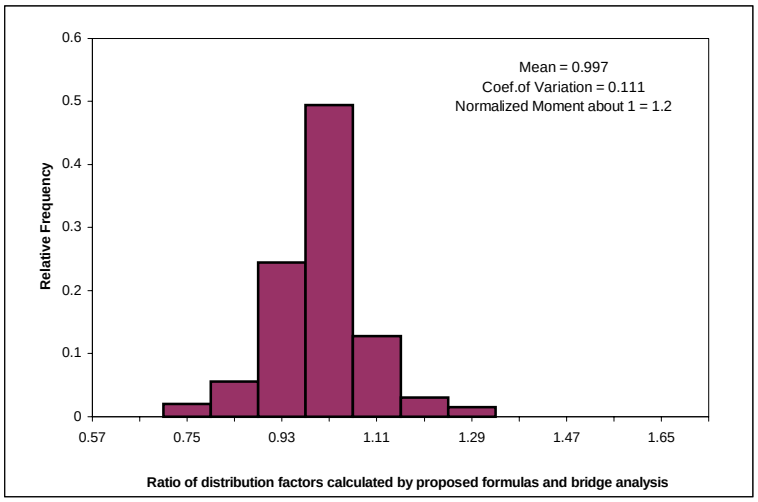

(a) New Formula

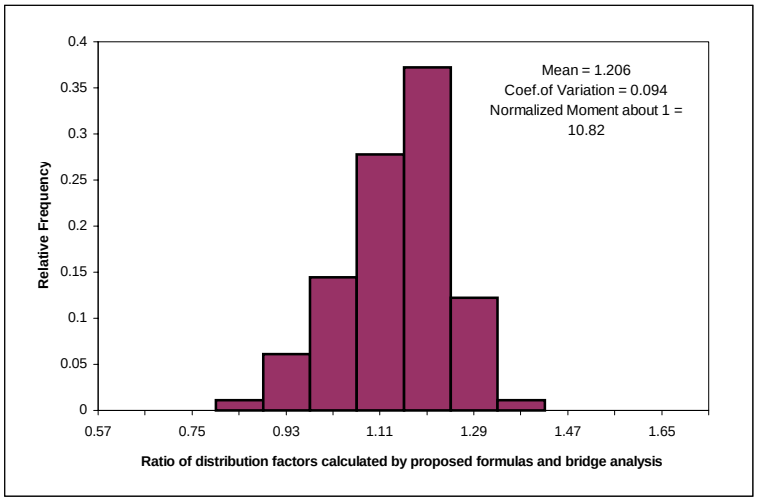

(b)LRFD Formula

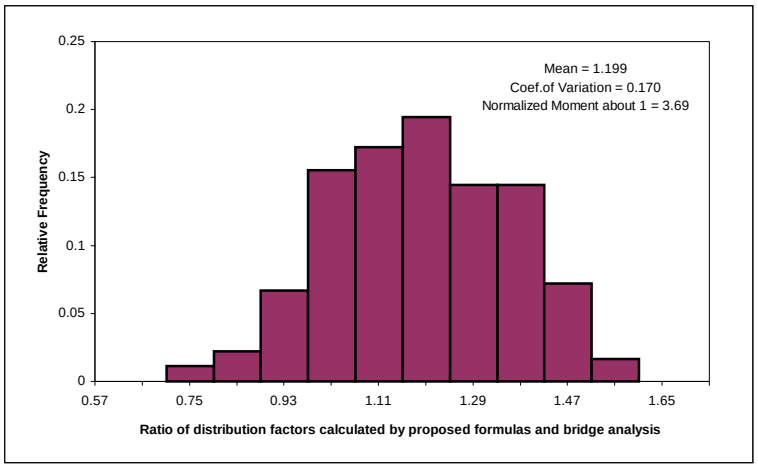

(c) Non-LRFD Formula

Figure C.20. Comparison of Distribution Factor Ratios calculated by the Proposed Formulas, LRFD Formulas, and Non-LRFD Formulas for All Vehicles, Concrete T-Beam, Bending Moment in Interior Girders for Single Lane

VITA

Juan Carlos Piñero Rivera was born on November 26, 1975 in Guaynabo, Puerto Rico, the youngest of three children of Raquel Rivera and Carlos Piñero. He attended the University of Puerto Rico – Mayagüez Campus, where he received a Bachelor of Science in Civil Engineering on May 1998. Upon graduation, a construction company hired him as a Project Engineer. In January 1999, he got married and began graduate studies in the Engineering Science and Mechanics Department at Virginia Polytechnic Institute and State University where he worked under the tutelage of Prof. M.P. Singh. He became a father of a beautiful baby boy in February 2000. During the last summer of his graduate studies in the ESM Department, he worked for as a structural engineer for a consulting firm in Puerto Rico. In August 2000, he joined the Civil and Environmental Engineering Department of Virginia Polytechnic Institute and State University to continue doctoral studies in the area of Construction Engineering and Management. He received the degree of Master of Science in Engineering Mechanics in May 2001.